Density Model for Risso's Dolphin (*Grampus griseus*) for the U.S. East Coast: Supplementary Report

Duke University Marine Geospatial Ecology Lab*

Model Version 3.3 - 2016-04-21

Citation

When referencing our methodology or results generally, please cite our open-access article:

Roberts JJ, Best BD, Mannocci L, Fujioka E, Halpin PN, Palka DL, Garrison LP, Mullin KD, Cole TVN, Khan CB, McLellan WM, Pabst DA, Lockhart GG (2016) Habitat-based cetacean density models for the U.S. Atlantic and Gulf of Mexico. Scientific Reports 6: 22615. doi: 10.1038/srep22615

To reference this specific model or Supplementary Report, please cite:

Roberts JJ, Best BD, Mannocci L, Fujioka E, Halpin PN, Palka DL, Garrison LP, Mullin KD, Cole TVN, Khan CB, McLellan WM, Pabst DA, Lockhart GG (2016) Density Model for Risso's Dolphin (*Grampus griseus*) for the U.S. East Coast Version 3.3, 2016-04-21, and Supplementary Report. Marine Geospatial Ecology Lab, Duke University, Durham, North Carolina.

Copyright and License

Revision History

Version	Date	Description of changes
1	2014-10-19	Initial version.
2	2014-11-21	Reconfigured detection hierarchy and adjusted NARWSS detection functions based on additional information from Tim Cole. Removed CumVGPM180 predictor. Updated documentation.
3	2014-12-05	Fixed bug that applied the wrong detection function to segments NE_narwss_1999_widgeon_hapo dataset. Refitted model. Updated documentation.
3.1	2015-03-06	Updated the documentation. No changes to the model.
3.2	2015-05-14	Updated calculation of CVs. Switched density rasters to logarithmic breaks. No changes to the model.
3.3	2016-04-21	Switched calculation of monthly 5% and 95% confidence interval rasters to the method used to produce the year-round rasters. (We intended this to happen in version 3.2 but I did not implement it properly.) No changes to the other rasters or the model itself.

*For questions, or to offer feedback about this model or report, please contact Jason Roberts (jason.roberts@duke.edu)

Survey Data

Survey	Period	Length (1000 km)	Hours	Sightings
NEFSC Aerial Surveys	1995-2008	70	412	148
NEFSC NARWSS Harbor Porpoise Survey	1999-1999	6	36	2
NEFSC North Atlantic Right Whale Sighting Survey	1999-2013	432	2330	86
NEFSC Shipboard Surveys	1995-2004	16	1143	352
NJDEP Aerial Surveys	2008-2009	11	60	0
NJDEP Shipboard Surveys	2008-2009	14	836	0
SEFSC Atlantic Shipboard Surveys	1992-2005	28	1731	77
SEFSC Mid Atlantic Tursiops Aerial Surveys	1995-2005	35	196	0
SEFSC Southeast Cetacean Aerial Surveys	1992-1995	8	42	0
UNCW Cape Hatteras Navy Surveys	2011-2013	19	125	9
UNCW Early Marine Mammal Surveys	2002-2002	18	98	0
UNCW Jacksonville Navy Surveys	2009-2013	66	402	42
UNCW Onslow Navy Surveys	2007-2011	49	282	5
UNCW Right Whale Surveys	2005-2008	114	586	0
Virginia Aquarium Aerial Surveys	2012-2014	9	53	0
Total		895	8332	721

Table 2: Survey effort and sightings used in this model. Effort is tallied as the cumulative length of on-effort transects and hours the survey team was on effort. Sightings are the number of on-effort encounters of the modeled species for which a perpendicular sighting distance (PSD) was available. Off effort sightings and those without PSDs were omitted from the analysis.

Season	Months	Length (1000 km)	Hours	Sightings
All_Year	All	897	8332	721

Table 3: Survey effort and on-effort sightings having perpendicular sighting distances.

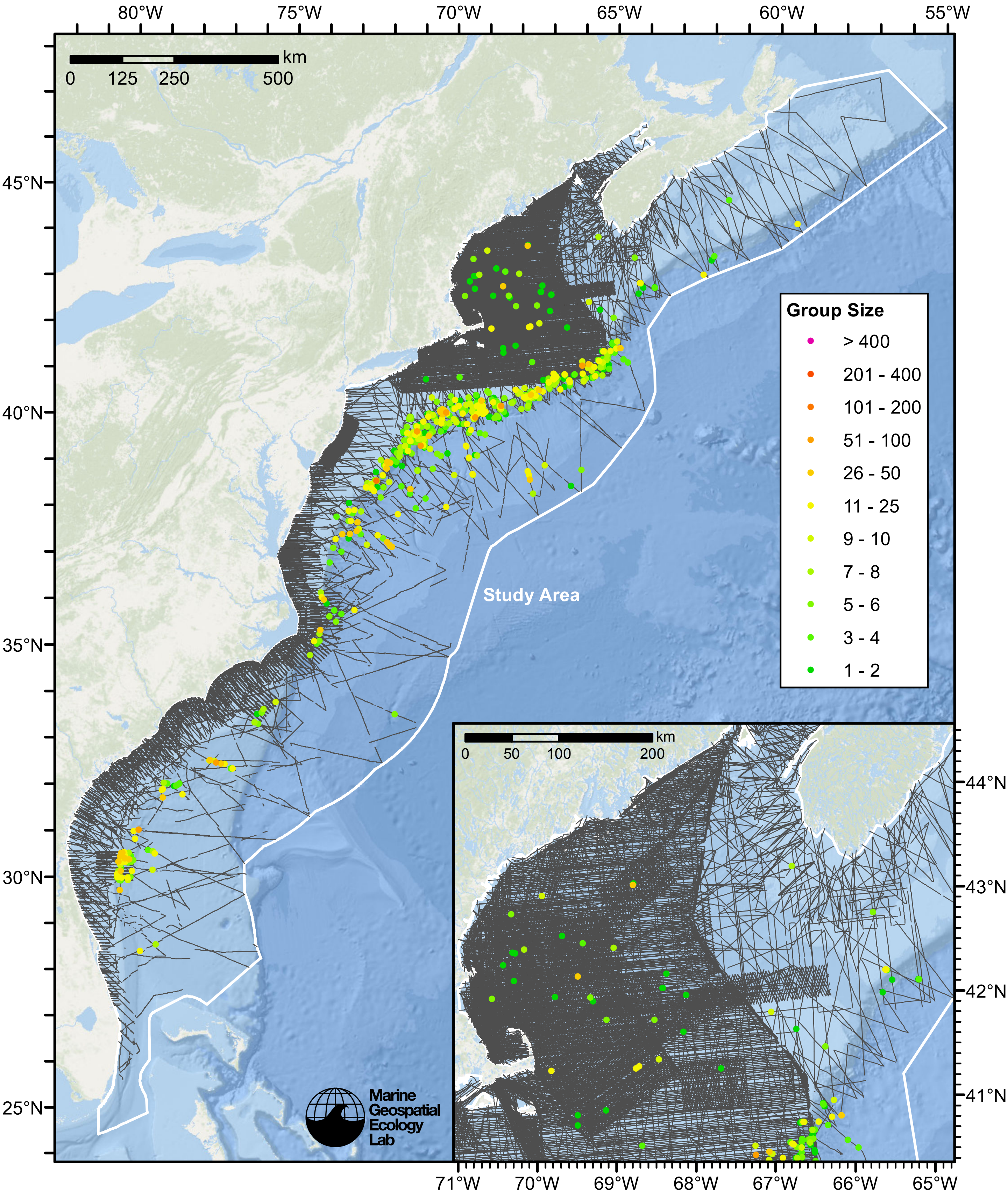

Figure 1: Risso's dolphin sightings and survey tracklines.

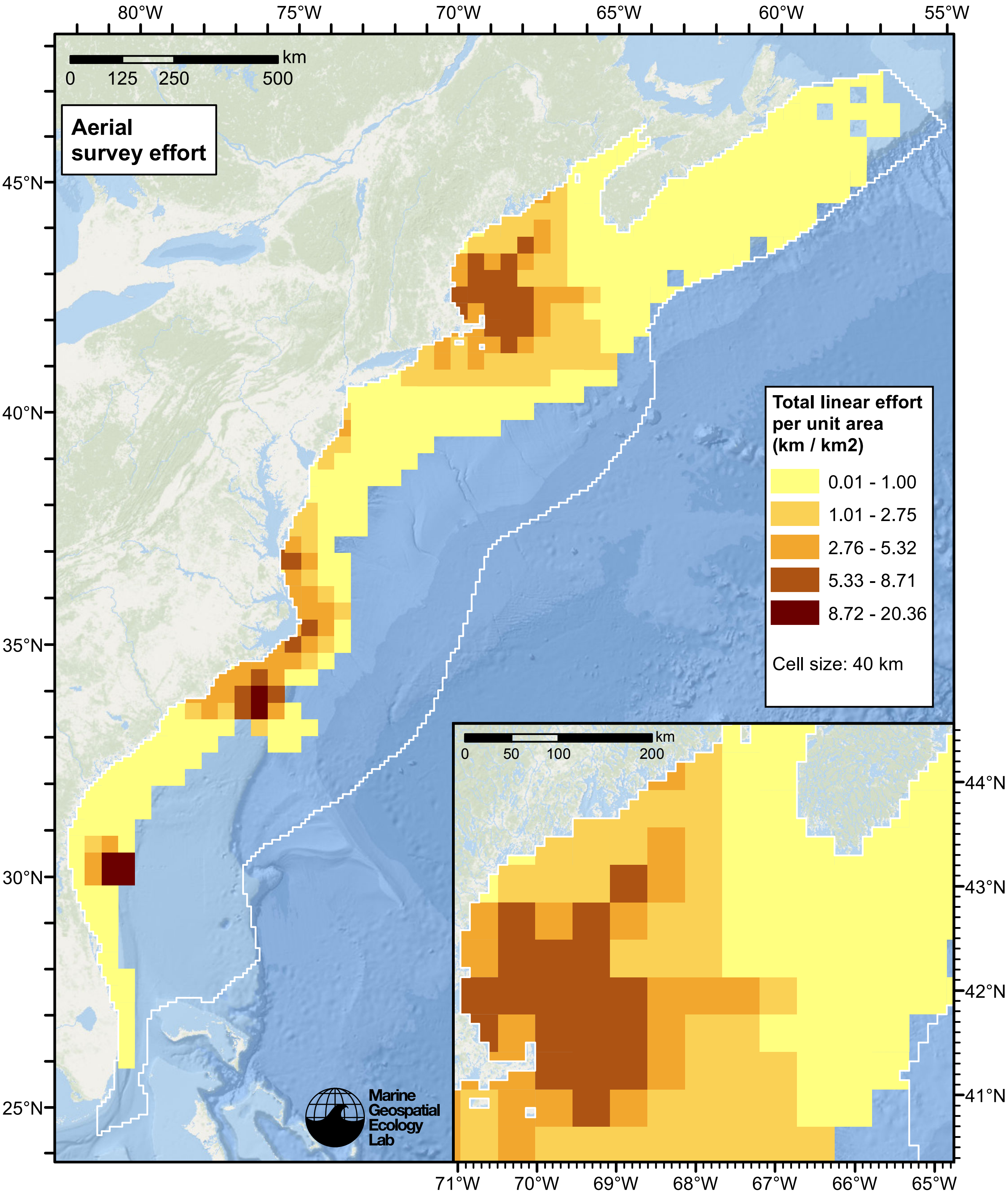

Figure 2: Aerial linear survey effort per unit area.

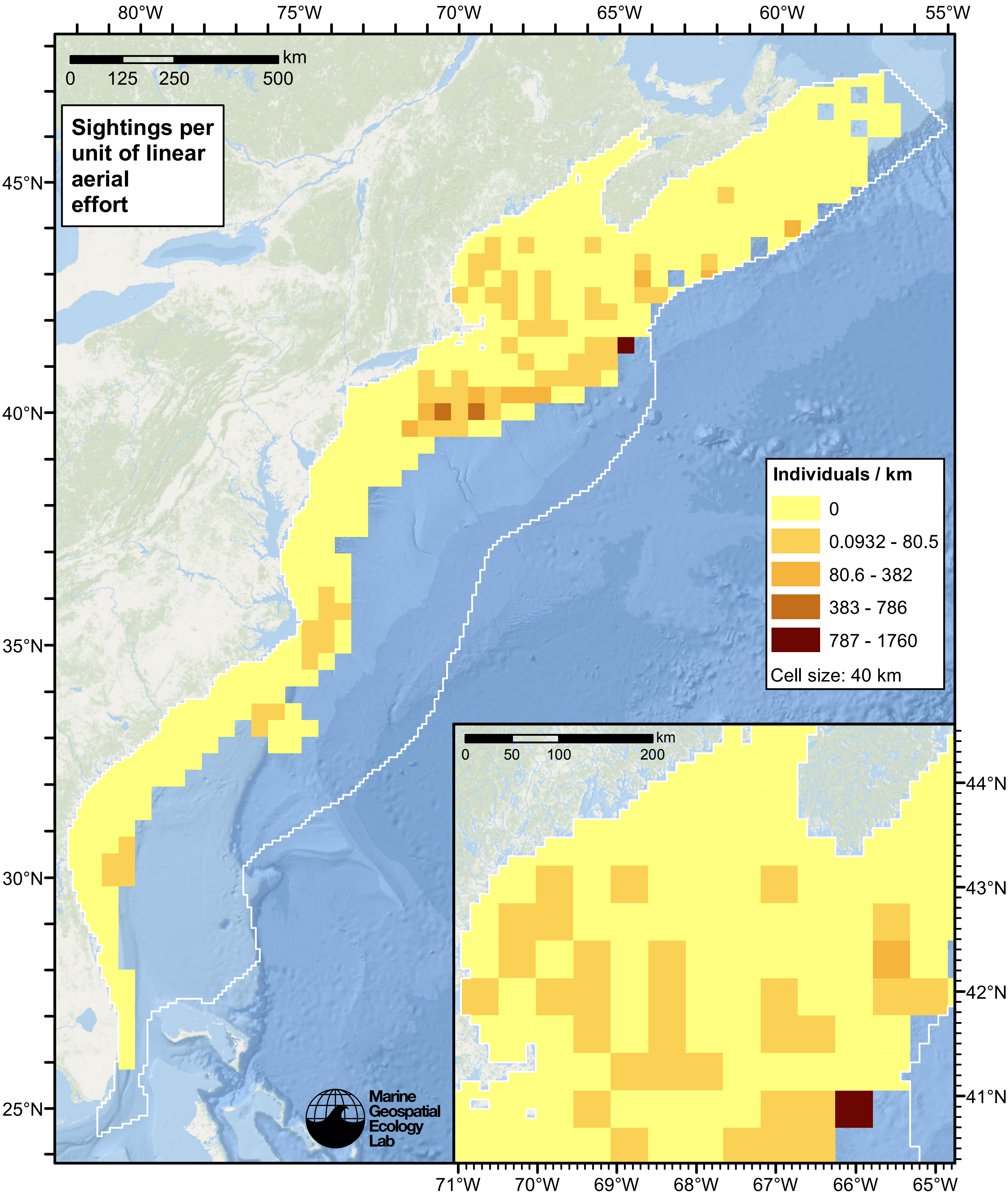

Figure 3: Risso's dolphin sightings per unit aerial linear survey effort.

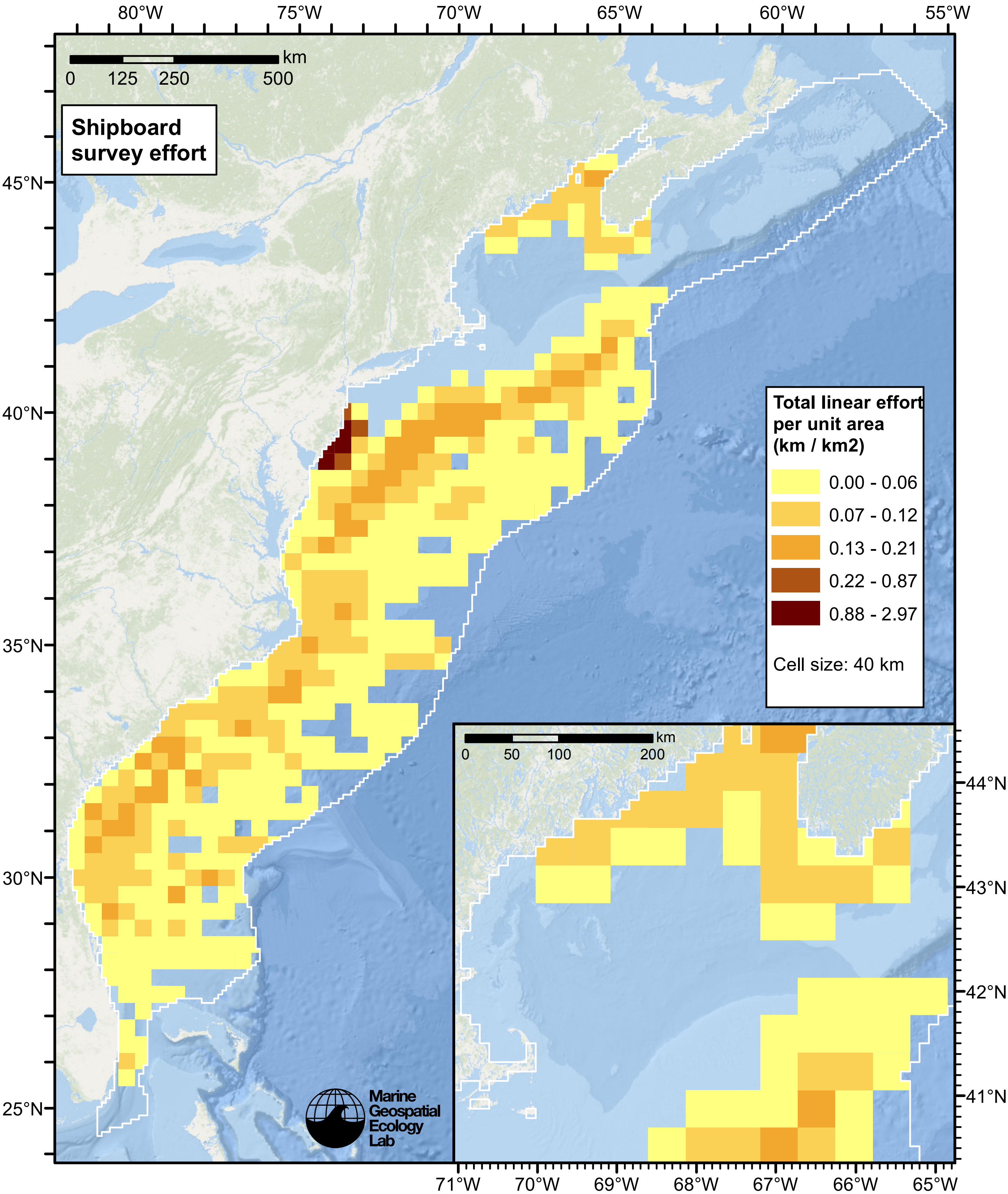

Figure 4: Shipboard linear survey effort per unit area.

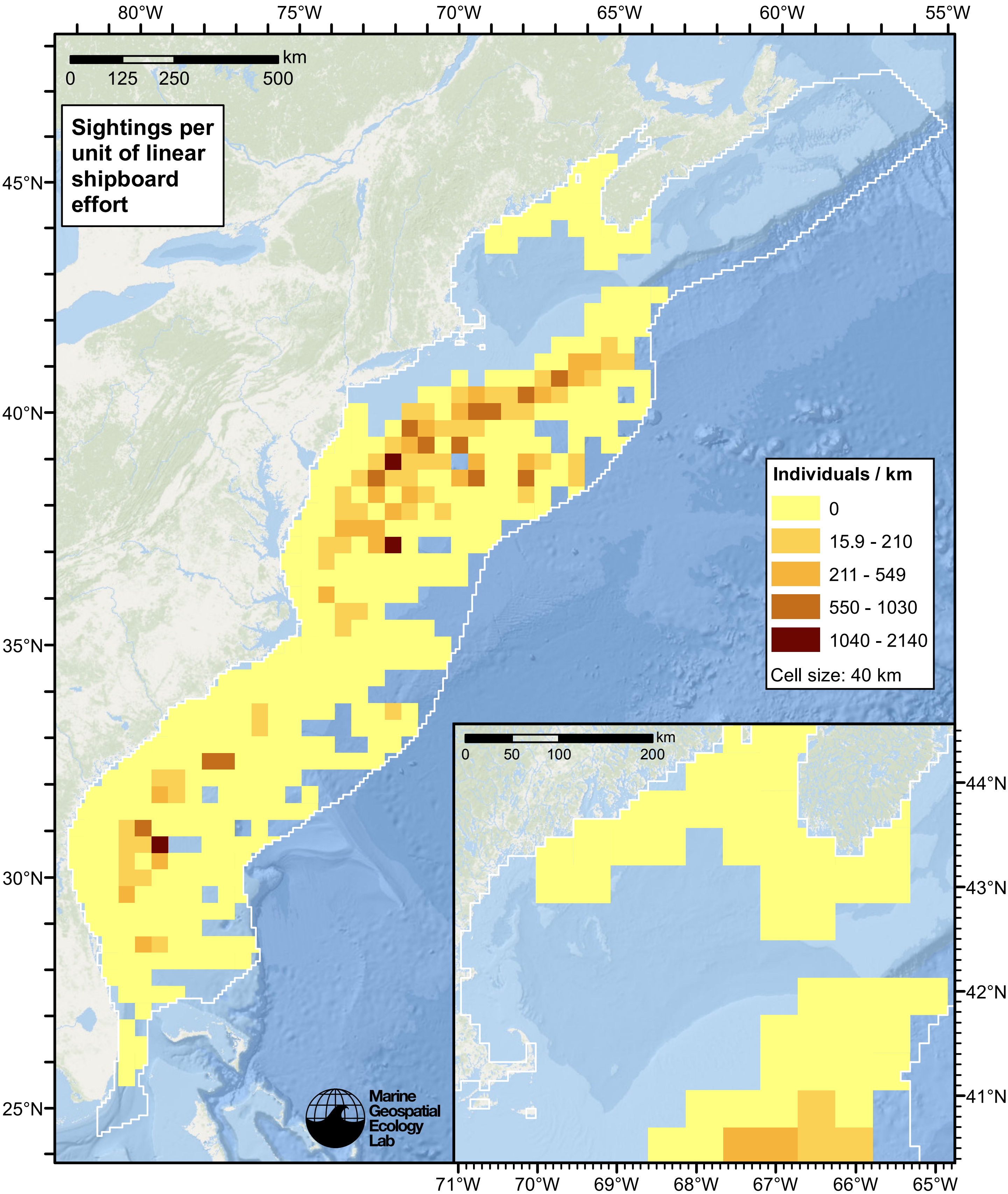

Figure 5: Risso's dolphin sightings per unit shipboard linear survey effort.

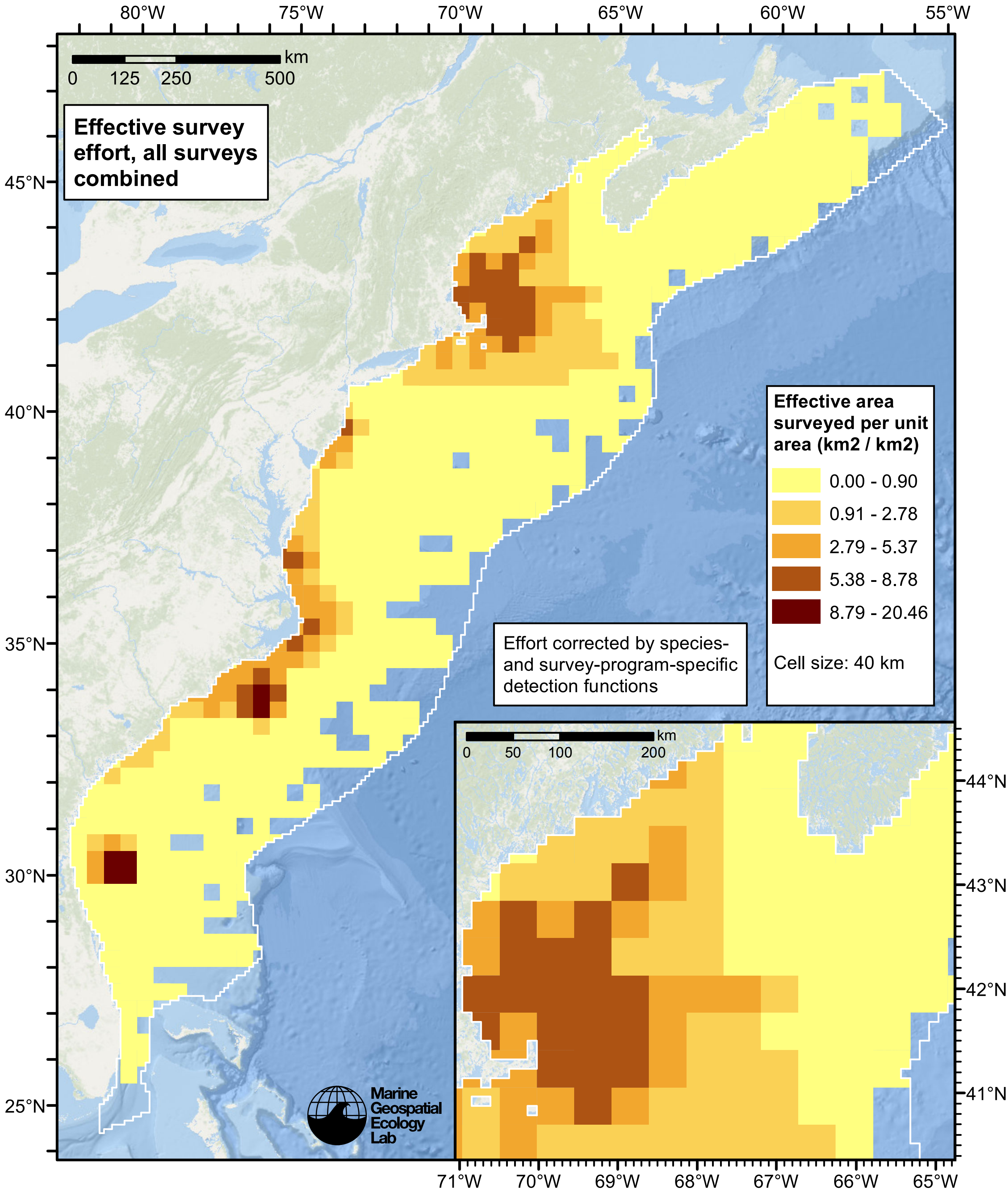

Figure 6: Effective survey effort per unit area, for all surveys combined. Here, effort is corrected by the species- and survey-program-specific detection functions used in fitting the density models.

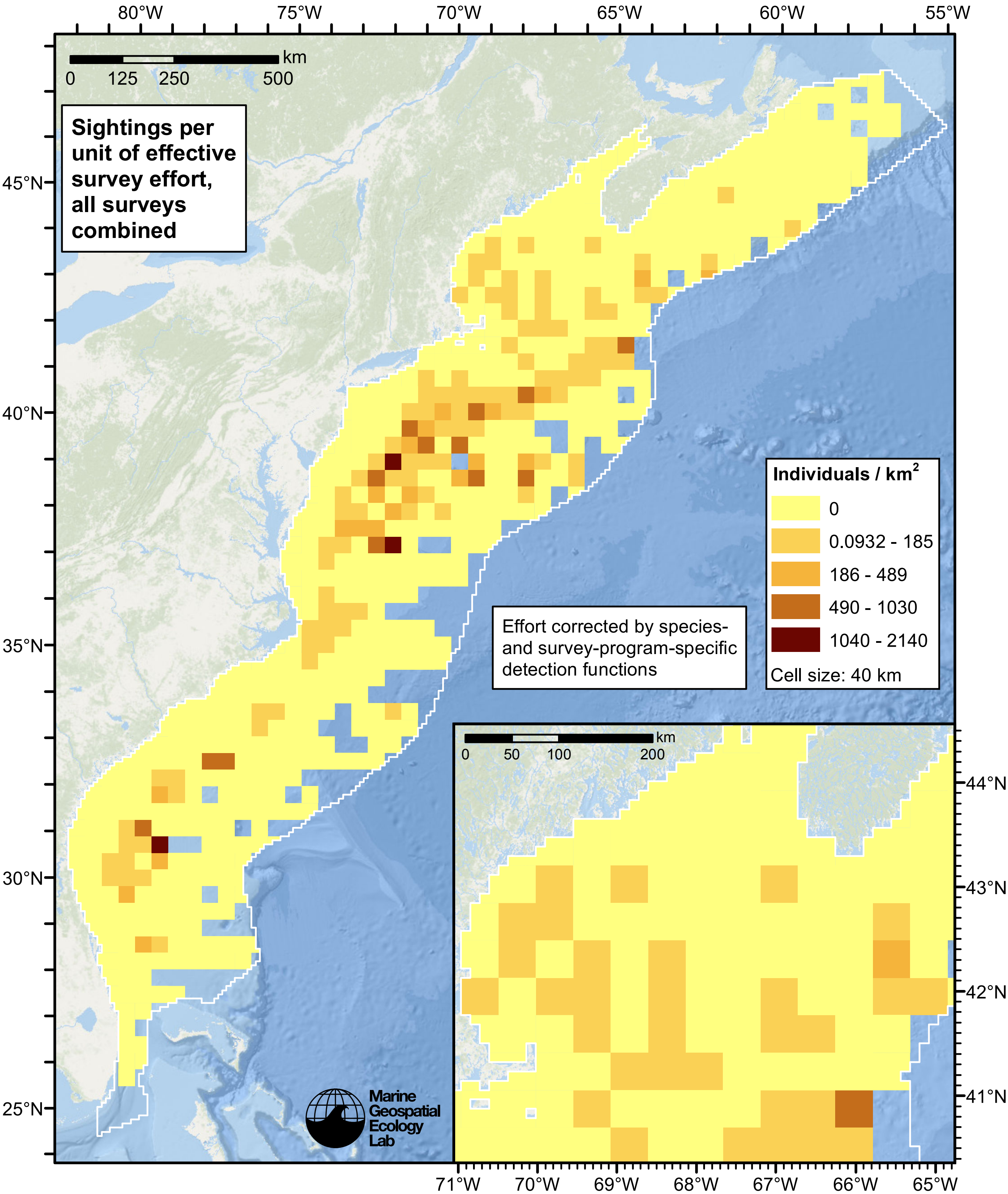

Figure 7: Risso's dolphin sightings per unit of effective survey effort, for all surveys combined. Here, effort is corrected by the species- and survey-program-specific detection functions used in fitting the density models.

Detection Functions

The detection hierarchy figures below show how sightings from multiple surveys were pooled to try to achieve Buckland et. al's (2001) recommendation that at least 60-80 sightings be used to fit a detection function. Leaf nodes, on the right, usually represent individual surveys, while the hierarchy to the left shows how they have been grouped according to how similar we believed the surveys were to each other in their detection performance.

At each node, the red or green number indicates the total number of sightings below that node in the hierarchy, and is colored green if 70 or more sightings were available, and red otherwise. If a grouping node has zero sightings–i.e. all of the surveys within it had zero sightings–it may be collapsed and shown as a leaf to save space.

Each histogram in the figure indicates a node where a detection function was fitted. The actual detection functions do not appear in this figure; they are presented in subsequent sections. The histogram shows the frequency of sightings by perpendicular sighting distance for all surveys contained by that node. Each survey (leaf node) recieves the detection function that is closest to it up the hierarchy. Thus, for common species, sufficient sightings may be available to fit detection functions deep in the hierarchy, with each function applying to only a few surveys, thereby allowing variability in detection performance between surveys to be addressed relatively finely. For rare species, so few sightings may be available that we have to pool many surveys together to try to meet Buckland's recommendation, and fit only a few coarse detection functions high in the hierarchy.

A blue Proxy Species tag indicates that so few sightings were available that, rather than ascend higher in the hierarchy to a point that we would pool grossly-incompatible surveys together, (e.g. shipboard surveys that used big-eye binoculars with those that used only naked eyes) we pooled sightings of similar species together instead. The list of species pooled is given in following sections.

Shipboard Surveys

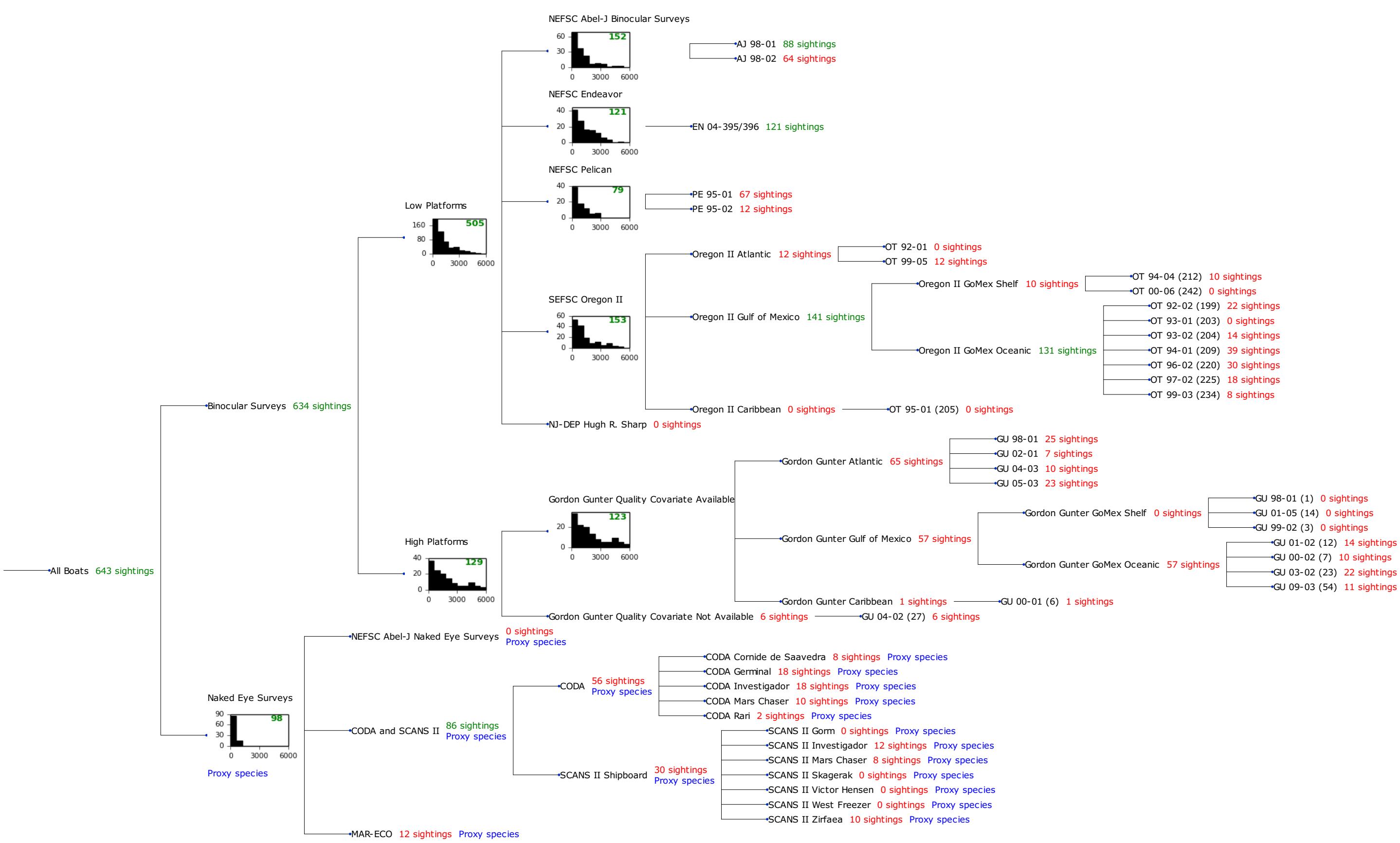

Figure 8: Detection hierarchy for shipboard surveys

Low Platforms

The sightings were right truncated at 5500m.

Covariate	Description
beaufort	Beaufort sea state.
size	Estimated size (number of individuals) of the sighted group.

Table 4: Covariates tested in candidate “multi-covariate distance sampling” (MCDS) detection functions.

Key	Adjustment	Order	Covariates	Succeeded	Δ AIC	Mean ESHW (m)
hr			beaufort, size	Yes	0.00	1643
hr			beaufort	Yes	1.45	1595
hr	poly	2		Yes	4.79	1278
hr	poly	4		Yes	6.77	1350
hr			size	Yes	11.68	1542
hr				Yes	14.00	1485
hn	cos	3		Yes	15.59	1511
hn	cos	2		Yes	17.61	1687
hn			beaufort, size	Yes	26.04	2063
hn			beaufort	Yes	40.52	2040
hn			size	Yes	41.59	2071
hn				Yes	54.28	2050
hn	herm	4		Yes	55.57	2047

Table 5: Candidate detection functions for Low Platforms. The first one listed was selected for the density model.

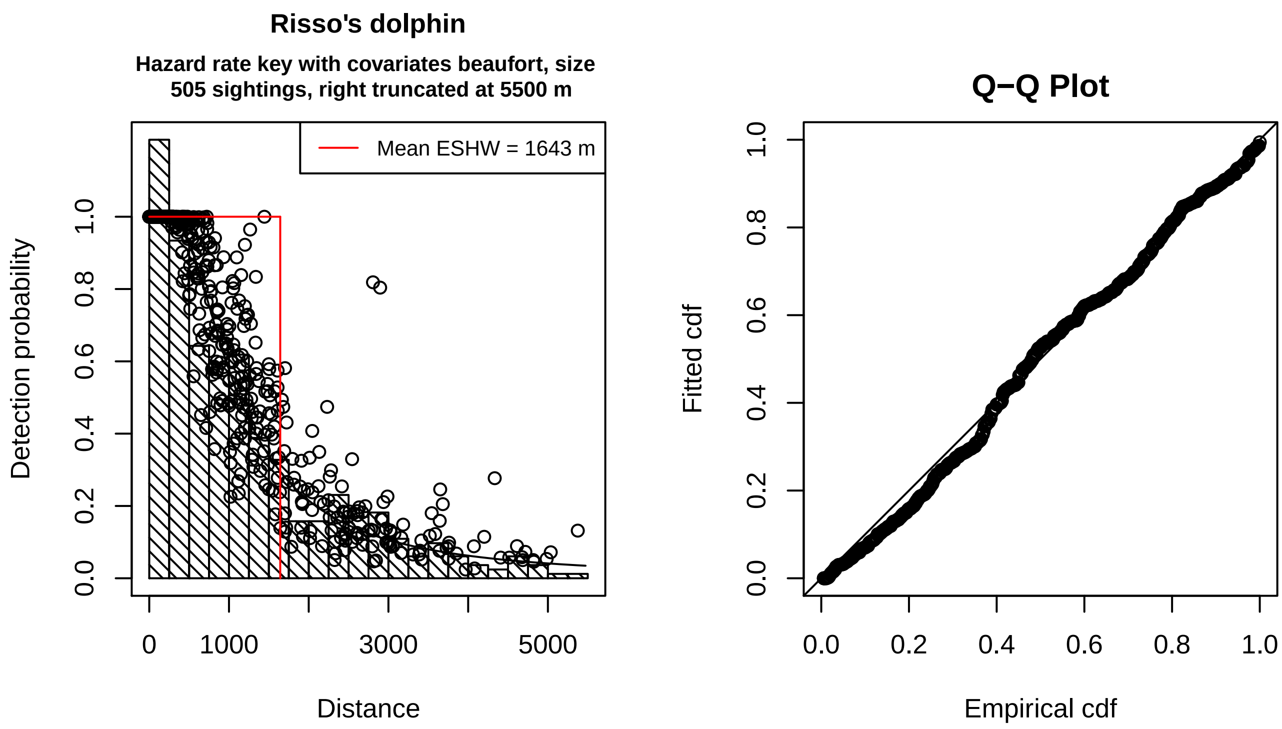

Figure 9: Detection function for Low Platforms that was selected for the density model

Statistical output for this detection function:

```
Summary for ds object
Number of observations :  505
Distance range         :  0  -  5500
AIC                    :  8149.828

Detection function:
 Hazard-rate key function

Detection function parameters
Scale Coefficients:
              estimate         se
(Intercept)  7.3694833 0.18769443
beaufort    -0.2454228 0.06201611
size         0.2182358 0.08027209

Shape parameters:
             estimate        se
(Intercept) 0.6837352 0.0819912

                        Estimate           SE         CV
Average p              0.2784291   0.01670321 0.05999090
N in covered region 1813.7471437 129.11969449 0.07118947
```

Additional diagnostic plots:

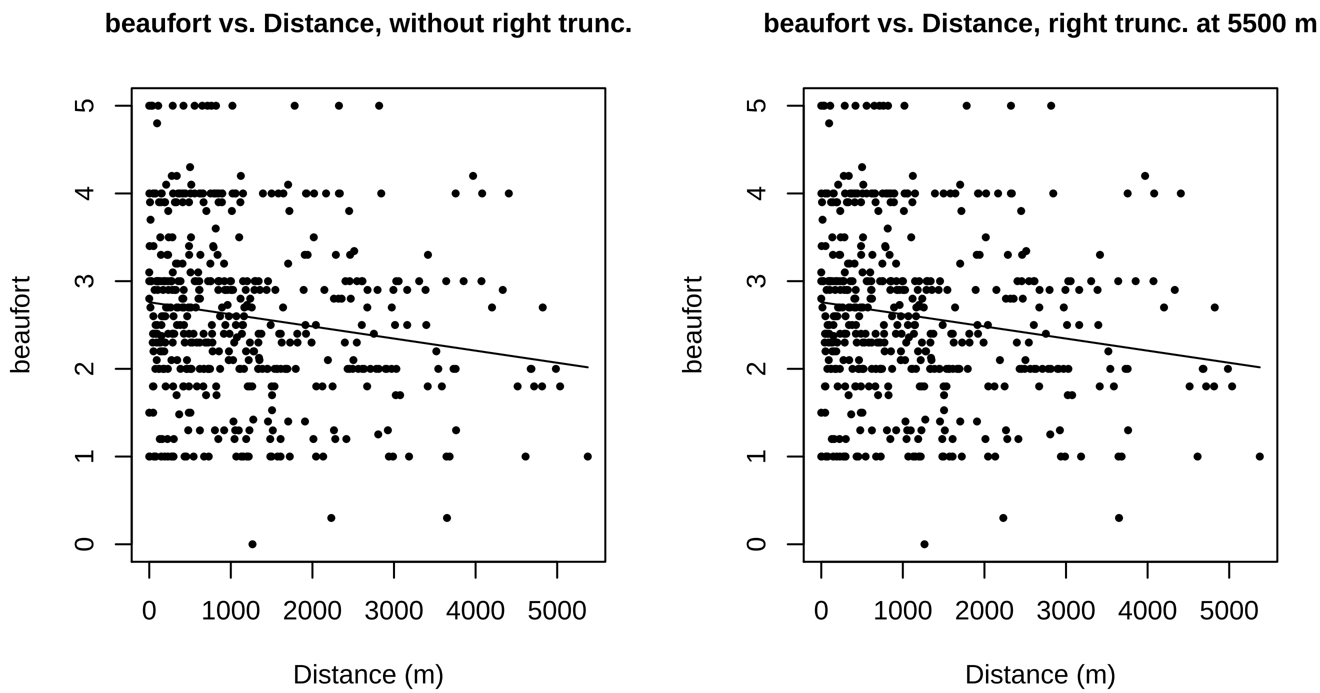

Figure 10: Scatterplots showing the relationship between Beaufort sea state and perpendicular sighting distance, for all sightings (left) and only those not right truncated (right). The line is a simple linear regression.

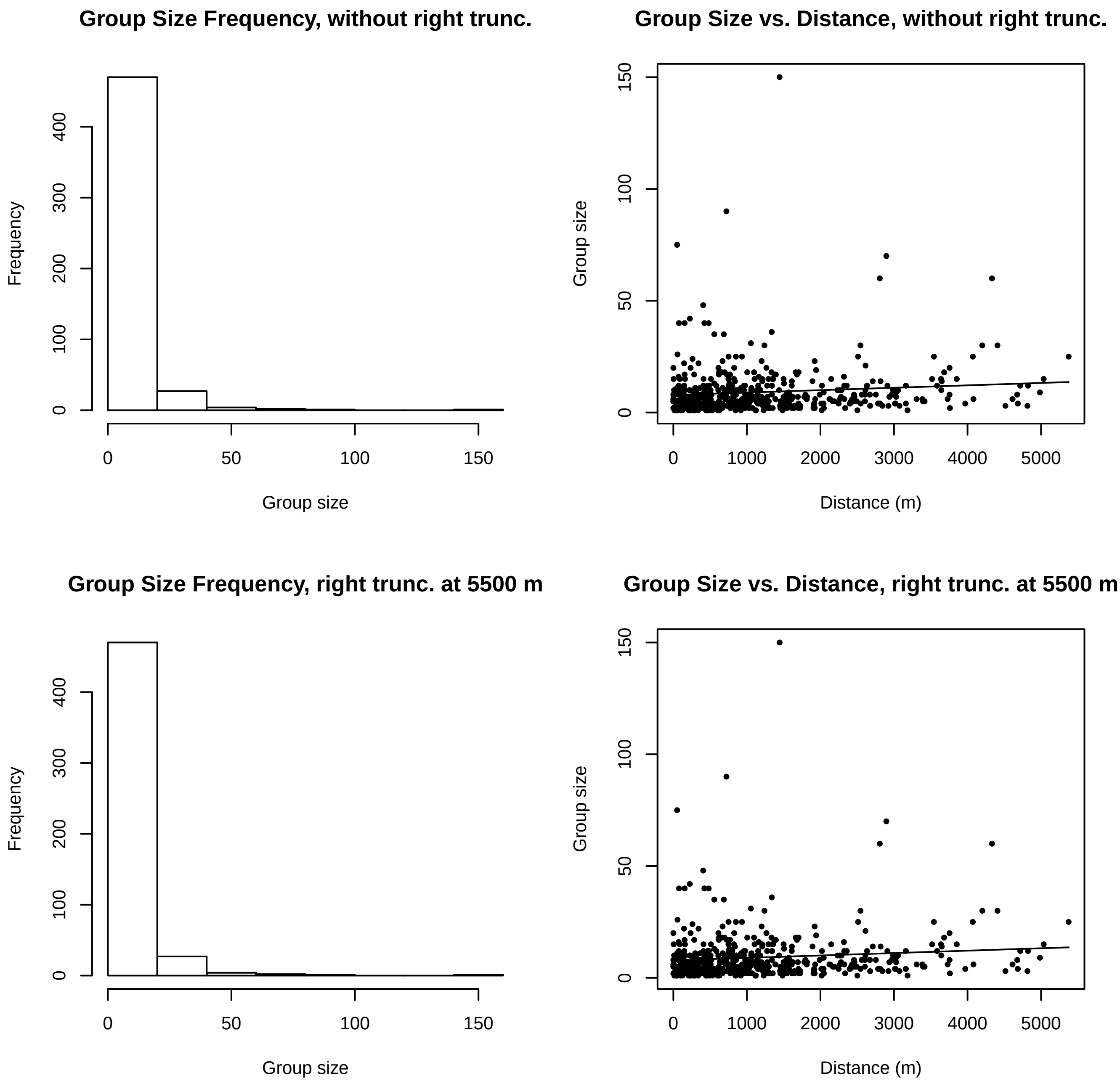

Figure 11: Histograms showing group size frequency and scatterplots showing the relationship between group size and perpendicular sighting distance, for all sightings (top row) and only those not right truncated (bottom row). In the scatterplot, the line is a simple linear regression.

NEFSC Abel-J Binocular Surveys

The sightings were right truncated at 3800m.

Covariate	Description
beaufort	Beaufort sea state.
quality	Survey-specific index of the quality of observation conditions, utilizing relevant factors other than Beaufort sea state (see methods).
size	Estimated size (number of individuals) of the sighted group.

Table 6: Covariates tested in candidate "multi-covariate distance sampling" (MCDS) detection functions.

Key	Adjustment	Order	Covariates	Succeeded	Δ AIC	Mean ESHW (m)
hr			quality, size	Yes	0.00	1264
hn	cos	2		Yes	0.74	1219
hr			beaufort, size	Yes	1.01	1286
hr			beaufort, quality, size	Yes	1.01	1281
hr			quality	Yes	1.21	1268
hr			beaufort	Yes	1.37	1339
hr			beaufort, quality	Yes	1.38	1340
hr			size	Yes	2.27	1210
hr				Yes	4.18	1158
hr	poly	2		Yes	4.46	1073
hr	poly	4		Yes	4.51	1080
hn			beaufort, quality	Yes	7.26	1604
hn			beaufort, quality, size	Yes	8.56	1600
hn			quality	Yes	9.42	1596
hn			quality, size	Yes	9.78	1594
hn			beaufort	Yes	9.98	1601
hn			beaufort, size	Yes	10.81	1600
hn	cos	3		Yes	12.70	1361
hn			size	Yes	13.14	1598
hn				Yes	13.45	1598
hn	herm	4		Yes	15.17	1594

Table 7: Candidate detection functions for NEFSC Abel-J Binocular Surveys. The first one listed was selected for the density model.

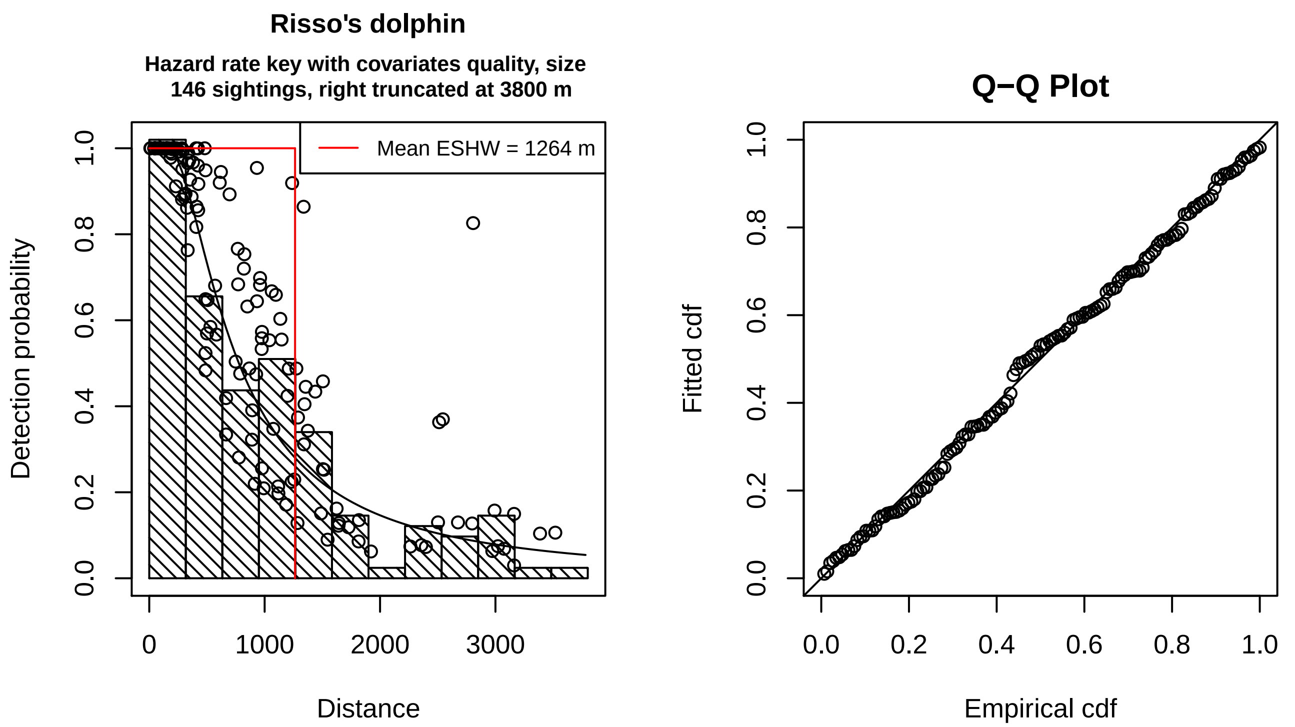

Figure 12: Detection function for NEFSC Abel-J Binocular Surveys that was selected for the density model

Statistical output for this detection function:

```
Summary for ds object
Number of observations :  146
Distance range         :  0  -  3800
AIC                    :  2284.244

Detection function:
 Hazard-rate key function

Detection function parameters
Scale Coefficients:
              estimate        se
(Intercept)  7.7174410 0.6905777
quality     -0.4444514 0.2062651
size         0.3162565 0.1683151

Shape parameters:
             estimate        se
(Intercept) 0.5538027 0.1616989

                       Estimate          SE        CV
Average p             0.2954145  0.03776618 0.1278413
N in covered region 494.2208431 72.33825516 0.1463683
```

Additional diagnostic plots:

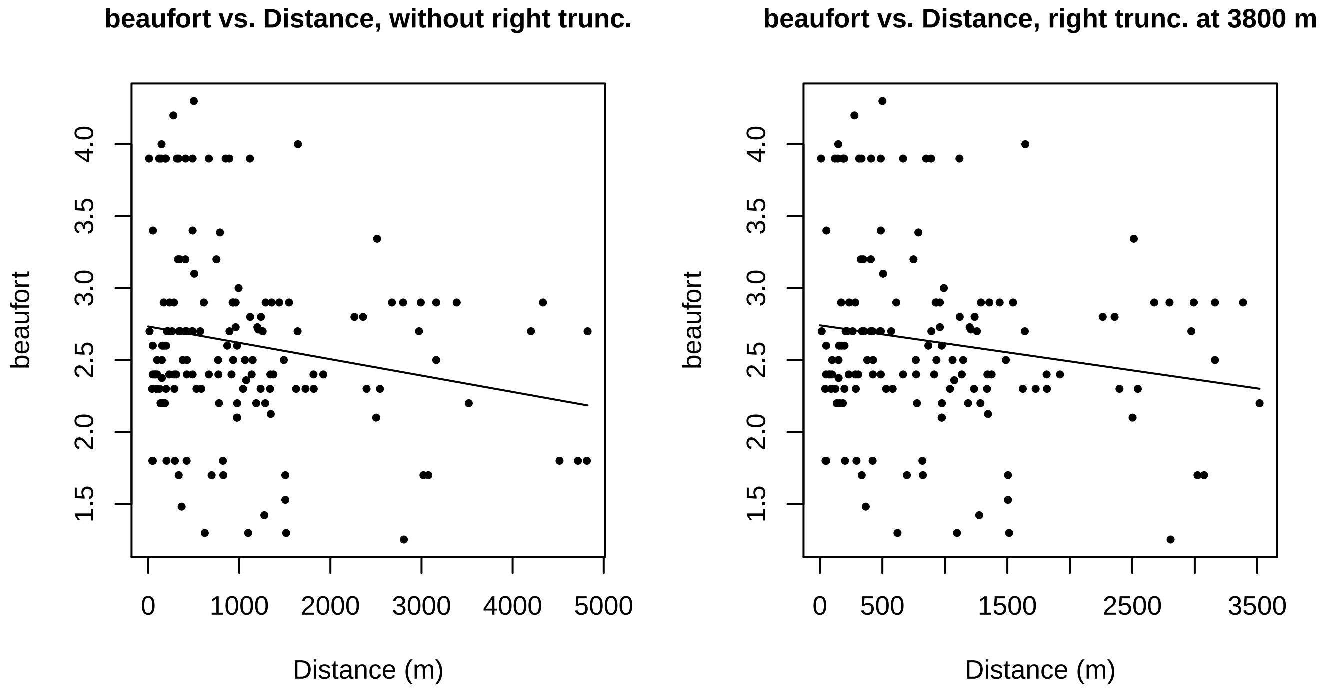

Figure 13: Scatterplots showing the relationship between Beaufort sea state and perpendicular sighting distance, for all sightings (left) and only those not right truncated (right). The line is a simple linear regression.

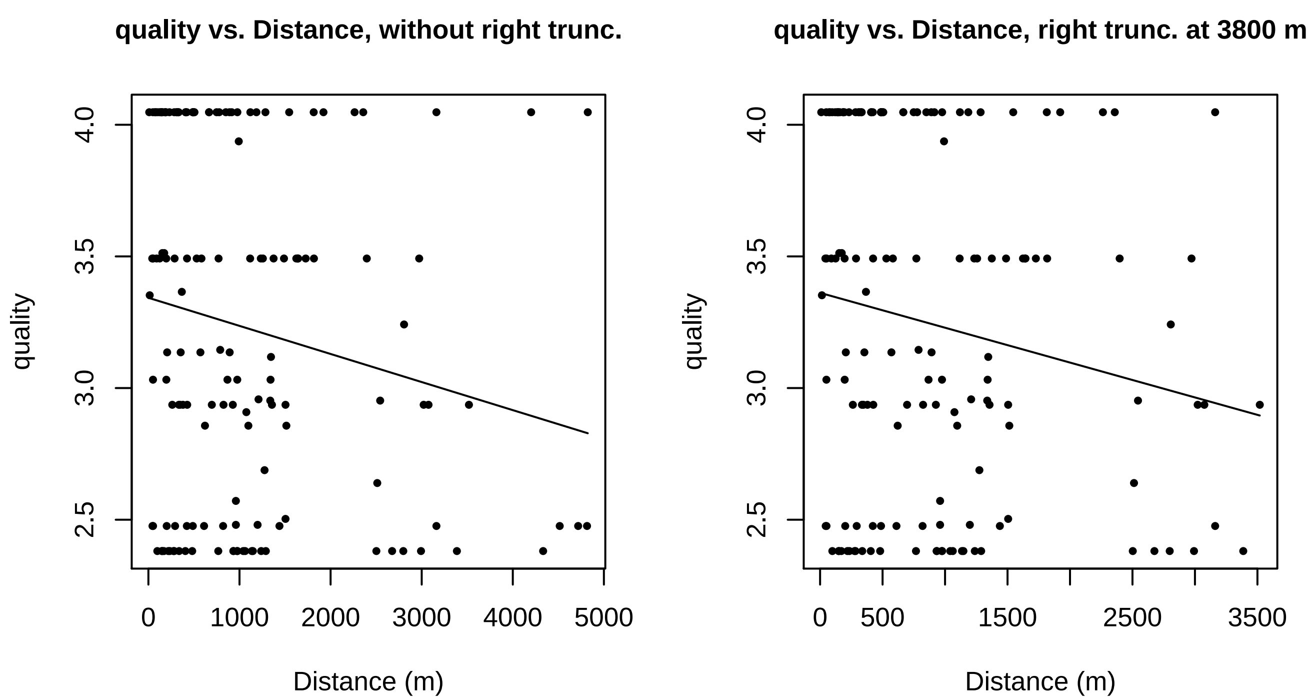

Figure 14: Scatterplots showing the relationship between the survey-specific index of the quality of observation conditions and perpendicular sighting distance, for all sightings (left) and only those not right truncated (right). Low values of the quality index correspond to better observation conditions. The line is a simple linear regression.

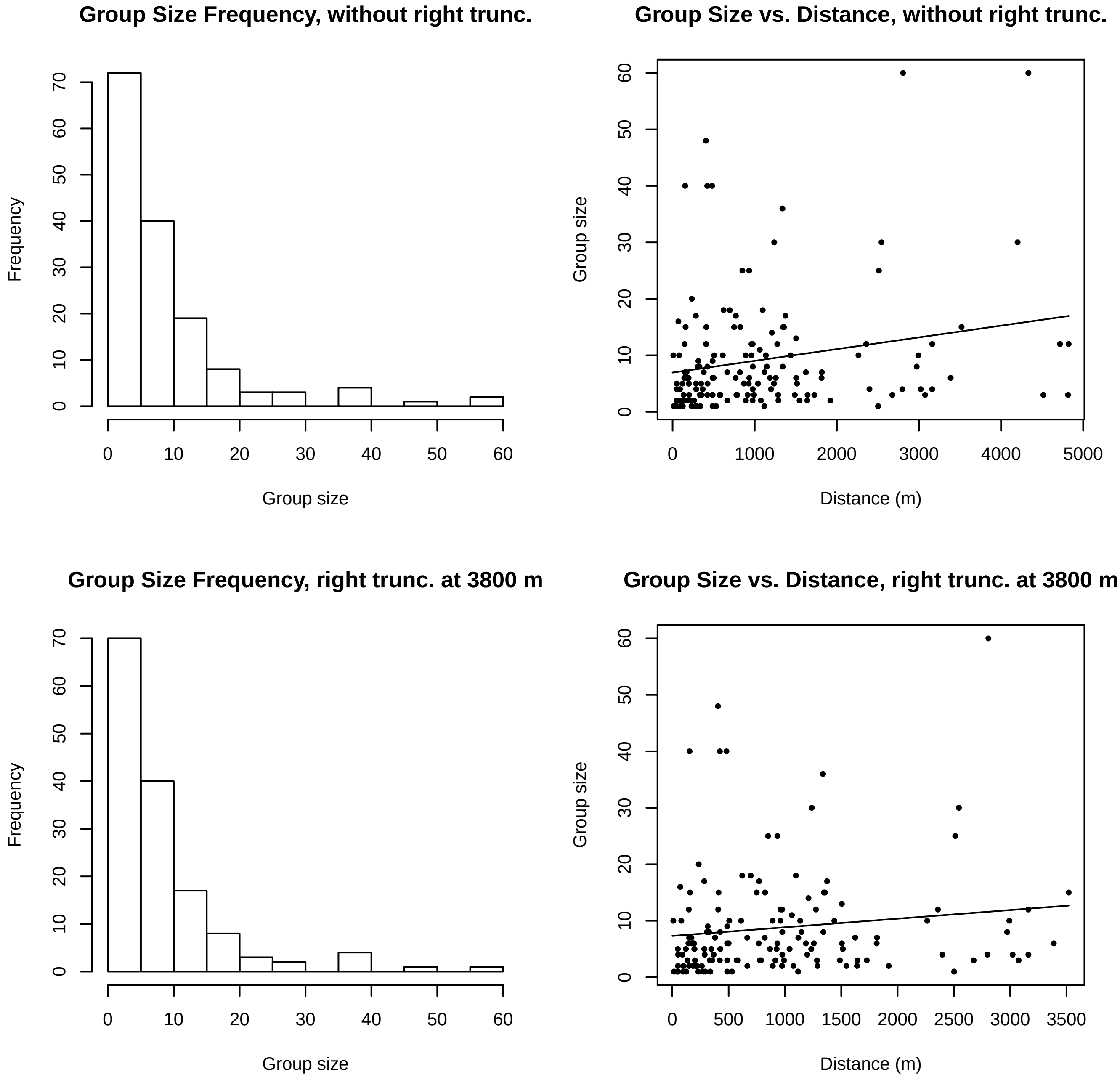

Figure 15: Histograms showing group size frequency and scatterplots showing the relationship between group size and perpendicular sighting distance, for all sightings (top row) and only those not right truncated (bottom row). In the scatterplot, the line is a simple linear regression.

NEFSC Endeavor

The sightings were right truncated at 4000m.

Covariate	Description
beaufort	Beaufort sea state.
quality	Survey-specific index of the quality of observation conditions, utilizing relevant factors other than Beaufort sea state (see methods).
size	Estimated size (number of individuals) of the sighted group.

Table 8: Covariates tested in candidate “multi-covariate distance sampling” (MCDS) detection functions.

Key	Adjustment	Order	Covariates	Succeeded	Δ AIC	Mean ESHW (m)
hr			beaufort	Yes	0.00	1947
hr			beaufort, size	Yes	2.00	1946
hn			beaufort	Yes	5.37	2171
hn	cos	3		Yes	6.90	1794
hn	cos	2		Yes	7.01	1854
hr				Yes	7.10	1716
hn				Yes	7.54	2166
hr	poly	4		Yes	7.95	1647
hr			size	Yes	8.98	1723
hr	poly	2		Yes	9.10	1716
hn	herm	4		Yes	9.40	2157
hn			quality	Yes	9.46	2166
hn			size	Yes	10.08	2237
hn			quality, size	Yes	12.08	2235
hr			quality	No		
hr			beaufort, quality	No		
hn			beaufort, quality	No		
hn			beaufort, size	No		
hr			quality, size	No		
hr			beaufort, quality, size	No		
hn			beaufort, quality, size	No		

Table 9: Candidate detection functions for NEFSC Endeavor. The first one listed was selected for the density model.

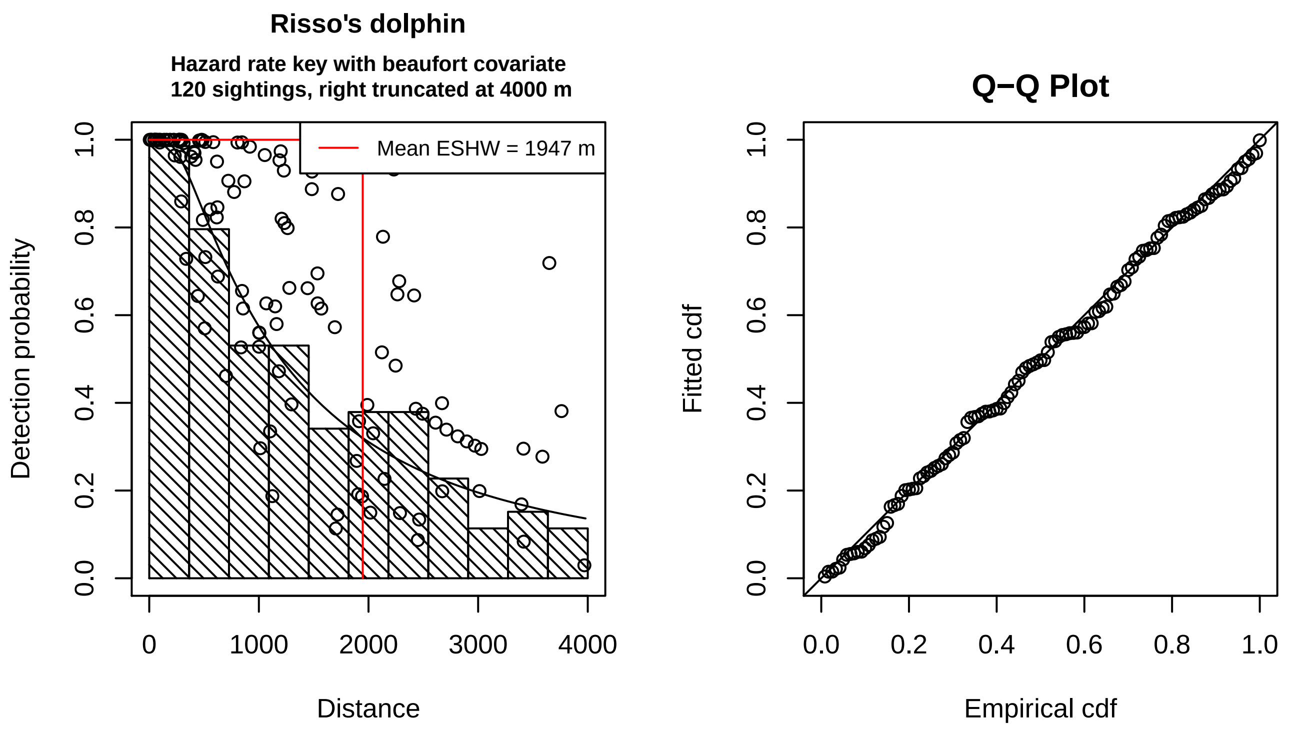

Figure 16: Detection function for NEFSC Endeavor that was selected for the density model

Statistical output for this detection function:

```
Summary for ds object
Number of observations :  120
Distance range         :  0  -  4000
AIC                    :  1940.546

Detection function:
 Hazard-rate key function

Detection function parameters
Scale Coefficients:
              estimate        se
(Intercept)  8.5401313 0.5526999
beaufort    -0.6061736 0.2167812

Shape parameters:
             estimate       se
(Intercept) 0.4240092 0.235498

                        Estimate          SE        CV
Average p              0.4135049  0.06772153 0.1637744
N in covered region 290.2021091 52.17201987 0.1797782
```

Additional diagnostic plots:

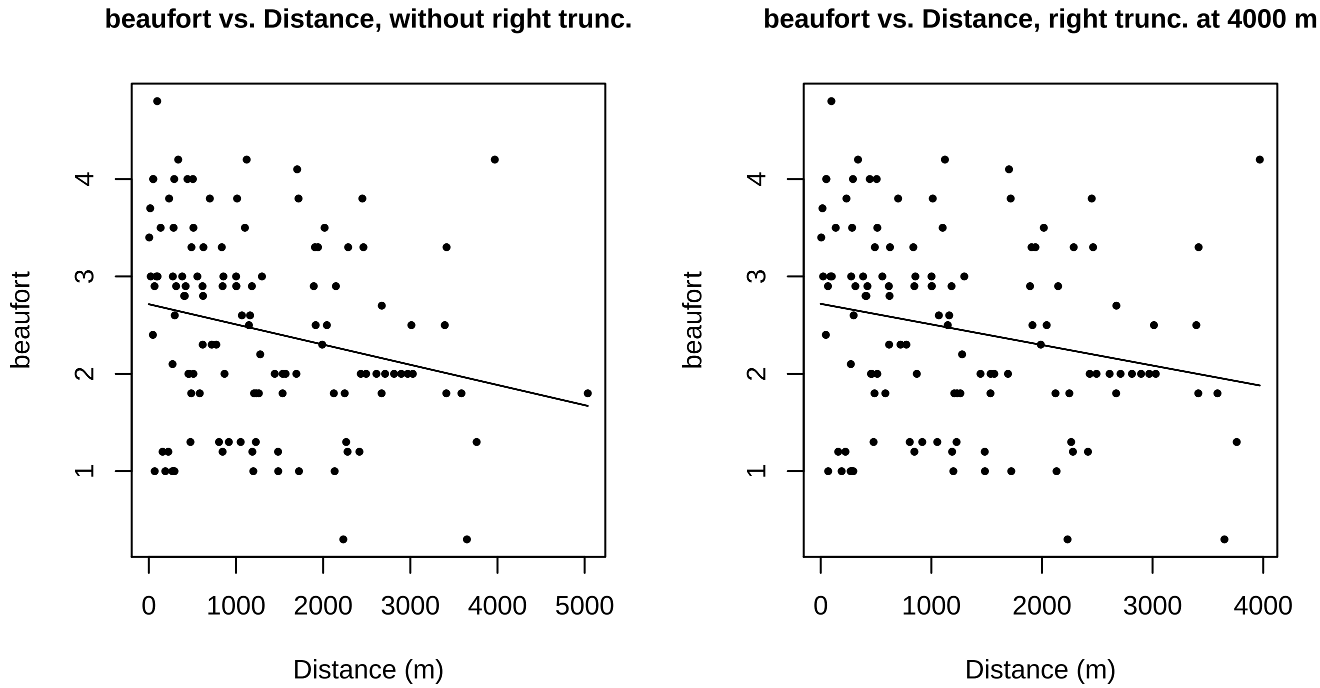

Figure 17: Scatterplots showing the relationship between Beaufort sea state and perpendicular sighting distance, for all sightings (left) and only those not right truncated (right). The line is a simple linear regression.

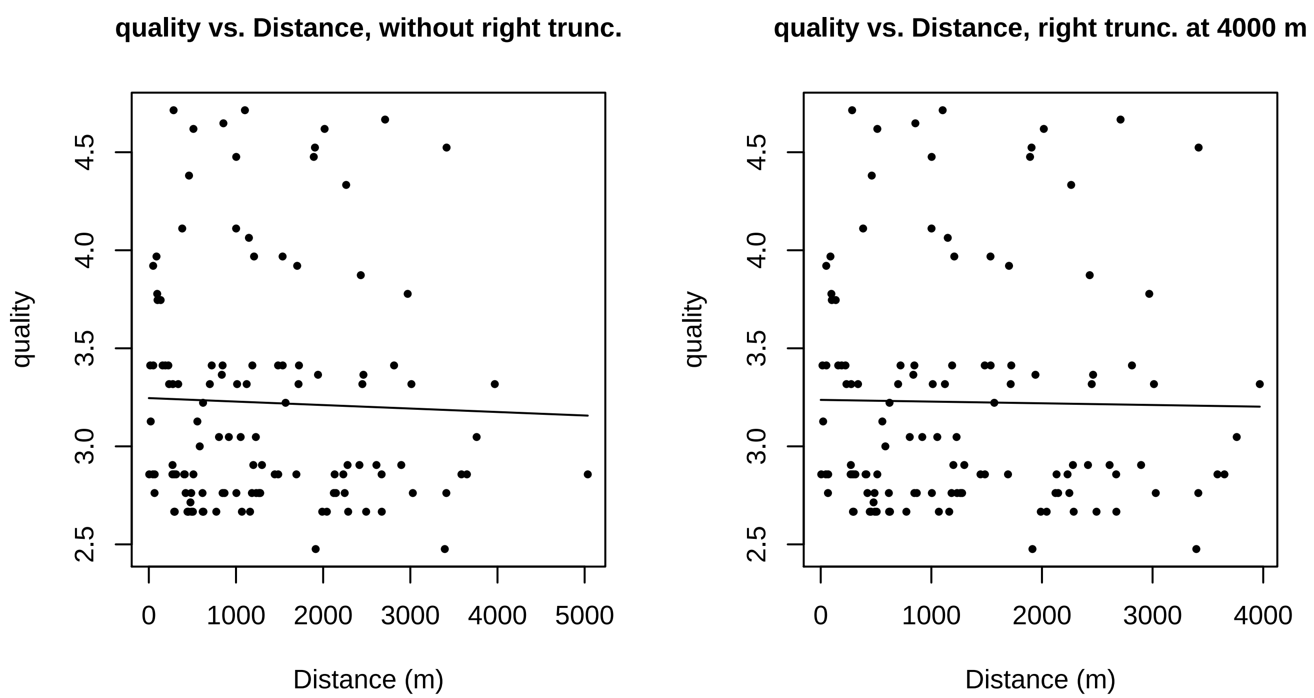

Figure 18: Scatterplots showing the relationship between the survey-specific index of the quality of observation conditions and perpendicular sighting distance, for all sightings (left) and only those not right truncated (right). Low values of the quality index correspond to better observation conditions. The line is a simple linear regression.

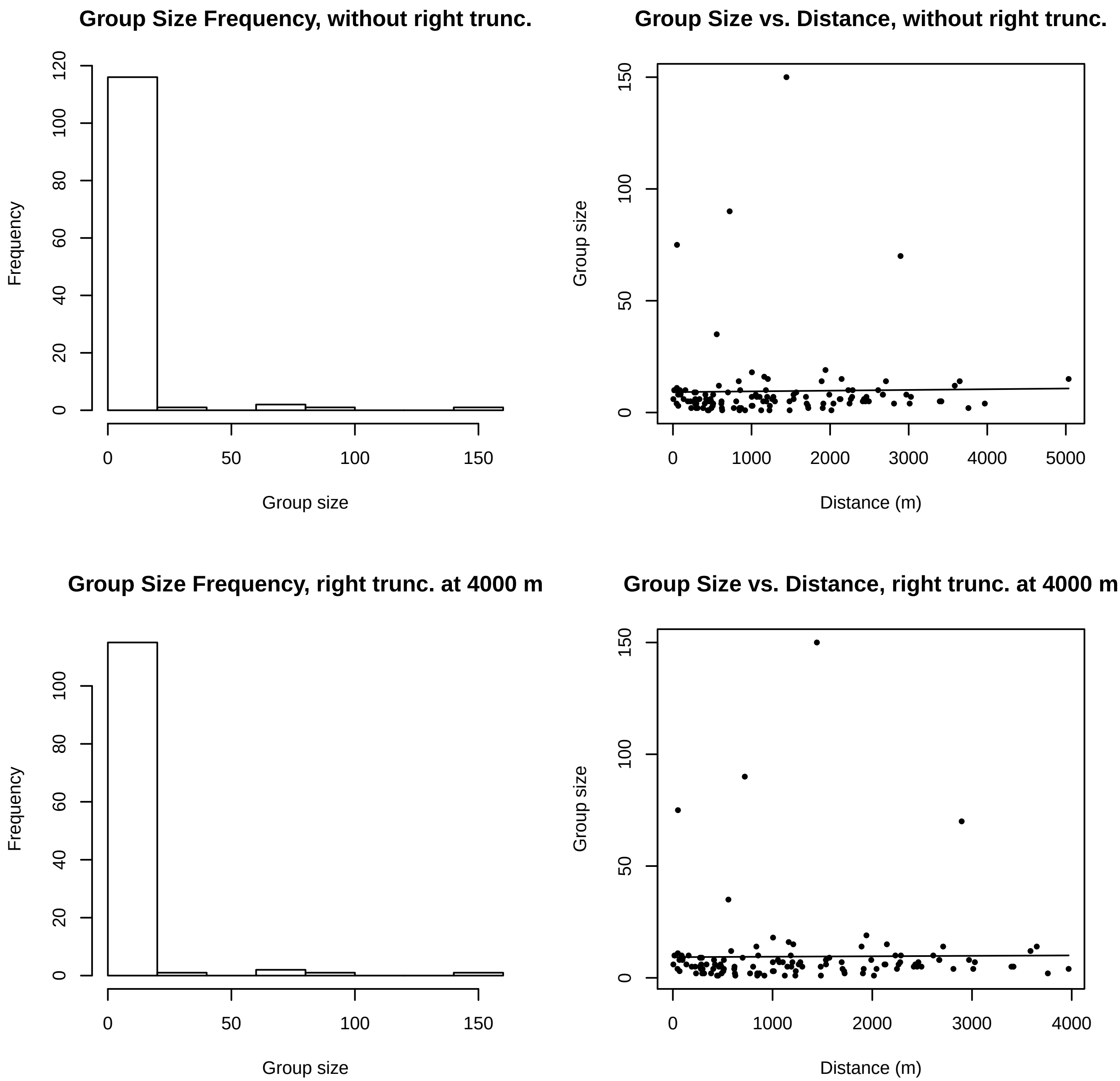

Figure 19: Histograms showing group size frequency and scatterplots showing the relationship between group size and perpendicular sighting distance, for all sightings (top row) and only those not right truncated (bottom row). In the scatterplot, the line is a simple linear regression.

NEFSC Pelican

The sightings were right truncated at 3000m.

Covariate	Description
beaufort	Beaufort sea state.
size	Estimated size (number of individuals) of the sighted group.

Table 10: Covariates tested in candidate "multi-covariate distance sampling" (MCDS) detection functions.

Key	Adjustment	Order	Covariates	Succeeded	Δ AIC	Mean ESHW (m)
hr			beaufort	Yes	0.00	1399
hr				Yes	2.37	1152
hn			beaufort	Yes	2.53	1615
hn	cos	2		Yes	3.15	1228
hr	poly	2		Yes	4.37	1152
hr	poly	4		Yes	4.37	1150
hn				Yes	6.26	1568
hn	cos	3		Yes	6.79	1311
hn	herm	4		Yes	8.04	1563
hr			size	No		
hn			size	No		
hr			beaufort, size	No		
hn			beaufort, size	No		

Table 11: Candidate detection functions for NEFSC Pelican. The first one listed was selected for the density model.

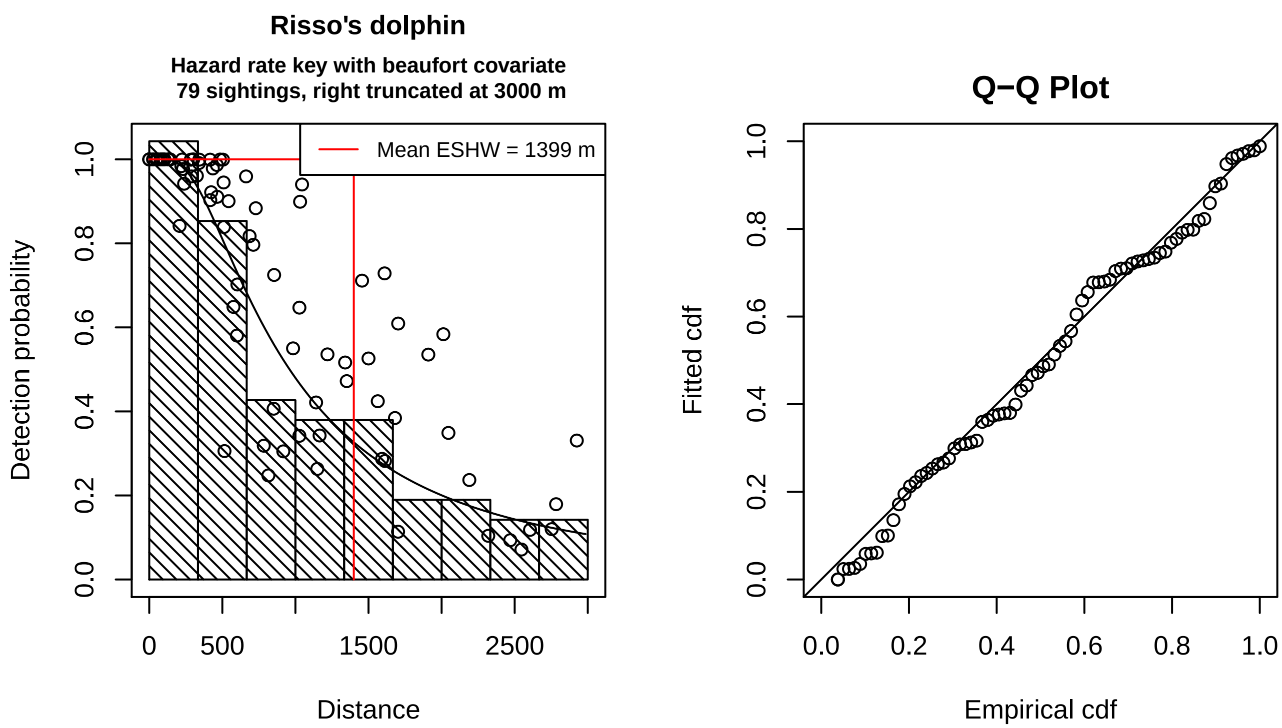

Figure 20: Detection function for NEFSC Pelican that was selected for the density model

Statistical output for this detection function:

```
Summary for ds object
```

```
Number of observations :  79
Distance range         :  0  -  3000
AIC                    :  1227.791

Detection function:
 Hazard-rate key function

Detection function parameters
Scale Coefficients:
              estimate        se
(Intercept)  8.3006234 0.7109885
beaufort    -0.6395938 0.2978920

Shape parameters:
             estimate        se
(Intercept) 0.5779257 0.2819418

                      Estimate          SE        CV
Average p             0.416197  0.07362142 0.1768908
N in covered region 189.813955 37.63690746 0.1982831
```

Additional diagnostic plots:

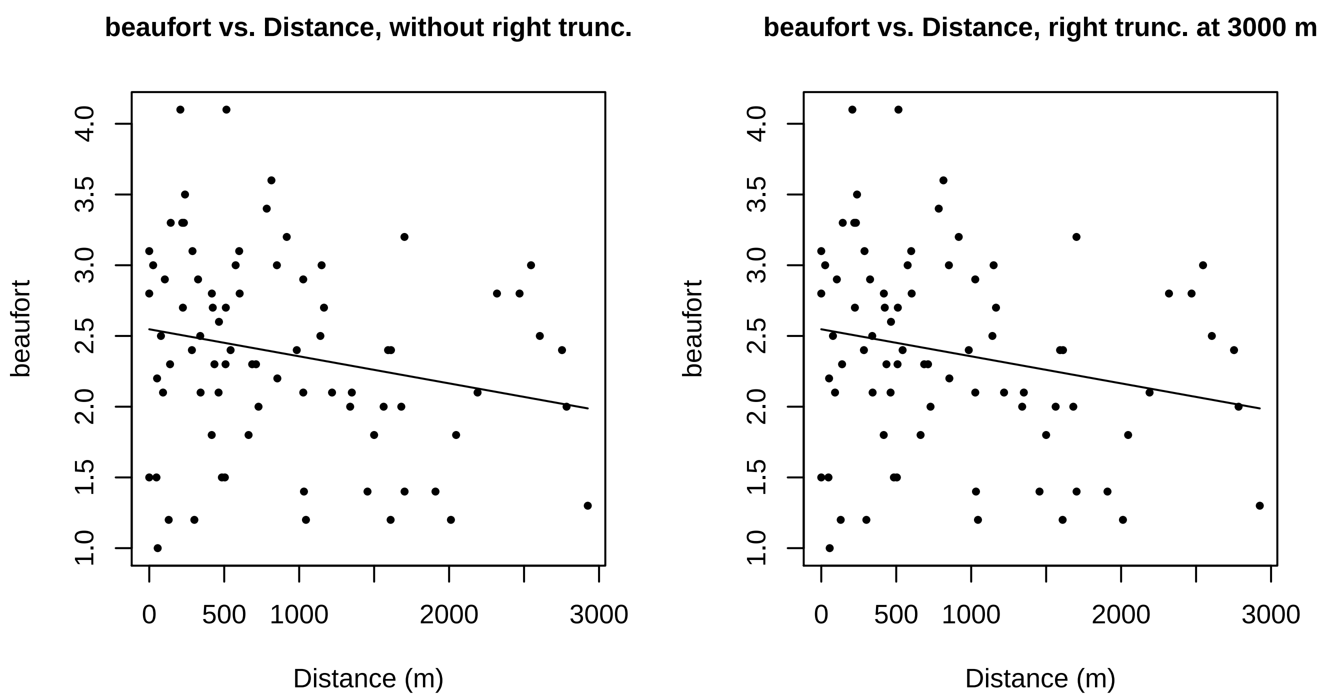

Figure 21: Scatterplots showing the relationship between Beaufort sea state and perpendicular sighting distance, for all sightings (left) and only those not right truncated (right). The line is a simple linear regression.

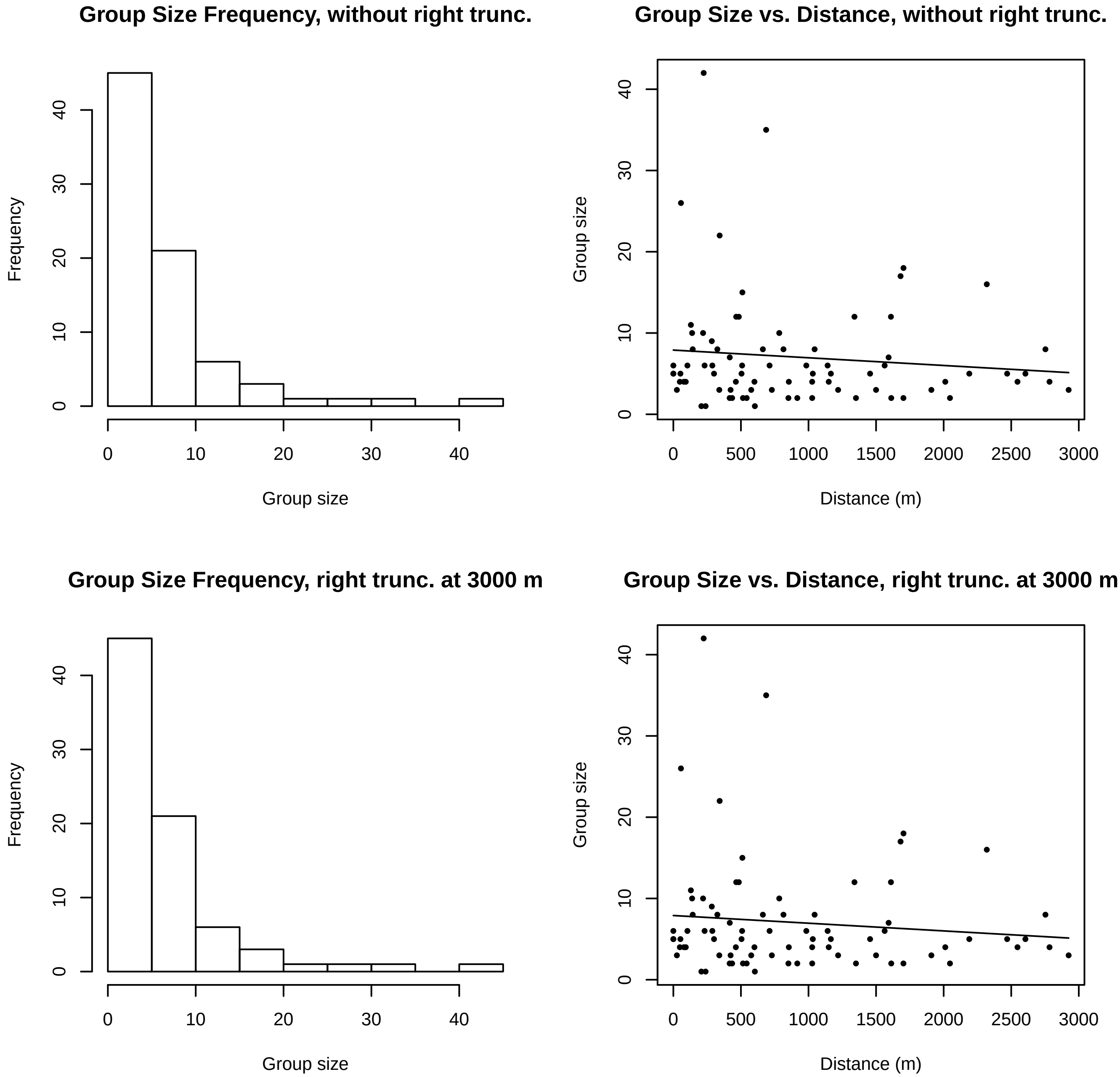

Figure 22: Histograms showing group size frequency and scatterplots showing the relationship between group size and perpendicular sighting distance, for all sightings (top row) and only those not right truncated (bottom row). In the scatterplot, the line is a simple linear regression.

SEFSC Oregon II

The sightings were right truncated at 6000m.

Covariate	Description
beaufort	Beaufort sea state.
quality	Survey-specific index of the quality of observation conditions, utilizing relevant factors other than Beaufort sea state (see methods).
size	Estimated size (number of individuals) of the sighted group.

Table 12: Covariates tested in candidate “multi-covariate distance sampling” (MCDS) detection functions.

Key	Adjustment	Order	Covariates	Succeeded	Δ AIC	Mean ESHW (m)
hr			beaufort, quality, size	Yes	0.00	1793
hr			quality, size	Yes	0.02	1675
hn	cos	3		Yes	2.49	1568
hr			beaufort, quality	Yes	3.64	1785
hr			quality	Yes	3.82	1700
hr			size	Yes	3.91	1558
hr	poly	4		Yes	3.99	1189
hr			beaufort, size	Yes	5.17	1601
hr				Yes	7.62	1550
hr			beaufort	Yes	8.25	1640
hr	poly	2		Yes	9.62	1550
hn			beaufort, quality, size	Yes	9.98	2296
hn	cos	2		Yes	10.88	1878
hn			beaufort, size	Yes	12.56	2322
hn			beaufort, quality	Yes	12.88	2319
hn			quality, size	Yes	16.18	2308
hn			size	Yes	17.93	2325
hn			beaufort	Yes	18.16	2324
hn			quality	Yes	19.68	2316
hn				Yes	22.59	2330
hn	herm	4		Yes	24.42	2326

Table 13: Candidate detection functions for SEFSC Oregon II. The first one listed was selected for the density model.

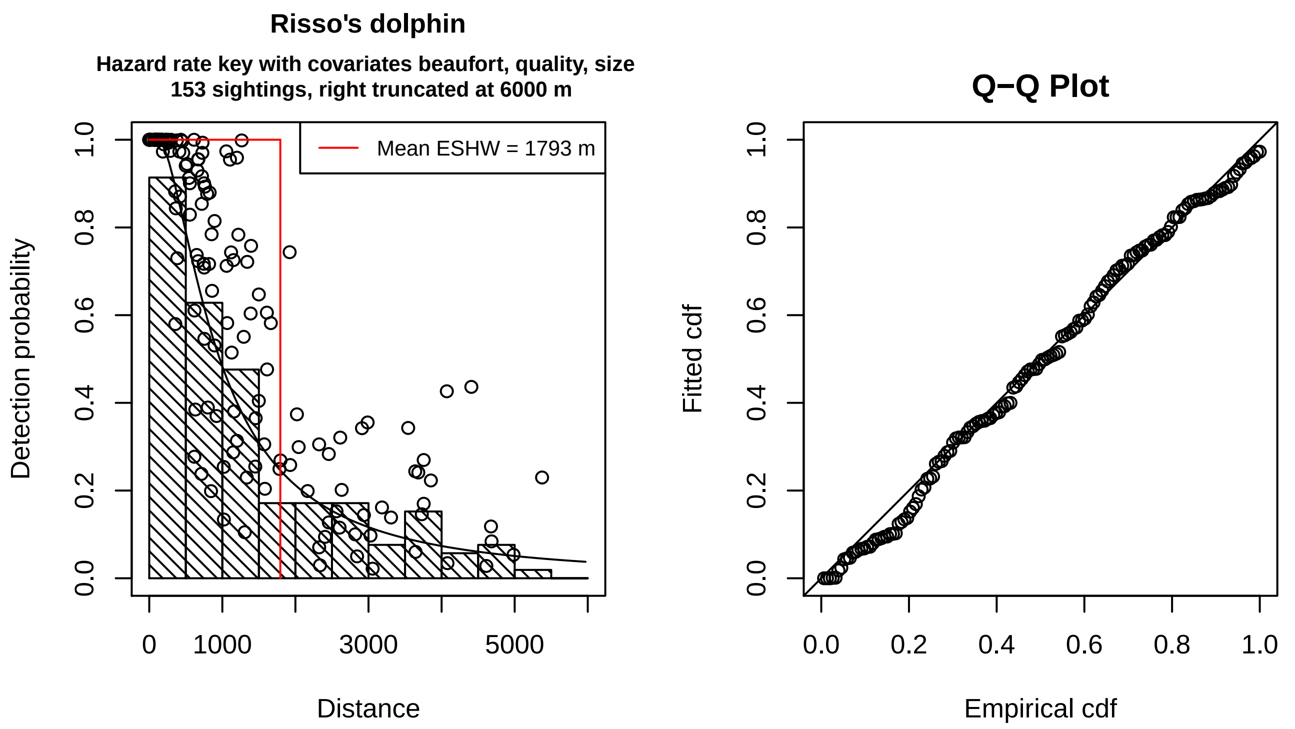

Figure 23: Detection function for SEFSC Oregon II that was selected for the density model

Statistical output for this detection function:

```
Summary for ds object
Number of observations :  153
Distance range         :  0  -  6000
AIC                    :  2502.88

Detection function:
 Hazard-rate key function

Detection function parameters
Scale Coefficients:
              estimate         se
(Intercept)  7.1973420 0.40695298
beaufort    -0.1514780 0.09856986
quality     -0.2685644 0.10211931
size         0.3420213 0.12661513

Shape parameters:
             estimate        se
(Intercept) 0.5816654 0.1476978

                       Estimate          SE        CV
Average p             0.2427283  0.03250746 0.1339253
N in covered region 630.3343107 96.11834299 0.1524879
```

Additional diagnostic plots:

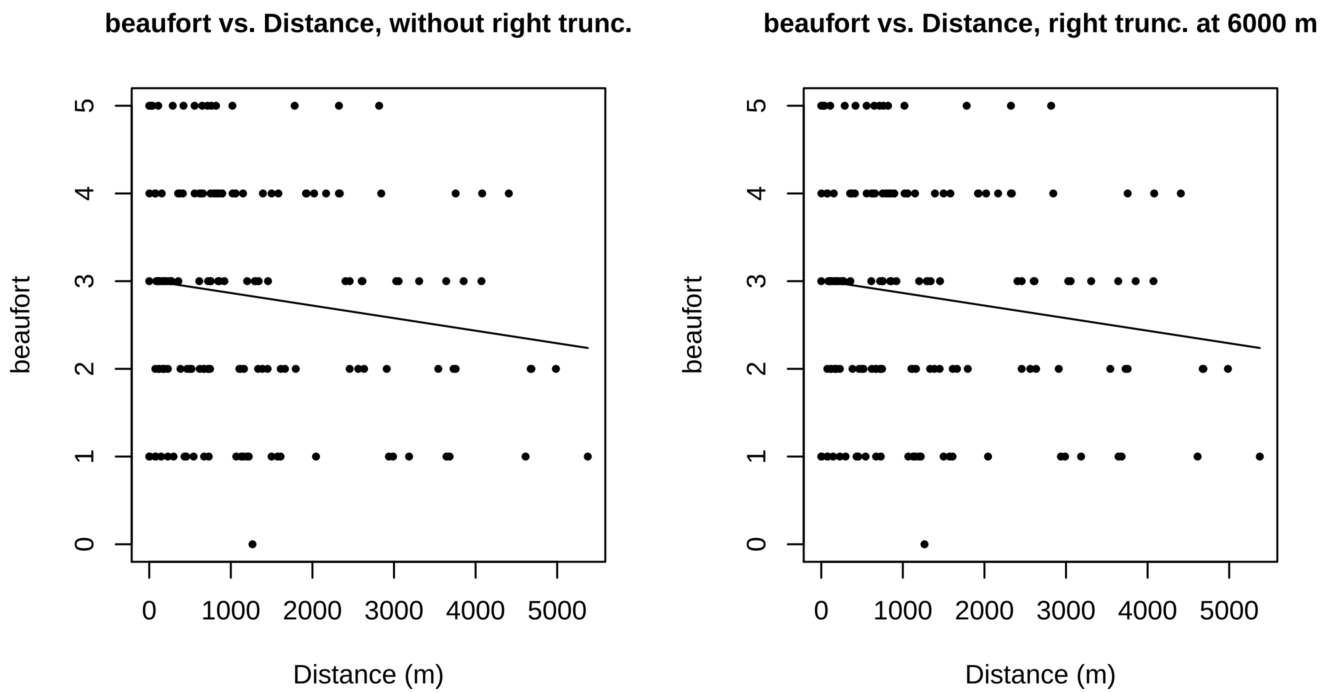

Figure 24: Scatterplots showing the relationship between Beaufort sea state and perpendicular sighting distance, for all sightings (left) and only those not right truncated (right). The line is a simple linear regression.

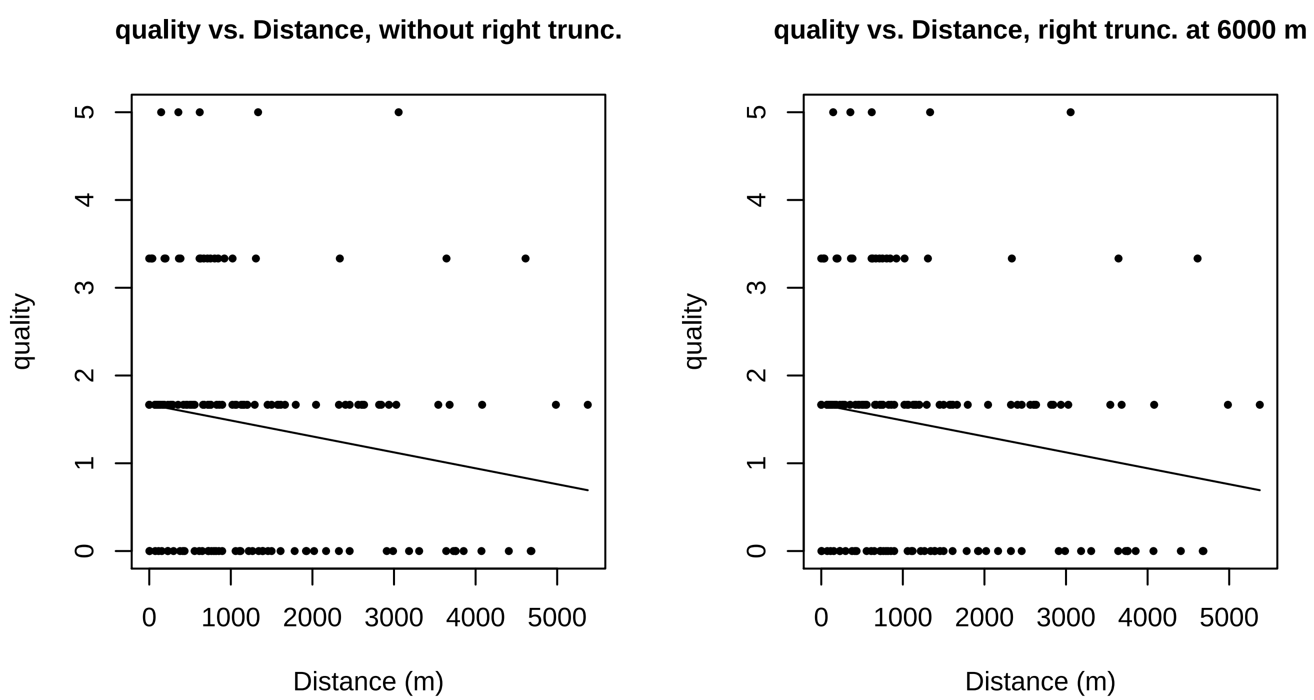

Figure 25: Scatterplots showing the relationship between the survey-specific index of the quality of observation conditions and perpendicular sighting distance, for all sightings (left) and only those not right truncated (right). Low values of the quality index correspond to better observation conditions. The line is a simple linear regression.

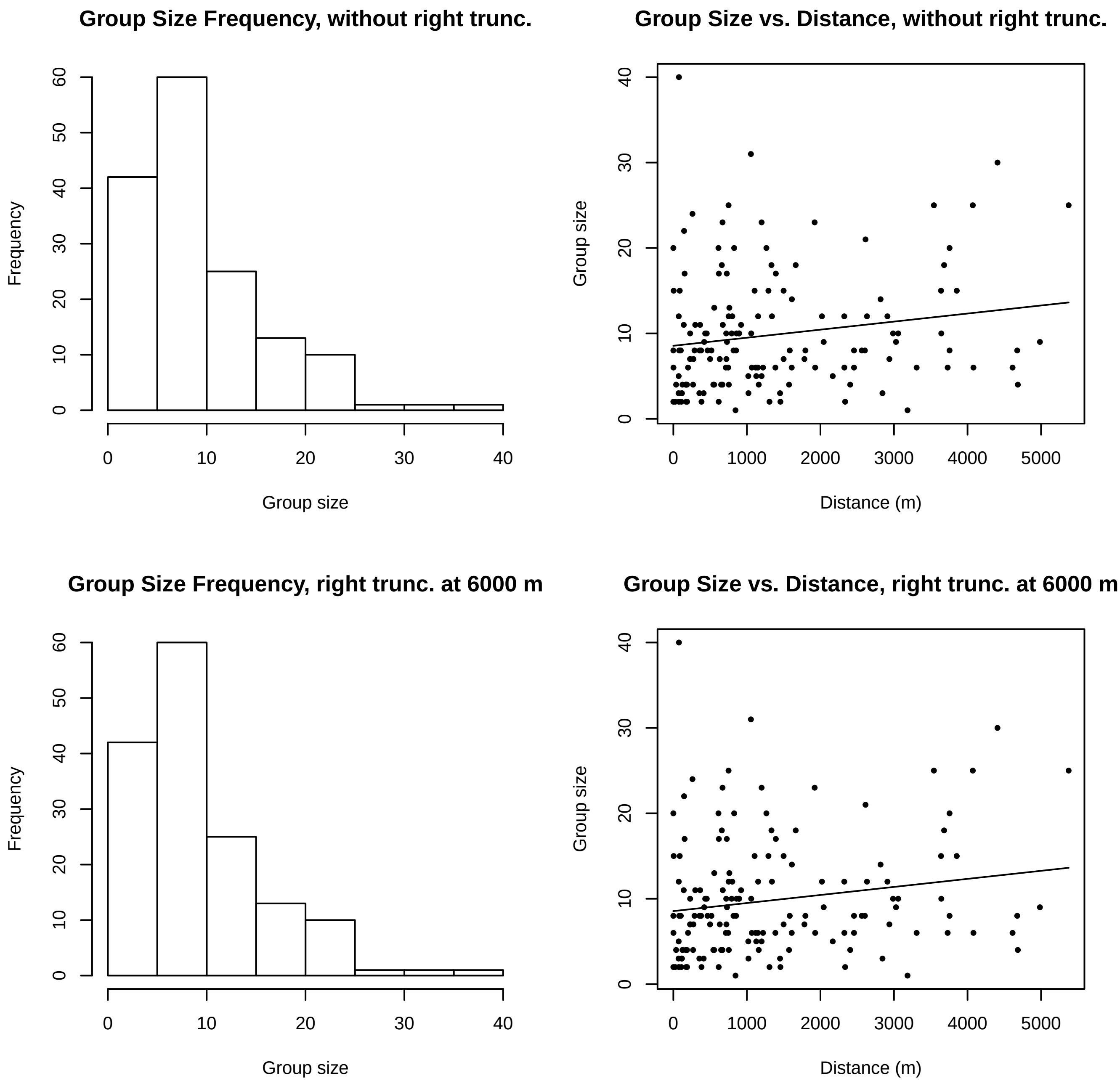

Figure 26: Histograms showing group size frequency and scatterplots showing the relationship between group size and perpendicular sighting distance, for all sightings (top row) and only those not right truncated (bottom row). In the scatterplot, the line is a simple linear regression.

High Platforms

The sightings were right truncated at 6100m.

Covariate	Description
beaufort	Beaufort sea state.
size	Estimated size (number of individuals) of the sighted group.

Table 14: Covariates tested in candidate "multi-covariate distance sampling" (MCDS) detection functions.

Key	Adjustment	Order	Covariates	Succeeded	Δ AIC	Mean ESHW (m)
hr			size	Yes	0.00	2426
hn	cos	2		Yes	0.50	2304
hr				Yes	1.46	2132
hr			beaufort, size	Yes	1.77	2449
hr			beaufort	Yes	2.20	2276
hr	poly	4		Yes	3.43	2095
hr	poly	2		Yes	3.46	2132
hn	cos	3		Yes	10.14	2553
hn				Yes	11.24	3106
hn			beaufort	Yes	11.25	3110
hn			size	Yes	12.15	3141
hn			beaufort, size	Yes	12.90	3119
hn	herm	4		Yes	12.90	3095

Table 15: Candidate detection functions for High Platforms. The first one listed was selected for the density model.

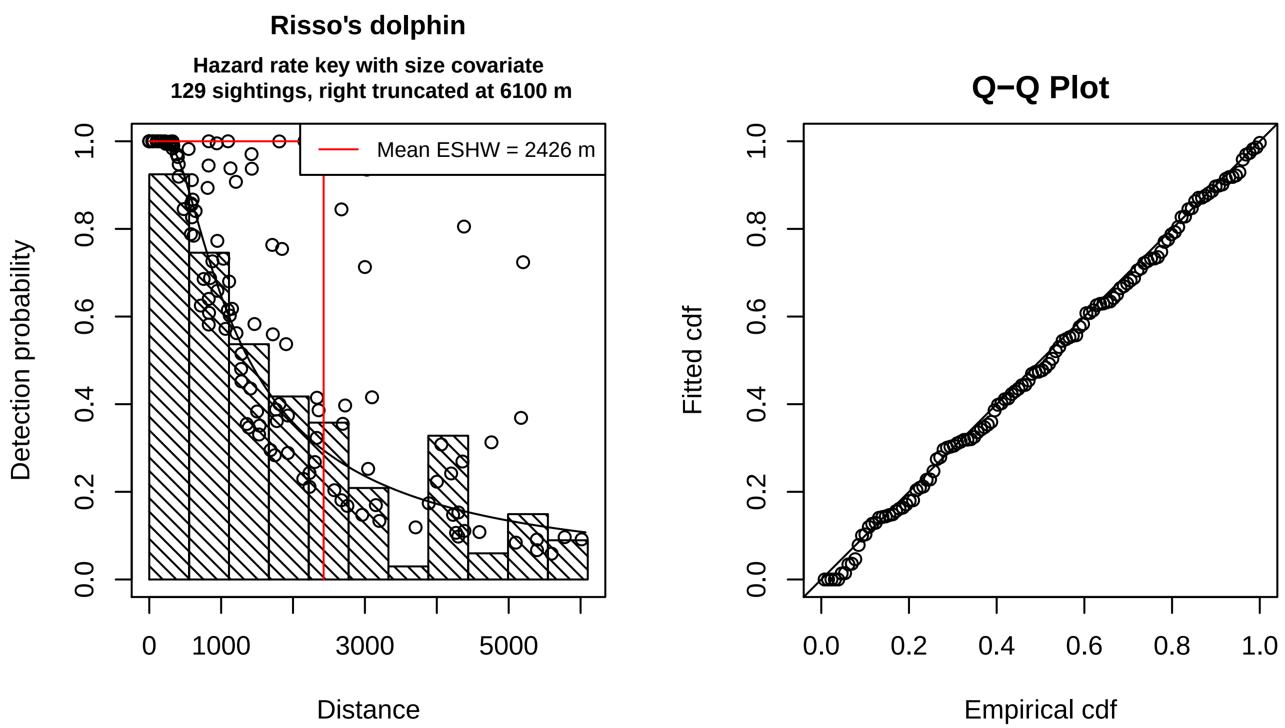

Figure 27: Detection function for High Platforms that was selected for the density model

Statistical output for this detection function:

```
Summary for ds object
```

```
Number of observations :  129
Distance range         :  0  -  6100
AIC                    :  2180.94

Detection function:
 Hazard-rate key function

Detection function parameters
Scale Coefficients:
             estimate        se
(Intercept) 6.4483550 0.4532456
size        0.7370187 0.3673670

Shape parameters:
             estimate        se
(Intercept) 0.3317178 0.1958107

                       Estimate           SE        CV
Average p             0.3498014  0.05748444 0.1643345
N in covered region 368.7807069 66.39806619 0.1800476
```

Additional diagnostic plots:

Figure 28: Scatterplots showing the relationship between Beaufort sea state and perpendicular sighting distance, for all sightings (left) and only those not right truncated (right). The line is a simple linear regression.

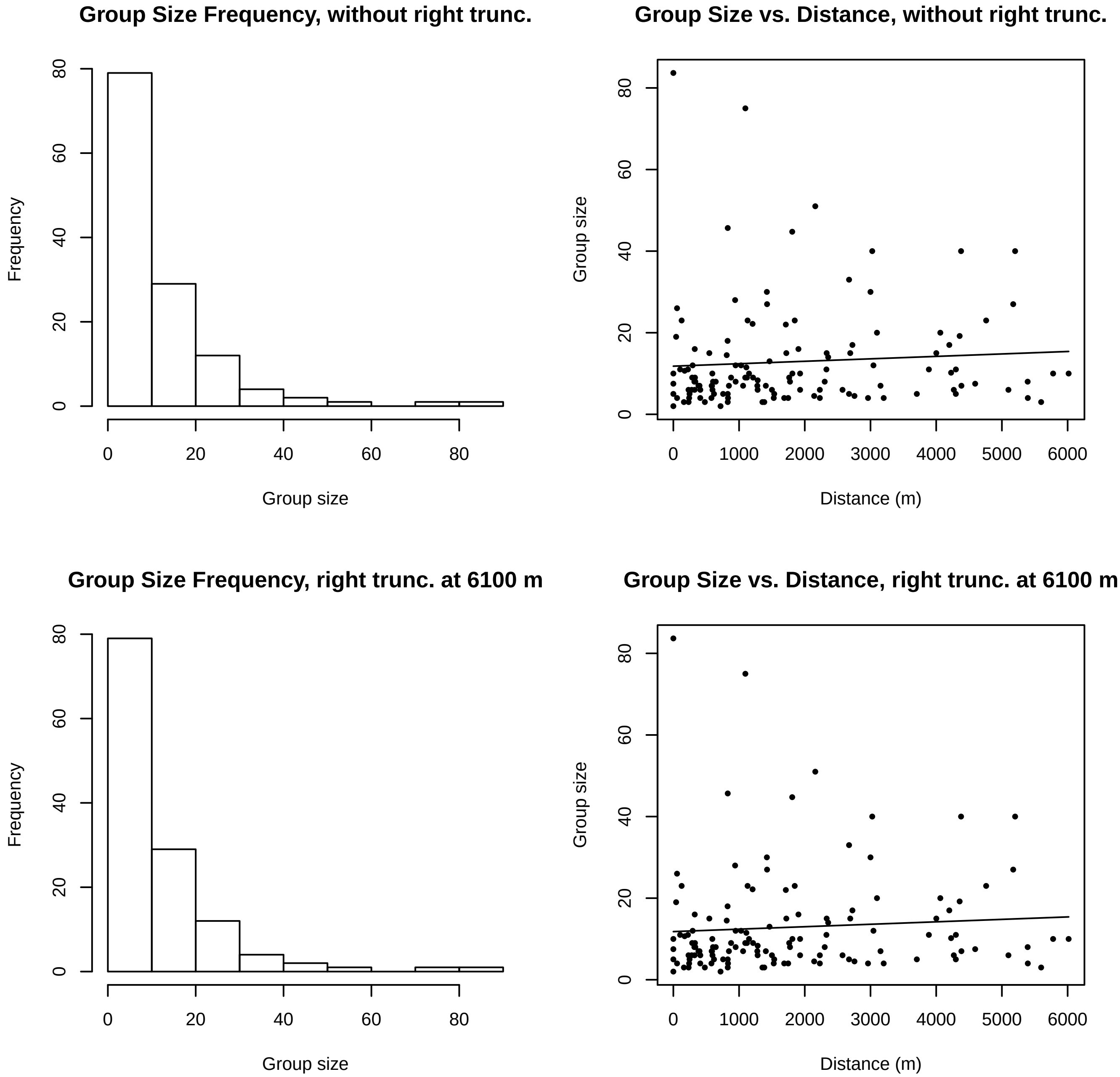

Figure 29: Histograms showing group size frequency and scatterplots showing the relationship between group size and perpendicular sighting distance, for all sightings (top row) and only those not right truncated (bottom row). In the scatterplot, the line is a simple linear regression.

Gordon Gunter Quality Covariate Available

The sightings were right truncated at 6100m.

Covariate	Description
beaufort	Beaufort sea state.
quality	Survey-specific index of the quality of observation conditions, utilizing relevant factors other than Beaufort sea state (see methods).
size	Estimated size (number of individuals) of the sighted group.

Table 16: Covariates tested in candidate “multi-covariate distance sampling” (MCDS) detection functions.

Key	Adjustment	Order	Covariates	Succeeded	Δ AIC	Mean ESHW (m)
hr			quality, size	Yes	0.00	2676
hr			size	Yes	0.37	2549
hr			quality	Yes	0.80	2472
hn	cos	2		Yes	1.45	2360
hr			beaufort, quality, size	Yes	1.83	2702
hr			beaufort, quality	Yes	1.86	2551
hr			beaufort, size	Yes	2.03	2600
hr				Yes	2.47	2168
hr			beaufort	Yes	2.82	2430
hr	poly	4		Yes	4.41	2091
hr	poly	2		Yes	4.47	2168
hn	cos	3		Yes	10.26	2636
hn			beaufort	Yes	10.63	3185
hn				Yes	10.93	3178
hn			size	Yes	11.58	3240
hn			quality	Yes	11.84	3203
hn			beaufort, size	Yes	12.23	3204
hn			beaufort, quality	Yes	12.25	3199
hn			quality, size	Yes	12.42	3268
hn	herm	4		Yes	12.62	3166
hn			beaufort, quality, size	Yes	13.61	3243

Table 17: Candidate detection functions for Gordon Gunter Quality Covariate Available. The first one listed was selected for the density model.

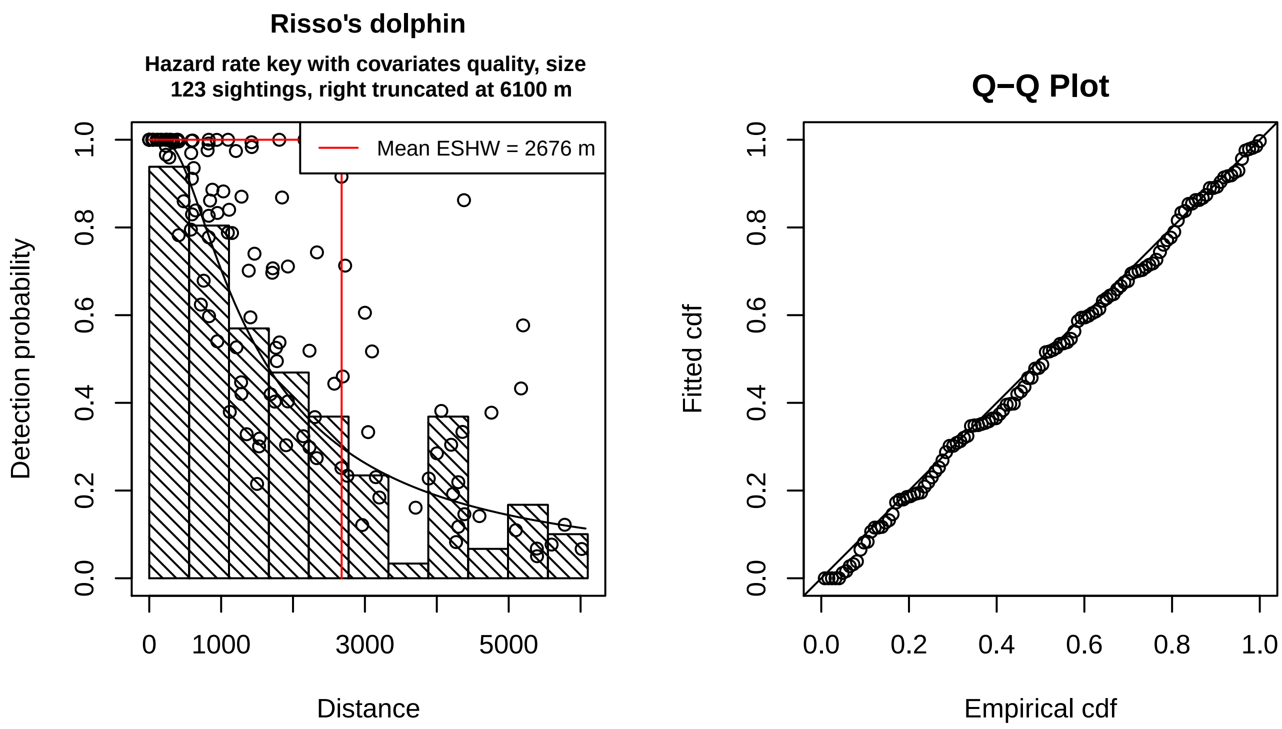

Figure 30: Detection function for Gordon Gunter Quality Covariate Available that was selected for the density model

Statistical output for this detection function:

```
Summary for ds object
Number of observations :  123
Distance range         :  0  -  6100
AIC                    :  2083.318

Detection function:
 Hazard-rate key function

Detection function parameters
Scale Coefficients:
              estimate        se
(Intercept)  7.2066038 0.4736353
quality     -0.2232128 0.1419035
size         0.6553273 0.3184299

Shape parameters:
             estimate        se
(Intercept) 0.4285349 0.2031903

                       Estimate          SE        CV
Average p             0.3747365  0.06095815 0.1626694
N in covered region 328.2306433 58.77494296 0.1790660
```

Additional diagnostic plots:

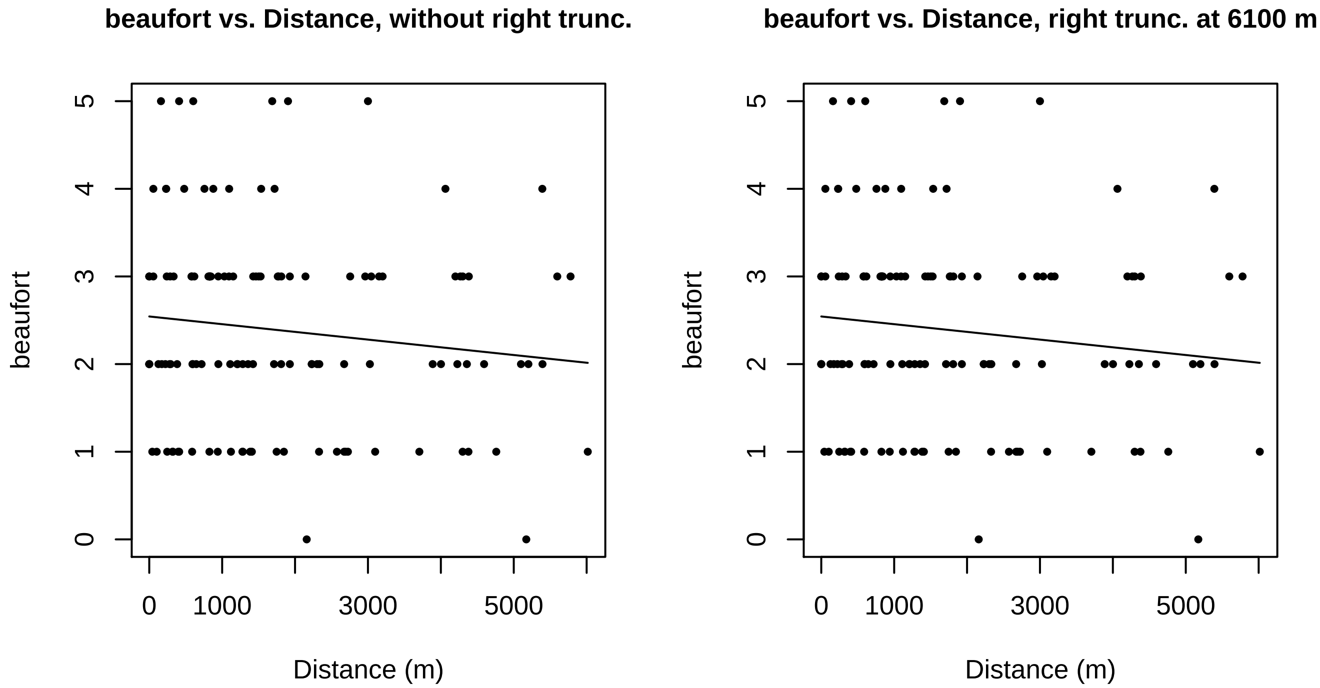

Figure 31: Scatterplots showing the relationship between Beaufort sea state and perpendicular sighting distance, for all sightings (left) and only those not right truncated (right). The line is a simple linear regression.

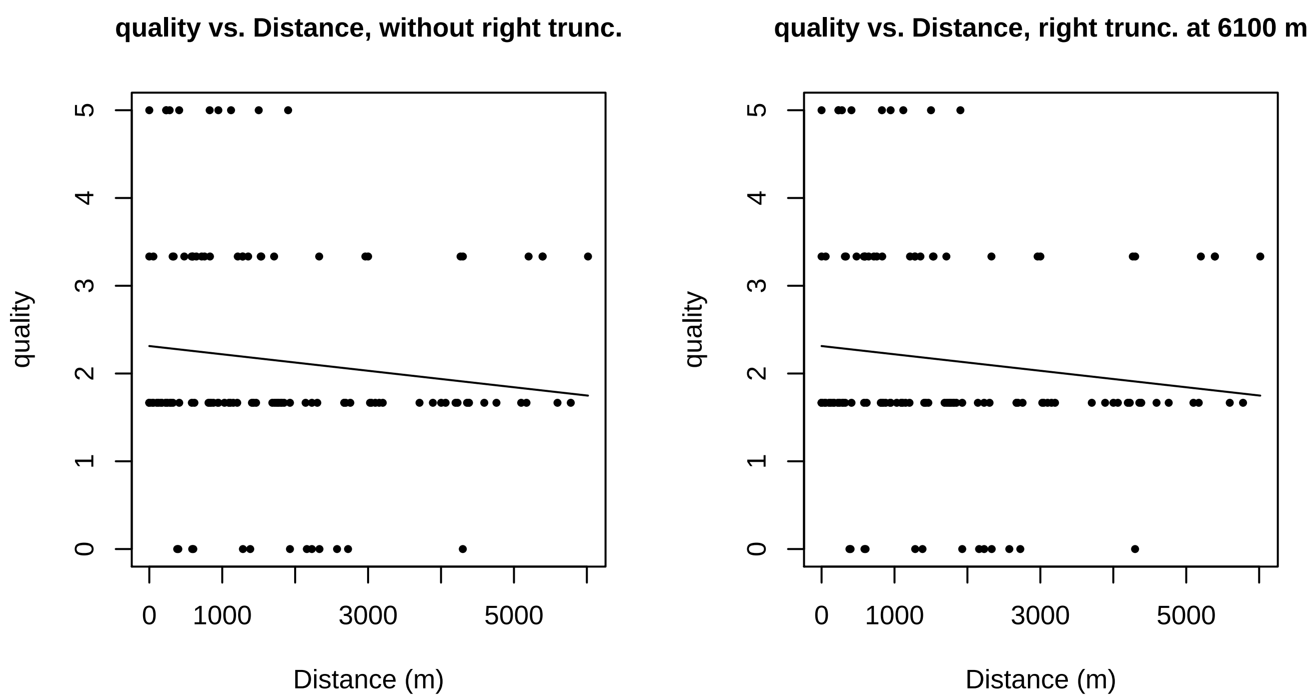

Figure 32: Scatterplots showing the relationship between the survey-specific index of the quality of observation conditions and perpendicular sighting distance, for all sightings (left) and only those not right truncated (right). Low values of the quality index correspond to better observation conditions. The line is a simple linear regression.

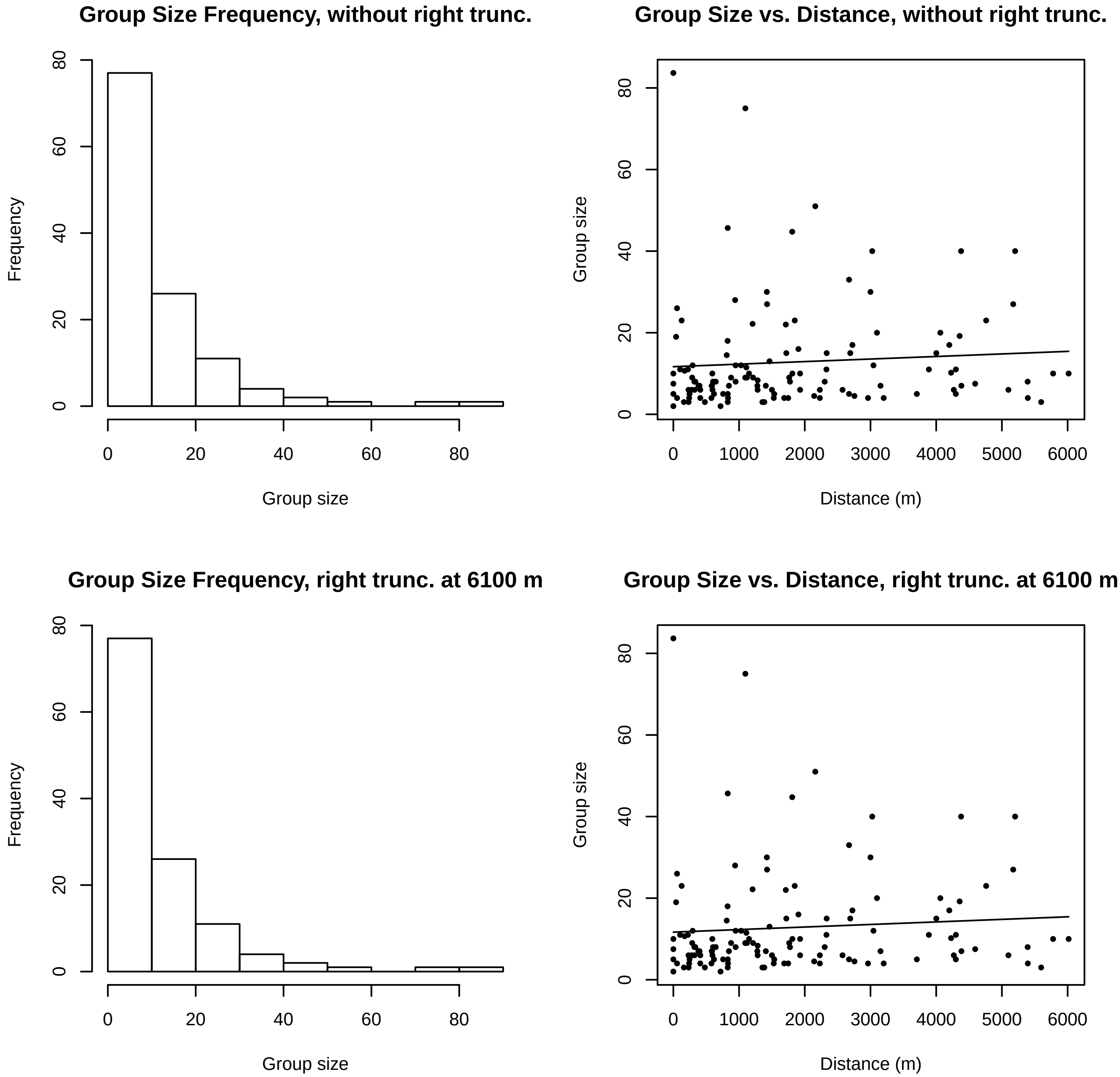

Figure 33: Histograms showing group size frequency and scatterplots showing the relationship between group size and perpendicular sighting distance, for all sightings (top row) and only those not right truncated (bottom row). In the scatterplot, the line is a simple linear regression.

Naked Eye Surveys

Because this taxon was sighted too infrequently to fit a detection function to its sightings alone, we fit a detection function to the pooled sightings of several other species that we believed would exhibit similar detectability. These "proxy species" are listed below.

Reported By Observer	Common Name	n
Delphinus capensis	Long-beaked common dolphin	0
Delphinus delphis	Short-beaked common dolphin	255

Delphinus delphis/Lagenorhynchus acutus	Short-beaked common or Atlantic white-sided dolphin	0
Delphinus delphis/Stenella	Short-beaked common dolphin or Stenella spp.	0
Delphinus delphis/Stenella coeruleoalba	Short-beaked common or striped dolphin	72
Grampus griseus	Risso's dolphin	9
Grampus griseus/Tursiops truncatus	Risso's or Bottlenose dolphin	0
Lagenodelphis hosei	Fraser's dolphin	0
Lagenorhynchus acutus	Atlantic white-sided dolphin	102
Lagenorhynchus albirostris	White-beaked dolphin	36
Lagenorhynchus albirostris/Lagenorhynchus acutus	White-beaked or white-sided dolphin	4
Stenella	Unidentified Stenella	0
Stenella attenuata	Pantropical spotted dolphin	0
Stenella attenuata/frontalis	Pantropical or Atlantic spotted dolphin	0
Stenella clymene	Clymene dolphin	0
Stenella coeruleoalba	Striped dolphin	48
Stenella frontalis	Atlantic spotted dolphin	0
Stenella frontalis/Tursiops truncatus	Atlantic spotted or Bottlenose dolphin	0
Stenella longirostris	Spinner dolphin	0
Steno bredanensis	Rough-toothed dolphin	0
Steno bredanensis/Tursiops truncatus	Bottlenose or rough-toothed dolphin	0
Tursiops truncatus	Bottlenose dolphin	41
Total		567

Table 18: Proxy species used to fit detection functions for Naked Eye Surveys. The number of sightings, n, is before truncation.

The sightings were right truncated at 1000m.

Covariate	Description
beaufort	Beaufort sea state.
size	Estimated size (number of individuals) of the sighted group.

Table 19: Covariates tested in candidate "multi-covariate distance sampling" (MCDS) detection functions.

Key	Adjustment	Order	Covariates	Succeeded	Δ AIC	Mean ESHW (m)
hr			beaufort, size	Yes	0.00	329
hr			beaufort	Yes	5.52	306
hr			size	Yes	7.76	330
hr	poly	2		Yes	8.35	253
hr	poly	4		Yes	11.34	266
hn	cos	2		Yes	14.63	339

hr				Yes	14.95	308
hn	cos	3		Yes	29.74	330
hn			beaufort, size	Yes	33.37	434
hn			size	Yes	39.64	433
hn			beaufort	Yes	47.43	427
hn				Yes	53.26	426
hn	herm	4		Yes	54.28	425

Table 20: Candidate detection functions for Naked Eye Surveys. The first one listed was selected for the density model.

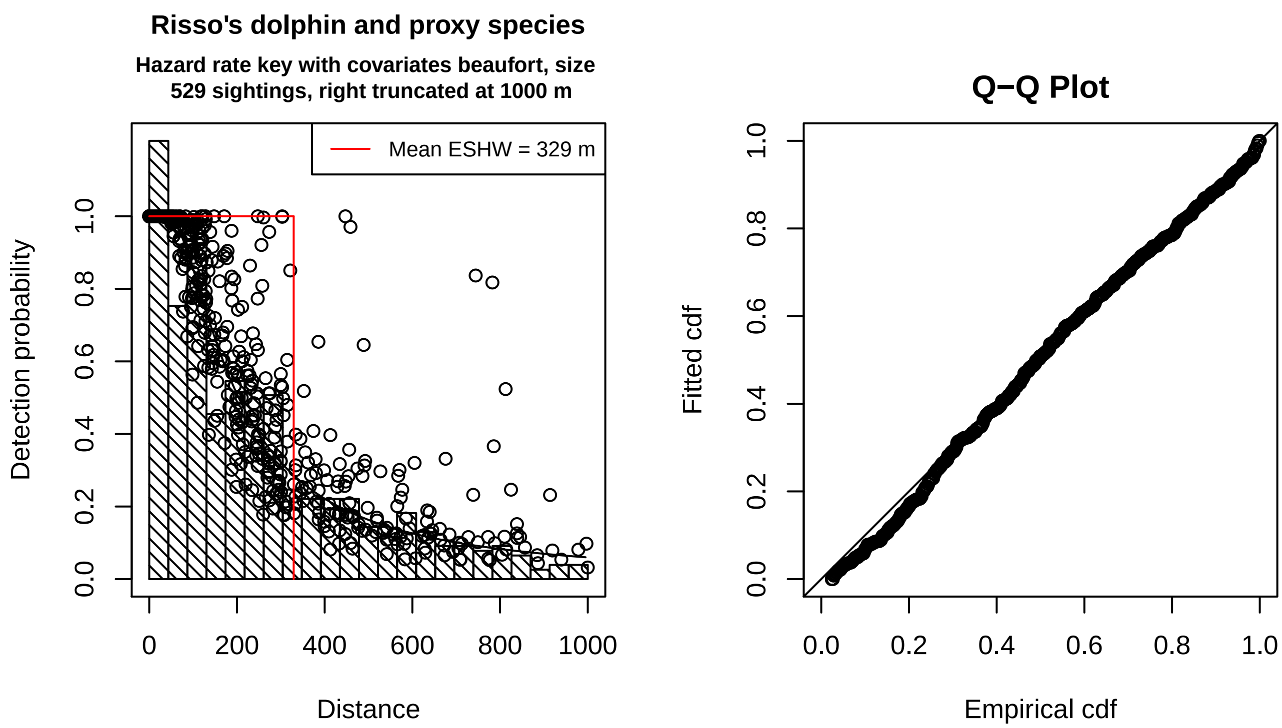

Figure 34: Detection function for Naked Eye Surveys that was selected for the density model

Statistical output for this detection function:

```
Summary for ds object
Number of observations :  529
Distance range         :  0  -  1000
AIC                    :  6866.942

Detection function:
 Hazard-rate key function

Detection function parameters
Scale Coefficients:
              estimate         se
(Intercept)  5.4796299 0.21489966
beaufort    -0.2095913 0.06594519
```

```
size         0.5152091 0.16341040

Shape parameters:
             estimate         se
(Intercept) 0.4966405 0.08804302

                        Estimate           SE         CV
Average p              0.2987683   0.02050381 0.06862779
N in covered region 1770.6030180 138.21190973 0.07805923
```

Additional diagnostic plots:

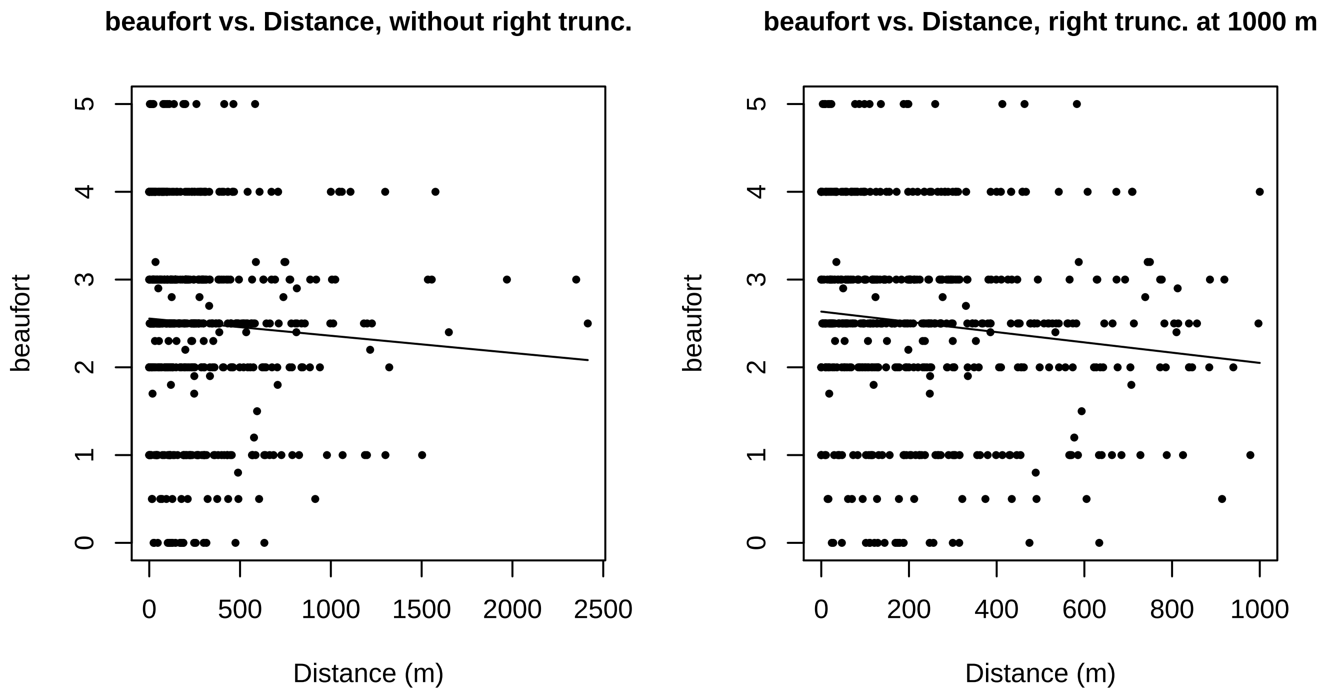

Figure 35: Scatterplots showing the relationship between Beaufort sea state and perpendicular sighting distance, for all sightings (left) and only those not right truncated (right). The line is a simple linear regression.

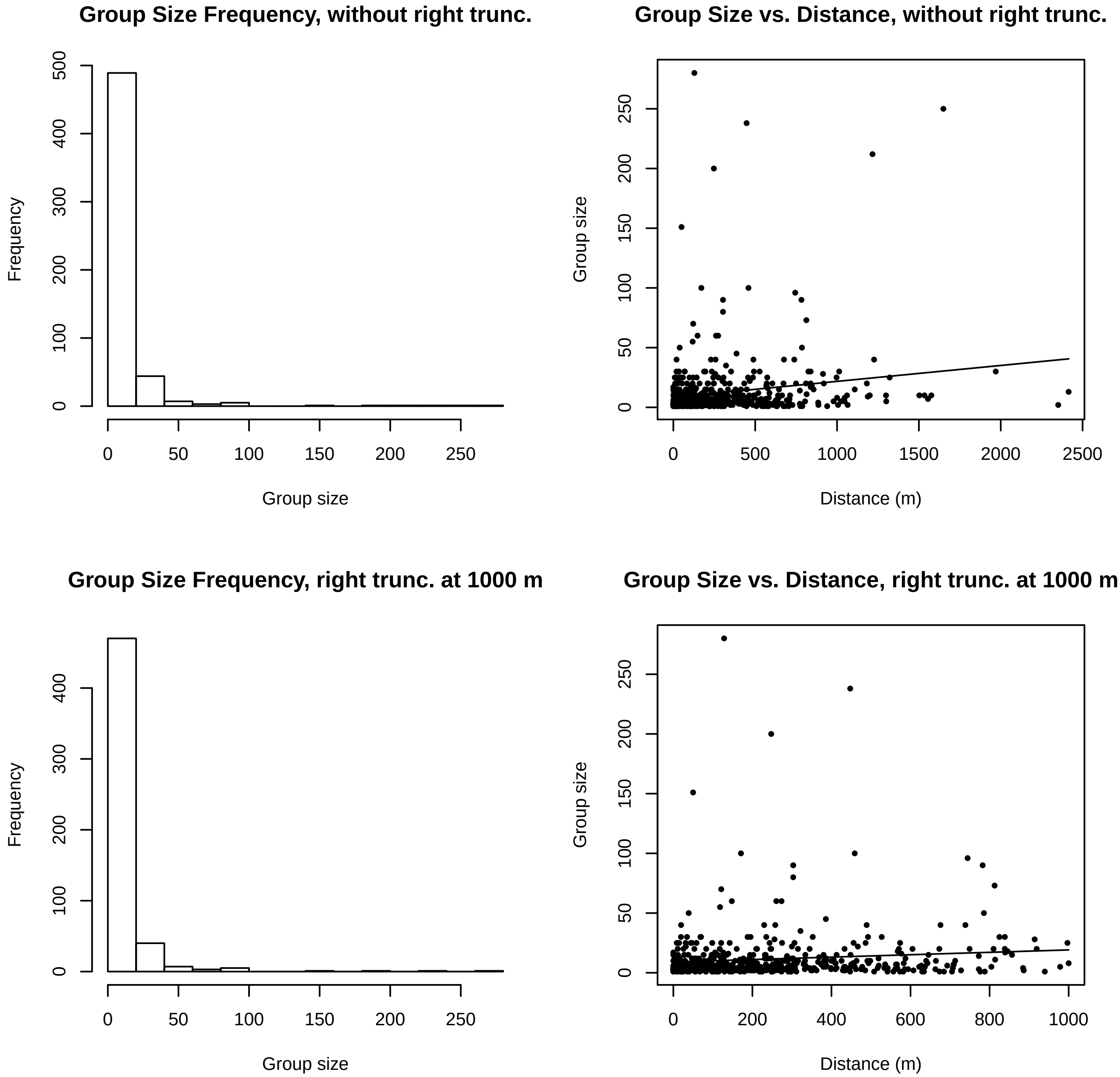

Figure 36: Histograms showing group size frequency and scatterplots showing the relationship between group size and perpendicular sighting distance, for all sightings (top row) and only those not right truncated (bottom row). In the scatterplot, the line is a simple linear regression.

CODA and SCANS II

Because this taxon was sighted too infrequently to fit a detection function to its sightings alone, we fit a detection function to the pooled sightings of several other species that we believed would exhibit similar detectability. These "proxy species" are listed below.

Reported By Observer	Common Name	n
Delphinus capensis	Long-beaked common dolphin	0
Delphinus delphis	Short-beaked common dolphin	227

Delphinus delphis/Lagenorhynchus acutus	Short-beaked common or Atlantic white-sided dolphin	0
Delphinus delphis/Stenella	Short-beaked common dolphin or Stenella spp.	0
Delphinus delphis/Stenella coeruleoalba	Short-beaked common or striped dolphin	57
Grampus griseus	Risso's dolphin	9
Grampus griseus/Tursiops truncatus	Risso's or Bottlenose dolphin	0
Lagenodelphis hosei	Fraser's dolphin	0
Lagenorhynchus acutus	Atlantic white-sided dolphin	56
Lagenorhynchus albirostris	White-beaked dolphin	32
Lagenorhynchus albirostris/Lagenorhynchus acutus	White-beaked or white-sided dolphin	4
Stenella	Unidentified Stenella	0
Stenella attenuata	Pantropical spotted dolphin	0
Stenella attenuata/frontalis	Pantropical or Atlantic spotted dolphin	0
Stenella clymene	Clymene dolphin	0
Stenella coeruleoalba	Striped dolphin	36
Stenella frontalis	Atlantic spotted dolphin	0
Stenella frontalis/Tursiops truncatus	Atlantic spotted or Bottlenose dolphin	0
Stenella longirostris	Spinner dolphin	0
Steno bredanensis	Rough-toothed dolphin	0
Steno bredanensis/Tursiops truncatus	Bottlenose or rough-toothed dolphin	0
Tursiops truncatus	Bottlenose dolphin	41
Total		462

Table 21: Proxy species used to fit detection functions for CODA and SCANS II. The number of sightings, n, is before truncation.

The sightings were right truncated at 1000m.

Covariate	Description
beaufort	Beaufort sea state.
quality	Survey-specific index of the quality of observation conditions, utilizing relevant factors other than Beaufort sea state (see methods).
size	Estimated size (number of individuals) of the sighted group.

Table 22: Covariates tested in candidate "multi-covariate distance sampling" (MCDS) detection functions.

Key	Adjustment	Order	Covariates	Succeeded	Δ AIC	Mean ESHW (m)
hr			quality, size	Yes	0.00	326
hr			quality	Yes	0.85	325
hr	poly	2		Yes	2.85	257
hr			beaufort, size	Yes	3.50	319

hr			beaufort	Yes	4.73	315
hr	poly	4		Yes	5.08	288
hn	cos	2		Yes	5.71	335
hr			size	Yes	6.16	322
hr				Yes	7.78	319
hn	cos	3		Yes	15.49	324
hn			quality, size	Yes	21.34	416
hn			beaufort, size	Yes	22.76	417
hn			beaufort, quality, size	Yes	23.17	416
hn			quality	Yes	25.50	413
hn			size	Yes	26.46	418
hn			beaufort, quality	Yes	27.47	413
hn			beaufort	Yes	28.47	414
hn				Yes	32.88	414
hn	herm	4		Yes	34.17	413
hr			beaufort, quality	No		
hr			beaufort, quality, size	No		

Table 23: Candidate detection functions for CODA and SCANS II. The first one listed was selected for the density model.

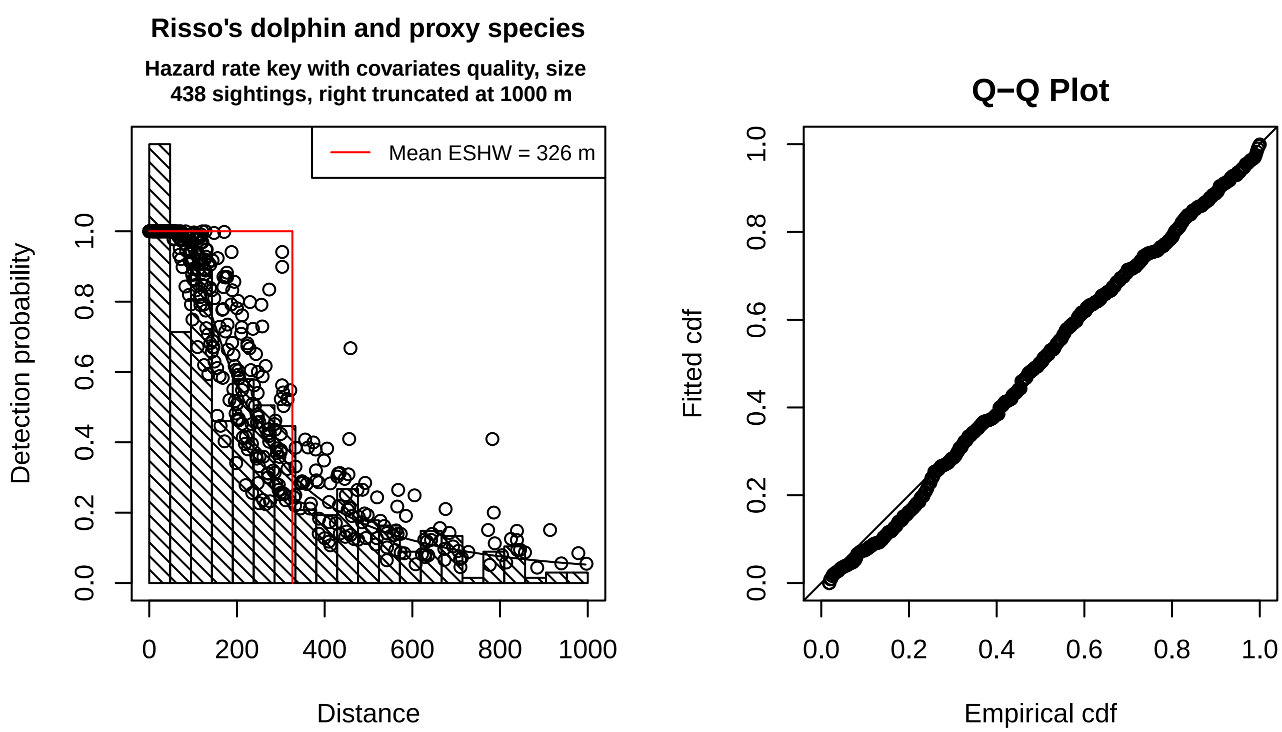

Figure 37: Detection function for CODA and SCANS II that was selected for the density model

Statistical output for this detection function:

```
Summary for ds object
Number of observations :  438
Distance range         :  0  -  1000
AIC                    :  5674.066

Detection function:
 Hazard-rate key function

Detection function parameters
Scale Coefficients:
              estimate         se
(Intercept)  5.4624136 0.17286880
quality     -0.1426257 0.05036964
size         0.2194236 0.11538504

Shape parameters:
             estimate         se
(Intercept) 0.5741026 0.09733169

                        Estimate           SE         CV
Average p              0.3097732   0.02170451 0.07006582
N in covered region 1413.9378602 114.19755693 0.08076561
```

Additional diagnostic plots:

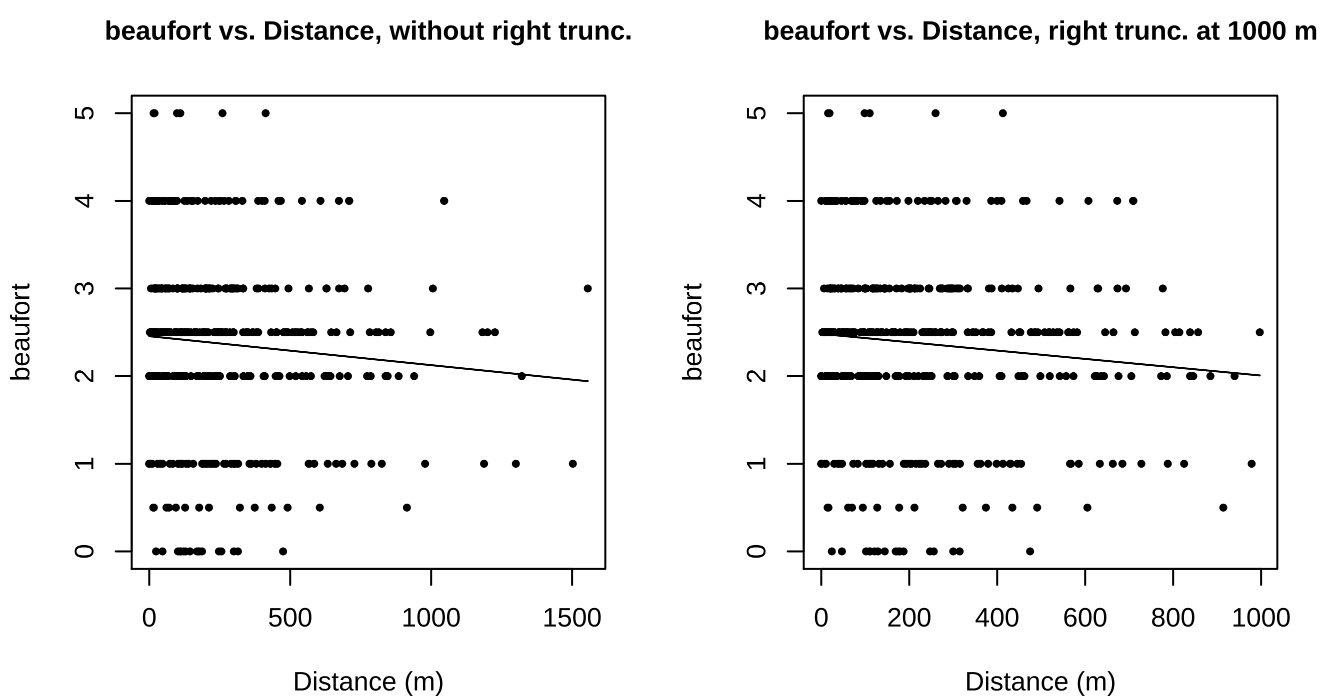

Figure 38: Scatterplots showing the relationship between Beaufort sea state and perpendicular sighting distance, for all sightings (left) and only those not right truncated (right). The line is a simple linear regression.

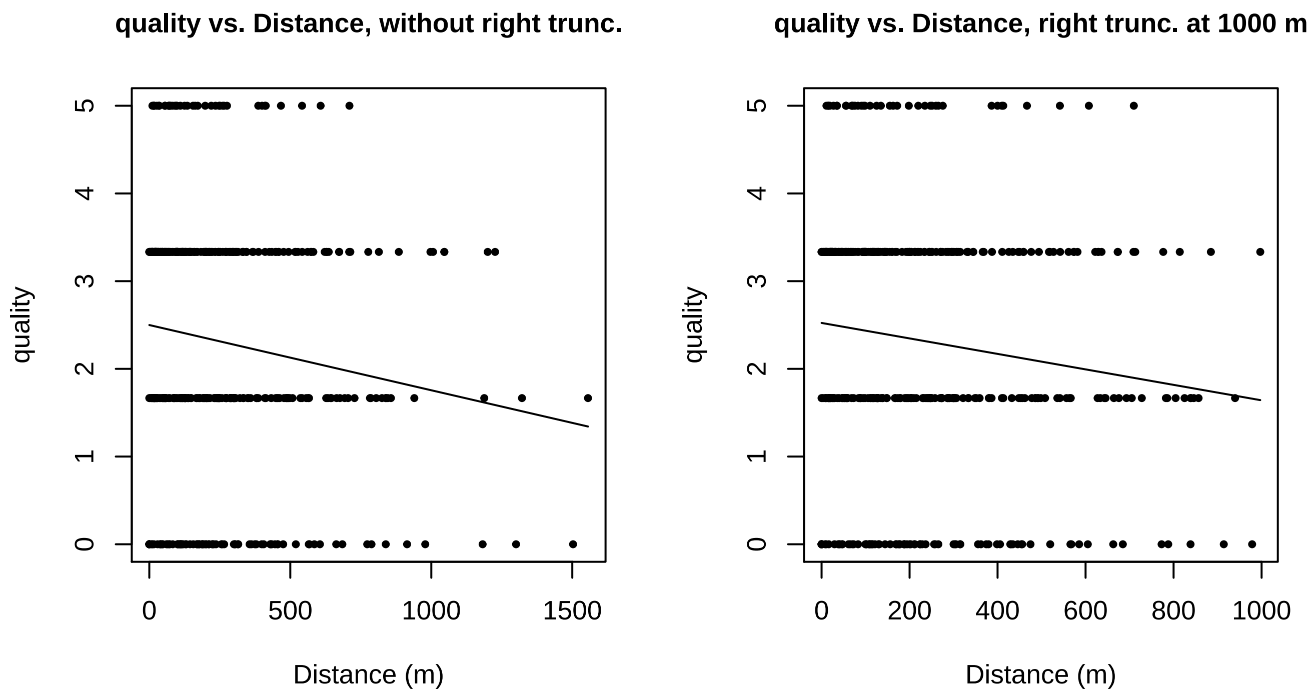

Figure 39: Scatterplots showing the relationship between the survey-specific index of the quality of observation conditions and perpendicular sighting distance, for all sightings (left) and only those not right truncated (right). Low values of the quality index correspond to better observation conditions. The line is a simple linear regression.

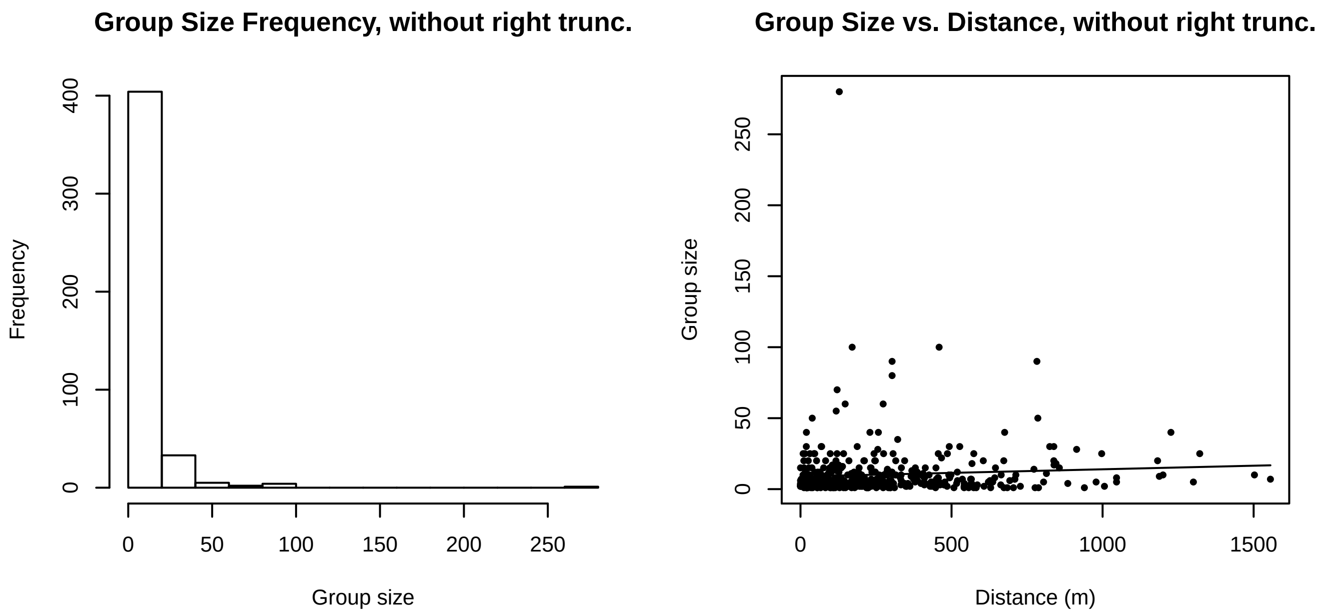

Figure 40: Histograms showing group size frequency and scatterplots showing the relationship between group size and perpendicular sighting distance, for all sightings (top row) and only those not right truncated (bottom row). In the scatterplot, the line is a simple linear regression.

Aerial Surveys

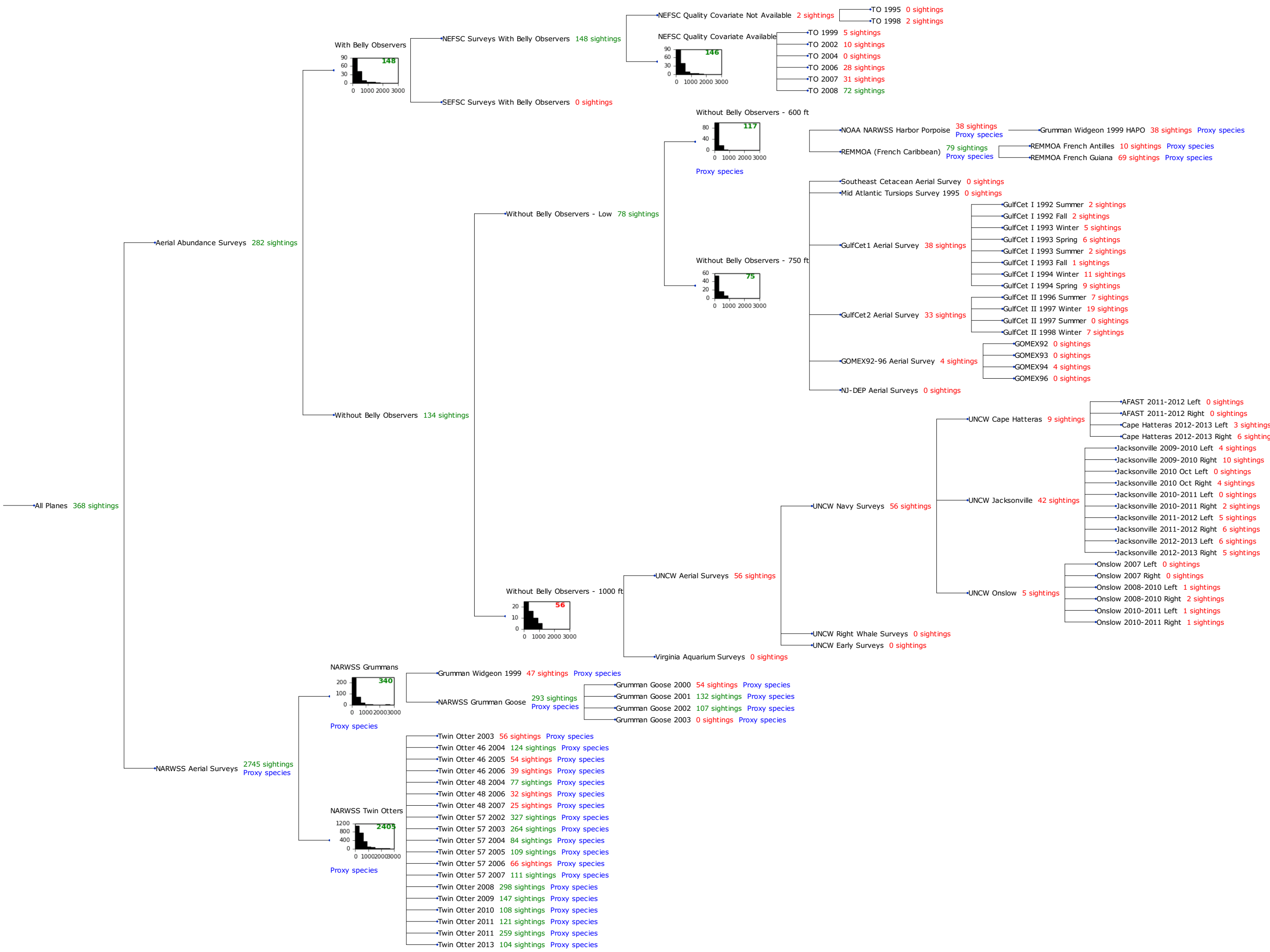

Figure 41: Detection hierarchy for aerial surveys

With Belly Observers

The sightings were right truncated at 1500m.

Covariate	Description
beaufort	Beaufort sea state.
size	Estimated size (number of individuals) of the sighted group.

Table 24: Covariates tested in candidate "multi-covariate distance sampling" (MCDS) detection functions.

Key	Adjustment	Order	Covariates	Succeeded	Δ AIC	Mean ESHW (m)
hr				Yes	0.00	474
hn	cos	2		Yes	0.96	436

hr			size	Yes	1.85	477
hr			beaufort	Yes	1.92	476
hr	poly	2		Yes	2.00	474
hr	poly	4		Yes	2.00	474
hr			beaufort, size	Yes	3.74	478
hn	cos	3		Yes	10.33	460
hn				Yes	10.66	533
hn			beaufort	Yes	11.82	533
hn			size	Yes	11.89	533
hn	herm	4		Yes	12.36	532
hn			beaufort, size	Yes	12.82	533

Table 25: Candidate detection functions for With Belly Observers. The first one listed was selected for the density model.

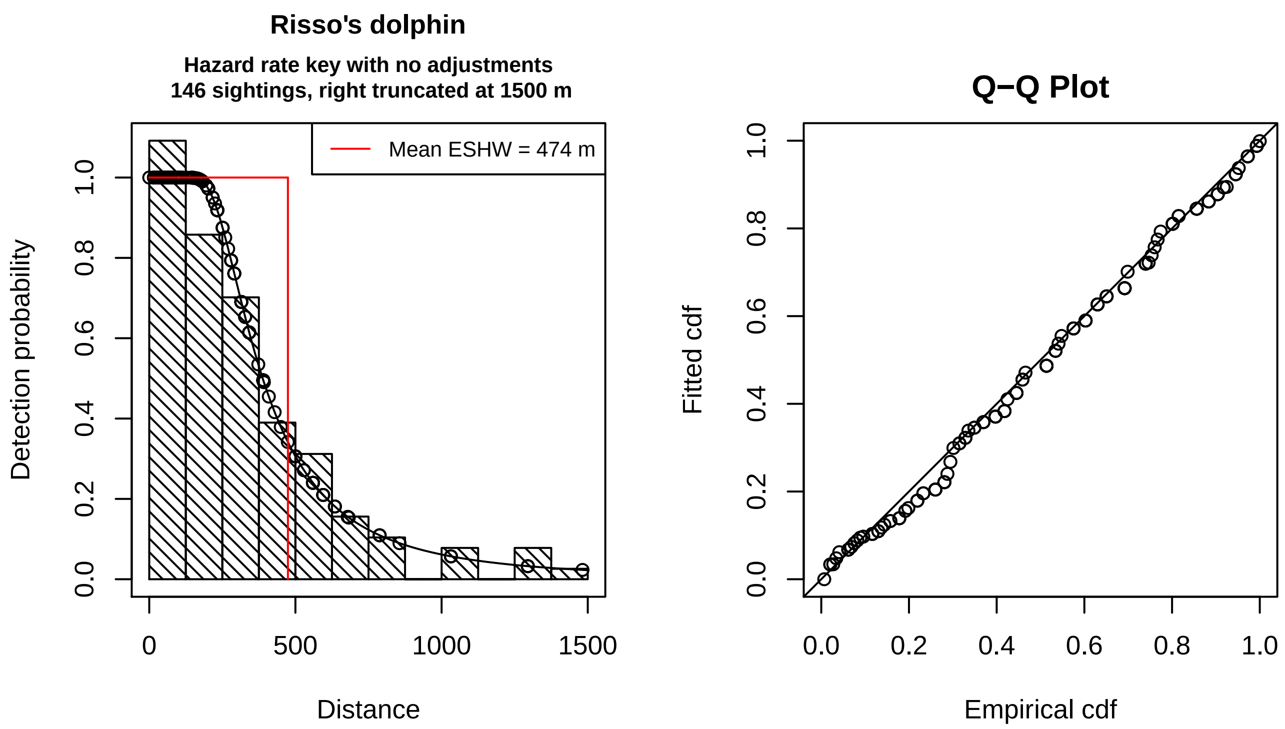

Figure 42: Detection function for With Belly Observers that was selected for the density model

Statistical output for this detection function:

```
Summary for ds object
Number of observations :  146
Distance range         :  0  -  1500
AIC                    :  1969.719

Detection function:
 Hazard-rate key function
```

```
Detection function parameters
Scale Coefficients:
            estimate       se
(Intercept) 5.815632 0.132012

Shape parameters:
             estimate        se
(Intercept) 0.9257516 0.1478857

                         Estimate          SE         CV
Average p               0.3162475  0.02818735 0.08913069
N in covered region 461.6637948 51.87818782 0.11237222
```

Additional diagnostic plots:

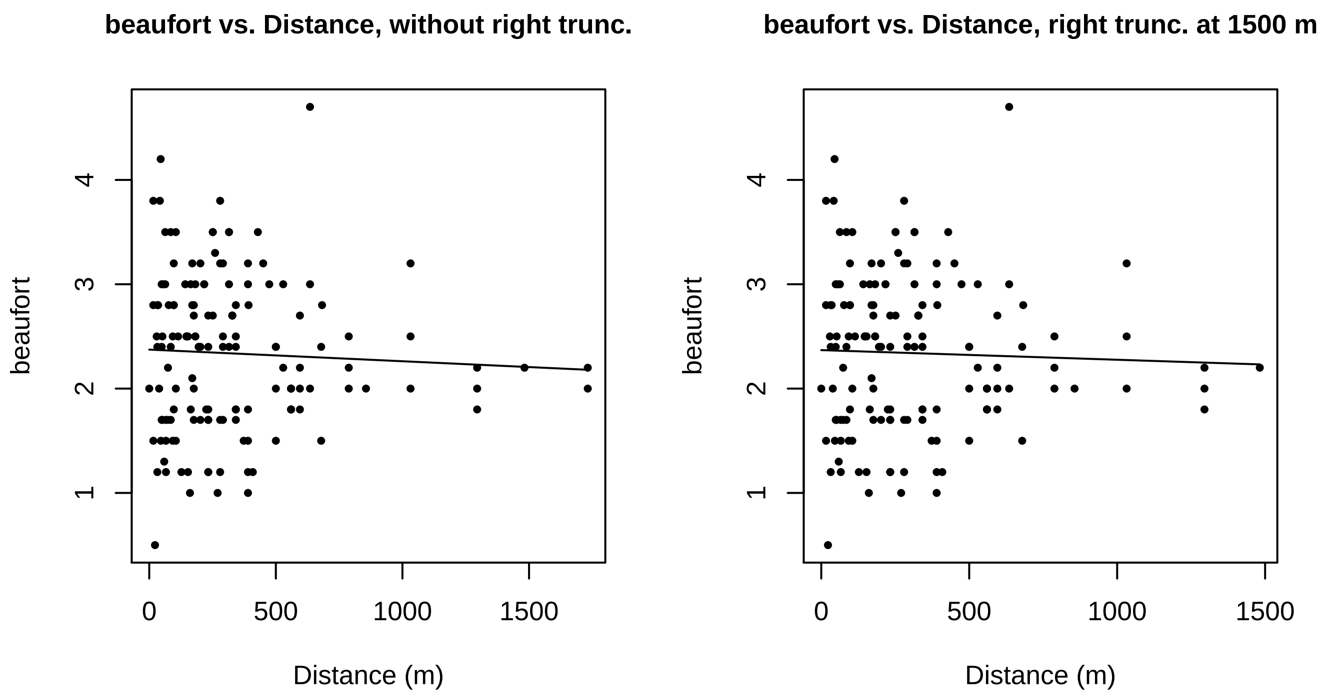

Figure 43: Scatterplots showing the relationship between Beaufort sea state and perpendicular sighting distance, for all sightings (left) and only those not right truncated (right). The line is a simple linear regression.

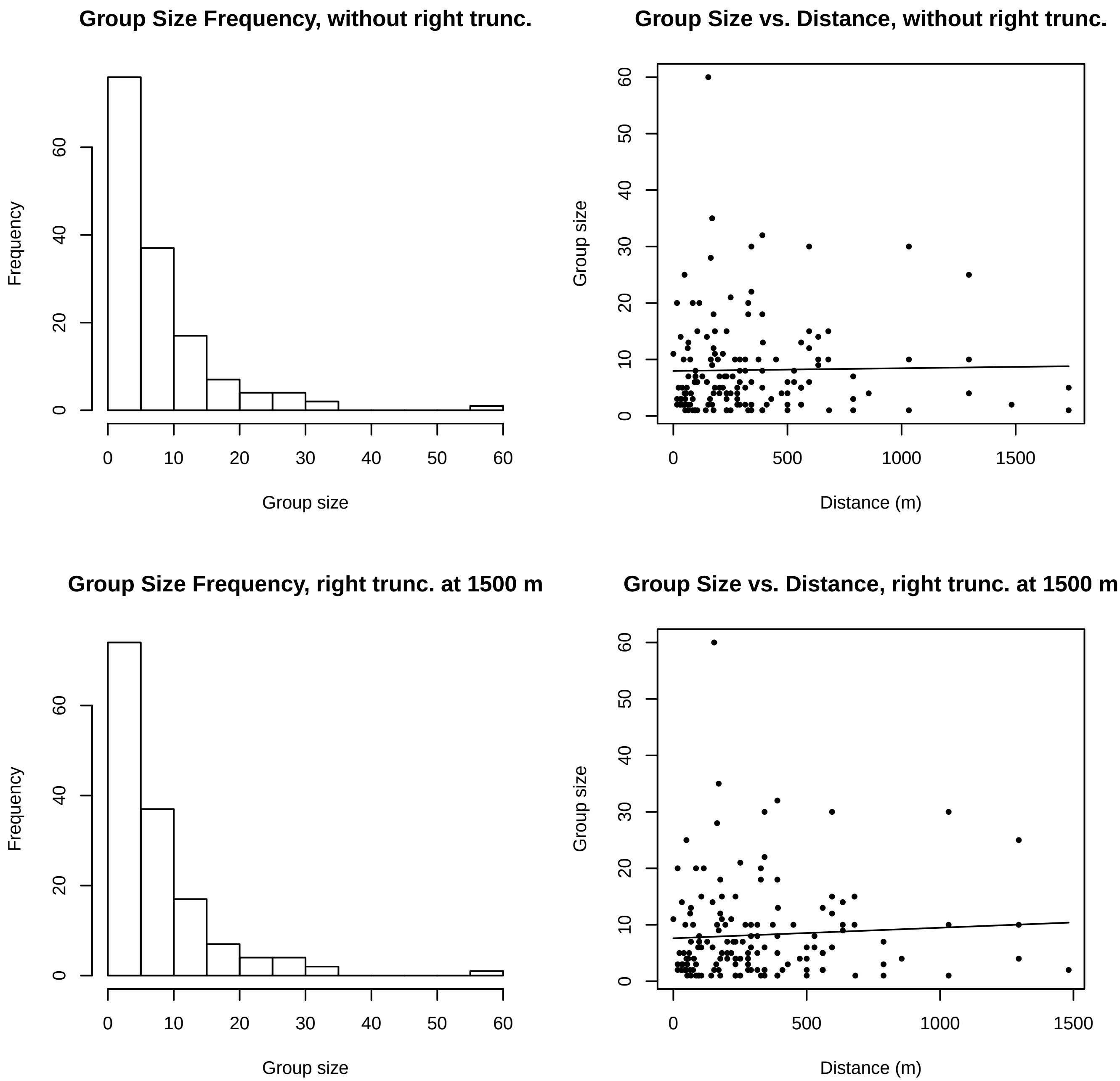

Figure 44: Histograms showing group size frequency and scatterplots showing the relationship between group size and perpendicular sighting distance, for all sightings (top row) and only those not right truncated (bottom row). In the scatterplot, the line is a simple linear regression.

NEFSC Quality Covariate Available

The sightings were right truncated at 1500m.

Covariate	Description
beaufort	Beaufort sea state.
quality	Survey-specific index of the quality of observation conditions, utilizing relevant factors other than Beaufort sea state (see methods).
size	Estimated size (number of individuals) of the sighted group.

Table 26: Covariates tested in candidate "multi-covariate distance sampling" (MCDS) detection functions.

Key	Adjustment	Order	Covariates	Succeeded	Δ AIC	Mean ESHW (m)
hr			quality	Yes	0.00	465
hr			quality, size	Yes	1.81	465
hr				Yes	3.42	465
hn	cos	2		Yes	4.33	430
hr			size	Yes	5.22	468
hr			beaufort	Yes	5.27	467
hr	poly	4		Yes	5.42	465
hr	poly	2		Yes	5.42	465
hr			beaufort, size	Yes	7.02	470
hn			quality	Yes	14.15	529
hn	cos	3		Yes	14.61	452
hn			quality, size	Yes	14.82	529
hn				Yes	15.40	530
hn			beaufort, quality	Yes	16.15	528
hn			beaufort	Yes	16.42	530
hn			size	Yes	16.44	530
hn			beaufort, quality, size	Yes	16.76	529
hn	herm	4		Yes	17.09	529
hn			beaufort, size	Yes	17.12	530
hr			beaufort, quality	No		
hr			beaufort, quality, size	No		

Table 27: Candidate detection functions for NEFSC Quality Covariate Available. The first one listed was selected for the density model.

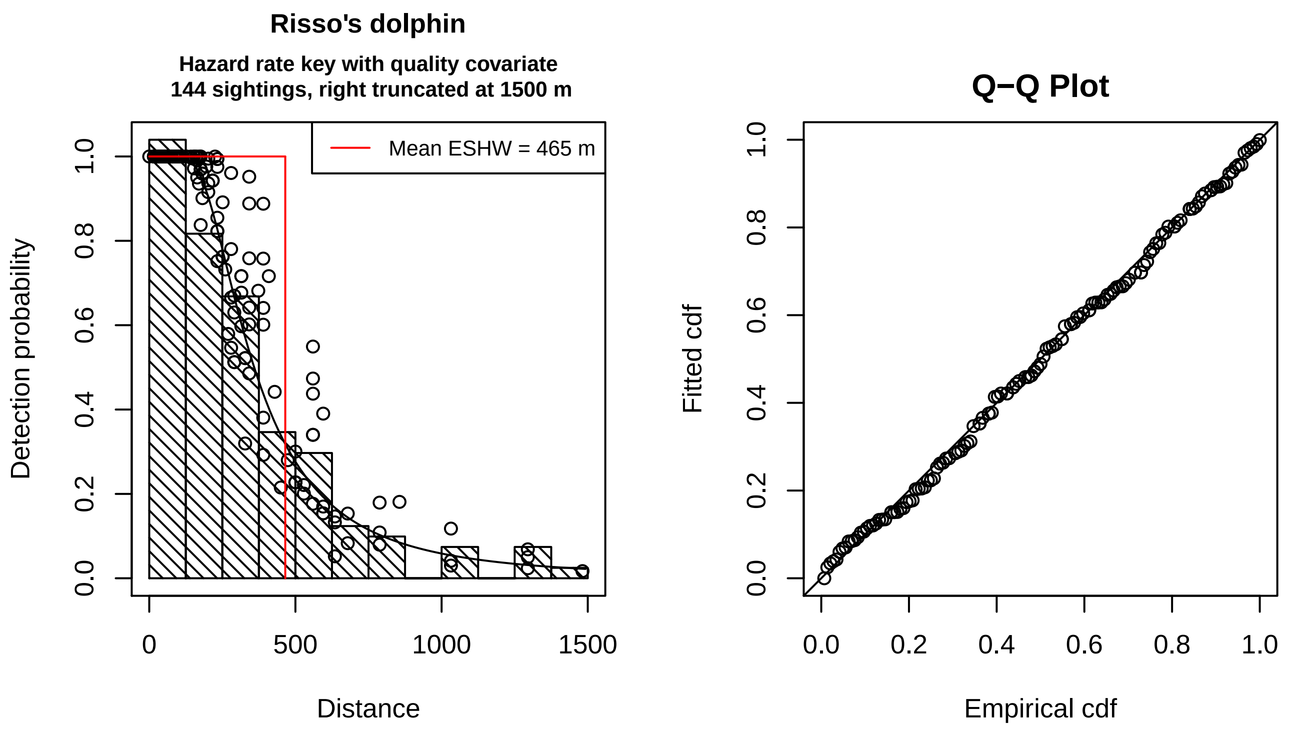

Figure 45: Detection function for NEFSC Quality Covariate Available that was selected for the density model

Statistical output for this detection function:

```
Summary for ds object
Number of observations :  144
Distance range         :  0  -  1500
AIC                    :  1936.432

Detection function:
 Hazard-rate key function

Detection function parameters
Scale Coefficients:
              estimate        se
(Intercept)  6.5850851 0.3536456
quality     -0.3133275 0.1280221

Shape parameters:
             estimate        se
(Intercept) 0.9134978 0.1432867

                       Estimate          SE        CV
Average p             0.2970435  0.02806221 0.0944717
N in covered region 484.7774676 57.15065316 0.1178905
```

Additional diagnostic plots:

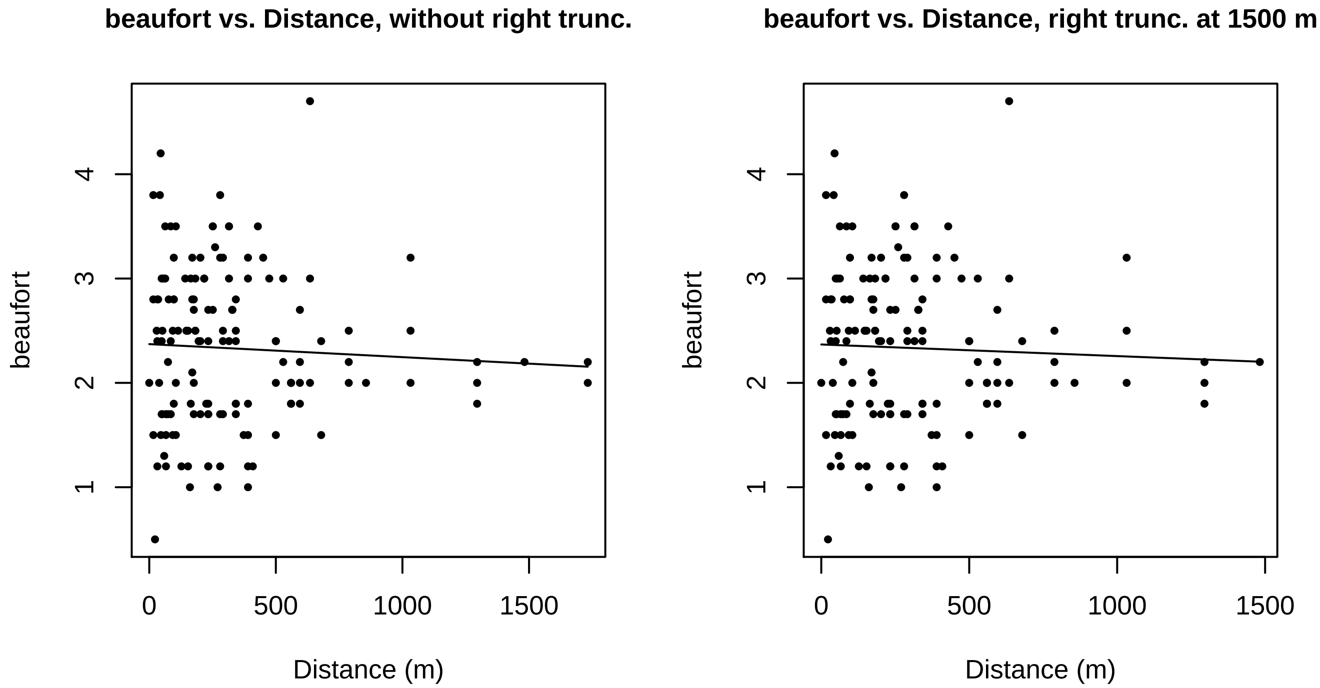

Figure 46: Scatterplots showing the relationship between Beaufort sea state and perpendicular sighting distance, for all sightings (left) and only those not right truncated (right). The line is a simple linear regression.

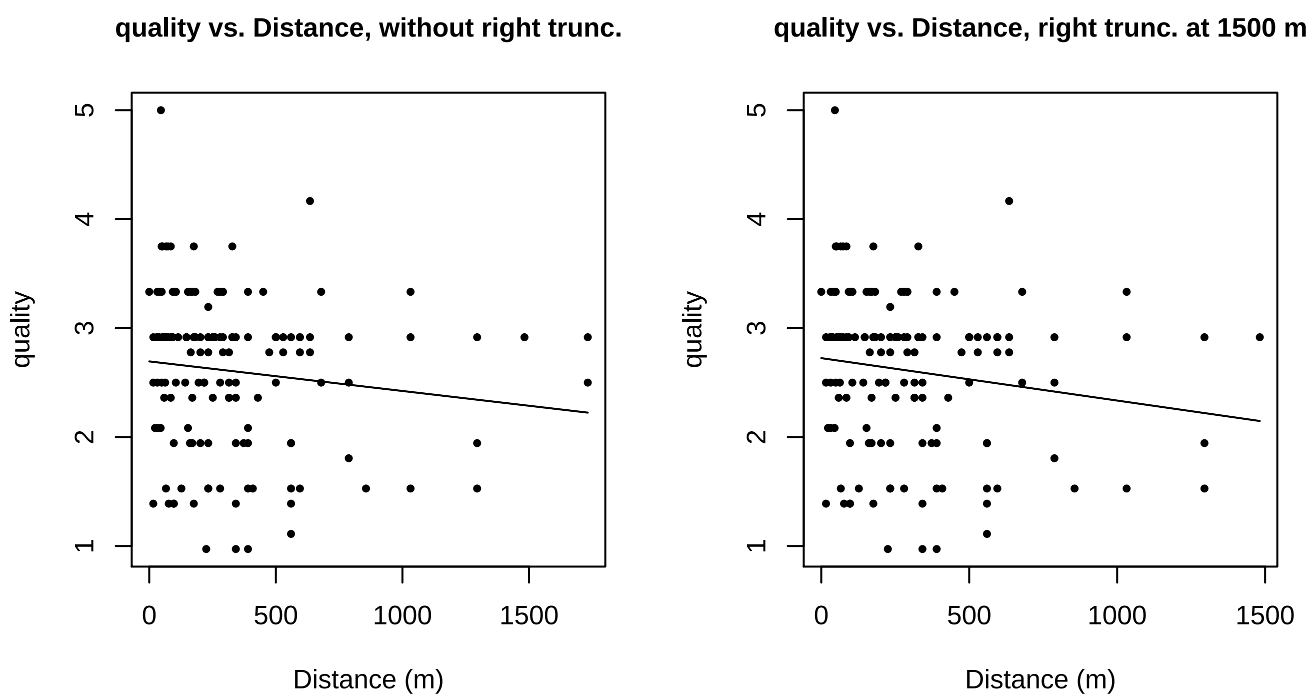

Figure 47: Scatterplots showing the relationship between the survey-specific index of the quality of observation conditions and perpendicular sighting distance, for all sightings (left) and only those not right truncated (right). Low values of the quality index correspond to better observation conditions. The line is a simple linear regression.

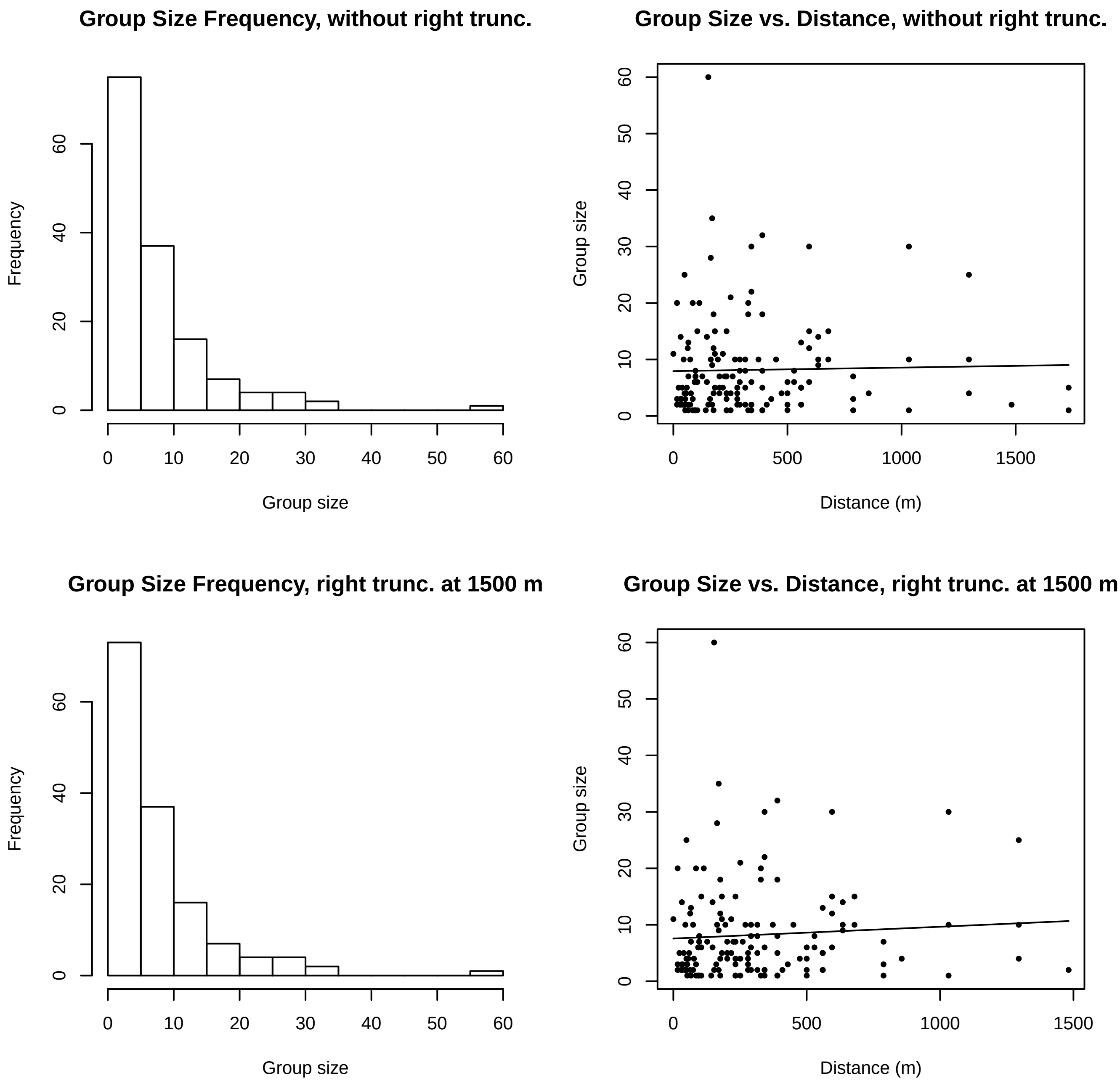

Figure 48: Histograms showing group size frequency and scatterplots showing the relationship between group size and perpendicular sighting distance, for all sightings (top row) and only those not right truncated (bottom row). In the scatterplot, the line is a simple linear regression.

Without Belly Observers - 600 ft

Because this taxon was sighted too infrequently to fit a detection function to its sightings alone, we fit a detection function to the pooled sightings of several other species that we believed would exhibit similar detectability. These "proxy species" are listed below.

Reported By Observer	Common Name	n
Delphinus capensis	Long-beaked common dolphin	0
Delphinus delphis	Short-beaked common dolphin	5

Delphinus delphis/Lagenorhynchus acutus	Short-beaked common or Atlantic white-sided dolphin	0
Delphinus delphis/Stenella	Short-beaked common dolphin or Stenella spp.	0
Delphinus delphis/Stenella coeruleoalba	Short-beaked common or striped dolphin	0
Grampus griseus	Risso's dolphin	3
Grampus griseus/Tursiops truncatus	Risso's or Bottlenose dolphin	0
Lagenodelphis hosei	Fraser's dolphin	4
Lagenorhynchus acutus	Atlantic white-sided dolphin	31
Lagenorhynchus albirostris	White-beaked dolphin	0
Lagenorhynchus albirostris/Lagenorhynchus acutus	White-beaked or white-sided dolphin	0
Stenella	Unidentified Stenella	0
Stenella attenuata	Pantropical spotted dolphin	4
Stenella attenuata/frontalis	Pantropical or Atlantic spotted dolphin	0
Stenella clymene	Clymene dolphin	0
Stenella coeruleoalba	Striped dolphin	0
Stenella frontalis	Atlantic spotted dolphin	0
Stenella frontalis/Tursiops truncatus	Atlantic spotted or Bottlenose dolphin	0
Stenella longirostris	Spinner dolphin	0
Steno bredanensis	Rough-toothed dolphin	0
Steno bredanensis/Tursiops truncatus	Bottlenose or rough-toothed dolphin	0
Tursiops truncatus	Bottlenose dolphin	70
Total		117

Table 28: Proxy species used to fit detection functions for Without Belly Observers - 600 ft. The number of sightings, n, is before truncation.

The sightings were right truncated at 600m.

Covariate	Description
beaufort	Beaufort sea state.
size	Estimated size (number of individuals) of the sighted group.

Table 29: Covariates tested in candidate "multi-covariate distance sampling" (MCDS) detection functions.

Key	Adjustment	Order	Covariates	Succeeded	Δ AIC	Mean ESHW (m)
hn				Yes	0.00	273
hr				Yes	0.47	313
hn	cos	3		Yes	0.63	294
hn	cos	2		Yes	1.46	297
hn	herm	4		Yes	1.66	292
hn			beaufort	Yes	1.82	273

hn			size	Yes	1.98	273
hr	poly	4		Yes	2.01	305
hr			beaufort	Yes	2.15	308
hr	poly	2		Yes	2.38	298
hn			beaufort, size	Yes	3.80	273
hr			size	No		
hr			beaufort, size	No		

Table 30: Candidate detection functions for Without Belly Observers - 600 ft. The first one listed was selected for the density model.

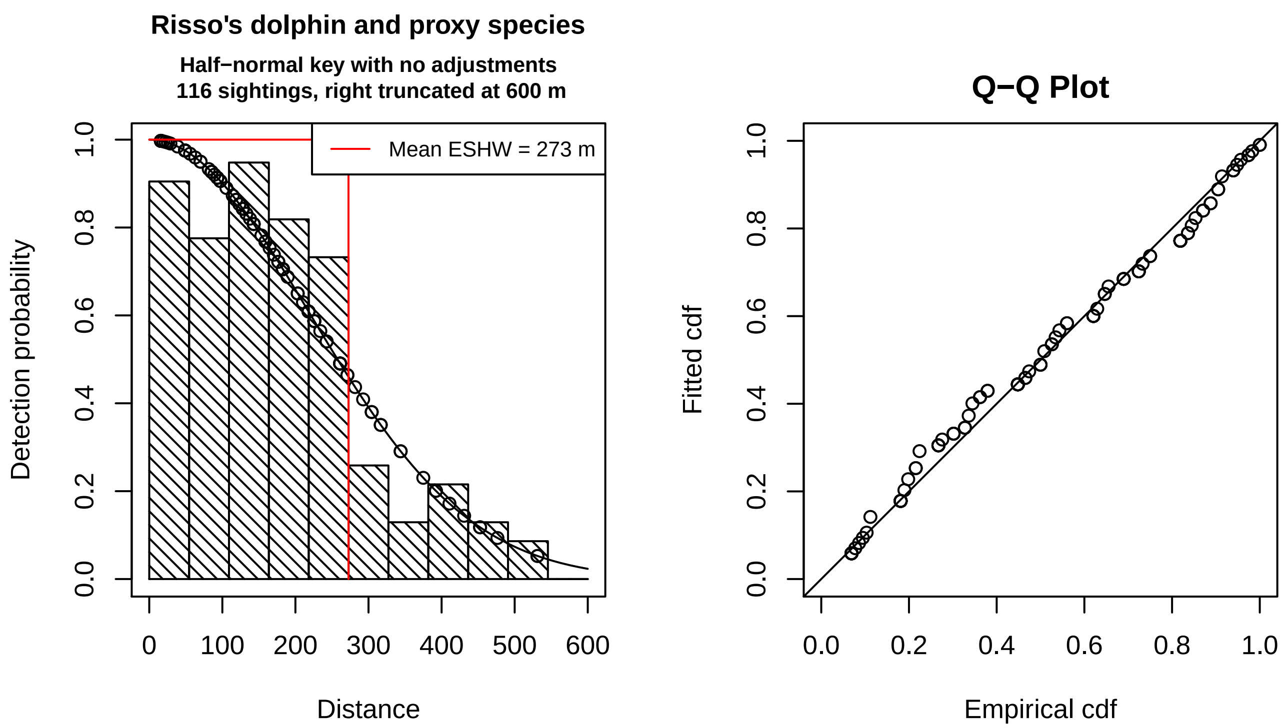

Figure 49: Detection function for Without Belly Observers - 600 ft that was selected for the density model

Statistical output for this detection function:

```
Summary for ds object
Number of observations :  116
Distance range         :  0  -  600
AIC                    :  1413.111

Detection function:
 Half-normal key function

Detection function parameters
Scale Coefficients:
            estimate         se
(Intercept) 5.388383 0.07654643
```

```
                      Estimate          SE         CV
Average p            0.4543498  0.03299346 0.07261686
N in covered region 255.3098755 25.50172372 0.09988538
```

Additional diagnostic plots:

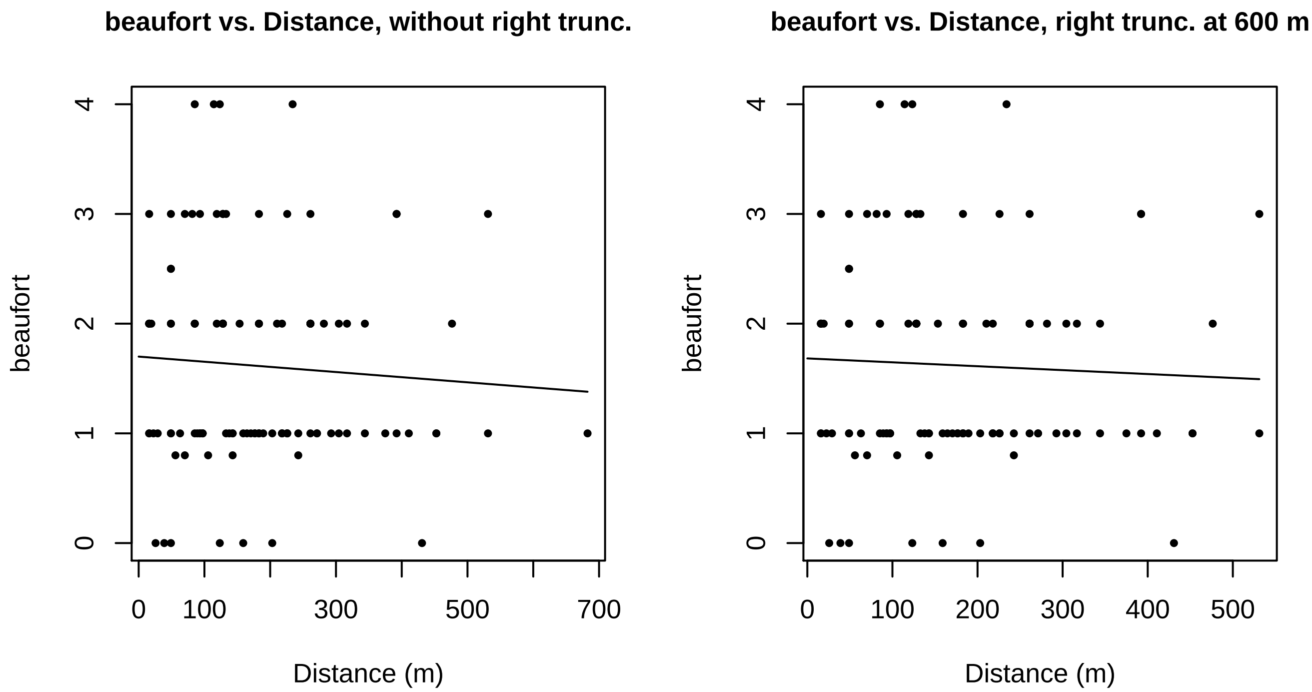

Figure 50: Scatterplots showing the relationship between Beaufort sea state and perpendicular sighting distance, for all sightings (left) and only those not right truncated (right). The line is a simple linear regression.

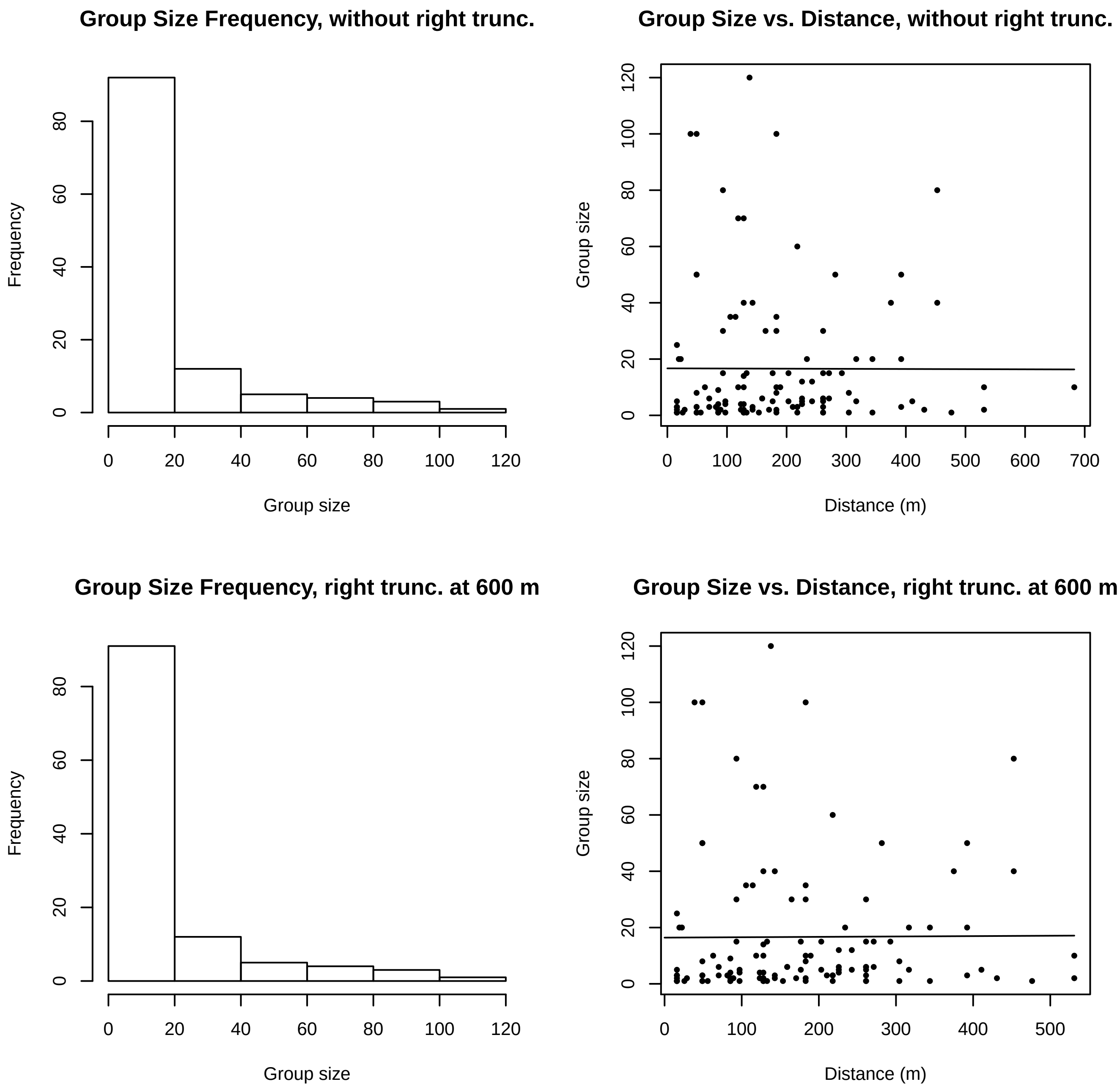

Figure 51: Histograms showing group size frequency and scatterplots showing the relationship between group size and perpendicular sighting distance, for all sightings (top row) and only those not right truncated (bottom row). In the scatterplot, the line is a simple linear regression.

Without Belly Observers - 750 ft

The sightings were right truncated at 1296m. The vertical sighting angles were heaped at 10 degree increments, so the candidate detection functions were fitted using linear bins scaled accordingly.

Covariate	Description
beaufort	Beaufort sea state.
quality	Survey-specific index of the quality of observation conditions, utilizing relevant factors other than Beaufort sea state (see methods).

size	Estimated size (number of individuals) of the sighted group.

Table 31: Covariates tested in candidate "multi-covariate distance sampling" (MCDS) detection functions.

Key	Adjustment	Order	Covariates	Succeeded	Δ AIC	Mean ESHW (m)
hr				Yes	0.00	379
hr			quality	Yes	2.00	379
hr	poly	2		Yes	2.00	379
hr	poly	4		Yes	2.00	379
hn	cos	2		Yes	2.15	360
hn	cos	3		Yes	2.20	332
hn				Yes	2.97	410
hn	herm	4		Yes	4.94	410
hn			beaufort	No		
hr			beaufort	No		
hn			quality	No		
hn			size	No		
hr			size	No		
hn			beaufort, quality	No		
hr			beaufort, quality	No		
hn			beaufort, size	No		
hr			beaufort, size	No		
hn			quality, size	No		
hr			quality, size	No		
hn			beaufort, quality, size	No		
hr			beaufort, quality, size	No		

Table 32: Candidate detection functions for Without Belly Observers - 750 ft. The first one listed was selected for the density model.

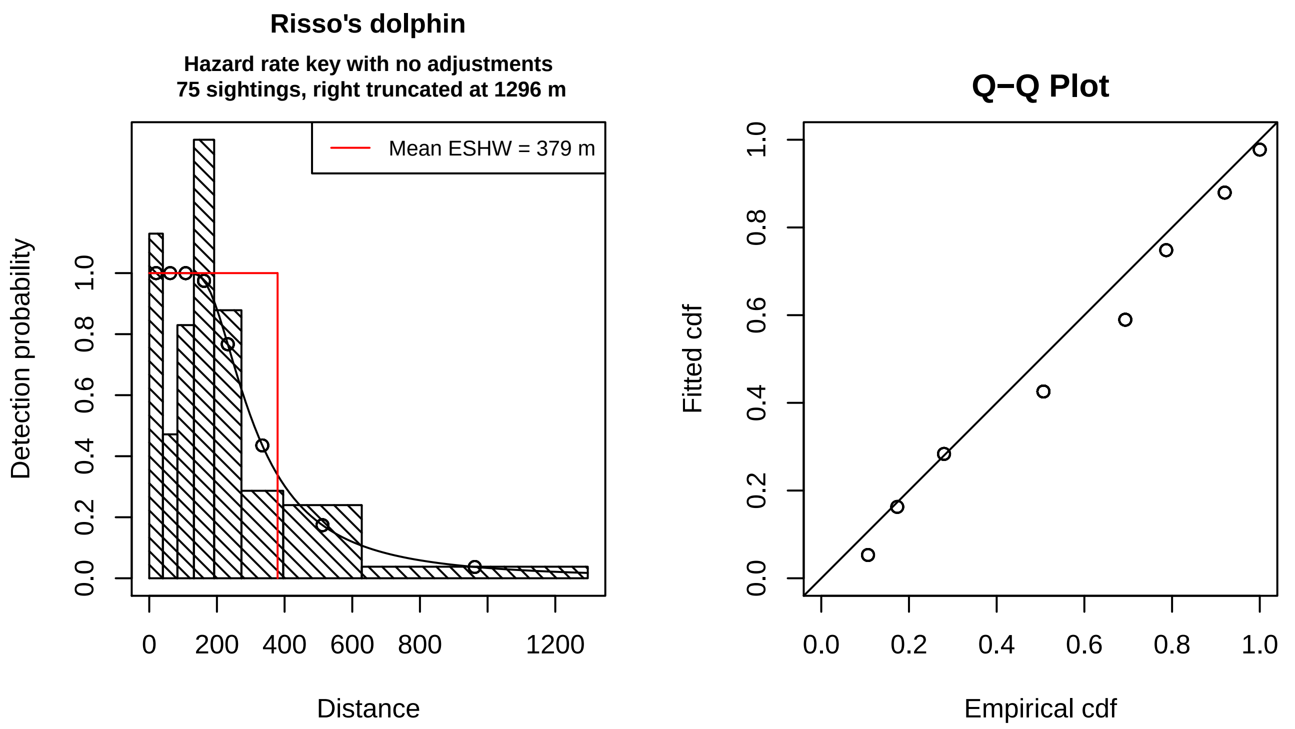

Figure 52: Detection function for Without Belly Observers - 750 ft that was selected for the density model

Statistical output for this detection function:

```
Summary for ds object
Number of observations :  75
Distance range         :  0  -  1296
AIC                    :  310.3734

Detection function:
 Hazard-rate key function

Detection function parameters
Scale Coefficients:
            estimate        se
(Intercept) 5.593894 0.2035062

Shape parameters:
             estimate        se
(Intercept) 0.9432286 0.2147999

                       Estimate         SE        CV
Average p             0.2927103  0.0395159 0.1350000
N in covered region 256.2260786 42.6102825 0.1662996
```

Additional diagnostic plots:

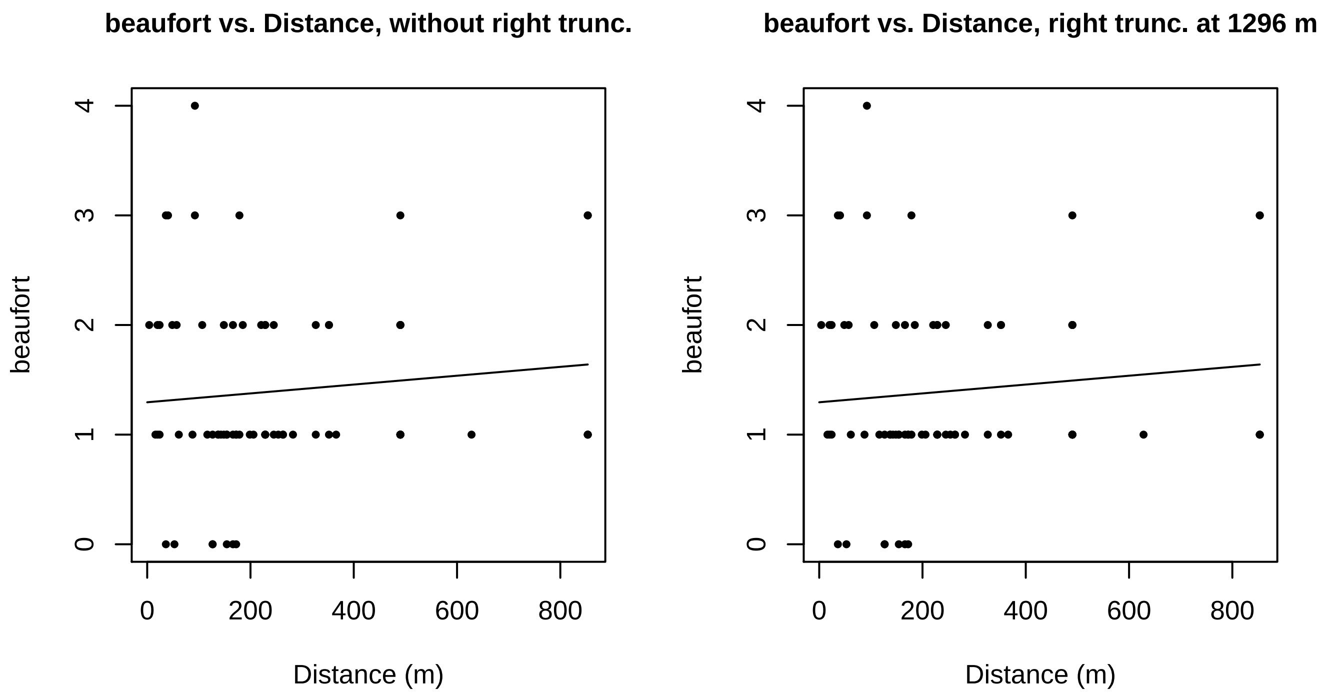

Figure 53: Scatterplots showing the relationship between Beaufort sea state and perpendicular sighting distance, for all sightings (left) and only those not right truncated (right). The line is a simple linear regression.

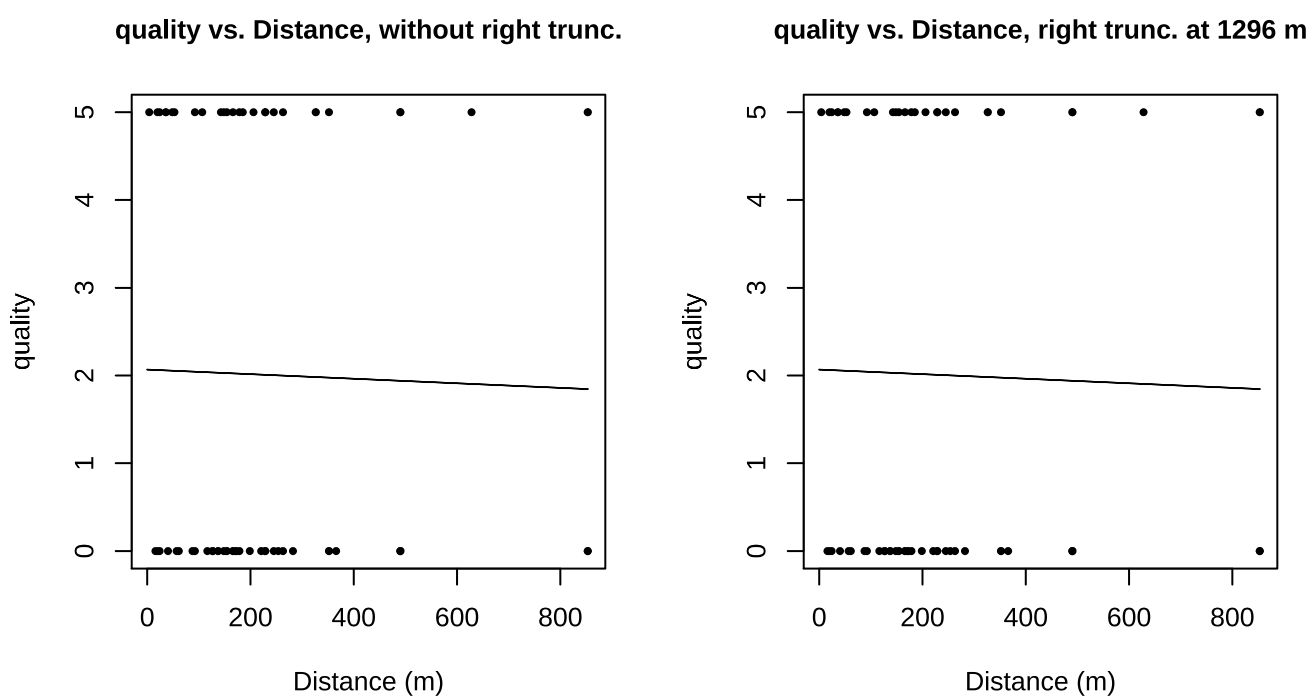

Figure 54: Scatterplots showing the relationship between the survey-specific index of the quality of observation conditions and perpendicular sighting distance, for all sightings (left) and only those not right truncated (right). Low values of the quality index correspond to better observation conditions. The line is a simple linear regression.

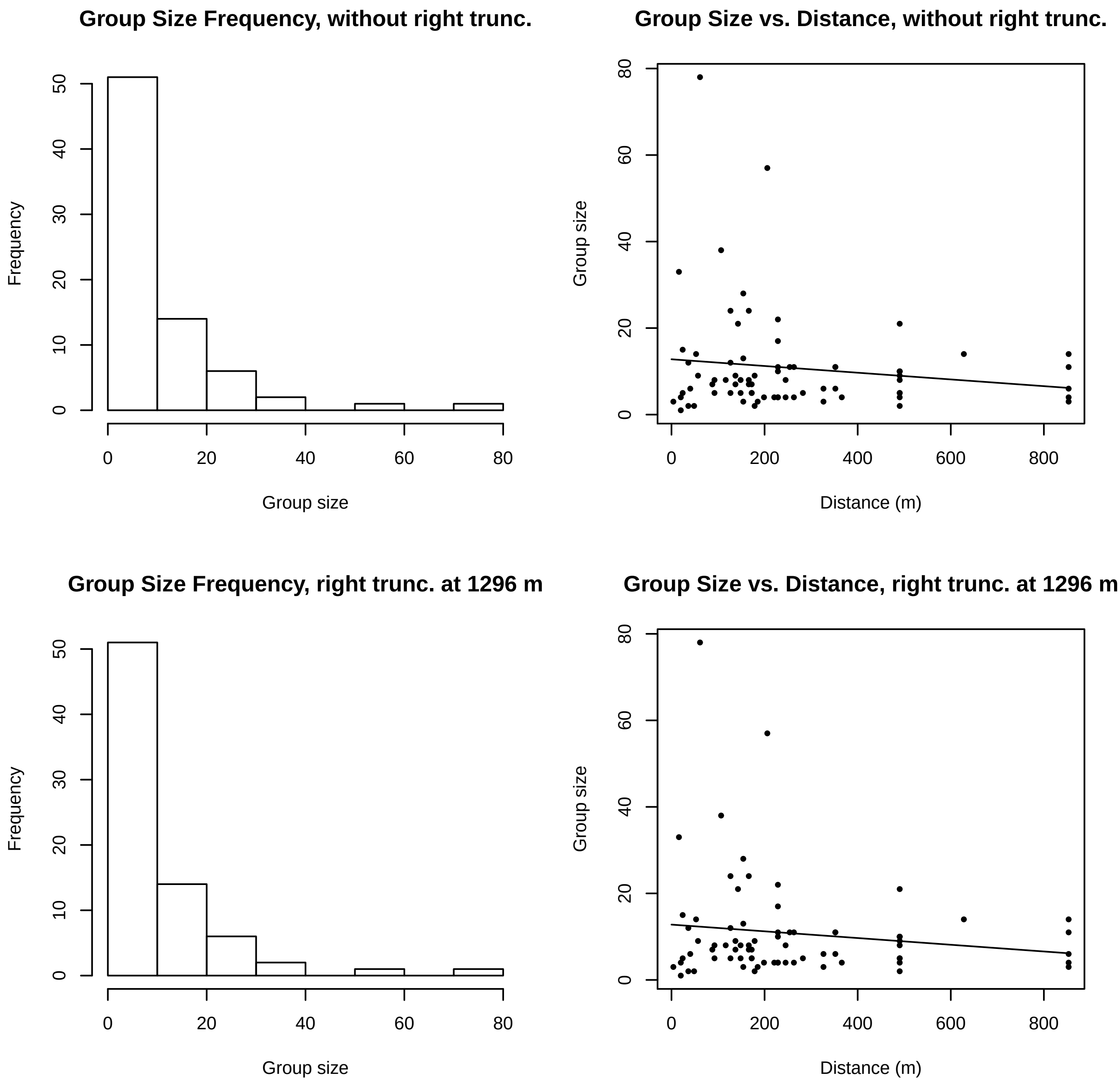

Figure 55: Histograms showing group size frequency and scatterplots showing the relationship between group size and perpendicular sighting distance, for all sightings (top row) and only those not right truncated (bottom row). In the scatterplot, the line is a simple linear regression.

Without Belly Observers - 1000 ft

The sightings were right truncated at 1200m.

Covariate	Description
beaufort	Beaufort sea state.
quality	Survey-specific index of the quality of observation conditions, utilizing relevant factors other than Beaufort sea state (see methods).
size	Estimated size (number of individuals) of the sighted group.

Table 33: Covariates tested in candidate “multi-covariate distance sampling” (MCDS) detection functions.

Key	Adjustment	Order	Covariates	Succeeded	Δ AIC	Mean ESHW (m)
hn				Yes	0.00	719
hr				Yes	1.53	738
hn	cos	3		Yes	1.67	748
hn			quality	Yes	1.88	719
hn	herm	4		Yes	1.96	716
hn	cos	2		Yes	1.96	745
hr			quality	Yes	3.51	759
hr	poly	2		Yes	3.53	738
hr	poly	4		Yes	3.53	738
hn			beaufort	No		
hr			beaufort	No		
hn			size	No		
hr			size	No		
hn			beaufort, quality	No		
hr			beaufort, quality	No		
hn			beaufort, size	No		
hr			beaufort, size	No		
hn			quality, size	No		
hr			quality, size	No		
hn			beaufort, quality, size	No		
hr			beaufort, quality, size	No		

Table 34: Candidate detection functions for Without Belly Observers - 1000 ft. The first one listed was selected for the density model.

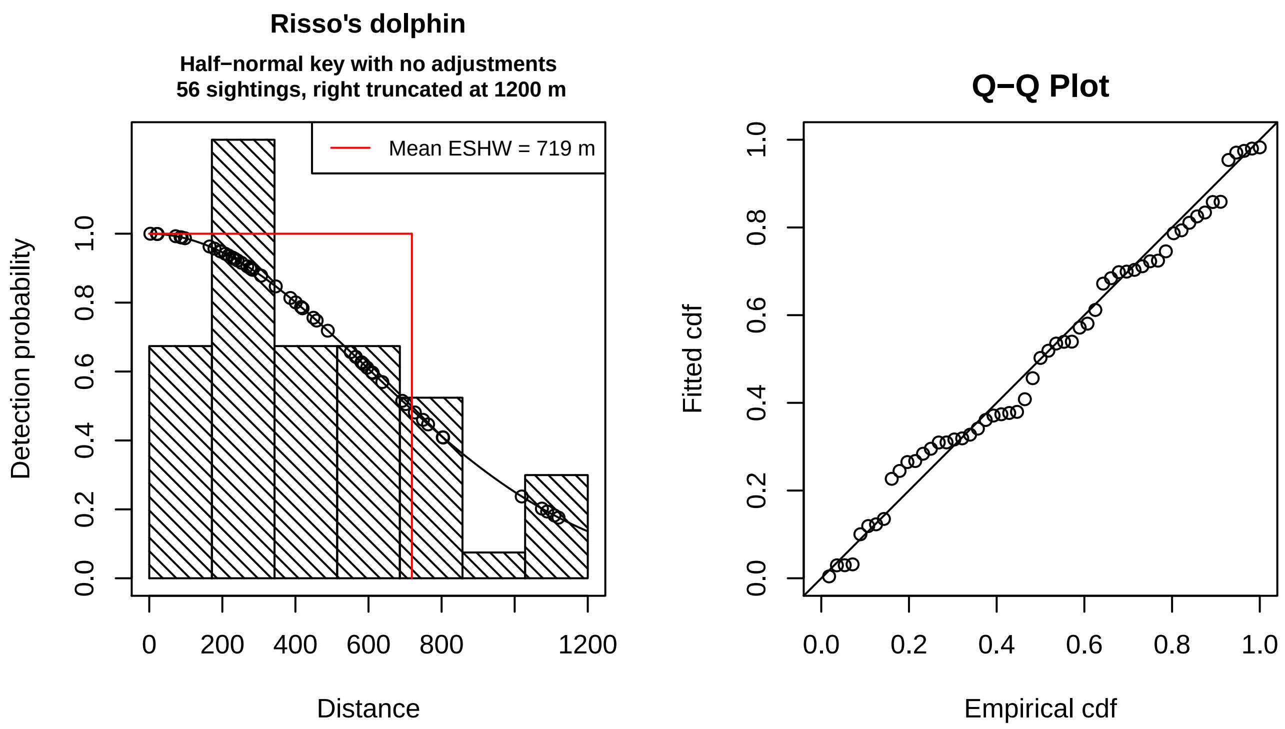

Figure 56: Detection function for Without Belly Observers - 1000 ft that was selected for the density model

Statistical output for this detection function:

```
Summary for ds object
Number of observations :  56
Distance range         :  0  -  1200
AIC                    :  781.9354

Detection function:
 Half-normal key function

Detection function parameters
Scale Coefficients:
            estimate        se
(Intercept) 6.398611 0.1444097

                        Estimate          SE        CV
Average p              0.5989218  0.06681563 0.1115599
N in covered region 93.5013479 13.09276323 0.1400275
```

Additional diagnostic plots:

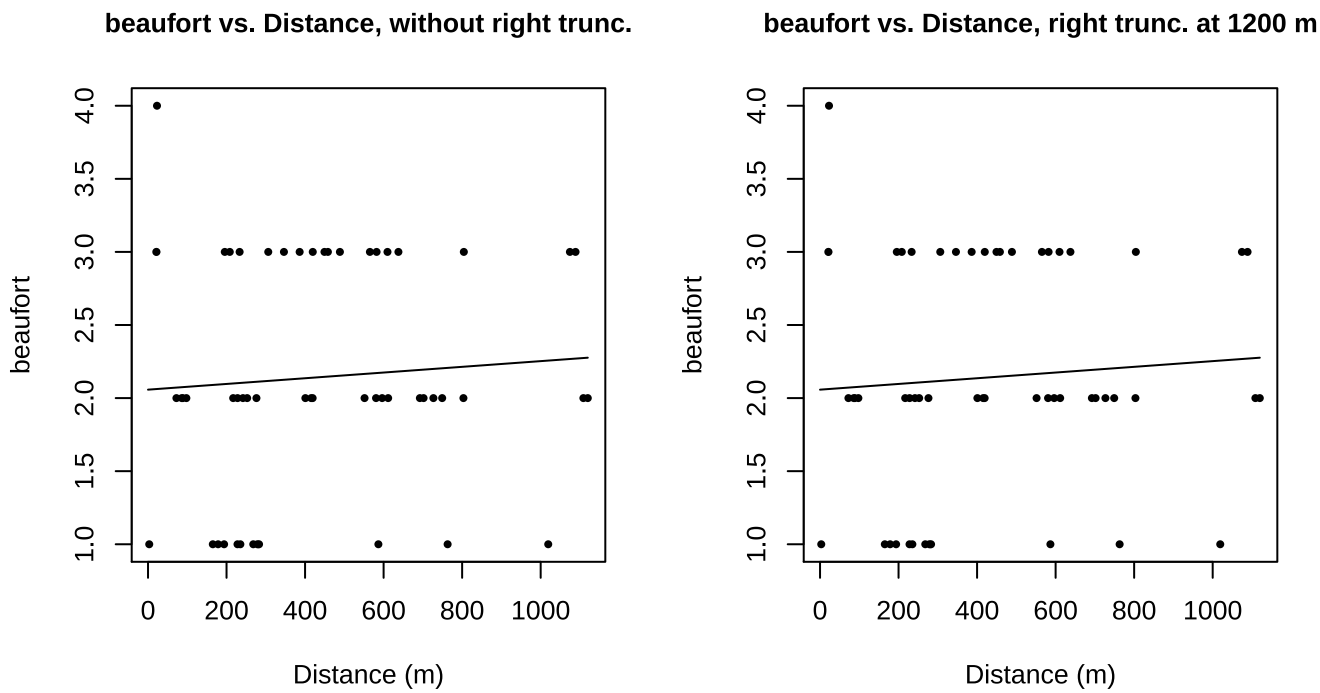

Figure 57: Scatterplots showing the relationship between Beaufort sea state and perpendicular sighting distance, for all sightings (left) and only those not right truncated (right). The line is a simple linear regression.

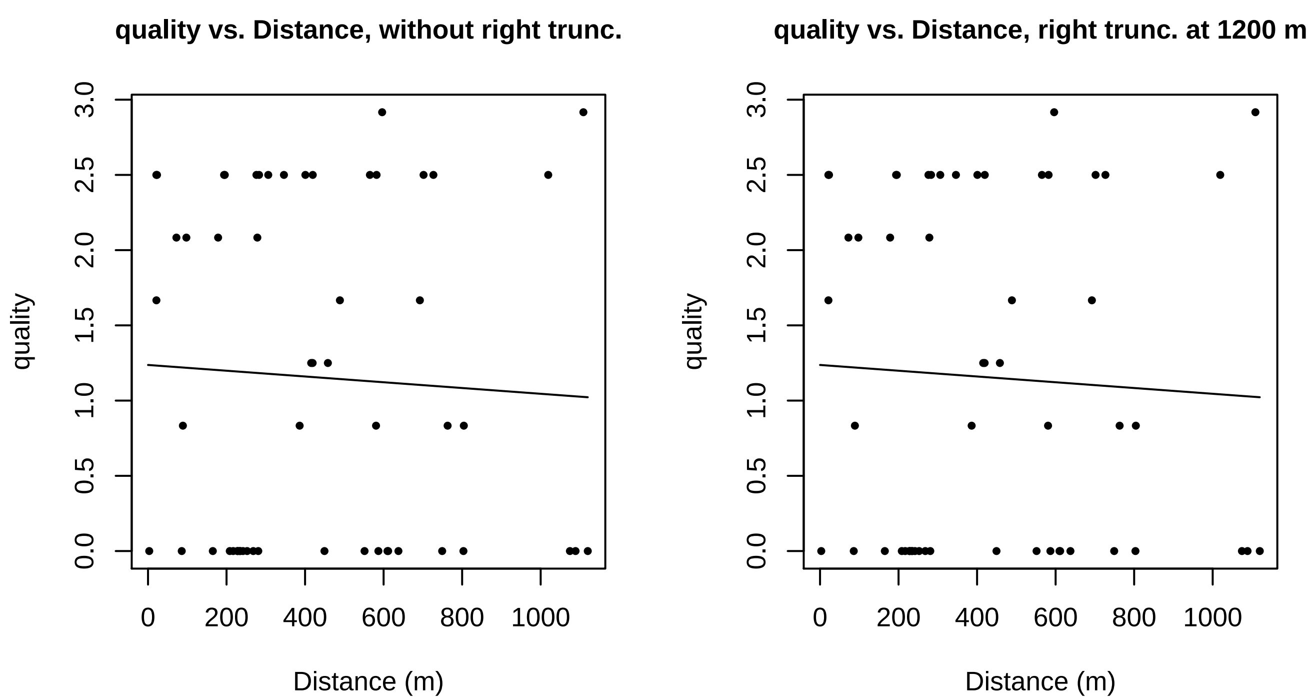

Figure 58: Scatterplots showing the relationship between the survey-specific index of the quality of observation conditions and perpendicular sighting distance, for all sightings (left) and only those not right truncated (right). Low values of the quality index correspond to better observation conditions. The line is a simple linear regression.

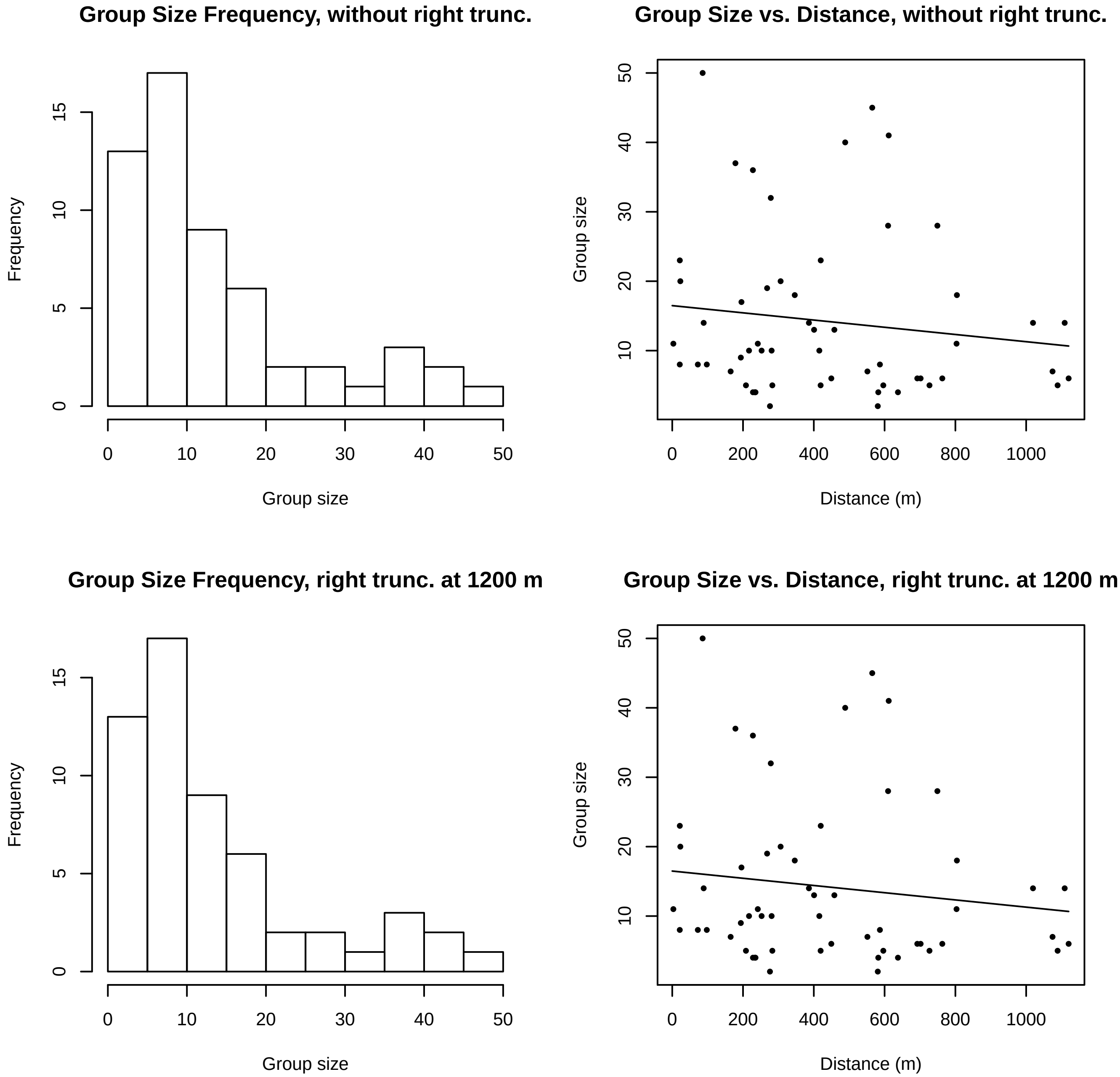

Figure 59: Histograms showing group size frequency and scatterplots showing the relationship between group size and perpendicular sighting distance, for all sightings (top row) and only those not right truncated (bottom row). In the scatterplot, the line is a simple linear regression.

NARWSS Grummans

Because this taxon was sighted too infrequently to fit a detection function to its sightings alone, we fit a detection function to the pooled sightings of several other species that we believed would exhibit similar detectability. These "proxy species" are listed below.

Reported By Observer	Common Name	n
Delphinus capensis	Long-beaked common dolphin	0
Delphinus delphis	Short-beaked common dolphin	42

Delphinus delphis/Lagenorhynchus acutus	Short-beaked common or Atlantic white-sided dolphin	0
Delphinus delphis/Stenella	Short-beaked common dolphin or Stenella spp.	0
Delphinus delphis/Stenella coeruleoalba	Short-beaked common or striped dolphin	0
Grampus griseus	Risso's dolphin	0
Grampus griseus/Tursiops truncatus	Risso's or Bottlenose dolphin	0
Lagenodelphis hosei	Fraser's dolphin	0
Lagenorhynchus acutus	Atlantic white-sided dolphin	288
Lagenorhynchus albirostris	White-beaked dolphin	3
Lagenorhynchus albirostris/Lagenorhynchus acutus	White-beaked or white-sided dolphin	0
Stenella	Unidentified Stenella	0
Stenella attenuata	Pantropical spotted dolphin	0
Stenella attenuata/frontalis	Pantropical or Atlantic spotted dolphin	0
Stenella clymene	Clymene dolphin	0
Stenella coeruleoalba	Striped dolphin	1
Stenella frontalis	Atlantic spotted dolphin	0
Stenella frontalis/Tursiops truncatus	Atlantic spotted or Bottlenose dolphin	0
Stenella longirostris	Spinner dolphin	0
Steno bredanensis	Rough-toothed dolphin	0
Steno bredanensis/Tursiops truncatus	Bottlenose or rough-toothed dolphin	0
Tursiops truncatus	Bottlenose dolphin	6
Total		340

Table 35: Proxy species used to fit detection functions for NARWSS Grummans. The number of sightings, n, is before truncation.

The sightings were right truncated at 800m. Due to a reduced frequency of sightings close to the trackline that plausibly resulted from the behavior of the observers and/or the configuration of the survey platform, the sightings were left truncted as well. Sightings closer than 107 m to the trackline were omitted from the analysis, and it was assumed that the the area closer to the trackline than this was not surveyed. This distance was estimated by inspecting histograms of perpendicular sighting distances.

Covariate	Description
beaufort	Beaufort sea state.
quality	Survey-specific index of the quality of observation conditions, utilizing relevant factors other than Beaufort sea state (see methods).
size	Estimated size (number of individuals) of the sighted group.

Table 36: Covariates tested in candidate "multi-covariate distance sampling" (MCDS) detection functions.

Key	Adjustment	Order	Covariates	Succeeded	Δ AIC	Mean ESHW (m)
hr			quality, size	Yes	0.00	235

hr			size	Yes	5.95	231
hr			beaufort, size	Yes	7.81	233
hr			quality	Yes	11.76	213
hn			size	Yes	14.26	231
hn			quality, size	Yes	14.51	233
hn			beaufort, size	Yes	16.23	231
hr				Yes	20.06	203
hr	poly	4		Yes	21.78	200
hr			beaufort	Yes	22.05	204
hr	poly	2		Yes	22.06	203
hn				Yes	33.54	223
hn			quality	Yes	33.86	223
hn	cos	3		Yes	34.13	179
hn	herm	4		Yes	35.13	222
hn	cos	2		No		
hn			beaufort	No		
hn			beaufort, quality	No		
hr			beaufort, quality	No		
hn			beaufort, quality, size	No		
hr			beaufort, quality, size	No		

Table 37: Candidate detection functions for NARWSS Grummans. The first one listed was selected for the density model.

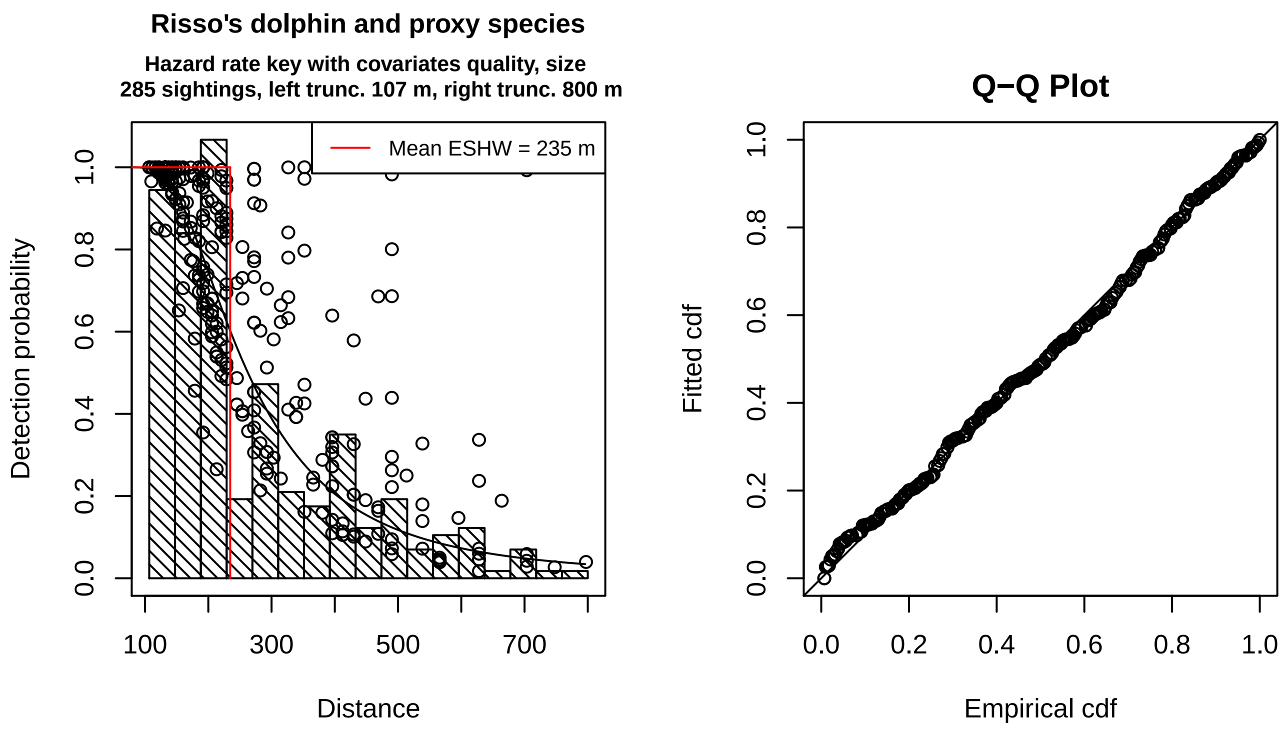

Figure 60: Detection function for NARWSS Grummans that was selected for the density model

Statistical output for this detection function:

```
Summary for ds object
Number of observations :  285
Distance range         :  106.5979  -  800
AIC                    :  3450.827

Detection function:
 Hazard-rate key function

Detection function parameters
Scale Coefficients:
              estimate         se
(Intercept)  5.5620259 0.12398130
quality     -0.2408179 0.09290192
size         0.2953779 0.09400126

Shape parameters:
            estimate        se
(Intercept) 1.119906 0.1056045

                       Estimate           SE        CV
Average p             0.2541682   0.03062592 0.1204947
N in covered region 1121.3045461 147.37019002 0.1314274
```

Additional diagnostic plots:

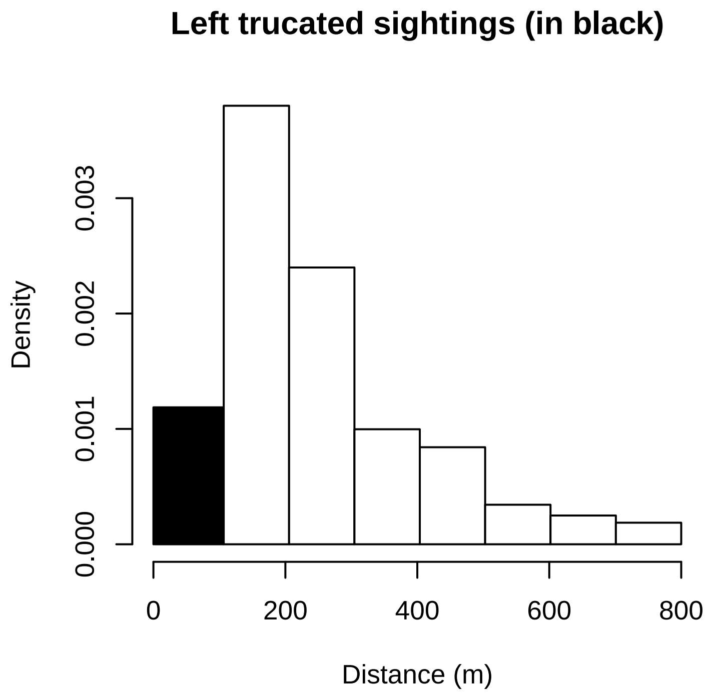

Figure 61: Density of sightings by perpendicular distance for NARWSS Grummans. Black bars on the left show sightings that were left truncated.

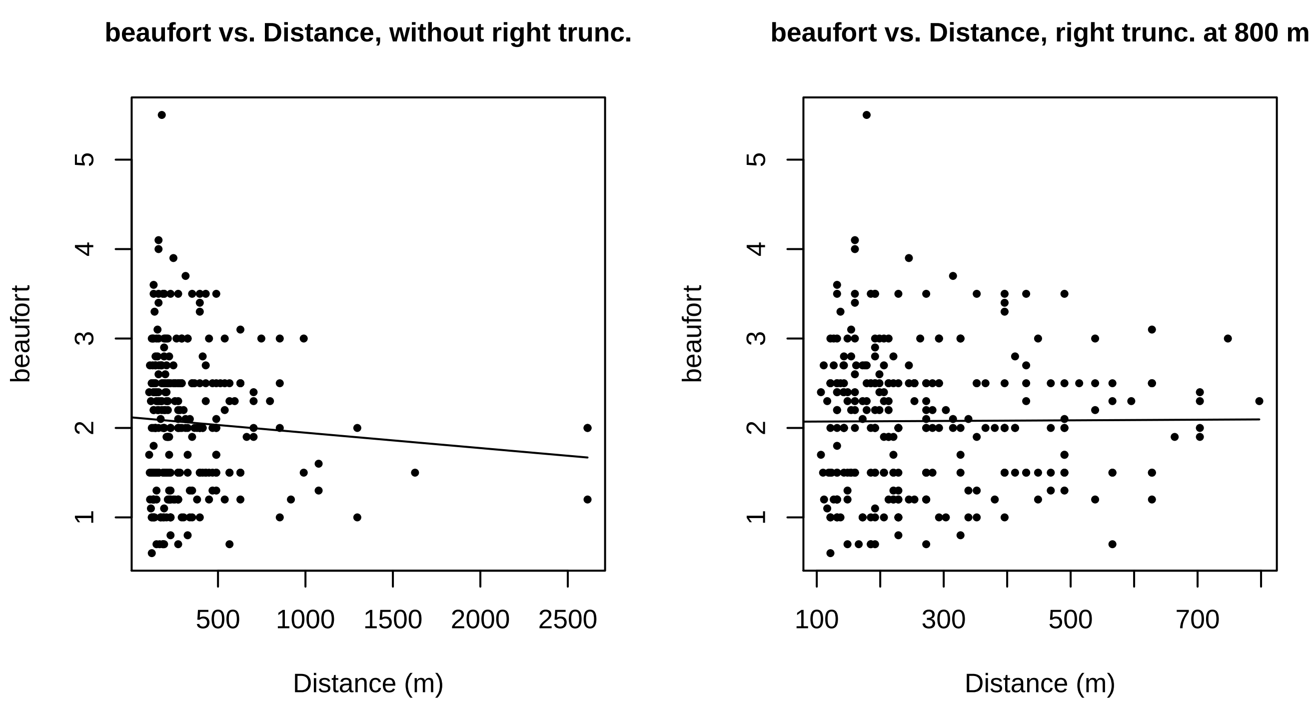

Figure 62: Scatterplots showing the relationship between Beaufort sea state and perpendicular sighting distance, for all sightings (left) and only those not right truncated (right). The line is a simple linear regression.

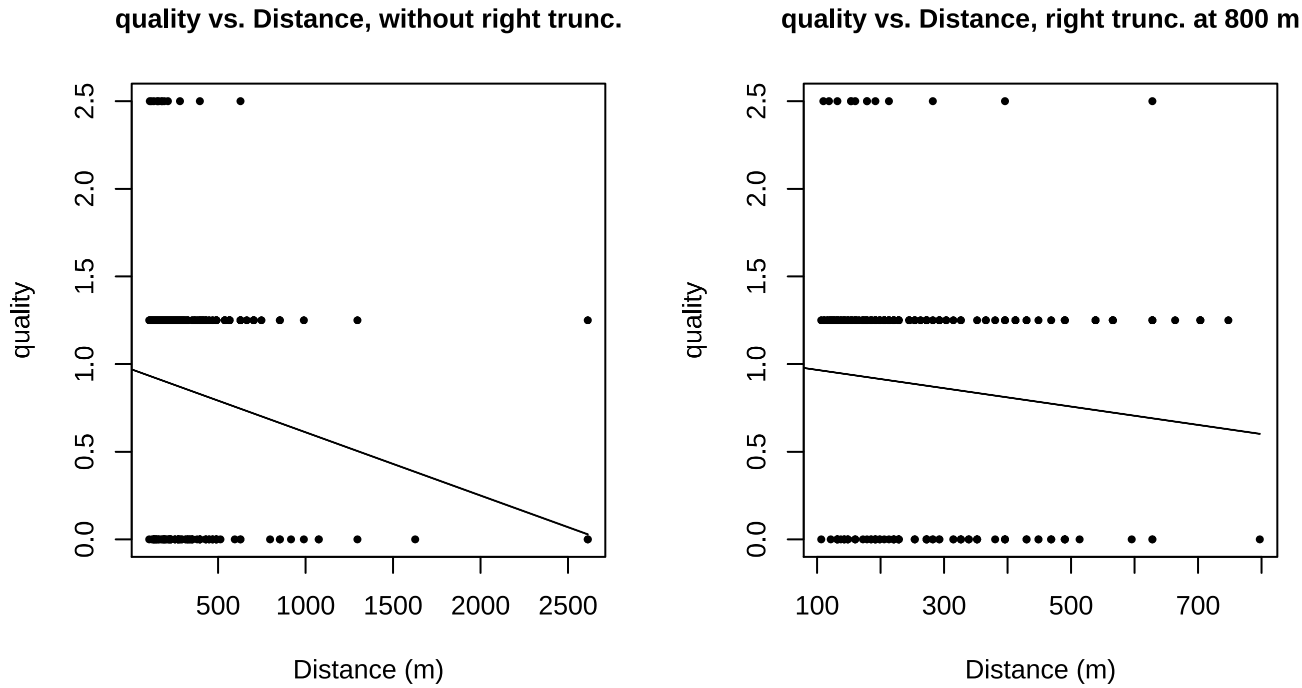

Figure 63: Scatterplots showing the relationship between the survey-specific index of the quality of observation conditions and perpendicular sighting distance, for all sightings (left) and only those not right truncated (right). Low values of the quality index correspond to better observation conditions. The line is a simple linear regression.

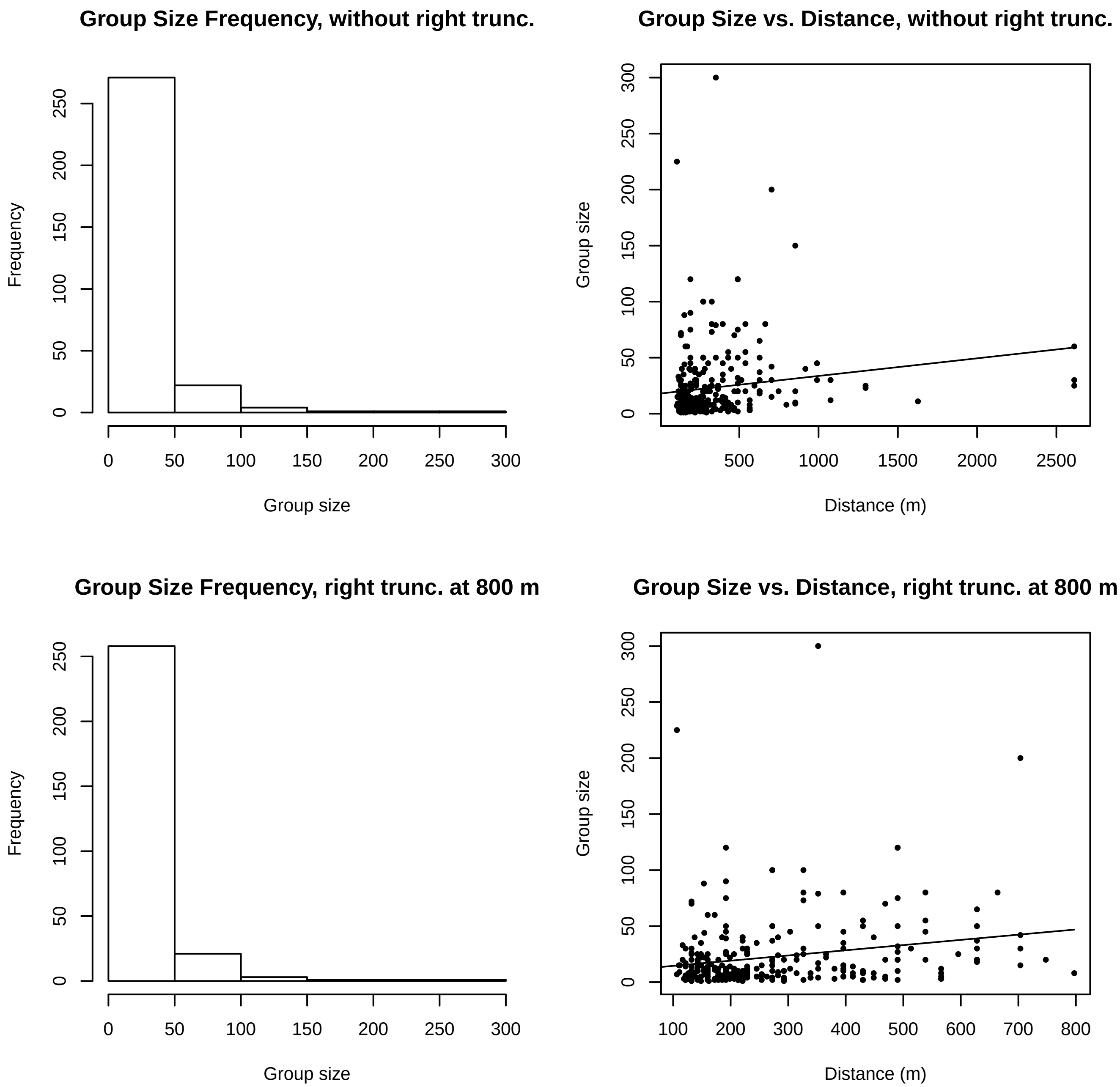

Figure 64: Histograms showing group size frequency and scatterplots showing the relationship between group size and perpendicular sighting distance, for all sightings (top row) and only those not right truncated (bottom row). In the scatterplot, the line is a simple linear regression.

NARWSS Twin Otters

Because this taxon was sighted too infrequently to fit a detection function to its sightings alone, we fit a detection function to the pooled sightings of several other species that we believed would exhibit similar detectability. These "proxy species" are listed below.

Reported By Observer	Common Name	n
Delphinus capensis	Long-beaked common dolphin	0
Delphinus delphis	Short-beaked common dolphin	539

Delphinus delphis/Lagenorhynchus acutus	Short-beaked common or Atlantic white-sided dolphin	0
Delphinus delphis/Stenella	Short-beaked common dolphin or Stenella spp.	0
Delphinus delphis/Stenella coeruleoalba	Short-beaked common or striped dolphin	0
Grampus griseus	Risso's dolphin	86
Grampus griseus/Tursiops truncatus	Risso's or Bottlenose dolphin	0
Lagenodelphis hosei	Fraser's dolphin	0
Lagenorhynchus acutus	Atlantic white-sided dolphin	1732
Lagenorhynchus albirostris	White-beaked dolphin	4
Lagenorhynchus albirostris/Lagenorhynchus acutus	White-beaked or white-sided dolphin	0
Stenella	Unidentified Stenella	1
Stenella attenuata	Pantropical spotted dolphin	0
Stenella attenuata/frontalis	Pantropical or Atlantic spotted dolphin	0
Stenella clymene	Clymene dolphin	0
Stenella coeruleoalba	Striped dolphin	4
Stenella frontalis	Atlantic spotted dolphin	0
Stenella frontalis/Tursiops truncatus	Atlantic spotted or Bottlenose dolphin	0
Stenella longirostris	Spinner dolphin	0
Steno bredanensis	Rough-toothed dolphin	0
Steno bredanensis/Tursiops truncatus	Bottlenose or rough-toothed dolphin	0
Tursiops truncatus	Bottlenose dolphin	39
Total		2405

Table 38: Proxy species used to fit detection functions for NARWSS Twin Otters. The number of sightings, n, is before truncation.

The sightings were right truncated at 2500m. Due to a reduced frequency of sightings close to the trackline that plausibly resulted from the behavior of the observers and/or the configuration of the survey platform, the sightings were left truncted as well. Sightings closer than 160 m to the trackline were omitted from the analysis, and it was assumed that the the area closer to the trackline than this was not surveyed. This distance was estimated by inspecting histograms of perpendicular sighting distances. The vertical sighting angles were heaped at 10 degree increments up to 80 degrees and 1 degree increments thereafter, so the candidate detection functions were fitted using linear bins scaled accordingly.

Covariate	Description
beaufort	Beaufort sea state.
quality	Survey-specific index of the quality of observation conditions, utilizing relevant factors other than Beaufort sea state (see methods).
size	Estimated size (number of individuals) of the sighted group.

Table 39: Covariates tested in candidate "multi-covariate distance sampling" (MCDS) detection functions.

Key	Adjustment	Order	Covariates	Succeeded	Δ AIC	Mean ESHW (m)

hr			beaufort, size	Yes	0.00	470
hr			size	Yes	5.29	463
hr			quality, size	Yes	7.11	463
hr	poly	2		Yes	9.16	430
hr	poly	4		Yes	10.71	442
hr			beaufort	Yes	17.46	464
hr				Yes	22.55	458
hr			quality	Yes	24.49	458
hn	cos	2		Yes	33.82	434
hn	cos	3		Yes	54.89	361
hn			beaufort, size	Yes	162.73	517
hn			size	Yes	162.85	518
hn			quality, size	Yes	164.00	518
hn			beaufort, quality, size	Yes	164.45	517
hn			beaufort	Yes	185.34	516
hn				Yes	186.28	516
hn	herm	4		Yes	186.91	516
hn			beaufort, quality	Yes	187.34	516
hn			quality	Yes	188.03	516
hr			beaufort, quality	No		
hr			beaufort, quality, size	No		

Table 40: Candidate detection functions for NARWSS Twin Otters. The first one listed was selected for the density model.

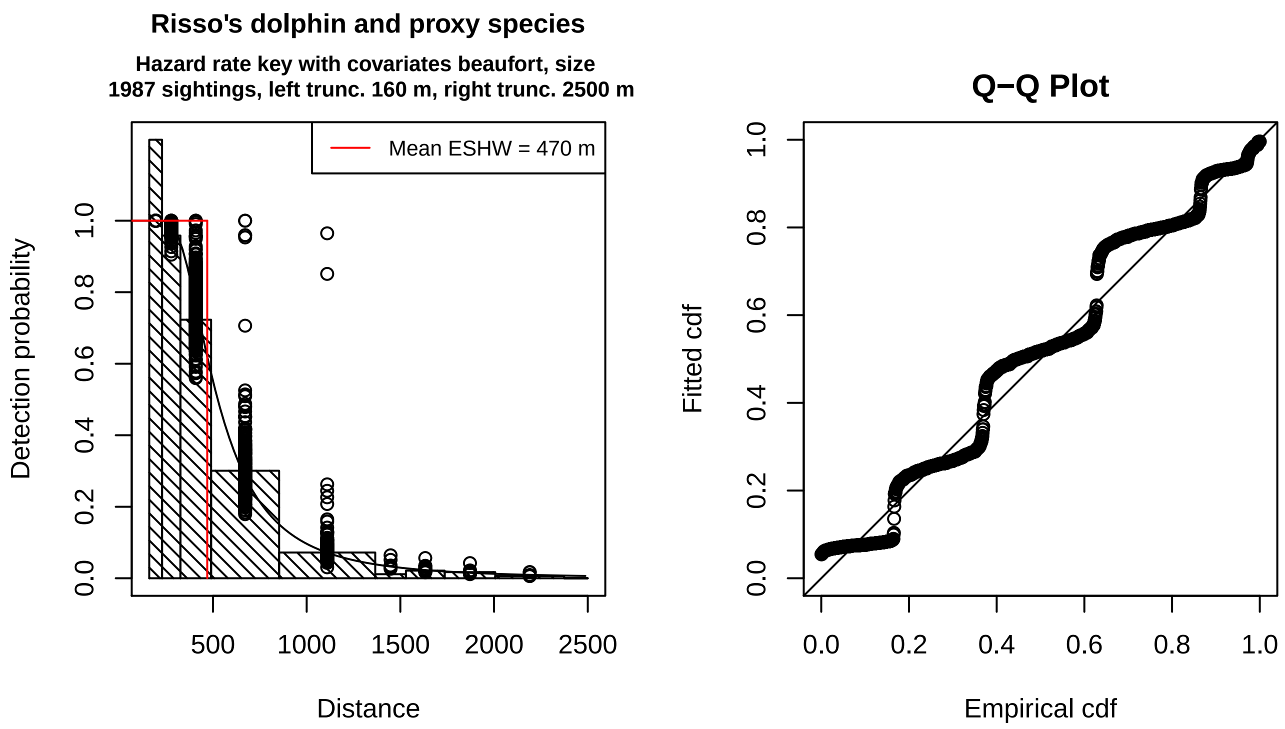

Figure 65: Detection function for NARWSS Twin Otters that was selected for the density model

Statistical output for this detection function:

```
Summary for ds object
Number of observations :  1987
Distance range         :  160.0674  -  2500
AIC                    :  6745.856

Detection function:
 Hazard-rate key function

Detection function parameters
Scale Coefficients:
              estimate         se
(Intercept)  6.26395198 0.06468196
beaufort    -0.07274292 0.02643651
size         0.08974254 0.02445737

Shape parameters:
            estimate        se
(Intercept) 1.110483 0.0356417

                        Estimate           SE         CV
Average p           1.845364e-01 5.774489e-03 0.03129187
N in covered region 1.076752e+04 4.016208e+02 0.03729928
```

Additional diagnostic plots:

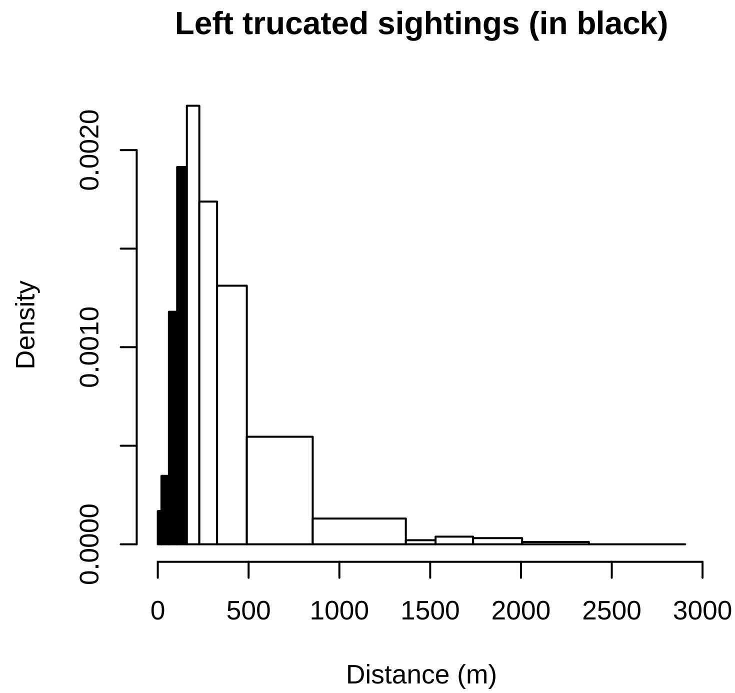

Figure 66: Density of sightings by perpendicular distance for NARWSS Twin Otters. Black bars on the left show sightings that were left truncated.

Figure 67: Scatterplots showing the relationship between Beaufort sea state and perpendicular sighting distance, for all sightings (left) and only those not right truncated (right). The line is a simple linear regression.

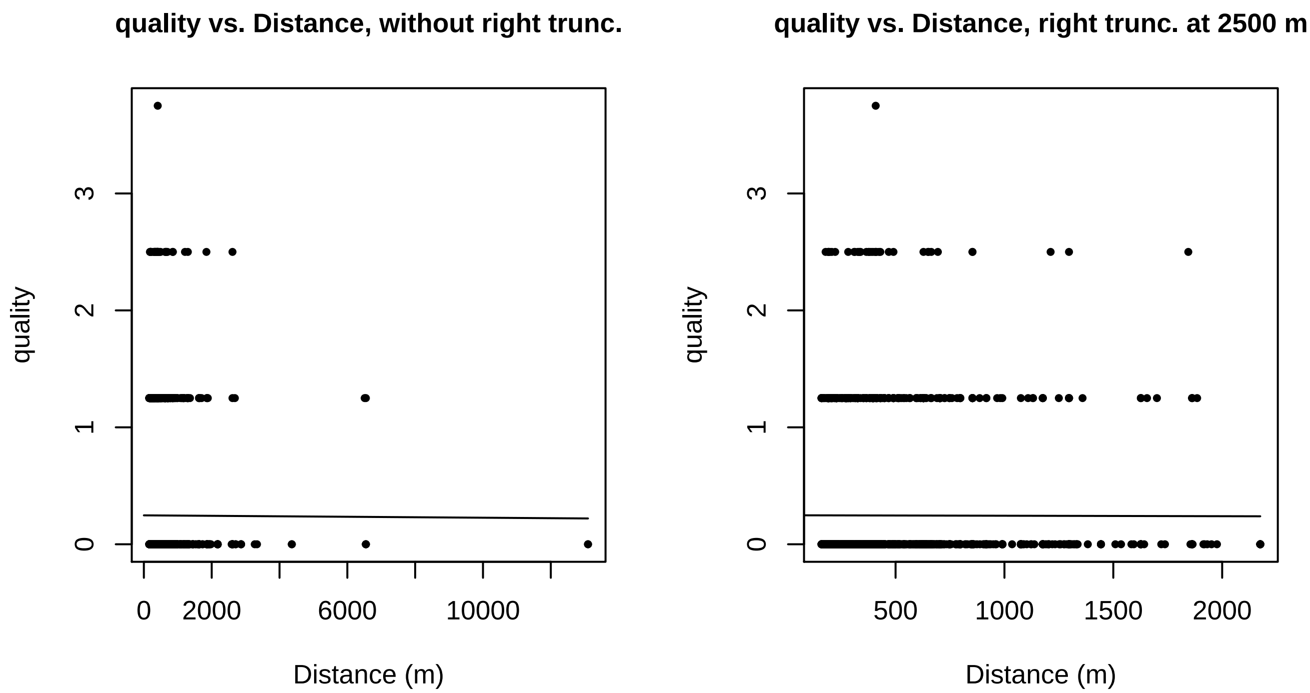

Figure 68: Scatterplots showing the relationship between the survey-specific index of the quality of observation conditions and perpendicular sighting distance, for all sightings (left) and only those not right truncated (right). Low values of the quality index correspond to better observation conditions. The line is a simple linear regression.

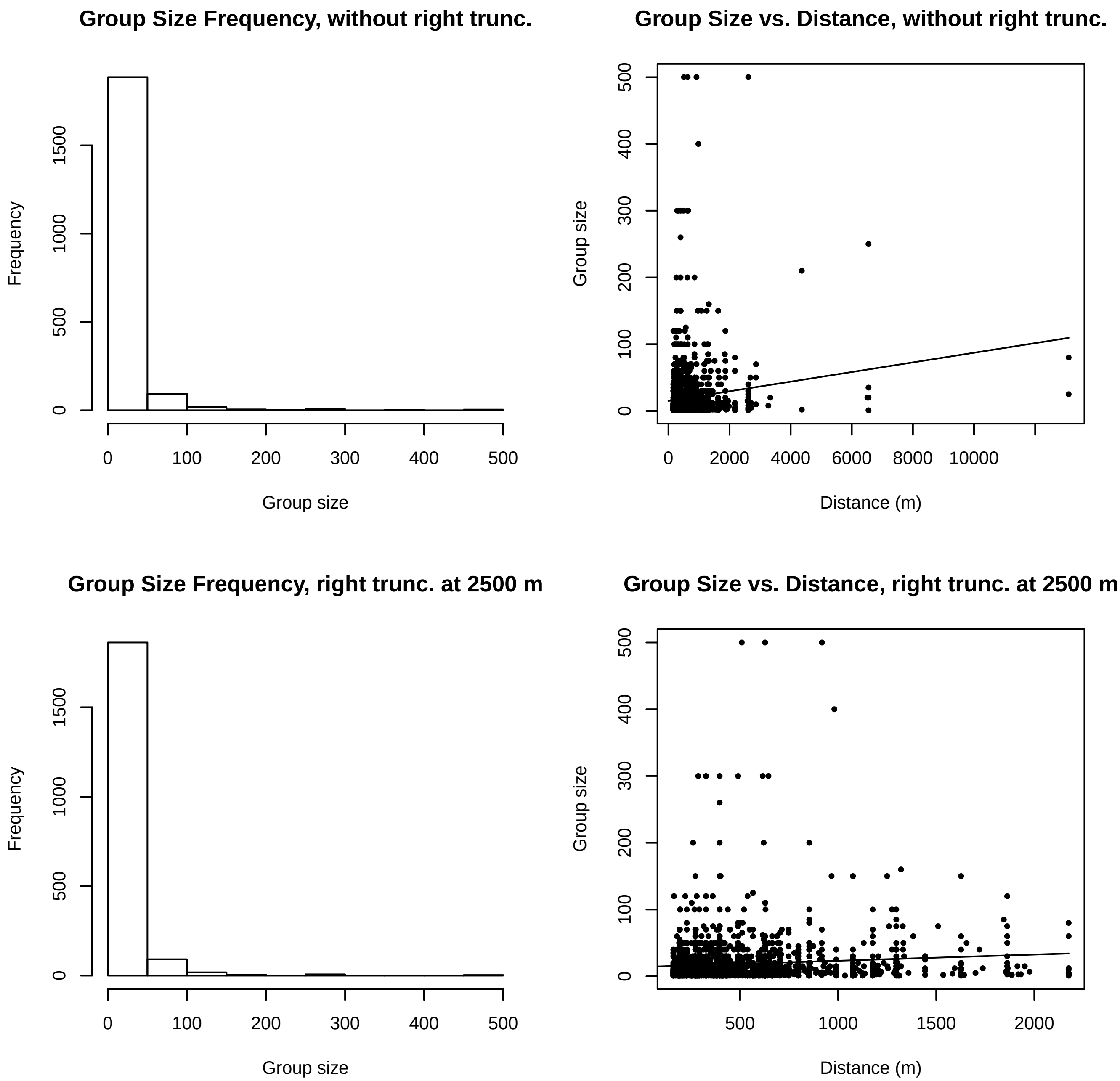

Figure 69: Histograms showing group size frequency and scatterplots showing the relationship between group size and perpendicular sighting distance, for all sightings (top row) and only those not right truncated (bottom row). In the scatterplot, the line is a simple linear regression.

g(0) Estimates

Platform	Surveys	Group Size	*g(0)*	Biases Addressed	Source
Shipboard	All	1-20	0.856	Perception	Barlow and Forney (2007)
		>20	0.970	Perception	Barlow and Forney (2007)
Shipboard	NEFSC Abel-J Binocular Surveys	Any	0.61	Perception	Palka (2006)
Shipboard	NEFSC Endeavor	Any	0.84	Perception	Palka (2006)
Aerial	All	1-5	0.43	Both	Palka (2006)
		>5	0.960	Both	Carretta et al. (2000)

Table 41: Estimates of *g(0)* used in this density model.

For shipboard surveys other than the NOAA NEFSC cruises for which Palka (2006) provided survey-specific estimates of g(0), we utilized Barlow and Forney's (2007) estimates for delphinids, produced from several years of dual-team surveys that used similar binoculars and protocols to the surveys in our study. This study provided separate estimates for small and large groups, but pooled sightings of several species together to provide a generic estimate for all delphinids, due to sample-size limitations. To our knowledge, there is no species-specific shipboard g(0) estimate that treats small and large groups separately, so we believe Barlow and Forney (2007) provide the best general- purpose alternative. Their estimate accounted for perception bias but not availability bias; dive times for dolphins are short enough that availability bias is not expected to be significant for dolphins observed from shipboard surveys.

For aerial surveys, we were unable to locate species-specific g(0) estimates in the literature. For small groups, defined here as 1-5 individuals, we used Palka's (2006) estimate of g(0) for groups of 1-5 small cetaceans, estimated from two years of aerial surveys using the Hiby (1999) circle-back method. This estimate accounted for both availability and perception bias, but pooled sightings of several species together to provide a generic estimate for all delphinids, due to sample-size limitations. For large groups, defined here as greater than 5 individuals, Palka (2006) assumed that g(0) was 1. When we discussed this with NOAA SWFSC reviewers, they agreed that it was safe to assume that the availability bias component of g(0) was 1 but insisted that perception bias should be slightly less than 1, because it was possible to miss large groups. We agreed to take a conservative approach and obtained our g(0) for large groups from Carretta et al. (2000), who estimated g(0) for both small and large groups of delphinids. We used Carretta et al.'s g(0) estimate for groups of 1-25 individuals (0.960), rather than their larger one for more than 25 individuals (0.994), to account for the fact that we were using Palka's definition of large groups as those with more than 5 individuals.

Density Models

A recent comprehensive review of the global distribution reported that Risso's dolphins "occur in all habitats from coastal to oceanic [but] show a strong preference for the mid-temperate waters of the continental shelf and slope between 30-45 degrees latitude", (Jefferson et al. 2014). This description is consistent with the sightings reported by the surveys we utilized: most sightings occurred on the continental slope close to the shelf break, while fewer sightings occurred on the shelf and in waters deeper than the slope. Little information is available about the seasonal distribution of Risso's dolphins in the study area. The population is reported to occupy the mid-Atlantic continental shelf edge year round, and may expand northward onto the shelf of Georges Bank and into the Gulf of Maine during spring, summer and fall, contracting southward in winter (Waring et al. 2014; CETAP 1982).

Given this year-round presence, we modeled Risso's dolphin abundance with a single, year-round model that incorporated all available survey data. We modeled the shelf and the slope/abyss separately, under the presumption that abundance might relate to different ecological processes in these two areas. Although survey effort off the continental shelf was sparse in non-summer months, we allowed the model to predict off-shelf during all months of the year. These predictions should be viewed with due caution.

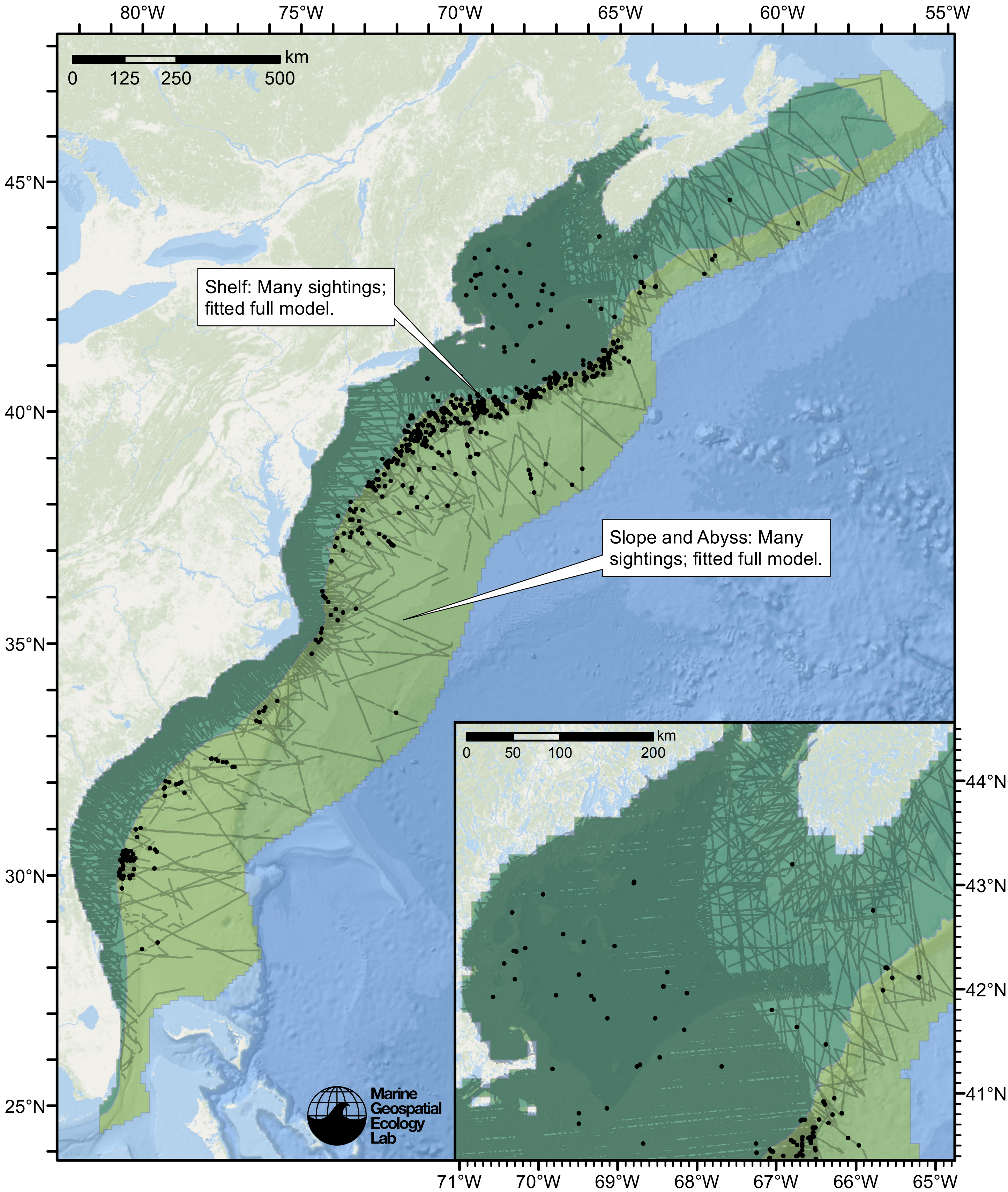

Figure 70: Risso's dolphin density model schematic. All on-effort sightings are shown, including those that were truncated when detection functions were fitted.

Climatological Model

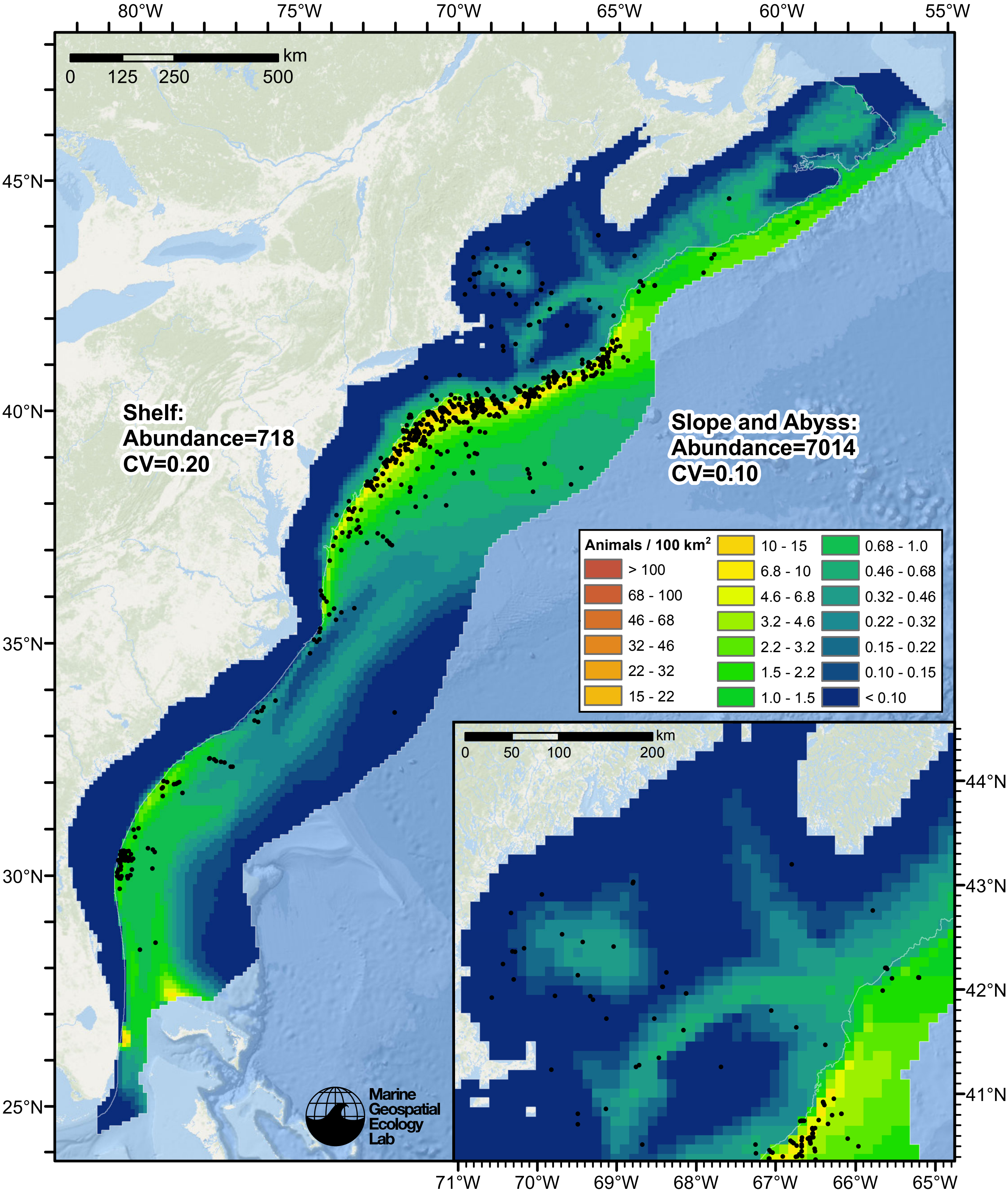

Figure 71: Risso's dolphin density predicted by the climatological model that explained the most deviance. Pixels are 10x10 km. The legend gives the estimated individuals per pixel; breaks are logarithmic. Abundance for each region was computed by summing the density cells occuring in that region.

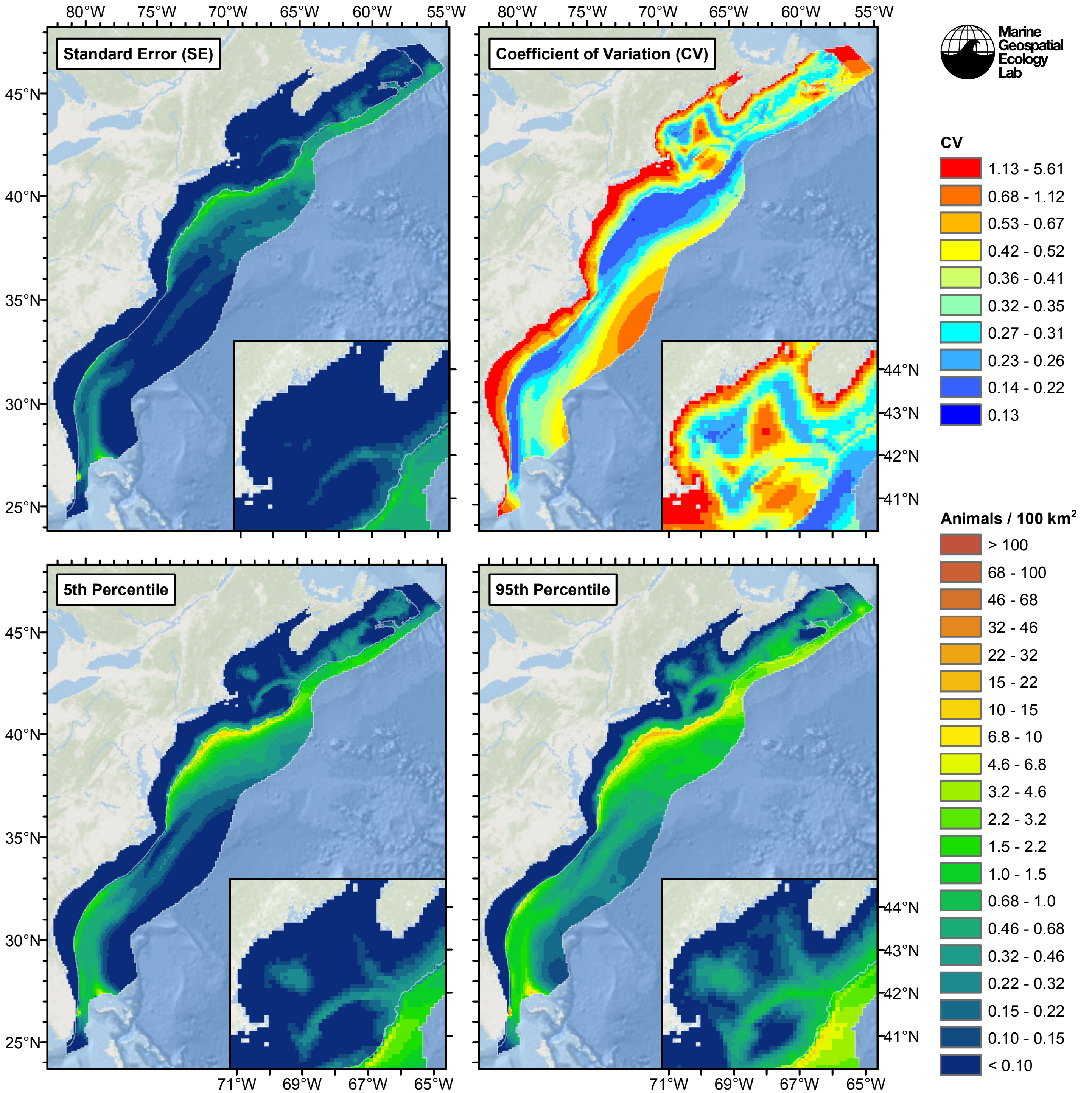

Figure 72: Estimated uncertainty for the climatological model that explained the most deviance. These estimates only incorporate the statistical uncertainty estimated for the spatial model (by the R mgcv package). They do not incorporate uncertainty in the detection functions, g(0) estimates, predictor variables, and so on.

Slope and Abyss

Statistical output

```
Rscript.exe: This is mgcv 1.8-2. For overview type 'help("mgcv-package")'.


Family: Tweedie(p=1.306)
```

```
Link function: log

Formula:
abundance ~ offset(log(area_km2)) + s(log10(Depth), bs = "ts",
    k = 5) + s(ClimSST, bs = "ts", k = 5) + s(I(ClimDistToFront1^(1/3)),
    bs = "ts", k = 5) + s(log10(pmax(ClimTKE, 1e-04)), bs = "ts",
    k = 5) + s(I(ClimDistToAEddy9/1000), bs = "ts", k = 5) +
    s(I(ClimDistToCEddy9/1000), bs = "ts", k = 5) + s(log10(pmax(ClimPkPB,
    0.01)), bs = "ts", k = 5)

Parametric coefficients:
            Estimate Std. Error t value Pr(>|t|)
(Intercept)  -4.7651     0.1038   -45.9   <2e-16 ***
---
Signif. codes:  0 '***' 0.001 '**' 0.01 '*' 0.05 '.' 0.1 ' ' 1

Approximate significance of smooth terms:
                                  edf Ref.df      F  p-value
s(log10(Depth))                3.2371      4  4.901 8.89e-05 ***
s(ClimSST)                     1.8838      4 12.459 1.84e-13 ***
s(I(ClimDistToFront1^(1/3)))   1.0478      4  5.041 2.70e-06 ***
s(log10(pmax(ClimTKE, 1e-04))) 2.6429      4  4.545 6.12e-05 ***
s(I(ClimDistToAEddy9/1000))    0.8552      4  1.204   0.0142 *
s(I(ClimDistToCEddy9/1000))    3.0212      4  6.313 1.83e-06 ***
s(log10(pmax(ClimPkPB, 0.01))) 3.5491      4 15.059 1.05e-14 ***
---
Signif. codes:  0 '***' 0.001 '**' 0.01 '*' 0.05 '.' 0.1 ' ' 1

R-sq.(adj) =  0.0932   Deviance explained = 47.5%
-REML = 3191.2  Scale est. = 43.783    n = 17198

All predictors were significant. This is the final model.
Creating term plots.
Diagnostic output from gam.check():

Method: REML   Optimizer: outer newton
full convergence after 14 iterations.
Gradient range [-1.372747e-05,4.728031e-06]
(score 3191.195 & scale 43.78282).
Hessian positive definite, eigenvalue range [0.3460342,1164.008].
Model rank =  29 / 29

Basis dimension (k) checking results. Low p-value (k-index<1) may
indicate that k is too low, especially if edf is close to k'.

                                  k'   edf k-index p-value
s(log10(Depth))                4.000 3.237   0.745    0.02
s(ClimSST)                     4.000 1.884   0.772    0.60
s(I(ClimDistToFront1^(1/3)))   4.000 1.048   0.754    0.08
s(log10(pmax(ClimTKE, 1e-04))) 4.000 2.643   0.718    0.00
s(I(ClimDistToAEddy9/1000))    4.000 0.855   0.767    0.31
s(I(ClimDistToCEddy9/1000))    4.000 3.021   0.752    0.03
s(log10(pmax(ClimPkPB, 0.01))) 4.000 3.549   0.737    0.00

Predictors retained during the model selection procedure: Depth, ClimSST, ClimDistToFront1, ClimTKE,
ClimDistToAEddy9, ClimDistToCEddy9, ClimPkPB

Predictors dropped during the model selection procedure: Slope, DistTo125m
```

Model term plots

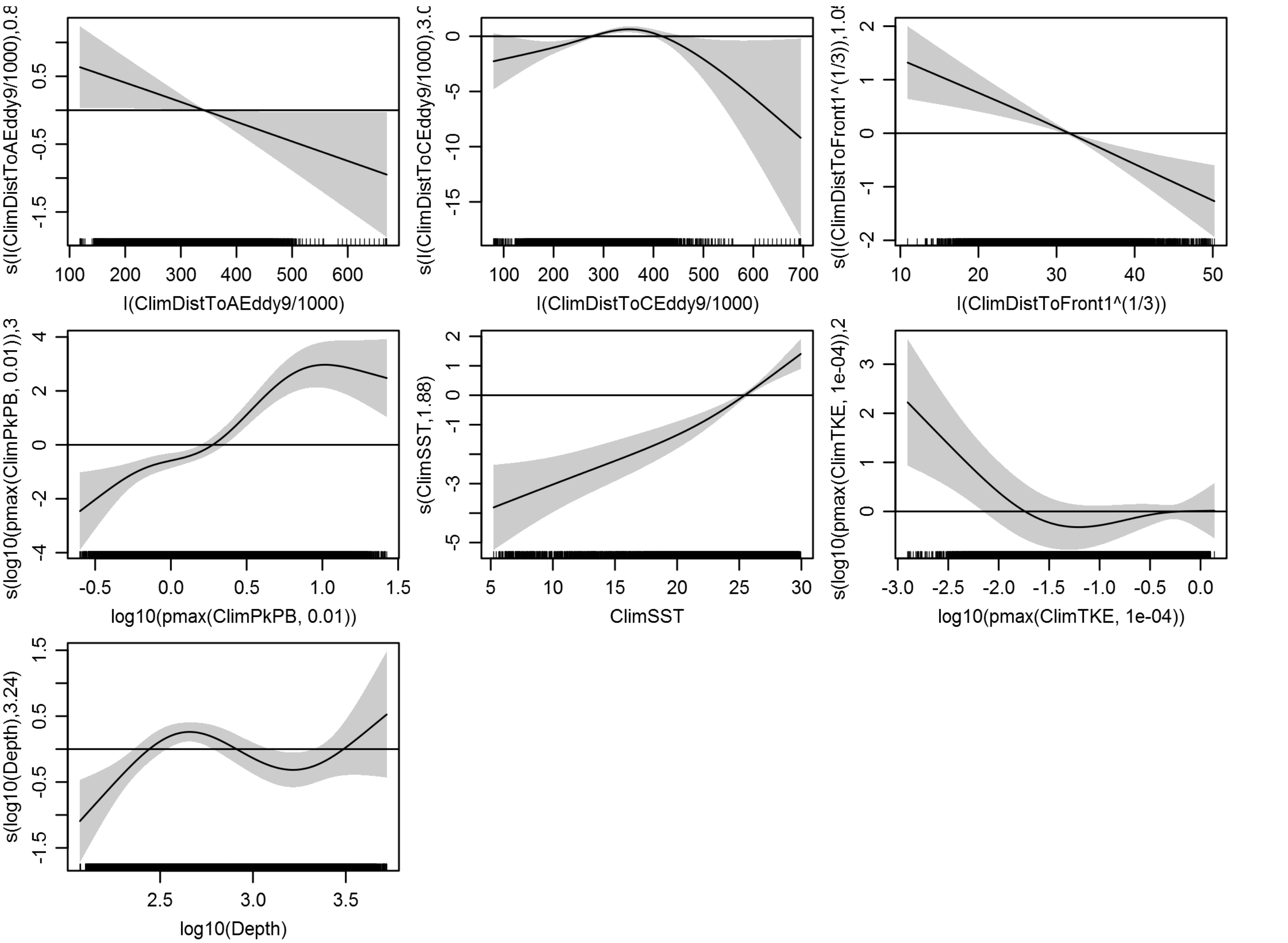

Diagnostic plots

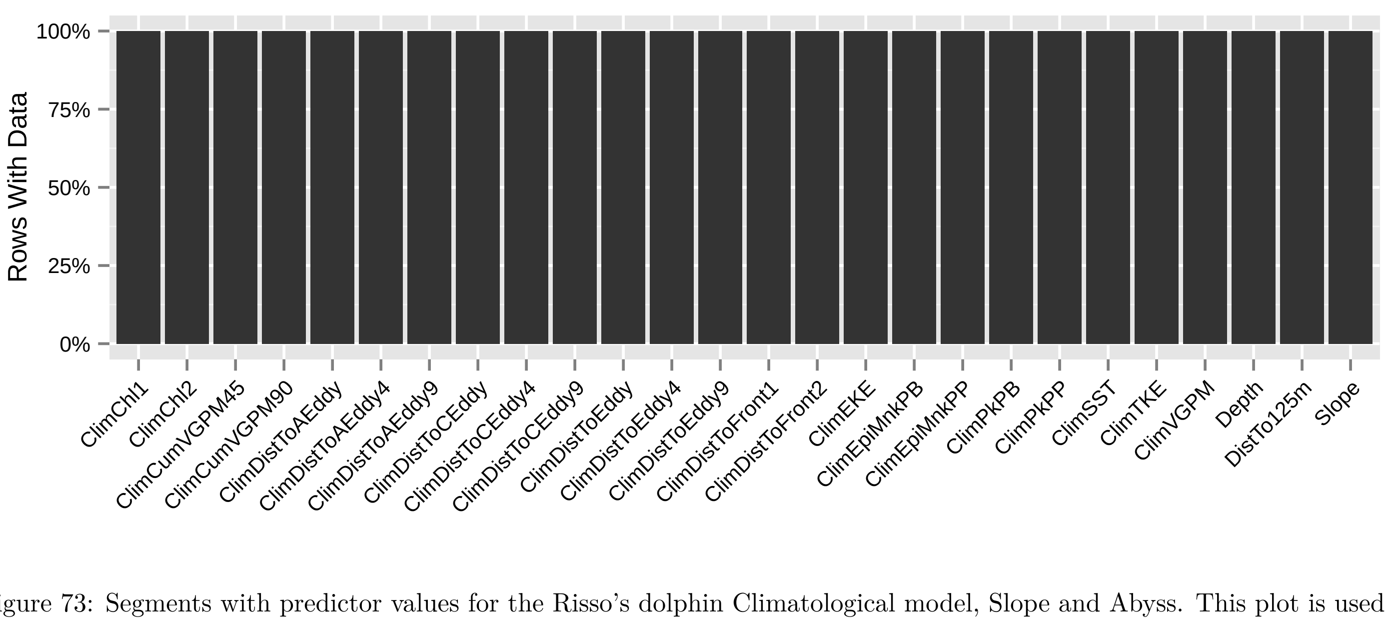

Figure 73: Segments with predictor values for the Risso's dolphin Climatological model, Slope and Abyss. This plot is used to assess how many segments would be lost by including a given predictor in a model.

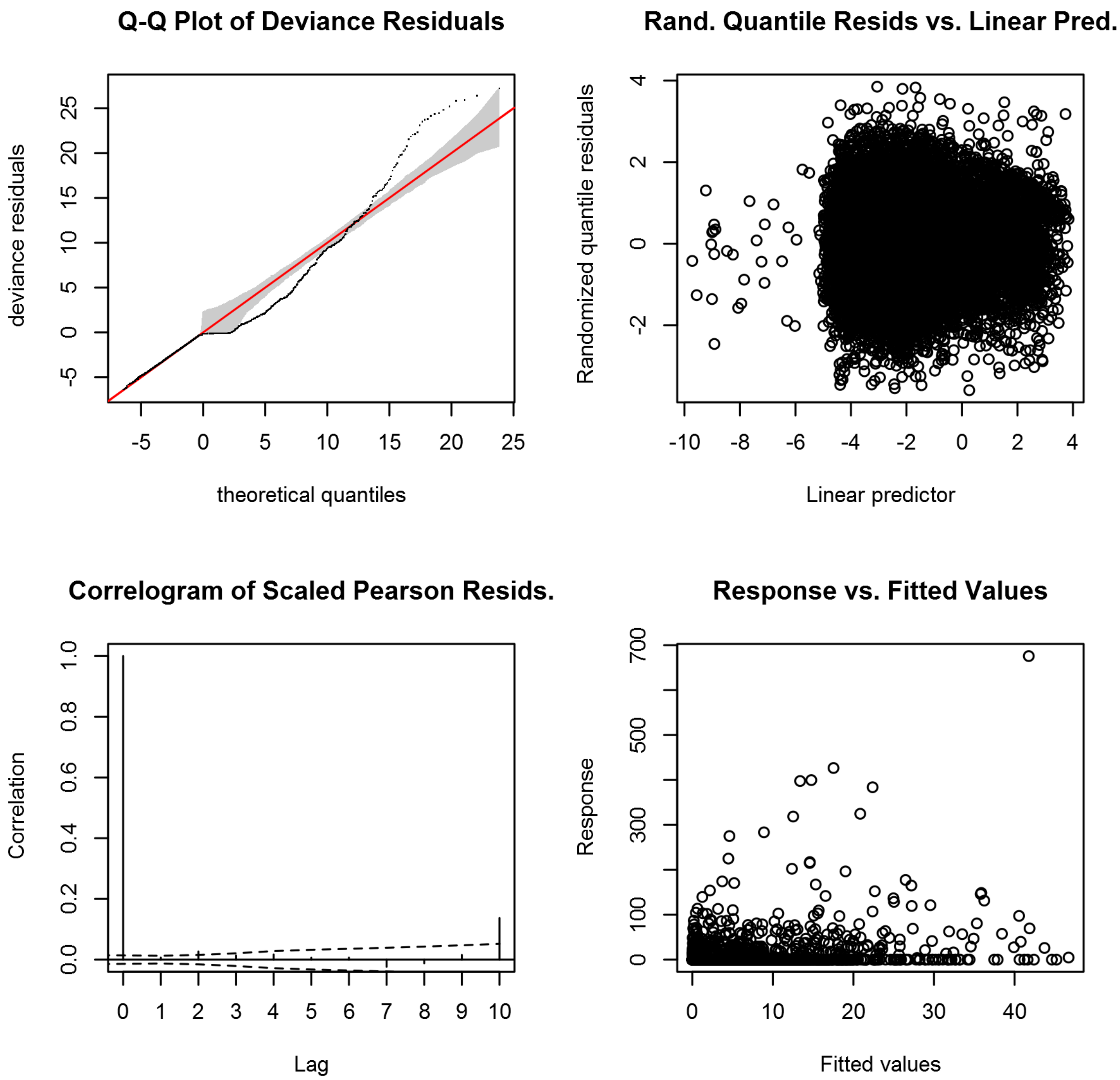

Figure 74: Statistical diagnostic plots for the Risso's dolphin Climatological model, Slope and Abyss.

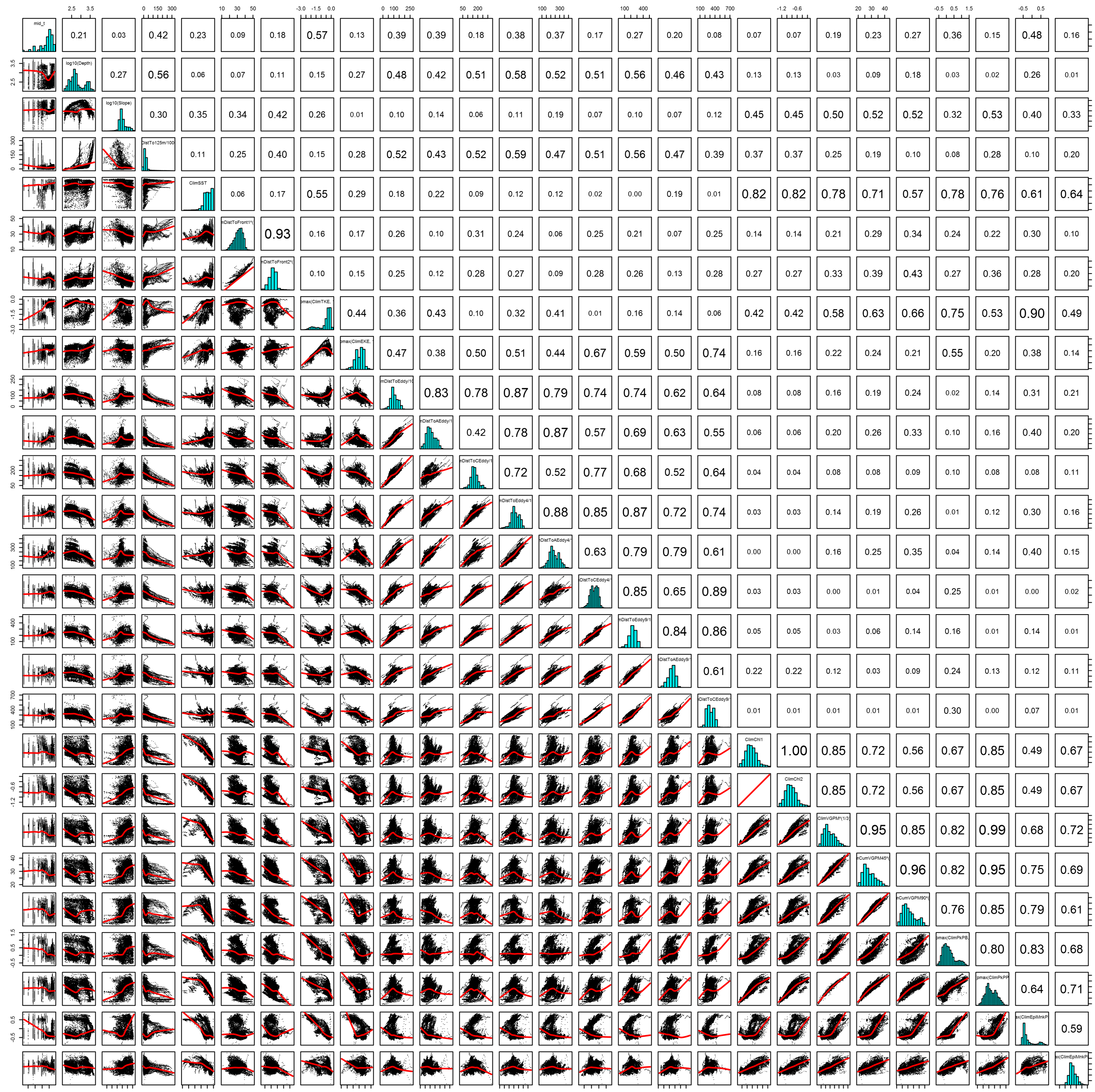

Figure 75: Scatterplot matrix for the Risso's dolphin Climatological model, Slope and Abyss. This plot is used to inspect the distribution of predictors (via histograms along the diagonal), simple correlation between predictors (via pairwise Pearson coefficients above the diagonal), and linearity of predictor correlations (via scatterplots below the diagonal). This plot is best viewed at high magnification.

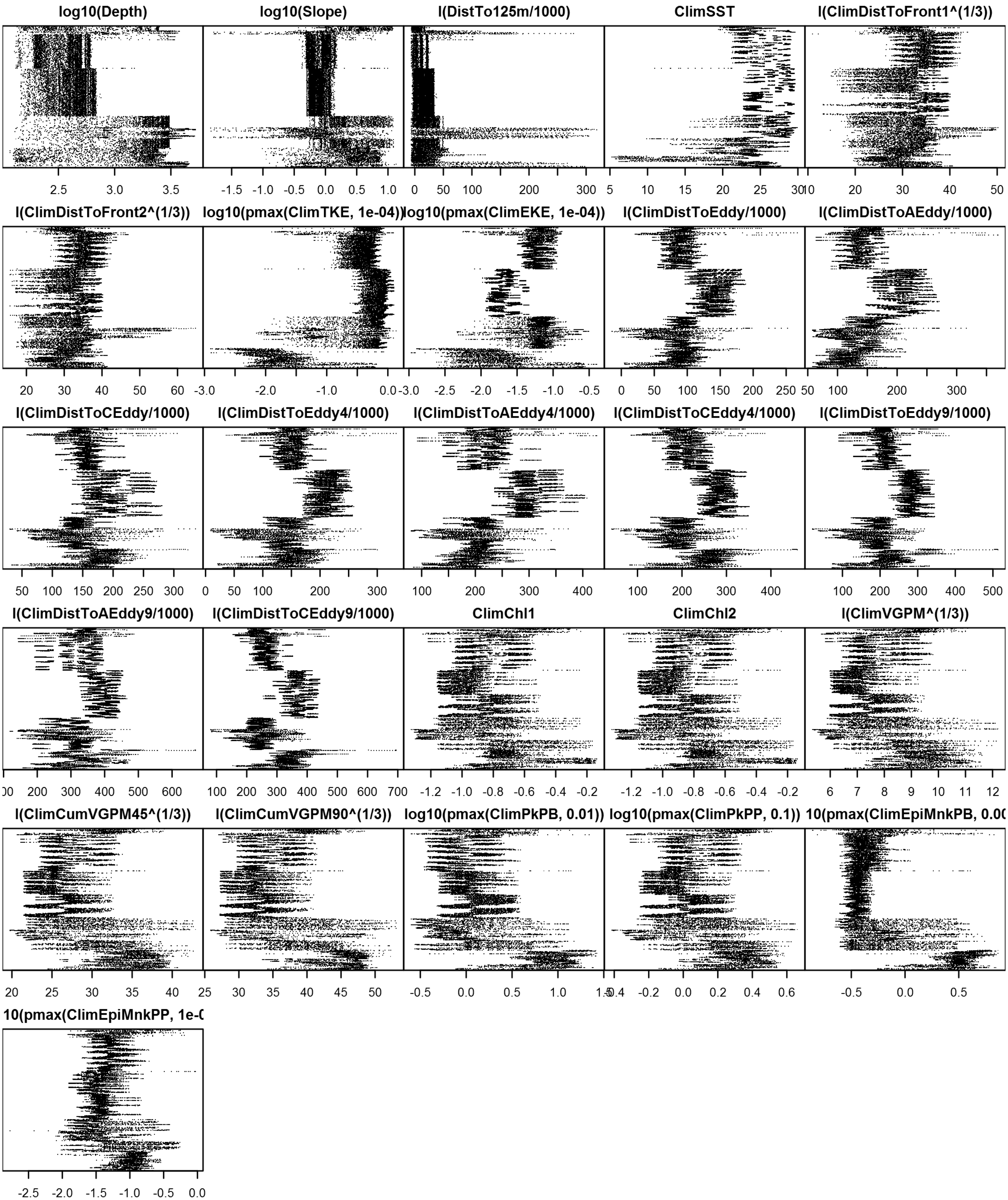

Figure 76: Dotplot for the Risso's dolphin Climatological model, Slope and Abyss. This plot is used to check for suspicious patterns and outliers in the data. Points are ordered vertically by transect ID, sequentially in time.

Shelf

Statistical output

```
Rscript.exe: This is mgcv 1.8-2. For overview type 'help("mgcv-package")'.


Family: Tweedie(p=1.328)
Link function: log

Formula:
abundance ~ offset(log(area_km2)) + s(log10(Depth), bs = "ts",
    k = 5) + s(sqrt(DistToShore/1000), bs = "ts", k = 5) + s(I(DistTo125m/1000),
    bs = "ts", k = 5) + s(ClimSST, bs = "ts", k = 5) + s(log10(pmax(ClimEpiMnkPB,
    0.001)), bs = "ts", k = 5)

Parametric coefficients:
            Estimate Std. Error t value Pr(>|t|)
(Intercept)  -9.3447     0.4535   -20.6   <2e-16 ***
---
Signif. codes:  0 '***' 0.001 '**' 0.01 '*' 0.05 '.' 0.1 ' ' 1

Approximate significance of smooth terms:
                                      edf Ref.df     F  p-value
s(log10(Depth))                    1.6180      4 2.984 0.000424 ***
s(sqrt(DistToShore/1000))          2.1658      4 5.184 8.51e-06 ***
s(I(DistTo125m/1000))              2.6077      4 4.333 0.000115 ***
s(ClimSST)                         1.0376      4 4.543 1.01e-05 ***
s(log10(pmax(ClimEpiMnkPB, 0.001))) 0.9495      4 3.407 8.77e-05 ***
---
Signif. codes:  0 '***' 0.001 '**' 0.01 '*' 0.05 '.' 0.1 ' ' 1

R-sq.(adj) =  0.00771   Deviance explained = 37.5%
-REML = 875.41  Scale est. = 134.98    n = 87038

All predictors were significant. This is the final model.
Creating term plots.
Diagnostic output from gam.check():

Method: REML   Optimizer: outer newton
full convergence after 15 iterations.
Gradient range [-0.0001562237,0.0001303444]
(score 875.4145 & scale 134.9759).
Hessian positive definite, eigenvalue range [0.1762516,415.9214].
Model rank =  21 / 21

Basis dimension (k) checking results. Low p-value (k-index<1) may
indicate that k is too low, especially if edf is close to k'.

                                       k'   edf k-index p-value
s(log10(Depth))                     4.000 1.618   0.656    0.00
s(sqrt(DistToShore/1000))           4.000 2.166   0.687    0.00
s(I(DistTo125m/1000))               4.000 2.608   0.671    0.01
s(ClimSST)                          4.000 1.038   0.725    0.00
s(log10(pmax(ClimEpiMnkPB, 0.001))) 4.000 0.949   0.695    0.00

Predictors retained during the model selection procedure: Depth, DistToShore, DistTo125m, ClimSST,
ClimEpiMnkPB
```

Predictors dropped during the model selection procedure: Slope, ClimDistToFront1, ClimTKE

Model term plots

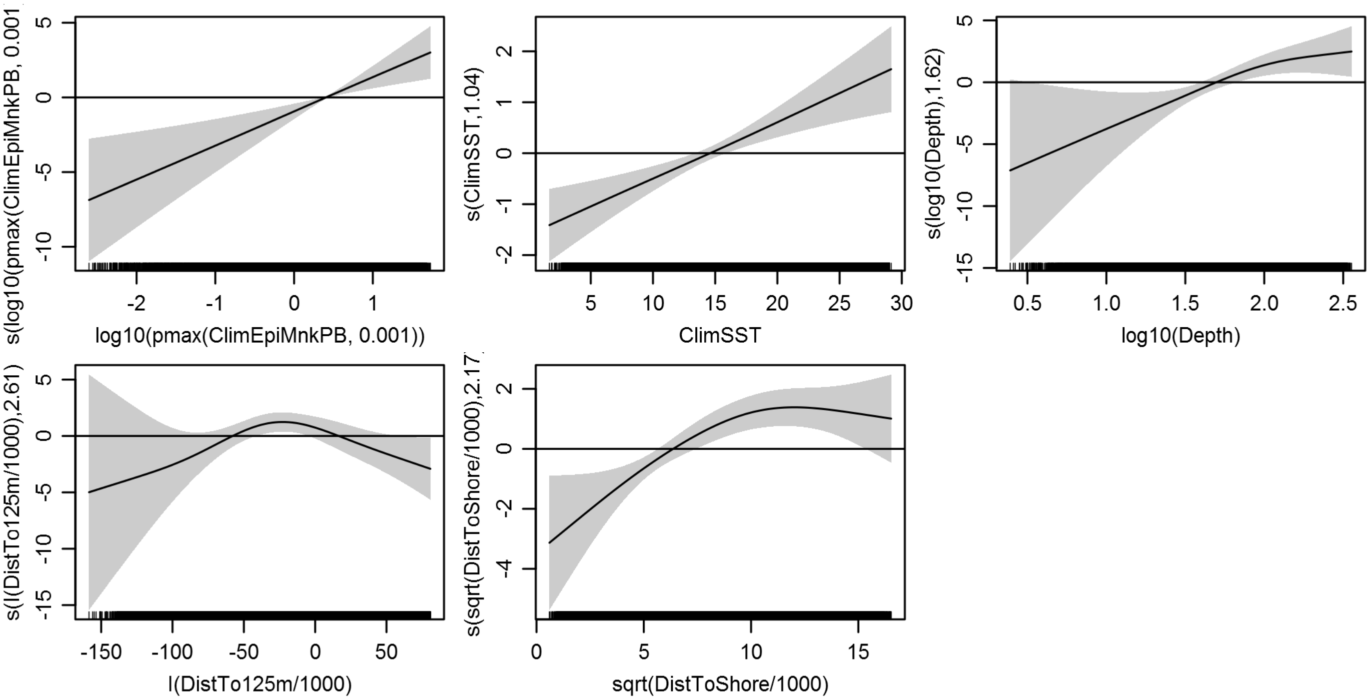

Diagnostic plots

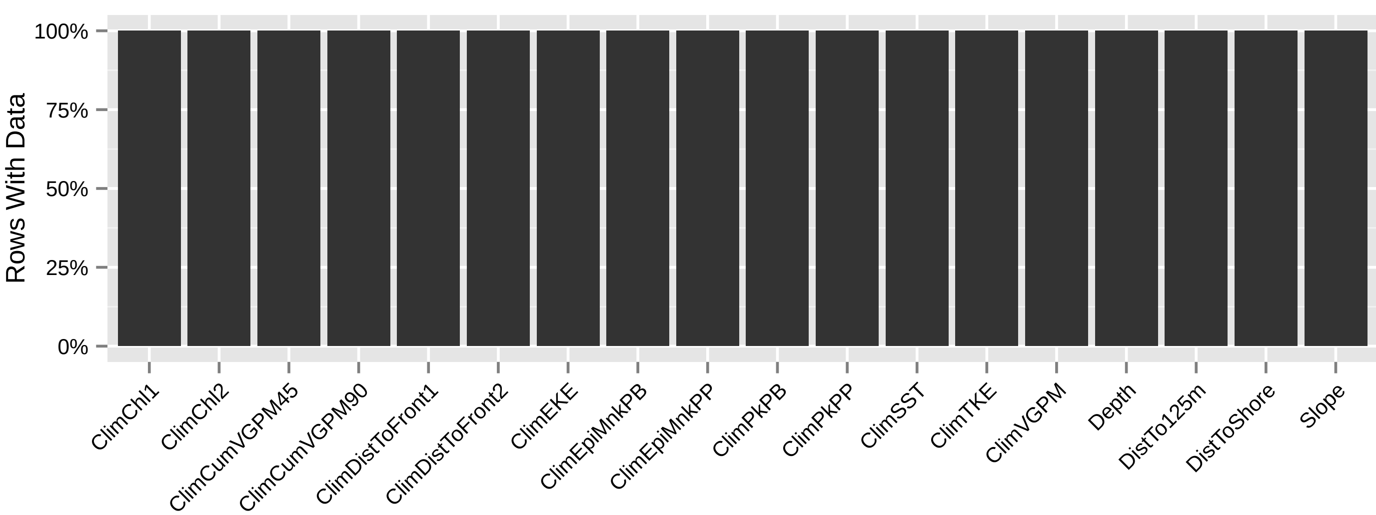

Figure 77: Segments with predictor values for the Risso's dolphin Climatological model, Shelf. This plot is used to assess how many segments would be lost by including a given predictor in a model.

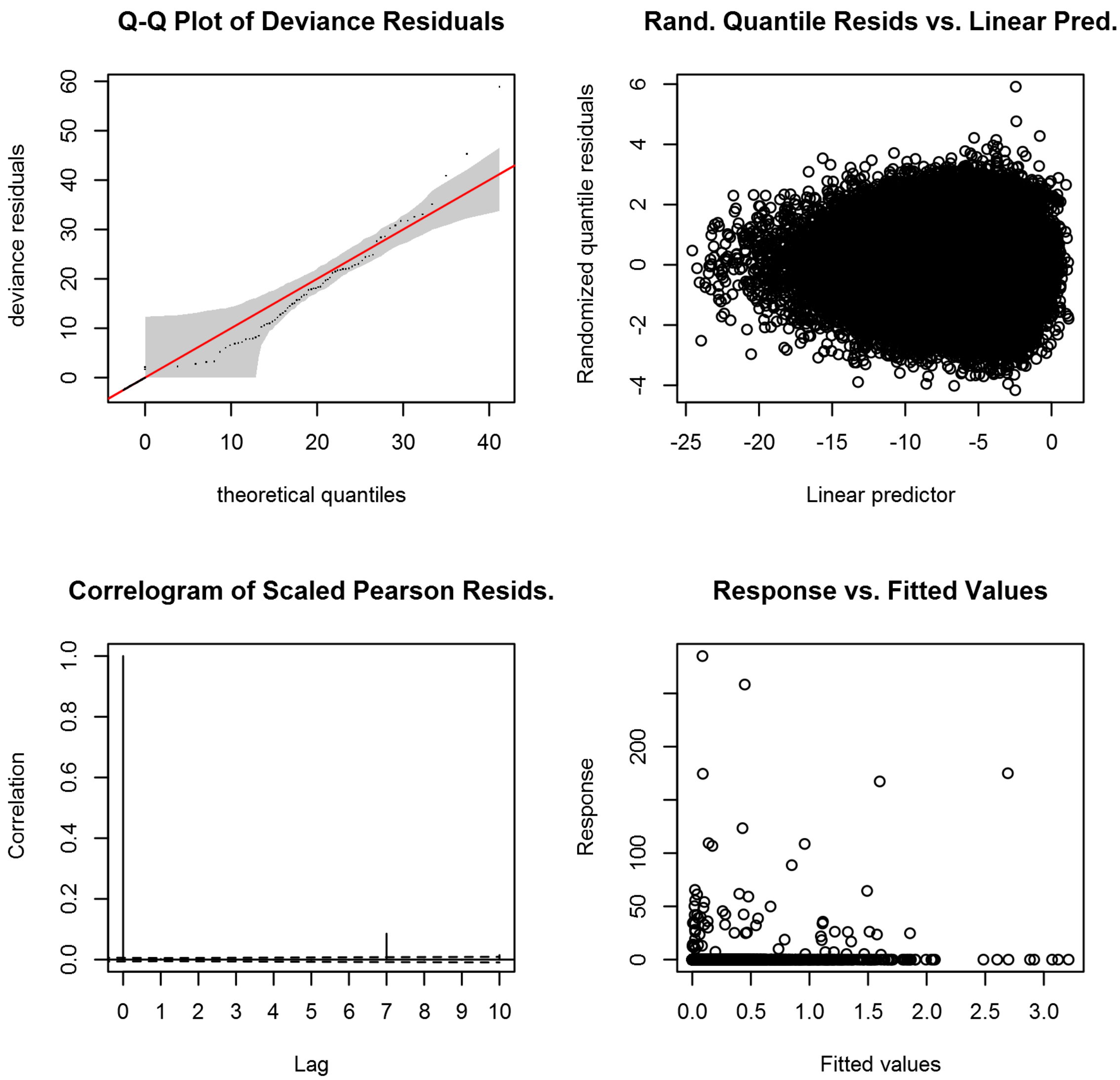

Figure 78: Statistical diagnostic plots for the Risso's dolphin Climatological model, Shelf.

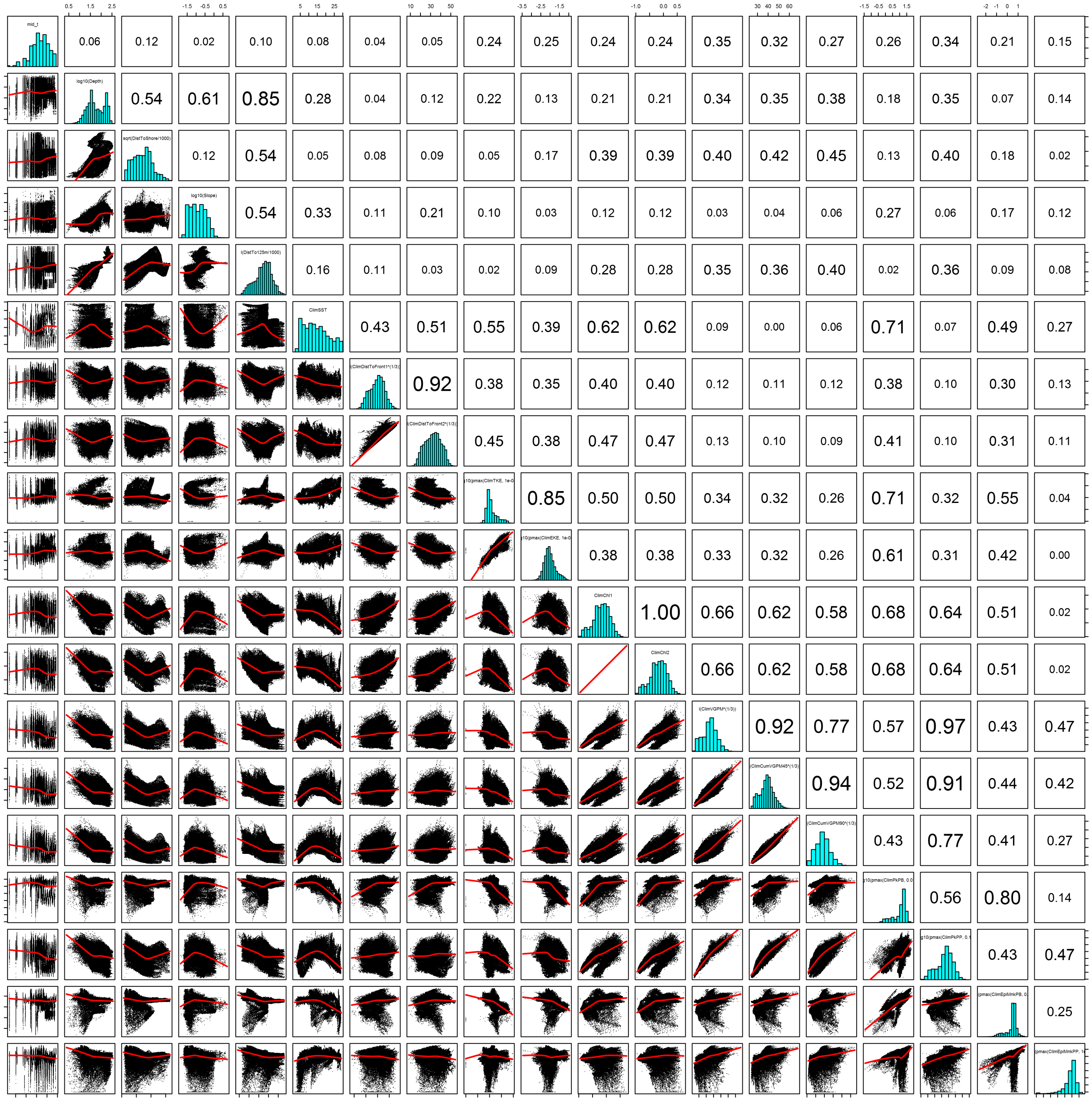

Figure 79: Scatterplot matrix for the Risso's dolphin Climatological model, Shelf. This plot is used to inspect the distribution of predictors (via histograms along the diagonal), simple correlation between predictors (via pairwise Pearson coefficients above the diagonal), and linearity of predictor correlations (via scatterplots below the diagonal). This plot is best viewed at high magnification.

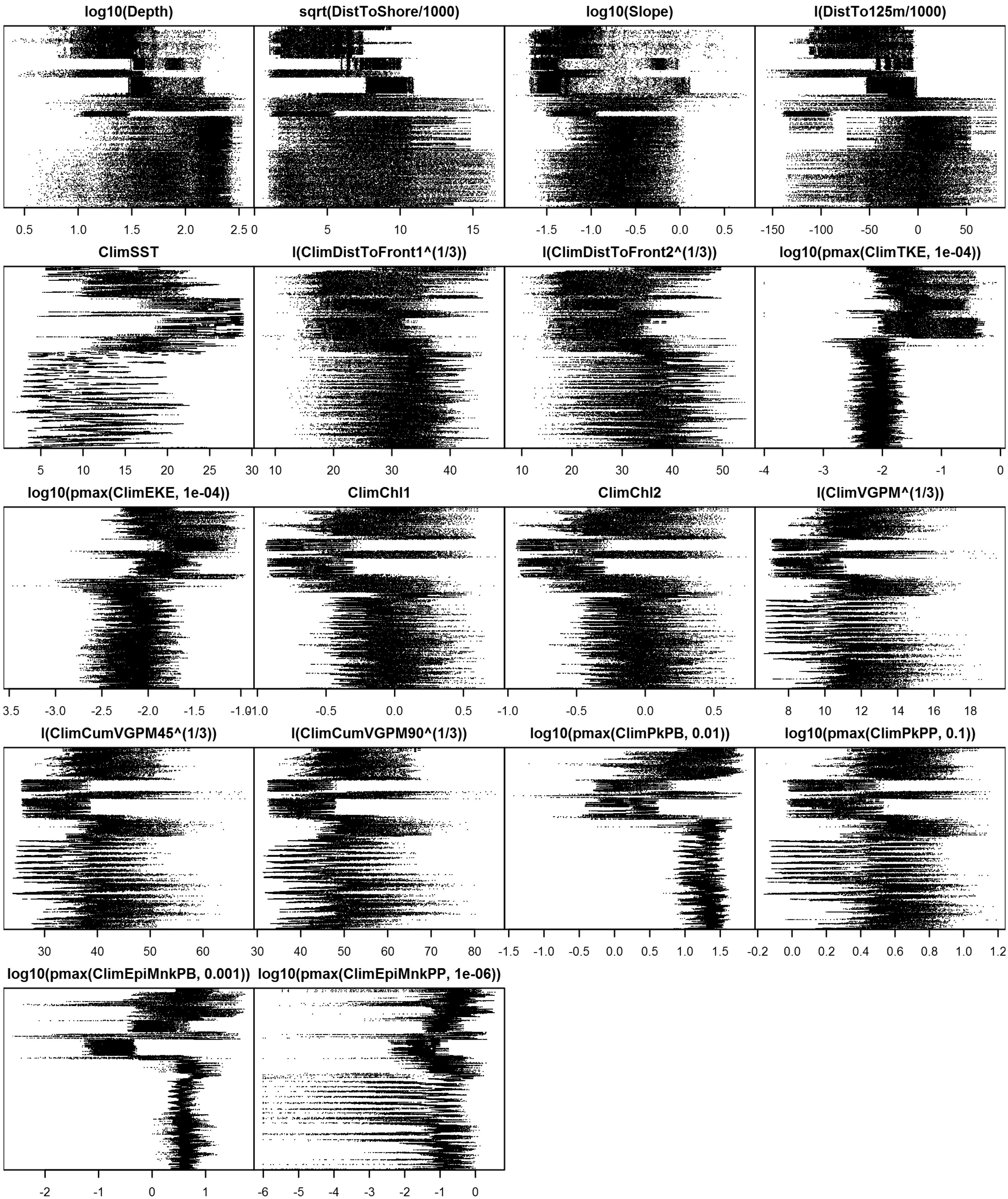

Figure 80: Dotplot for the Risso's dolphin Climatological model, Shelf. This plot is used to check for suspicious patterns and outliers in the data. Points are ordered vertically by transect ID, sequentially in time.

Contemporaneous Model

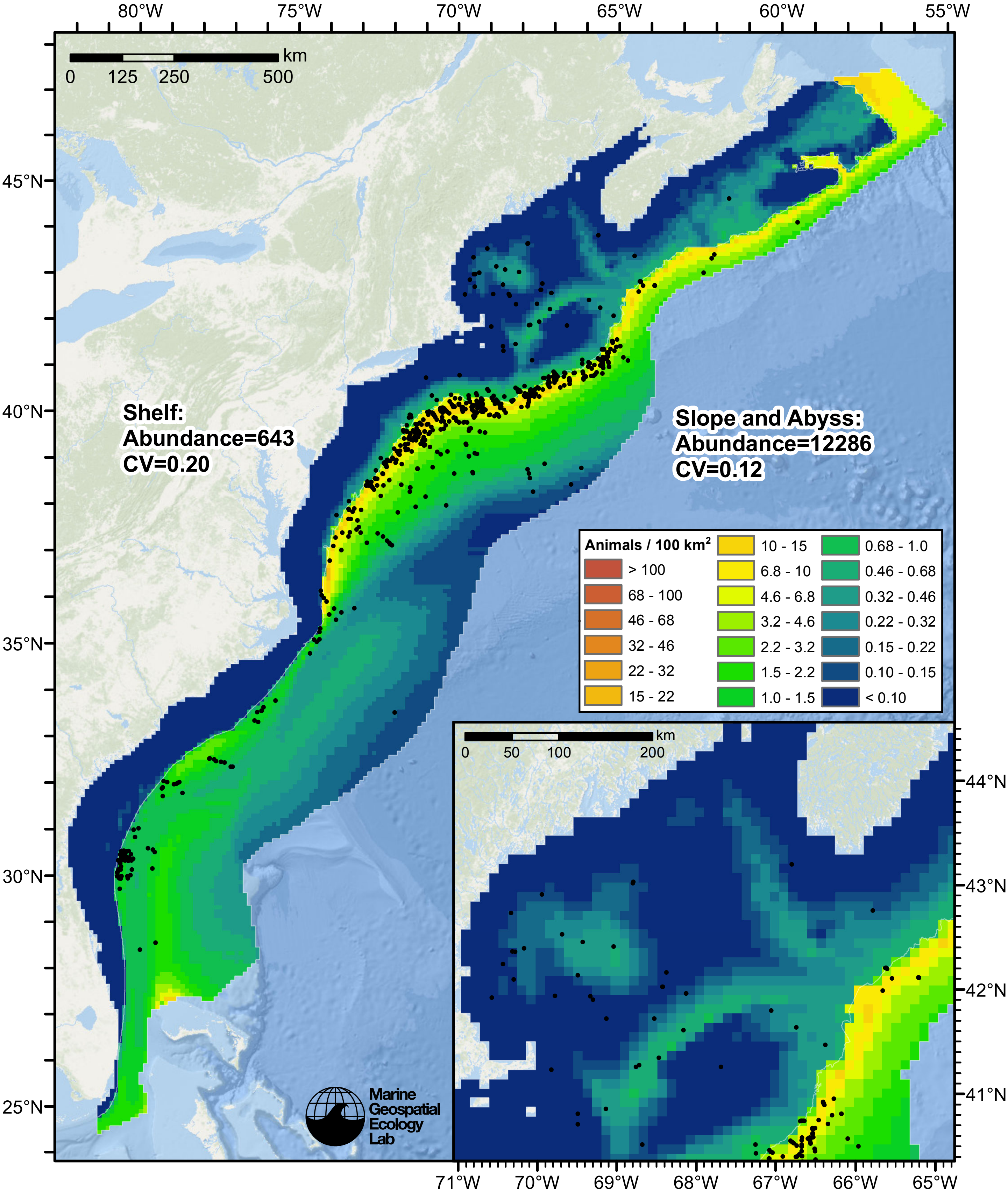

Figure 81: Risso's dolphin density predicted by the contemporaneous model that explained the most deviance. Pixels are 10x10 km. The legend gives the estimated individuals per pixel; breaks are logarithmic. Abundance for each region was computed by summing the density cells occuring in that region.

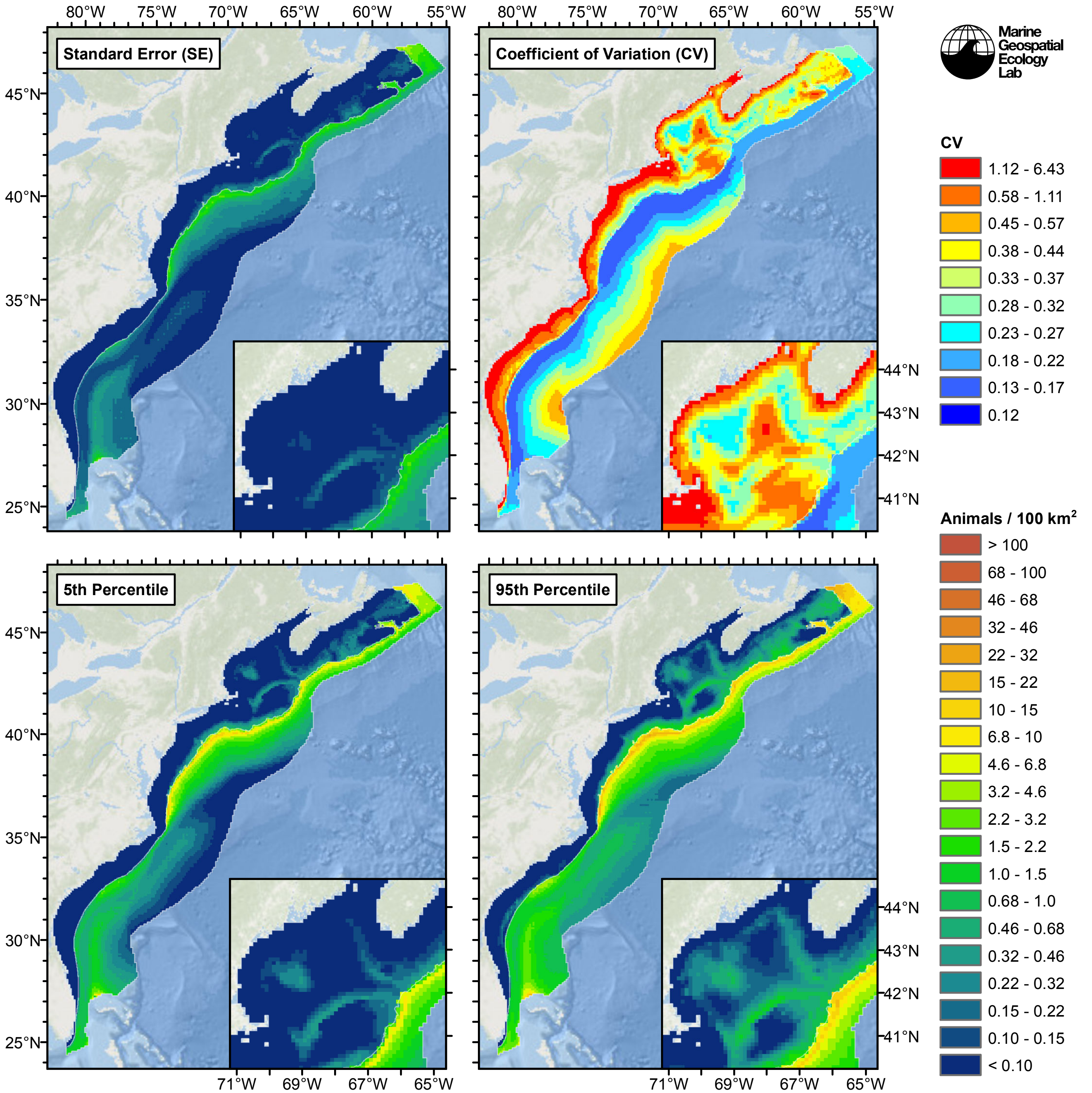

Figure 82: Estimated uncertainty for the contemporaneous model that explained the most deviance. These estimates only incorporate the statistical uncertainty estimated for the spatial model (by the R mgcv package). They do not incorporate uncertainty in the detection functions, g(0) estimates, predictor variables, and so on.

Slope and Abyss

Statistical output

```
Rscript.exe: This is mgcv 1.8-2. For overview type 'help("mgcv-package")'.


Family: Tweedie(p=1.304)
```

```
Link function: log

Formula:
abundance ~ offset(log(area_km2)) + s(log10(Depth), bs = "ts",
    k = 5) + s(I(DistTo125m/1000), bs = "ts", k = 5) + s(SST,
    bs = "ts", k = 5) + s(log10(pmax(TKE, 1e-04)), bs = "ts",
    k = 5) + s(I(DistToCEddy/1000), bs = "ts", k = 5) + s(I(CumVGPM90^(1/3)),
    bs = "ts", k = 5)

Parametric coefficients:
            Estimate Std. Error t value Pr(>|t|)
(Intercept)  -4.3456     0.0953   -45.6   <2e-16 ***
---
Signif. codes:  0 '***' 0.001 '**' 0.01 '*' 0.05 '.' 0.1 ' ' 1

Approximate significance of smooth terms:
                              edf Ref.df      F  p-value
s(log10(Depth))            2.8787      4  5.813 6.13e-06 ***
s(I(DistTo125m/1000))      0.8832      4  1.644  0.00364 **
s(SST)                     1.0112      4  6.281 2.18e-07 ***
s(log10(pmax(TKE, 1e-04))) 1.3128      4 23.683  < 2e-16 ***
s(I(DistToCEddy/1000))     1.0517      4  4.412 1.43e-05 ***
s(I(CumVGPM90^(1/3)))      1.7442      4 11.934 3.02e-13 ***
---
Signif. codes:  0 '***' 0.001 '**' 0.01 '*' 0.05 '.' 0.1 ' ' 1

R-sq.(adj) =  0.0757   Deviance explained = 43.5%
-REML = 2824.6  Scale est. = 50.126    n = 16520

All predictors were significant. This is the final model.
Creating term plots.
Diagnostic output from gam.check():

Method: REML   Optimizer: outer newton
full convergence after 8 iterations.
Gradient range [-0.001750243,0.001072948]
(score 2824.551 & scale 50.12625).
Hessian positive definite, eigenvalue range [0.248364,1029.473].
Model rank =  25 / 25

Basis dimension (k) checking results. Low p-value (k-index<1) may
indicate that k is too low, especially if edf is close to k'.

                              k'   edf k-index p-value
s(log10(Depth))            4.000 2.879   0.790    0.14
s(I(DistTo125m/1000))      4.000 0.883   0.818    0.92
s(SST)                     4.000 1.011   0.779    0.02
s(log10(pmax(TKE, 1e-04))) 4.000 1.313   0.788    0.12
s(I(DistToCEddy/1000))     4.000 1.052   0.815    0.87
s(I(CumVGPM90^(1/3)))      4.000 1.744   0.770    0.00

Predictors retained during the model selection procedure: Depth, DistTo125m, SST, TKE, DistToCEddy,
CumVGPM90

Predictors dropped during the model selection procedure: Slope, DistToFront1, DistToAEddy
```

Model term plots

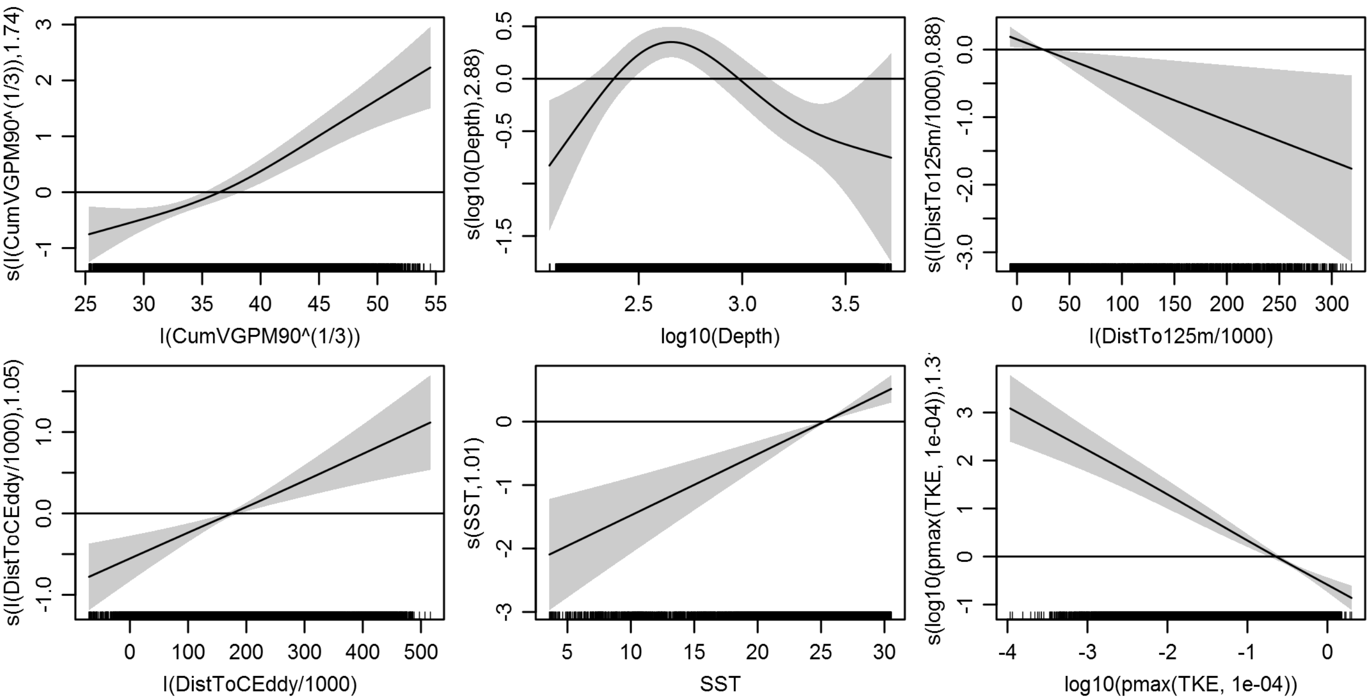

Diagnostic plots

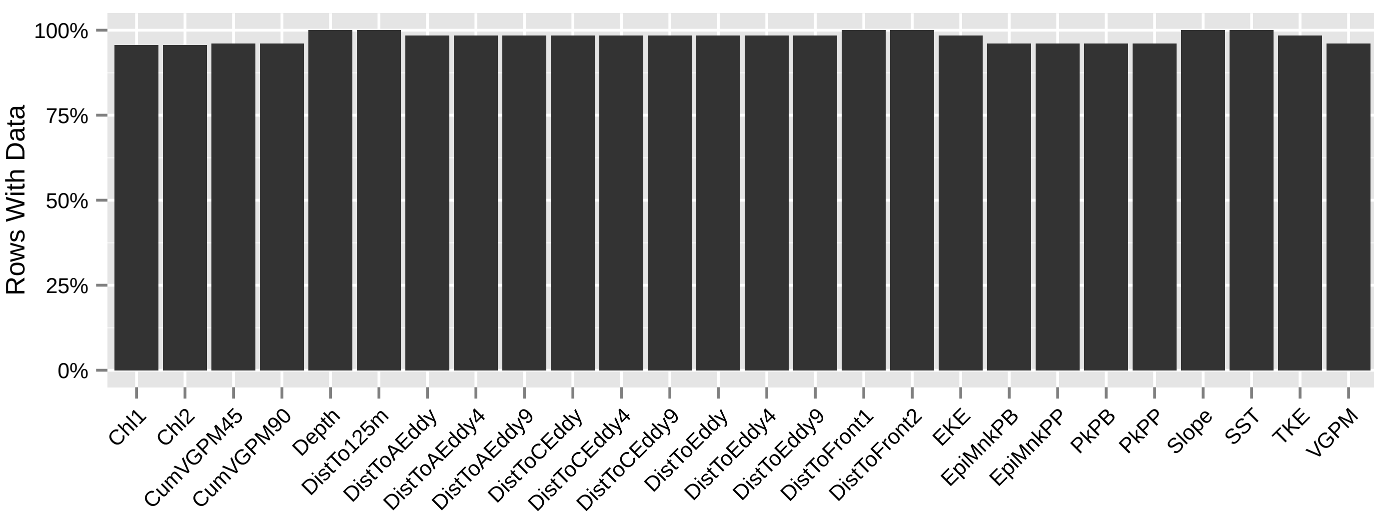

Figure 83: Segments with predictor values for the Risso's dolphin Contemporaneous model, Slope and Abyss. This plot is used to assess how many segments would be lost by including a given predictor in a model.

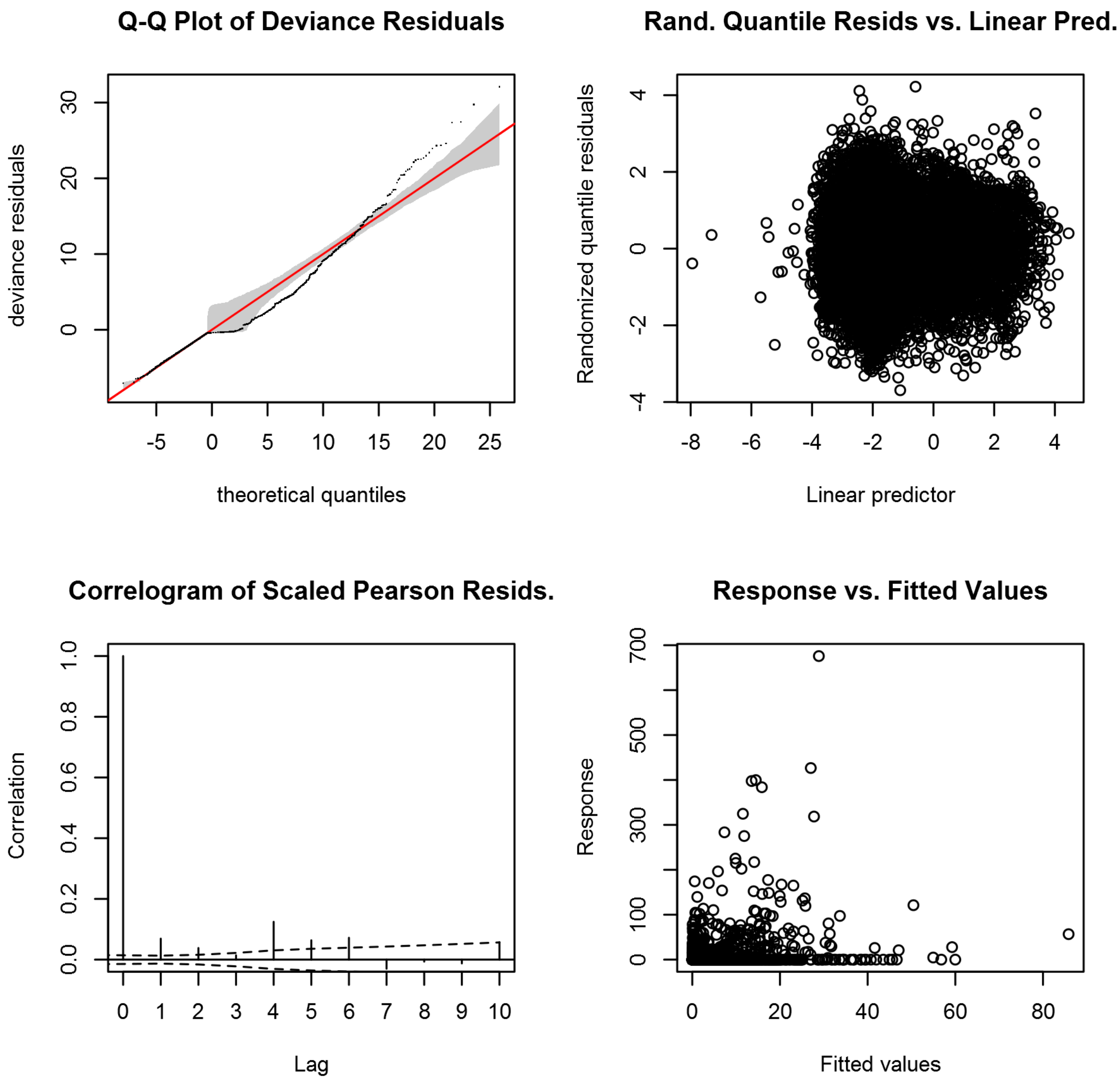

Figure 84: Statistical diagnostic plots for the Risso's dolphin Contemporaneous model, Slope and Abyss.

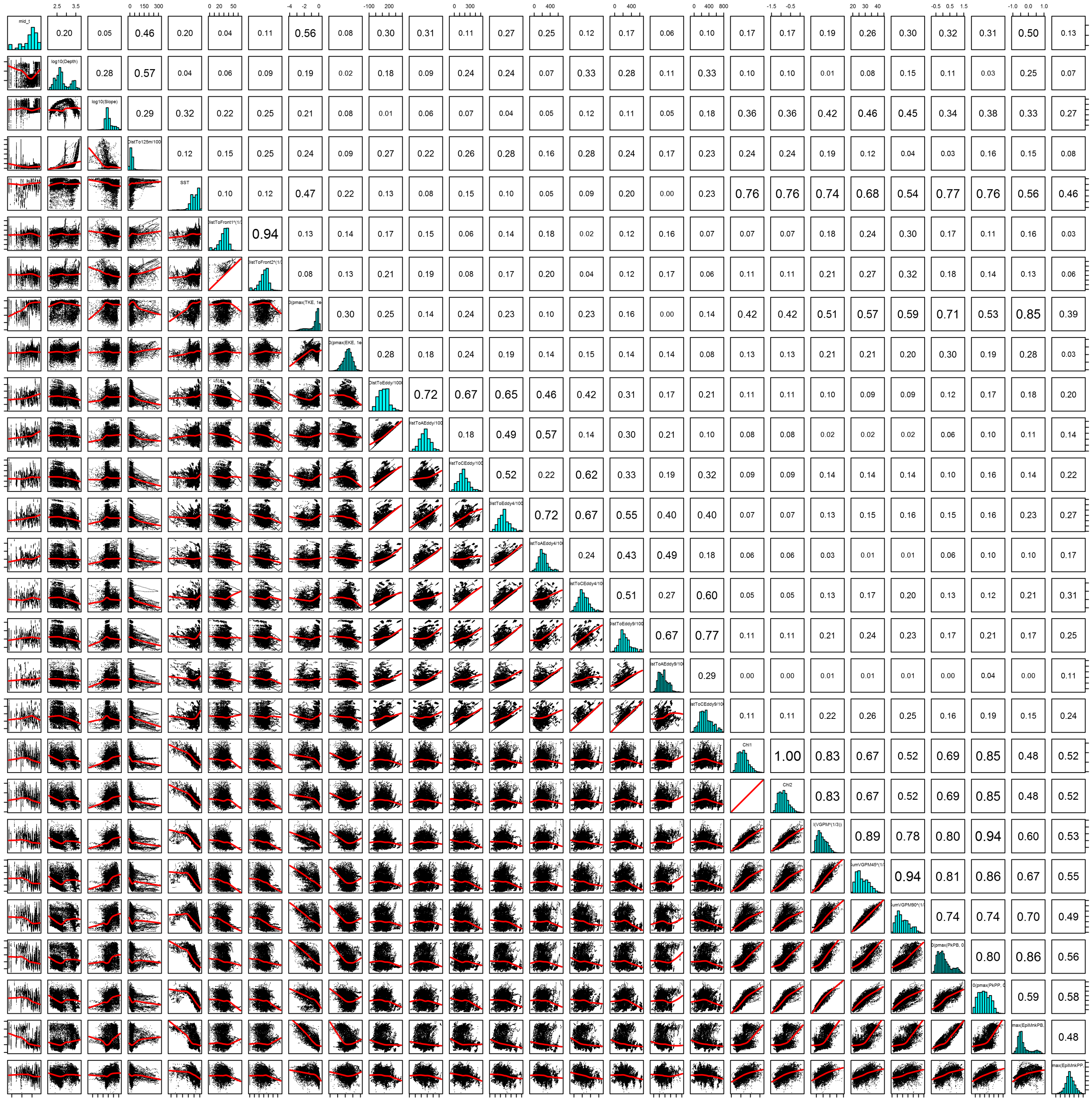

Figure 85: Scatterplot matrix for the Risso's dolphin Contemporaneous model, Slope and Abyss. This plot is used to inspect the distribution of predictors (via histograms along the diagonal), simple correlation between predictors (via pairwise Pearson coefficients above the diagonal), and linearity of predictor correlations (via scatterplots below the diagonal). This plot is best viewed at high magnification.

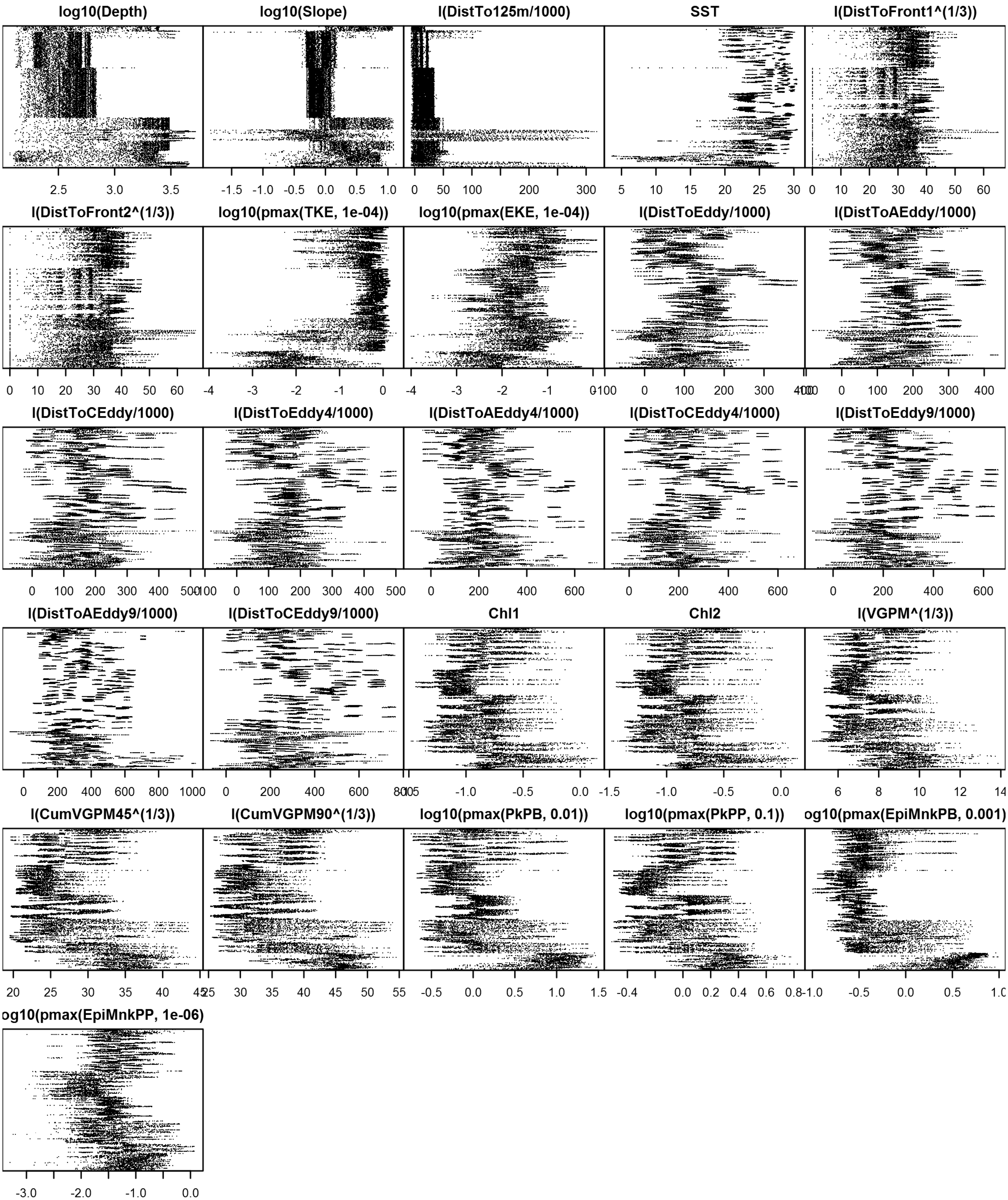

Figure 86: Dotplot for the Risso's dolphin Contemporaneous model, Slope and Abyss. This plot is used to check for suspicious patterns and outliers in the data. Points are ordered vertically by transect ID, sequentially in time.

Shelf

Statistical output

```
Rscript.exe: This is mgcv 1.8-2. For overview type 'help("mgcv-package")'.


Family: Tweedie(p=1.319)
Link function: log

Formula:
abundance ~ offset(log(area_km2)) + s(log10(Depth), bs = "ts",
    k = 5) + s(sqrt(DistToShore/1000), bs = "ts", k = 5) + s(I(DistTo125m/1000),
    bs = "ts", k = 5) + s(SST, bs = "ts", k = 5) + s(I(DistToFront1^(1/3)),
    bs = "ts", k = 5) + s(log10(pmax(TKE, 1e-04)), bs = "ts",
    k = 5)

Parametric coefficients:
            Estimate Std. Error t value Pr(>|t|)
(Intercept)  -9.4440     0.4865  -19.41   <2e-16 ***
---
Signif. codes:  0 '***' 0.001 '**' 0.01 '*' 0.05 '.' 0.1 ' ' 1

Approximate significance of smooth terms:
                              edf Ref.df     F  p-value
s(log10(Depth))            1.9539      4 4.974 5.34e-06 ***
s(sqrt(DistToShore/1000))  2.1209      4 4.926 1.41e-05 ***
s(I(DistTo125m/1000))      2.5427      4 3.507 0.000703 ***
s(SST)                     1.0405      4 4.182 1.88e-05 ***
s(I(DistToFront1^(1/3)))   0.9085      4 1.763 0.004434 **
s(log10(pmax(TKE, 1e-04))) 2.1588      4 3.351 0.000573 ***
---
Signif. codes:  0 '***' 0.001 '**' 0.01 '*' 0.05 '.' 0.1 ' ' 1

R-sq.(adj) =  0.00918   Deviance explained = 38.9%
-REML = 874.84  Scale est. = 127.6     n = 85972

All predictors were significant. This is the final model.
Creating term plots.
Diagnostic output from gam.check():

Method: REML   Optimizer: outer newton
full convergence after 18 iterations.
Gradient range [-9.987849e-06,8.817002e-06]
(score 874.838 & scale 127.5983).
Hessian positive definite, eigenvalue range [0.3489611,417.2089].
Model rank =  25 / 25

Basis dimension (k) checking results. Low p-value (k-index<1) may
indicate that k is too low, especially if edf is close to k'.

                              k'   edf k-index p-value
s(log10(Depth))            4.000 1.954   0.632    0.00
s(sqrt(DistToShore/1000))  4.000 2.121   0.661    0.00
s(I(DistTo125m/1000))      4.000 2.543   0.638    0.00
s(SST)                     4.000 1.040   0.725    0.16
s(I(DistToFront1^(1/3)))   4.000 0.909   0.731    0.44
s(log10(pmax(TKE, 1e-04))) 4.000 2.159   0.715    0.00
```

`Predictors retained during the model selection procedure: Depth, DistToShore, DistTo125m, SST, DistToFront1, TKE`

`Predictors dropped during the model selection procedure: Slope`

Model term plots

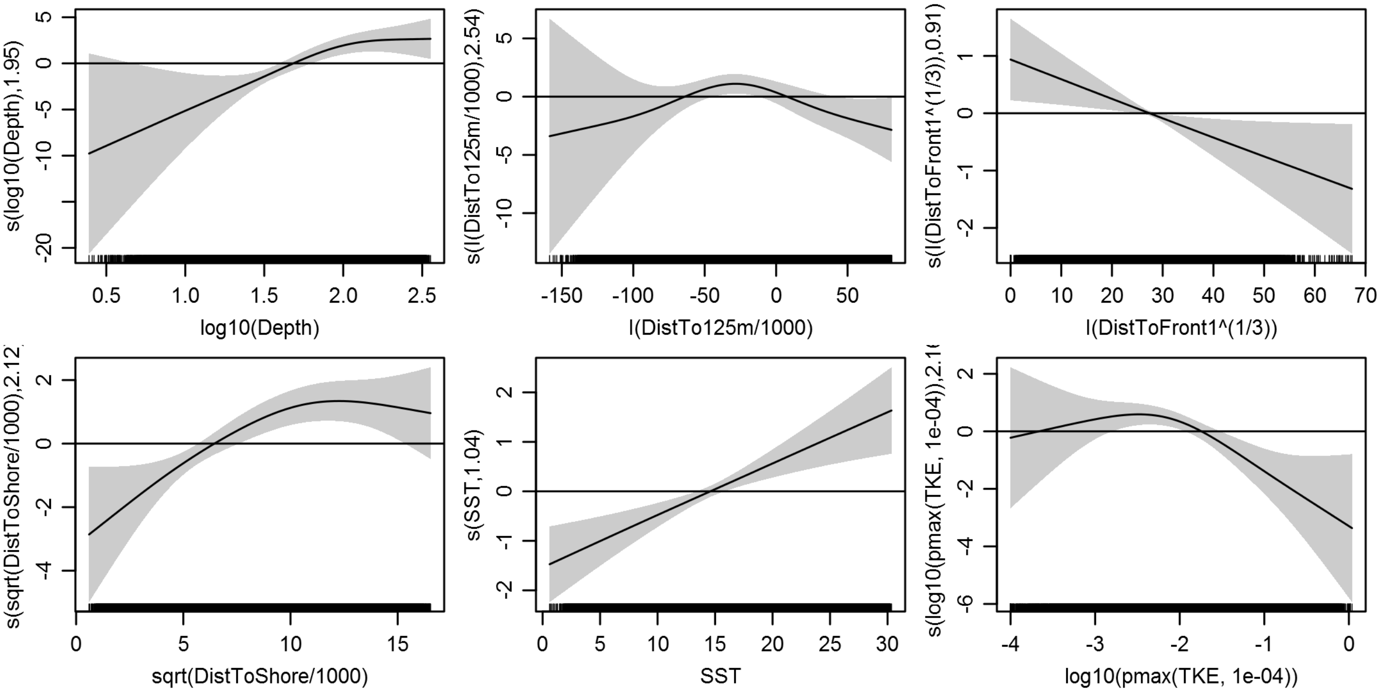

Diagnostic plots

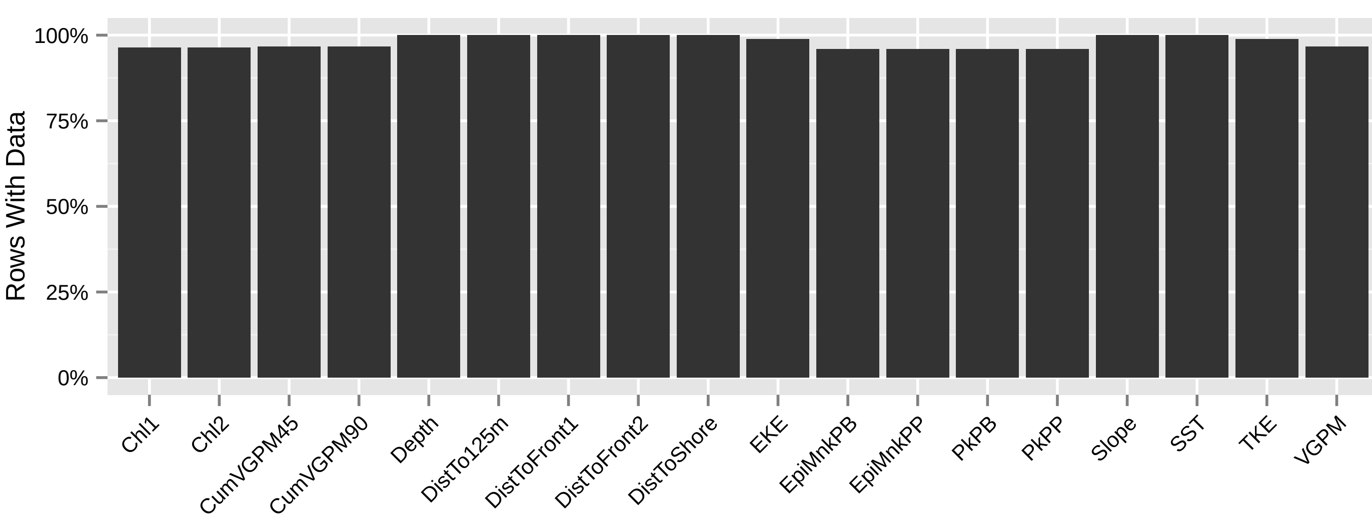

Figure 87: Segments with predictor values for the Risso's dolphin Contemporaneous model, Shelf. This plot is used to assess how many segments would be lost by including a given predictor in a model.

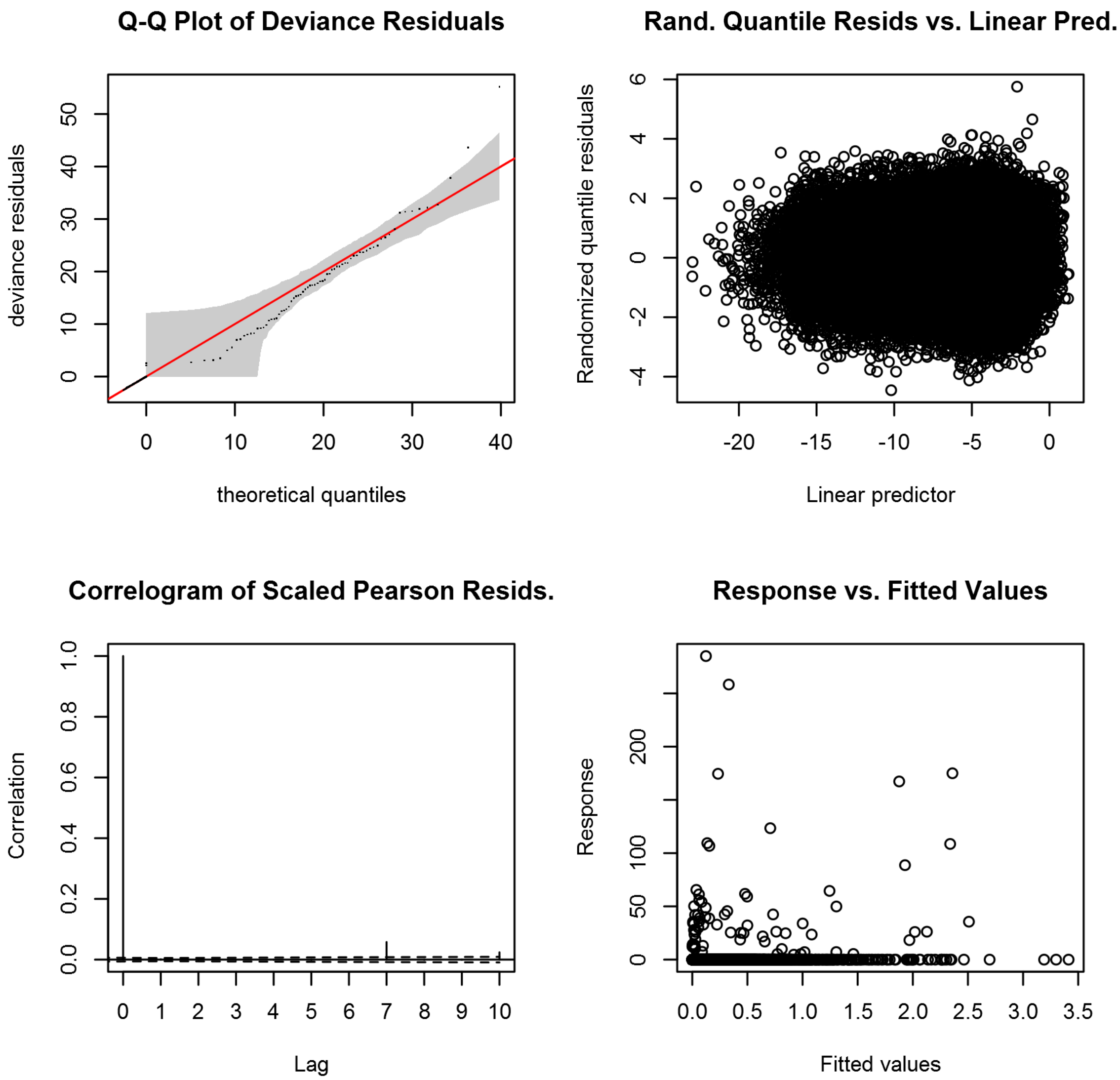

Figure 88: Statistical diagnostic plots for the Risso's dolphin Contemporaneous model, Shelf.

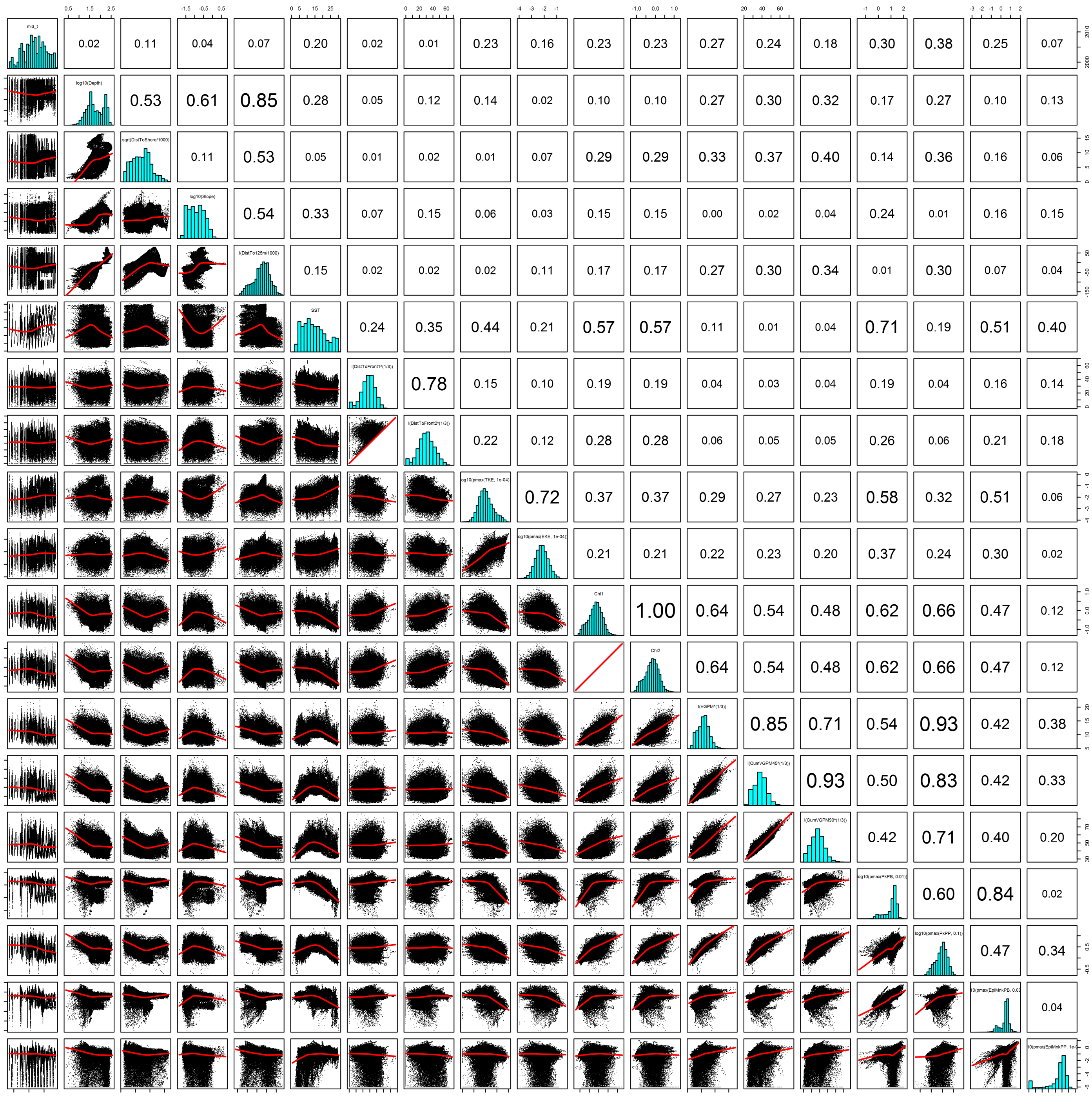

Figure 89: Scatterplot matrix for the Risso's dolphin Contemporaneous model, Shelf. This plot is used to inspect the distribution of predictors (via histograms along the diagonal), simple correlation between predictors (via pairwise Pearson coefficients above the diagonal), and linearity of predictor correlations (via scatterplots below the diagonal). This plot is best viewed at high magnification.

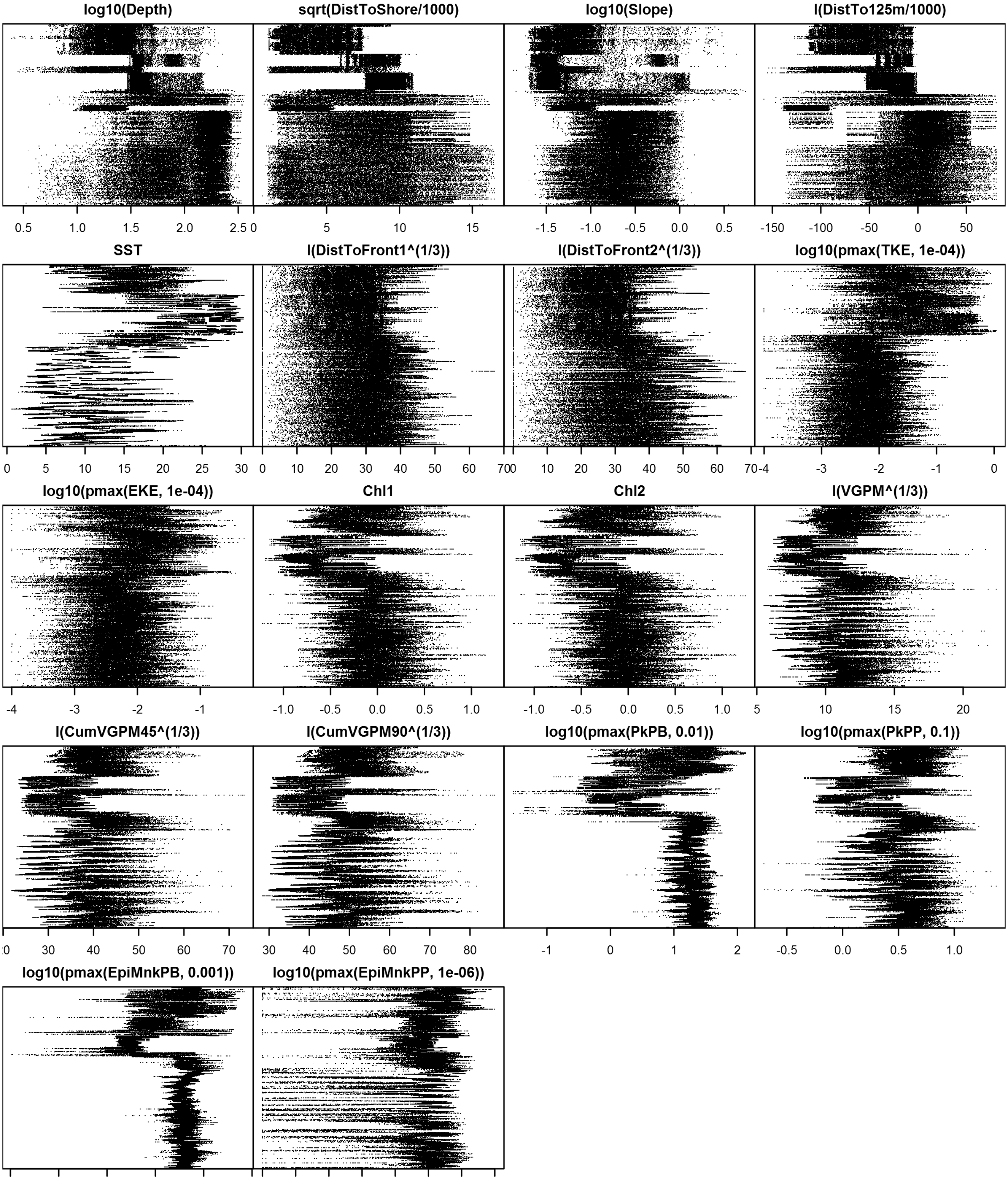

Figure 90: Dotplot for the Risso's dolphin Contemporaneous model, Shelf. This plot is used to check for suspicious patterns and outliers in the data. Points are ordered vertically by transect ID, sequentially in time.

Climatological Same Segments Model

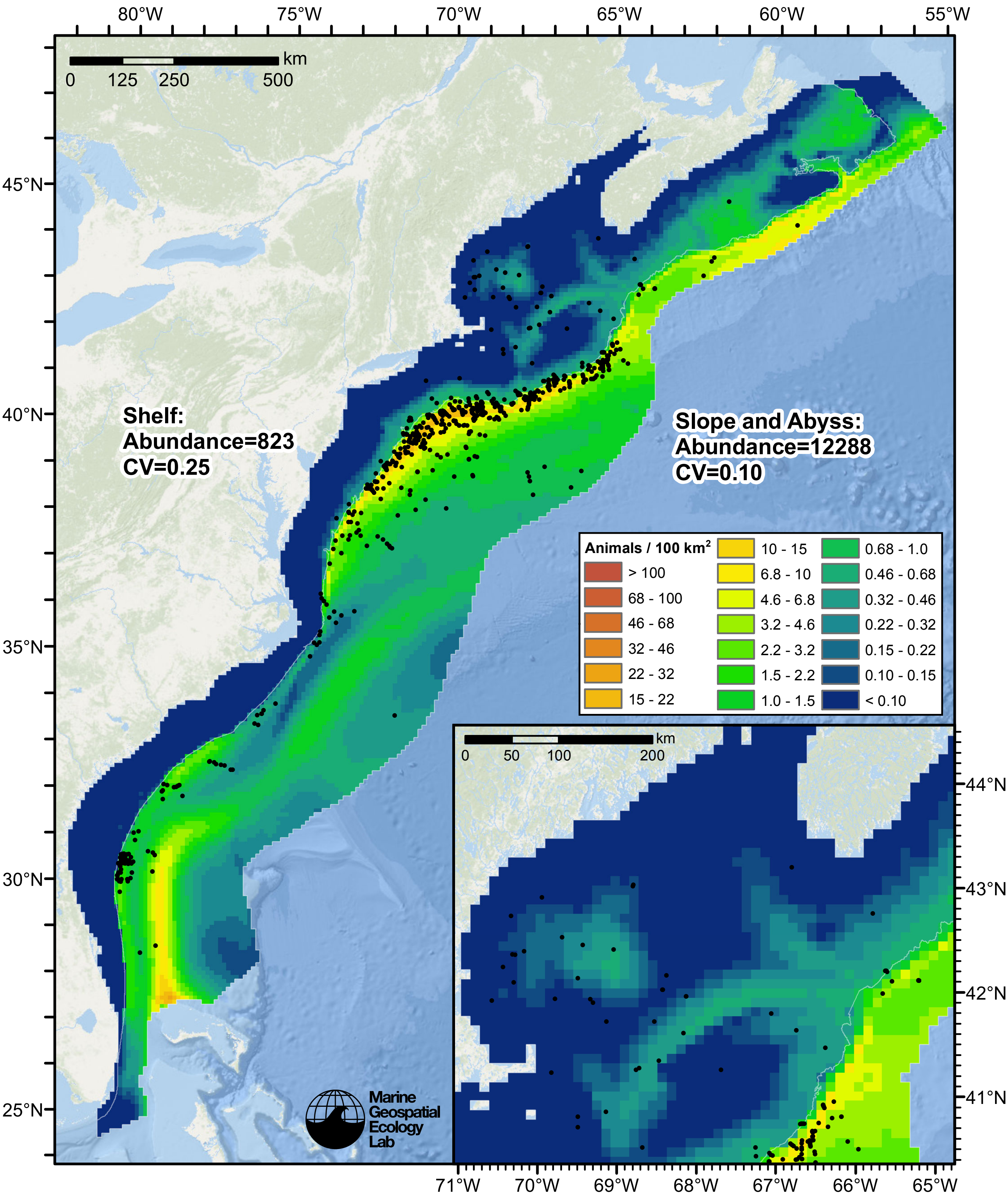

Figure 91: Risso's dolphin density predicted by the climatological same segments model that explained the most deviance. Pixels are 10x10 km. The legend gives the estimated individuals per pixel; breaks are logarithmic. Abundance for each region was computed by summing the density cells occuring in that region.

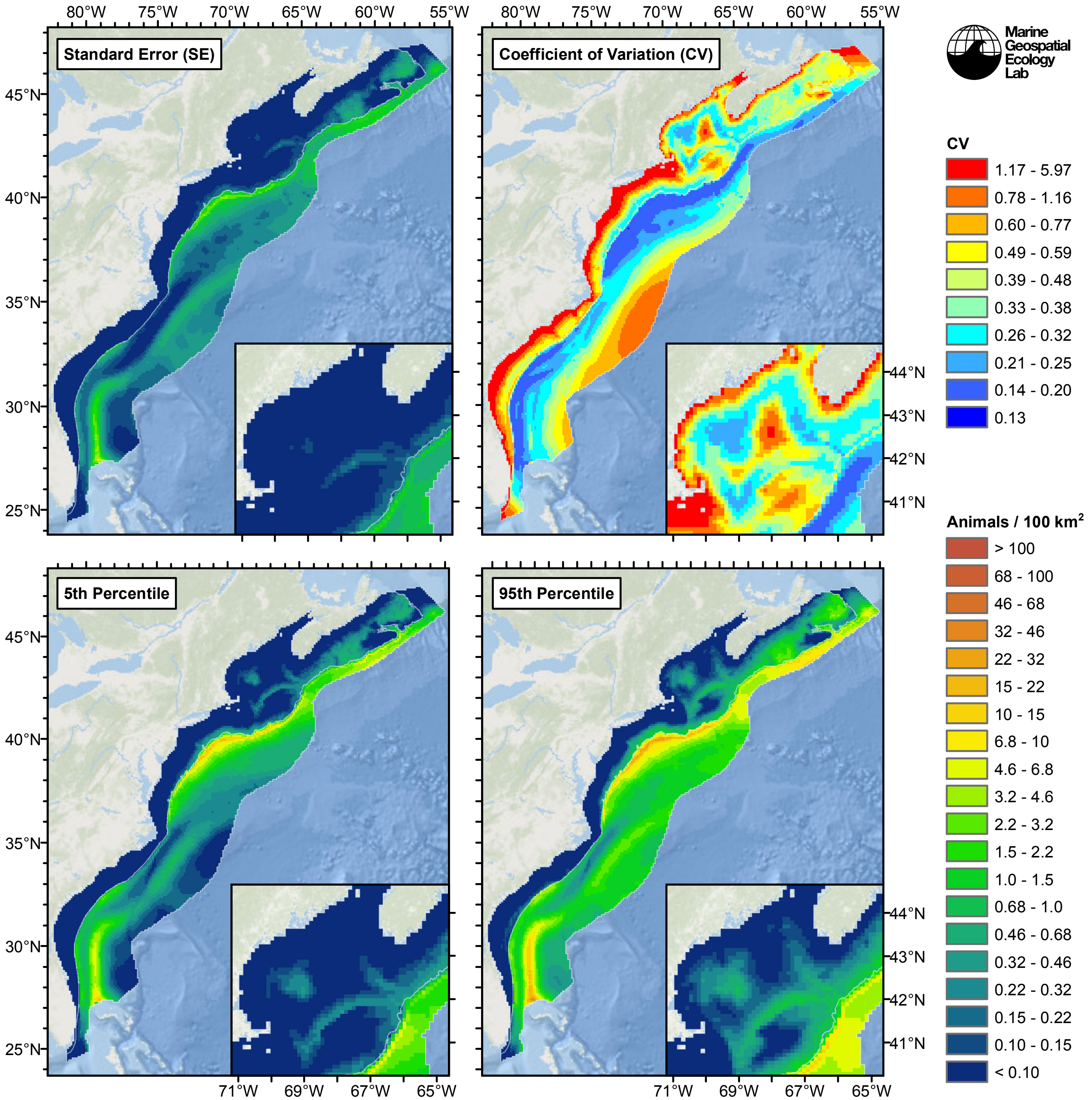

Figure 92: Estimated uncertainty for the climatological same segments model that explained the most deviance. These estimates only incorporate the statistical uncertainty estimated for the spatial model (by the R mgcv package). They do not incorporate uncertainty in the detection functions, g(0) estimates, predictor variables, and so on.

Slope and Abyss

Statistical output

```
Rscript.exe: This is mgcv 1.8-2. For overview type 'help("mgcv-package")'.


Family: Tweedie(p=1.297)
```

```
Link function: log

Formula:
abundance ~ offset(log(area_km2)) + s(log10(Depth), bs = "ts",
    k = 5) + s(I(ClimDistToFront1^(1/3)), bs = "ts", k = 5) +
    s(log10(pmax(ClimTKE, 1e-04)), bs = "ts", k = 5) + s(I(ClimDistToAEddy9/1000),
    bs = "ts", k = 5) + s(I(ClimDistToCEddy9/1000), bs = "ts",
    k = 5) + s(ClimChl1, bs = "ts", k = 5)

Parametric coefficients:
            Estimate Std. Error t value Pr(>|t|)
(Intercept)  -4.6940     0.1093  -42.96   <2e-16 ***
---
Signif. codes:  0 '***' 0.001 '**' 0.01 '*' 0.05 '.' 0.1 ' ' 1

Approximate significance of smooth terms:
                                  edf Ref.df      F  p-value
s(log10(Depth))                3.4356      4  6.037 1.02e-05 ***
s(I(ClimDistToFront1^(1/3)))   1.6746      4  8.675 8.52e-10 ***
s(log10(pmax(ClimTKE, 1e-04))) 1.6335      4 19.707  < 2e-16 ***
s(I(ClimDistToAEddy9/1000))    0.9115      4  1.638  0.00572 **
s(I(ClimDistToCEddy9/1000))    3.3800      4 15.028 8.45e-15 ***
s(ClimChl1)                    3.2135      4 11.478 3.81e-11 ***
---
Signif. codes:  0 '***' 0.001 '**' 0.01 '*' 0.05 '.' 0.1 ' ' 1

R-sq.(adj) =  0.104   Deviance explained = 48.3%
-REML = 2781.8  Scale est. = 46.92     n = 16520

All predictors were significant. This is the final model.
Creating term plots.
Diagnostic output from gam.check():

Method: REML   Optimizer: outer newton
full convergence after 13 iterations.
Gradient range [-0.0006087949,6.638799e-05]
(score 2781.802 & scale 46.91957).
Hessian positive definite, eigenvalue range [0.1498019,1022.906].
Model rank =  25 / 25

Basis dimension (k) checking results. Low p-value (k-index<1) may
indicate that k is too low, especially if edf is close to k'.

                                  k'   edf k-index p-value
s(log10(Depth))                4.000 3.436   0.766    0.07
s(I(ClimDistToFront1^(1/3)))   4.000 1.675   0.786    0.65
s(log10(pmax(ClimTKE, 1e-04))) 4.000 1.634   0.762    0.07
s(I(ClimDistToAEddy9/1000))    4.000 0.912   0.773    0.20
s(I(ClimDistToCEddy9/1000))    4.000 3.380   0.770    0.14
s(ClimChl1)                    4.000 3.214   0.769    0.10
```

Predictors retained during the model selection procedure: Depth, ClimDistToFront1, ClimTKE, ClimDistToAEddy9, ClimDistToCEddy9, ClimChl1

Predictors dropped during the model selection procedure: Slope, DistTo125m, ClimSST

Model term plots

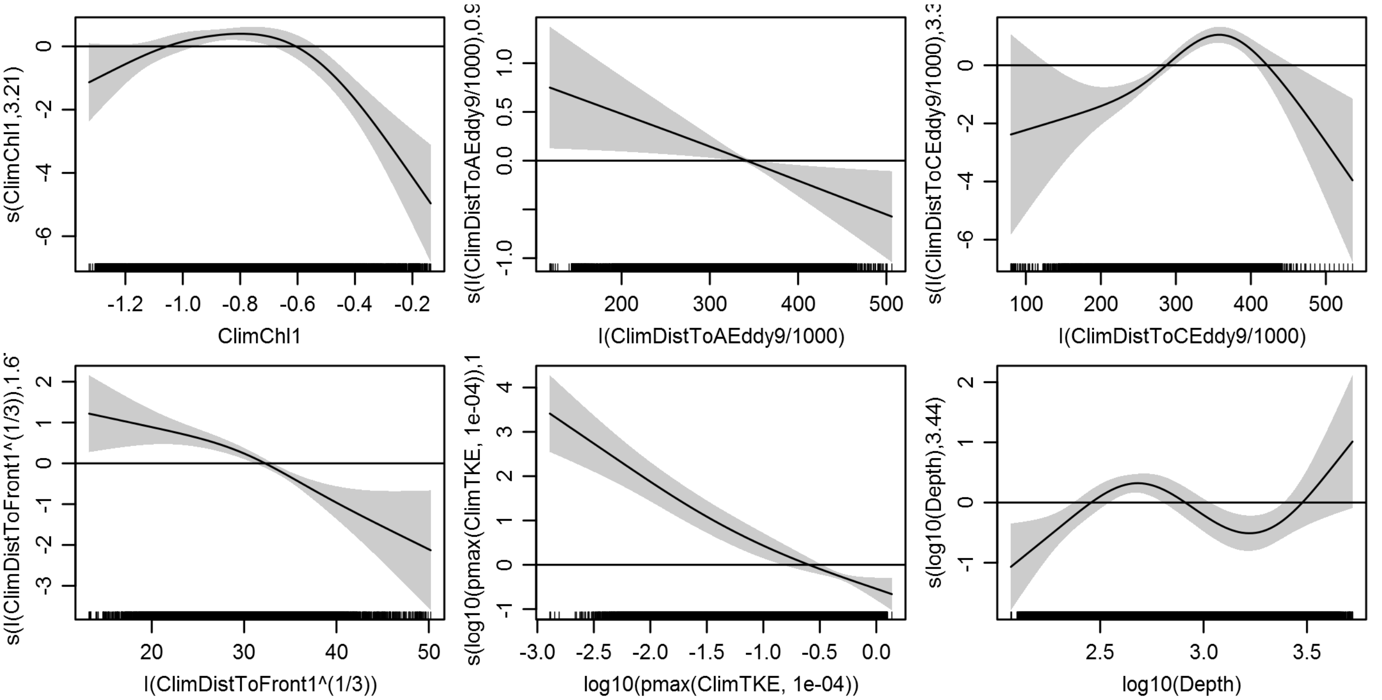

Diagnostic plots

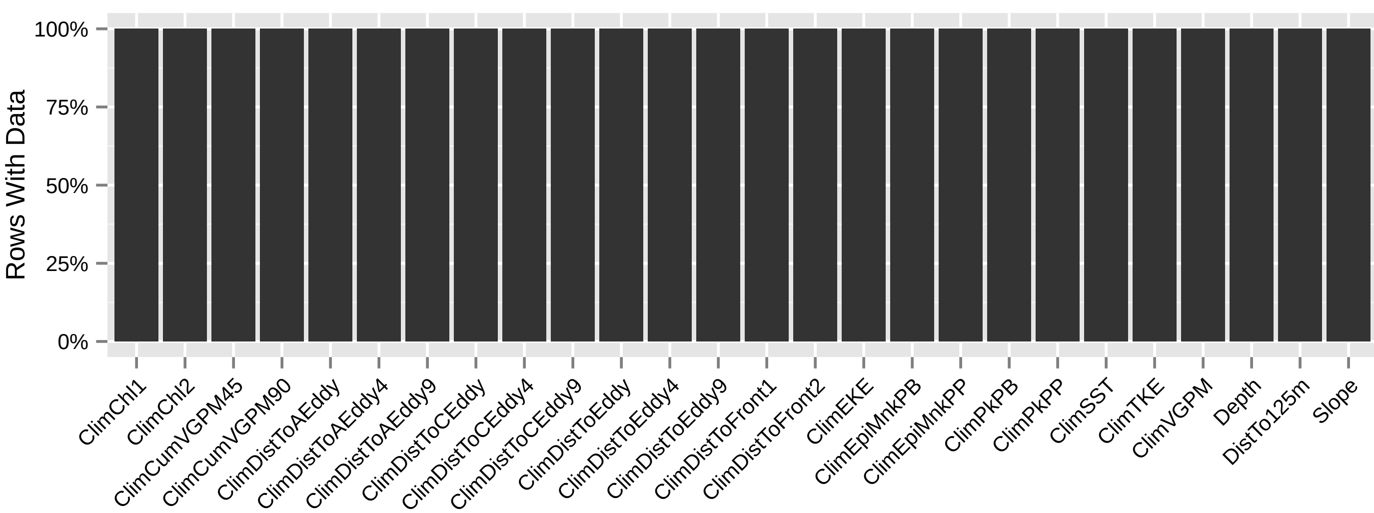

Figure 93: Segments with predictor values for the Risso's dolphin Climatological model, Slope and Abyss. This plot is used to assess how many segments would be lost by including a given predictor in a model.

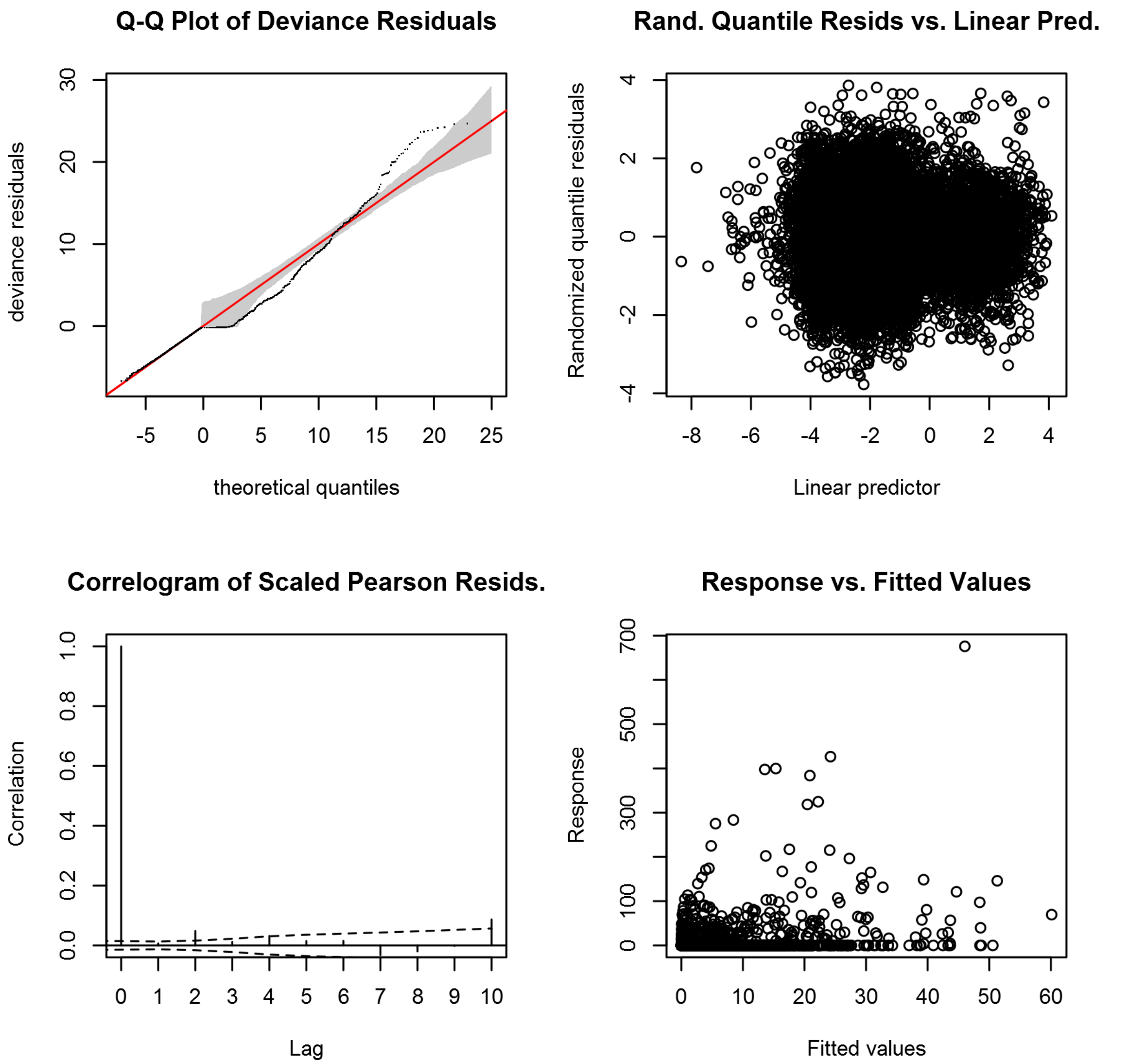

Figure 94: Statistical diagnostic plots for the Risso's dolphin Climatological model, Slope and Abyss.

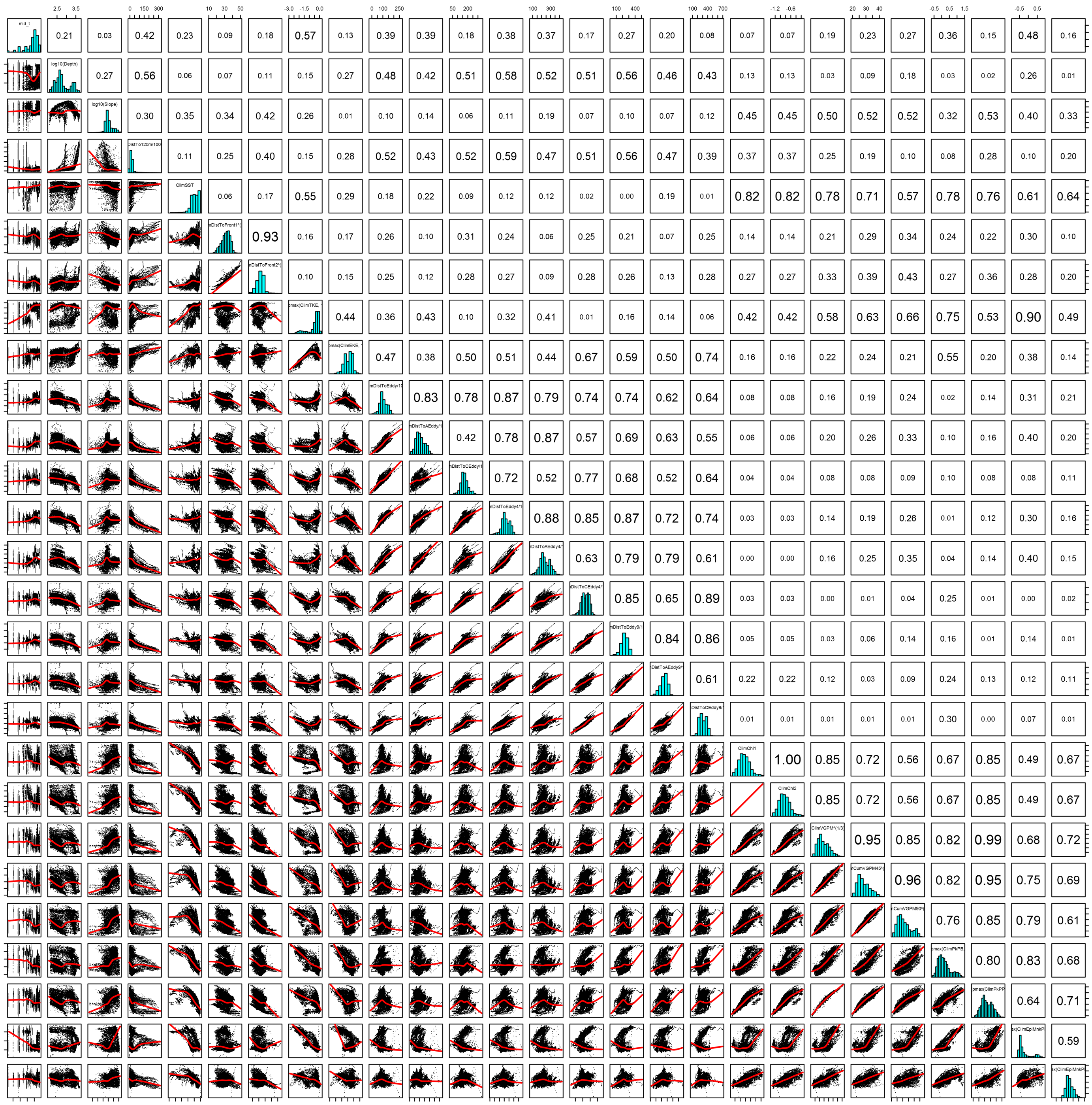

Figure 95: Scatterplot matrix for the Risso's dolphin Climatological model, Slope and Abyss. This plot is used to inspect the distribution of predictors (via histograms along the diagonal), simple correlation between predictors (via pairwise Pearson coefficients above the diagonal), and linearity of predictor correlations (via scatterplots below the diagonal). This plot is best viewed at high magnification.

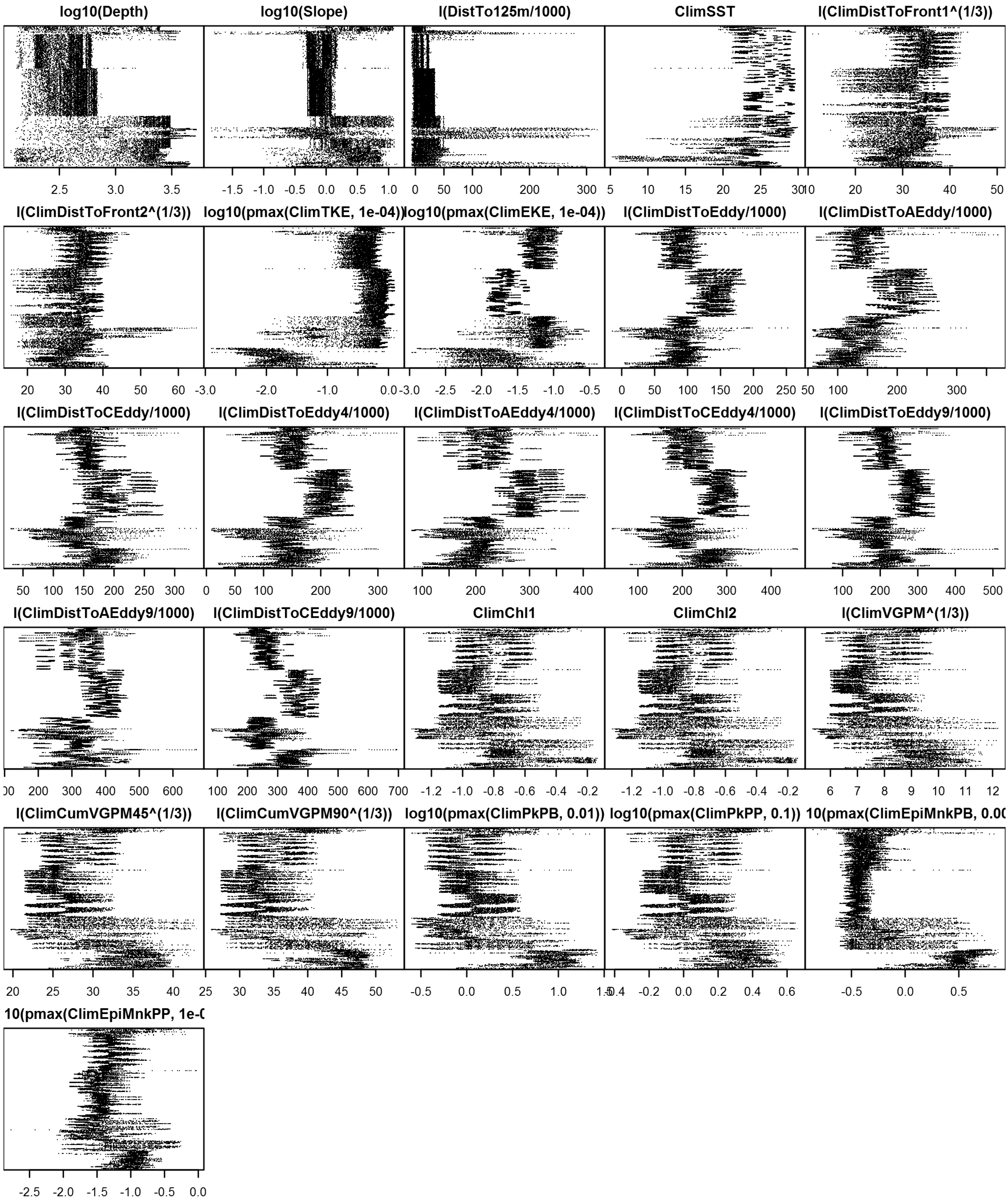

Figure 96: Dotplot for the Risso's dolphin Climatological model, Slope and Abyss. This plot is used to check for suspicious patterns and outliers in the data. Points are ordered vertically by transect ID, sequentially in time.

Shelf

Statistical output

```
Rscript.exe: This is mgcv 1.8-2. For overview type 'help("mgcv-package")'.


Family: Tweedie(p=1.327)
Link function: log

Formula:
abundance ~ offset(log(area_km2)) + s(log10(Depth), bs = "ts",
    k = 5) + s(sqrt(DistToShore/1000), bs = "ts", k = 5) + s(I(DistTo125m/1000),
    bs = "ts", k = 5) + s(ClimSST, bs = "ts", k = 5) + s(log10(pmax(ClimTKE,
    1e-04)), bs = "ts", k = 5)

Parametric coefficients:
            Estimate Std. Error t value Pr(>|t|)
(Intercept)  -9.3163     0.4765  -19.55   <2e-16 ***
---
Signif. codes:  0 '***' 0.001 '**' 0.01 '*' 0.05 '.' 0.1 ' ' 1

Approximate significance of smooth terms:
                                 edf Ref.df     F  p-value
s(log10(Depth))                1.704      4 3.619 9.13e-05 ***
s(sqrt(DistToShore/1000))      1.928      4 4.824 1.33e-05 ***
s(I(DistTo125m/1000))          2.564      4 4.319 0.000111 ***
s(ClimSST)                     1.053      4 4.666 6.60e-06 ***
s(log10(pmax(ClimTKE, 1e-04))) 1.000      4 2.914 0.000293 ***
---
Signif. codes:  0 '***' 0.001 '**' 0.01 '*' 0.05 '.' 0.1 ' ' 1

R-sq.(adj) =  0.0085   Deviance explained = 36.7%
-REML = 876.68  Scale est. = 135.36    n = 85972

All predictors were significant. This is the final model.
Creating term plots.
Diagnostic output from gam.check():

Method: REML   Optimizer: outer newton
full convergence after 16 iterations.
Gradient range [-0.0004794311,0.000365987]
(score 876.6838 & scale 135.3616).
Hessian positive definite, eigenvalue range [0.2728189,418.5886].
Model rank =  21 / 21

Basis dimension (k) checking results. Low p-value (k-index<1) may
indicate that k is too low, especially if edf is close to k'.

                                  k'   edf k-index p-value
s(log10(Depth))                4.000 1.704   0.657    0.00
s(sqrt(DistToShore/1000))      4.000 1.928   0.676    0.00
s(I(DistTo125m/1000))          4.000 2.564   0.661    0.00
s(ClimSST)                     4.000 1.053   0.741    0.28
s(log10(pmax(ClimTKE, 1e-04))) 4.000 1.000   0.708    0.00

Predictors retained during the model selection procedure: Depth, DistToShore, DistTo125m, ClimSST,
ClimTKE
```

```
Predictors dropped during the model selection procedure: Slope, ClimDistToFront1
```

Model term plots

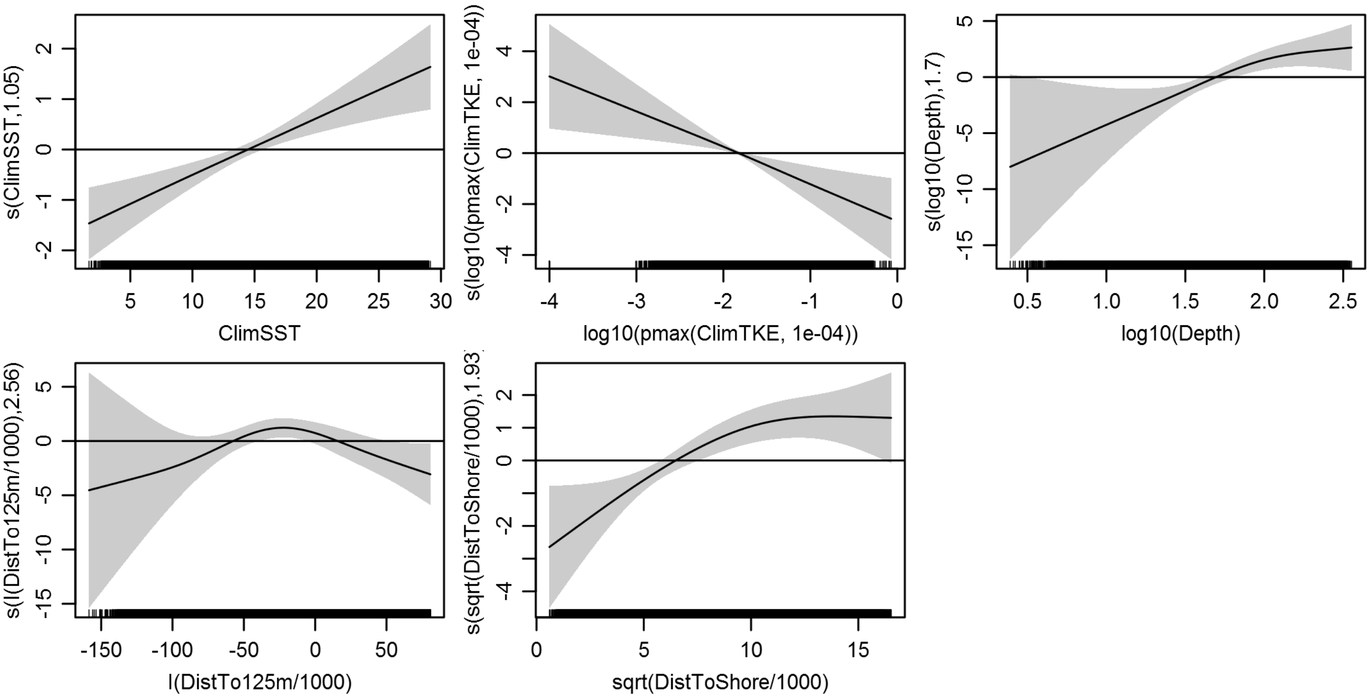

Diagnostic plots

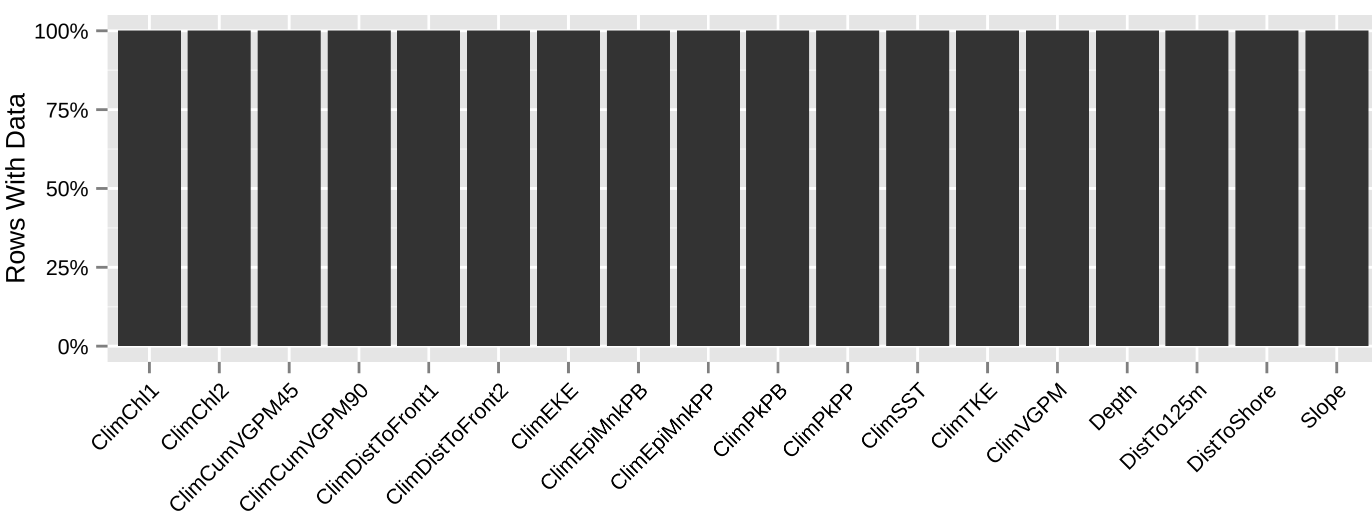

Figure 97: Segments with predictor values for the Risso's dolphin Climatological model, Shelf. This plot is used to assess how many segments would be lost by including a given predictor in a model.

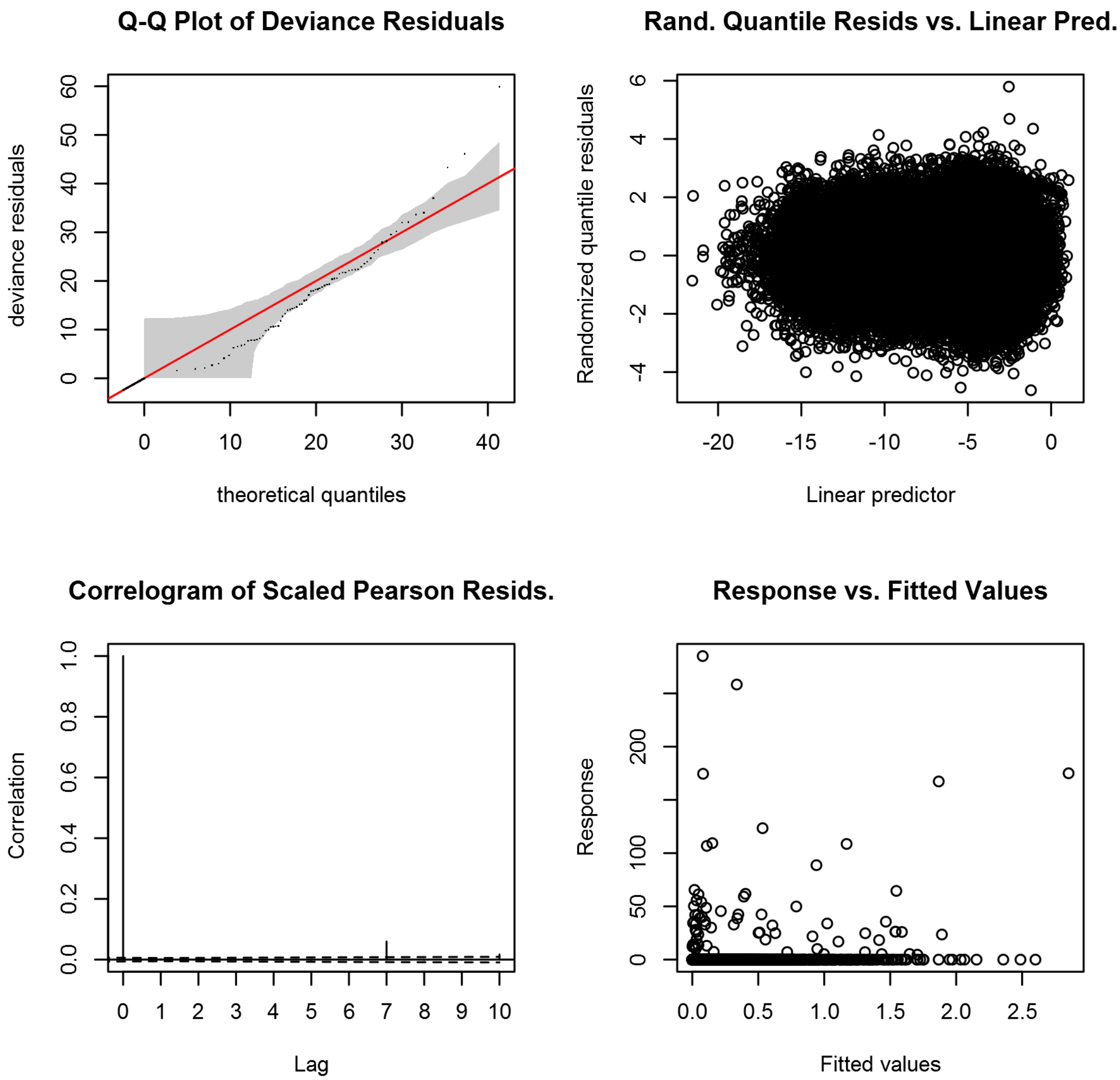

Figure 98: Statistical diagnostic plots for the Risso's dolphin Climatological model, Shelf.

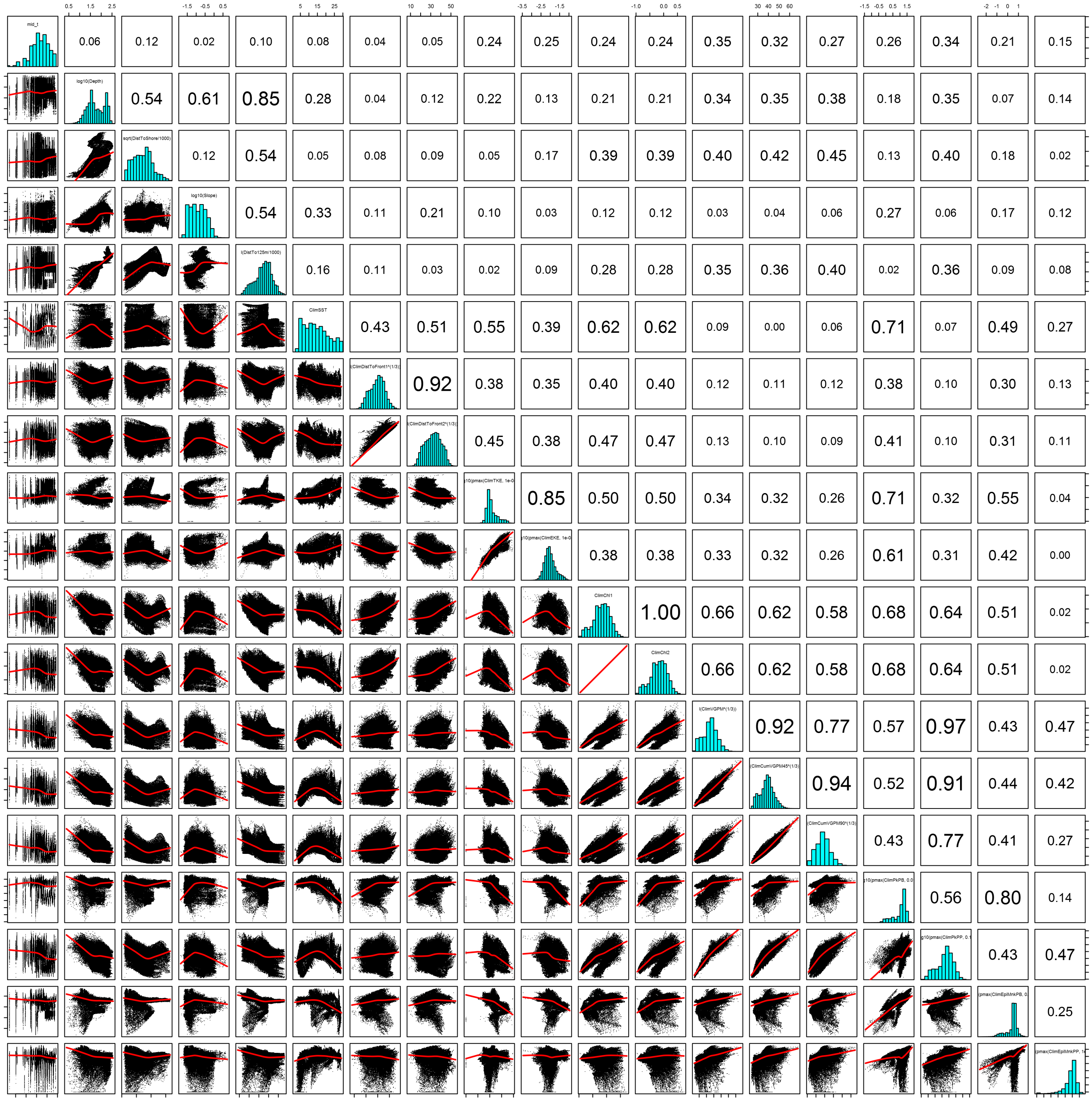

Figure 99: Scatterplot matrix for the Risso's dolphin Climatological model, Shelf. This plot is used to inspect the distribution of predictors (via histograms along the diagonal), simple correlation between predictors (via pairwise Pearson coefficients above the diagonal), and linearity of predictor correlations (via scatterplots below the diagonal). This plot is best viewed at high magnification.

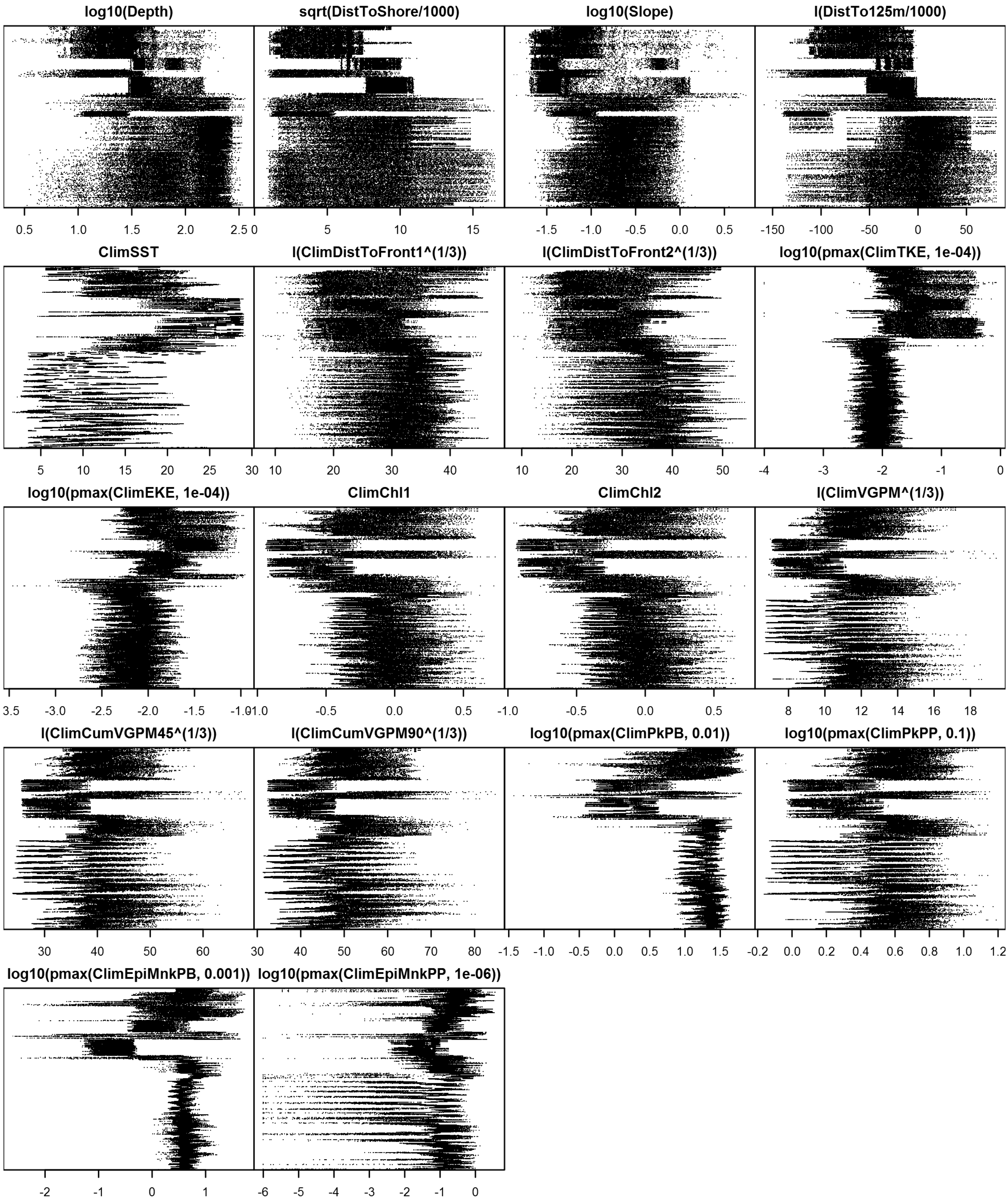

Figure 100: Dotplot for the Risso's dolphin Climatological model, Shelf. This plot is used to check for suspicious patterns and outliers in the data. Points are ordered vertically by transect ID, sequentially in time.

Model Comparison

Spatial Model Performance

The table below summarizes the performance of the candidate spatial models that were tested. For each subregion, the first model contained only physiographic predictors. Subsequent models added additional suites of predictors of based on when they became available via remote sensing.

For each model, three versions were fitted; the % Dev Expl columns give the % deviance explained by each one. The "climatological" models were fitted to 8-day climatologies of the environmental predictors. Because the environmental predictors were always available, no segments were lost, allowing these models to consider the maximal amount of survey data. The "contemporaneous" models were fitted to day-of-sighting images of the environmental predictors; these were smoothed to reduce data loss due to clouds, but some segments still failed to retrieve environmental values and were lost. Finally, the "climatological same segments" models fitted climatological predictors to the segments retained by the contemporaneous model, so that the explantory power of the two types of predictors could be directly compared. For each of the three models, predictors were selected independently via shrinkage smoothers; thus the three models did not necessarily utilize the same predictors.

Predictors derived from ocean currents first became available in January 1993 after the launch of the TOPEX/Poseidon satellite; productivity predictors first became available in September 1997 after the launch of the SeaWiFS sensor. Contemporaneous and climatological same segments models considering these predictors usually suffered data loss. Date Range shows the years spanned by the retained segments. The Segments column gives the number of segments retained; % Lost gives the percentage lost.

Predictors	Climatol % Dev Expl	Contemp % Dev Expl	Climatol Same Segs % Dev Expl	Segments	% Lost	Date Range
Slope and Abyss:						
Phys	28.0			17198		1992-2013
Phys+SST	33.3	31.0	33.3	17198	0.0	1992-2013
Phys+SST+Curr	45.9	41.9	45.8	16939	1.5	1995-2013
Phys+SST+Curr+Prod	47.5	43.5	48.3	16520	3.9	1998-2013
Shelf:						
Phys	34.5			87038		1992-2014
Phys+SST	34.8	36.2	34.8	87038	0.0	1992-2014
Phys+SST+Curr	36.9	38.9	36.7	85972	1.2	1995-2013
Phys+SST+Curr+Prod	37.5	38.2	36.4	83417	4.2	1998-2013

Table 42: Deviance explained by the candidate density models.

Abundance Estimates

The table below shows the estimated mean abundance (number of animals) within the study area, for the models that explained the most deviance for each model type. Mean abundance was calculated by first predicting density maps for a series of time steps, then computing the abundance for each map, and then averaging the abundances. For the climatological models, we used 8-day climatologies, resulting in 46 abundance maps. For the contemporaneous models, we used daily images, resulting in 365 predicted abundance maps per year that the prediction spanned. The Dates column gives the dates to which the estimates apply. For our models, these are the years for which both survey data and remote sensing data were available.

The Assumed g(0)=1 column specifies whether the abundance estimate assumed that detection was certain along the survey trackline. Studies that assumed this did not correct for availability or perception bias, and therefore underestimated abundance. The In our models column specifies whether the survey data from the study was also used in our models. If not, the study provides a completely independent estimate of abundance.

Dates	Model or study	Estimated abundance	CV	Assumed g(0)=1	In our models
1992-2014	Climatological model*	7732	0.09	No	
1998-2013	Contemporaneous model	12929	0.11	No	
1992-2014	Climatological same segments model	13111	0.09	No	
Jun-Aug 2011	Central Virginia to lower Bay of Fundy (Waring et al. 2014)	15197	0.55	No	No
Jun-Aug 2011	Central Florida to central Virginia (Waring et al. 2014)	3053	0.44	No	No
Jun-Aug 2011	Central Florida to lower Bay of Fundy, combined	18250	0.46	No	No
August 2006	Southern Gulf of Maine to Bay of Fundy and Gulf of St. Lawrence (Waring et al. 2014)	14408	0.38	No	Yes
Jun-Aug 2004	Maryland to Bay of Fundy (Waring et al. 2013)	15053	0.78	No	Yes
Jun-Aug 2004	Florida to Maryland (Waring et al. 2013)	5426	0.54	No	Yes
Jun-Aug 2004	Florida to Bay of Fundy, combined	20479	0.59	No	Yes

Table 43: Estimated mean abundance within the study area. We selected the model marked with * as our best estimate of the abundance and distribution of this taxon. For comparison, independent abundance estimates from NOAA technical reports and/or the scientific literature are shown. Please see the Discussion section below for our evaluation of our models compared to the other estimates. Note that our abundance estimates are averaged over the whole year, while the other studies may have estimated abundance for specific months or seasons. Our coefficients of variation (CVs) underestimate the true uncertainty in our estimates, as they only incorporated the uncertainty of the GAM stage of our models. Other sources of uncertainty include the detection functions and g(0) estimates. It was not possible to incorporate these into our CVs without undertaking a computationally-prohibitive bootstrap; we hope to attempt that in a future version of our models.

Density Maps

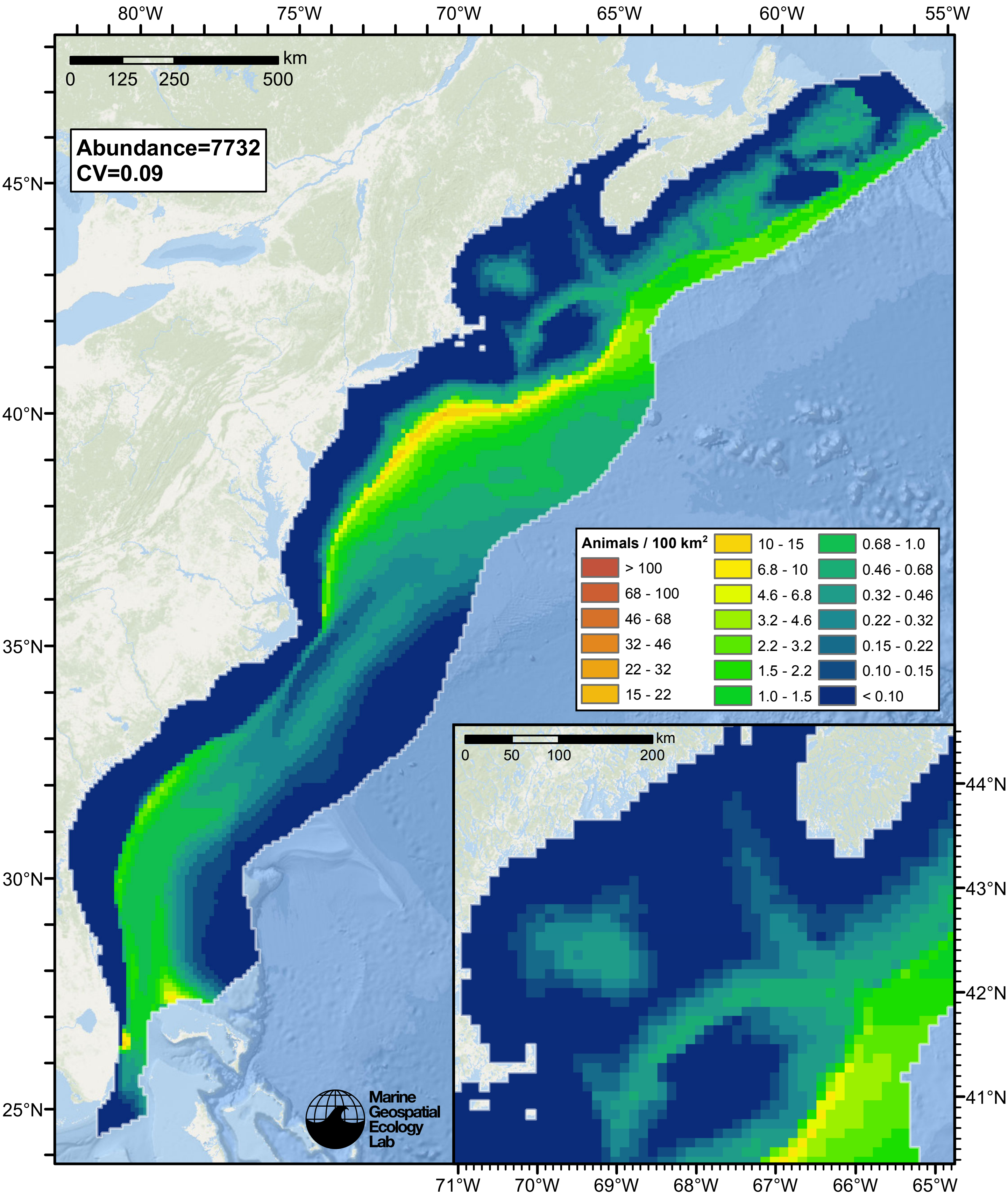

Figure 101: Risso's dolphin density and abundance predicted by the climatological model that explained the most deviance. Regions inside the study area (white line) where the background map is visible are areas we did not model (see text).

Contemporaneous Model

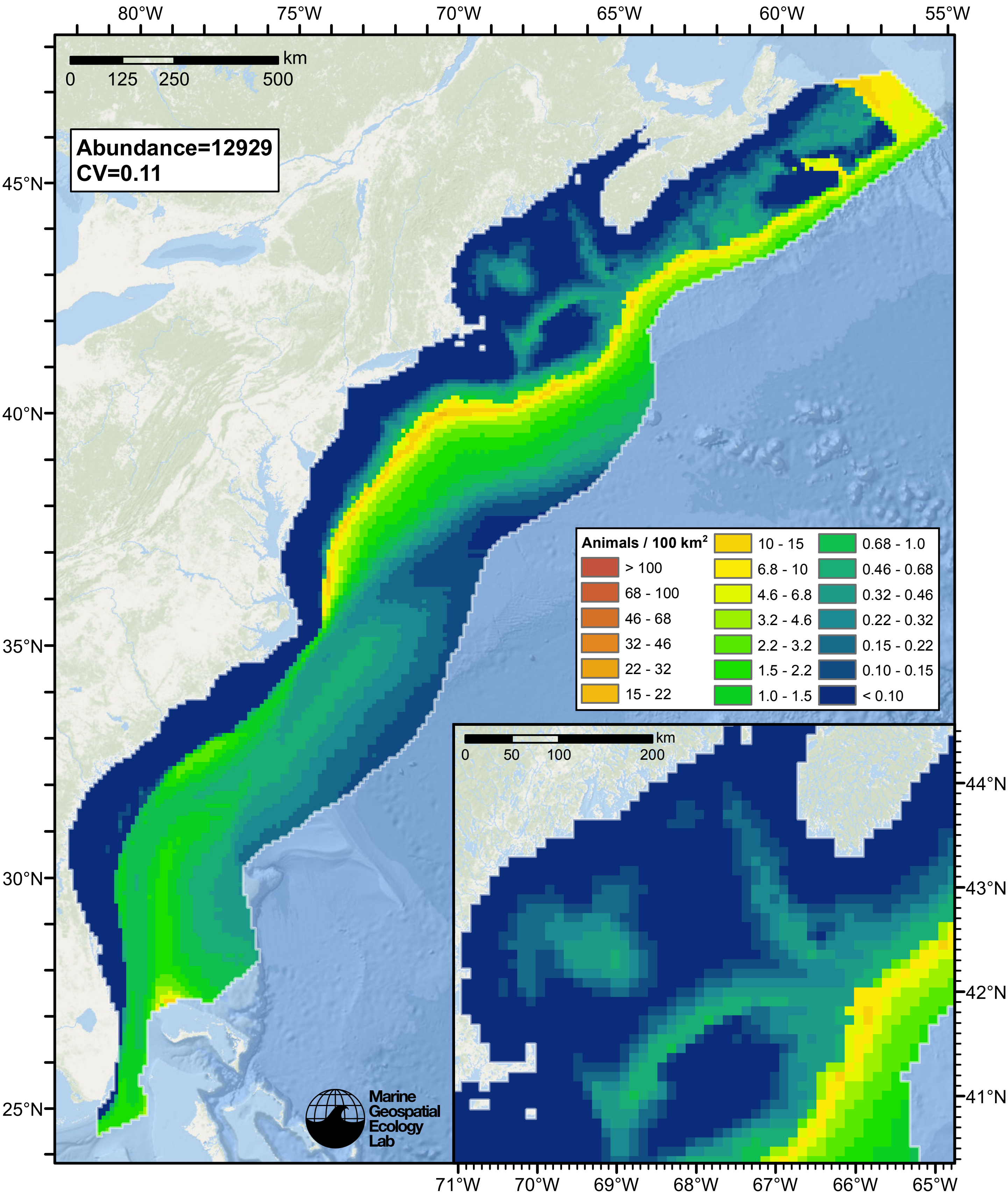

Figure 102: Risso's dolphin density and abundance predicted by the contemporaneous model that explained the most deviance. Regions inside the study area (white line) where the background map is visible are areas we did not model (see text).

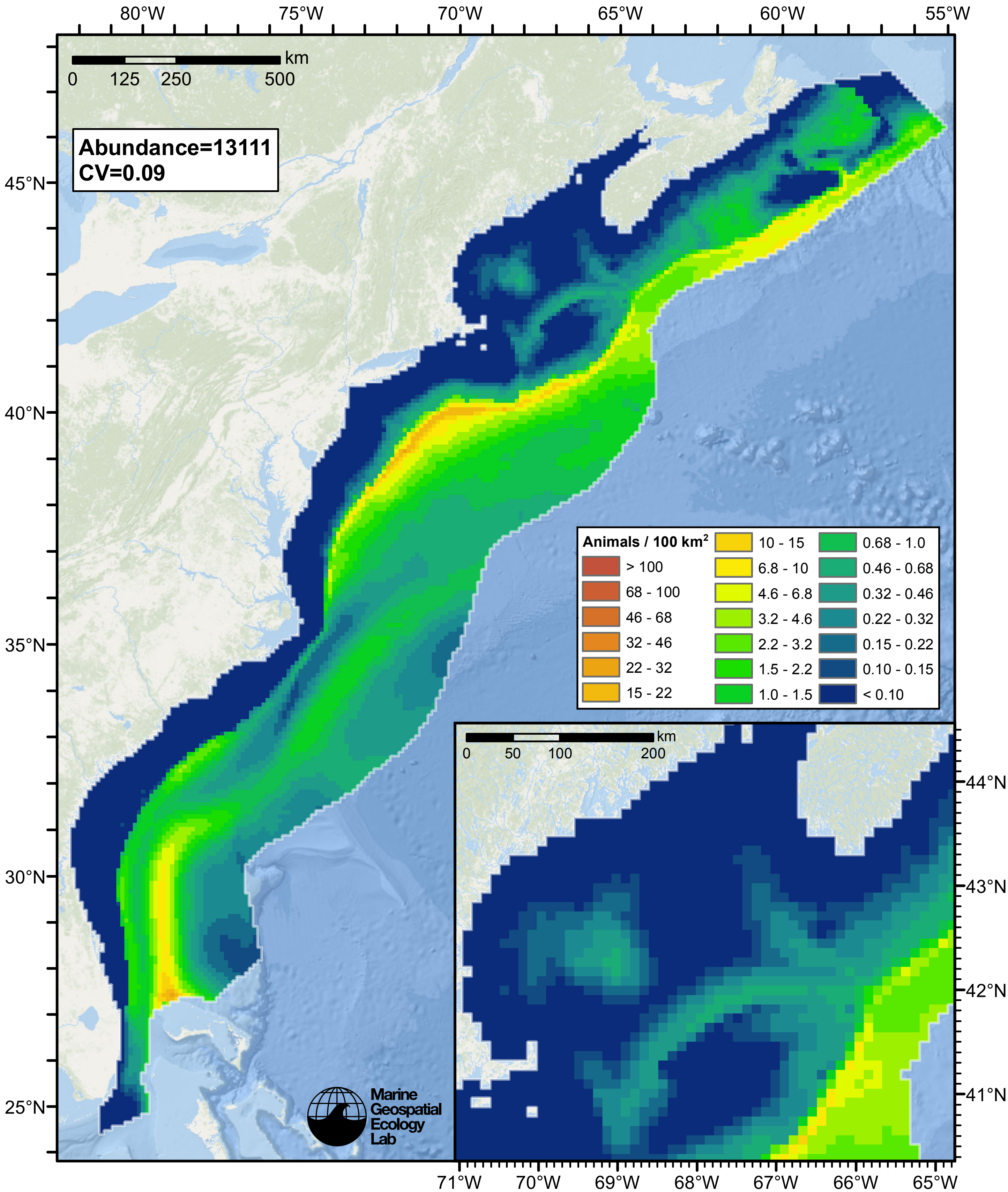

Figure 103: Risso's dolphin density and abundance predicted by the climatological same segments model that explained the most deviance. Regions inside the study area (white line) where the background map is visible are areas we did not model (see text).

Temporal Variability

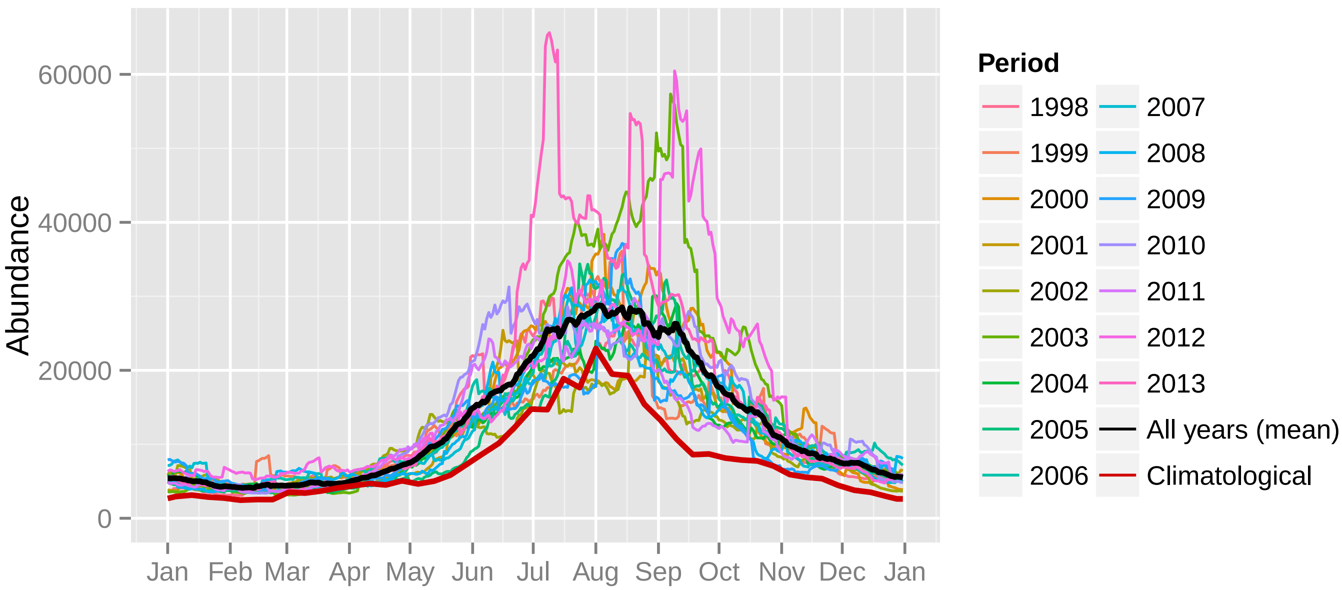

Figure 104: Comparison of Risso's dolphin abundance predicted at a daily time step for different time periods. Individual years were predicted using contemporaneous models. "All years (mean)" averages the individual years, giving the mean annual abundance of the contemporaneous model. "Climatological" was predicted using the climatological model. The results for the climatological same segments model are not shown.

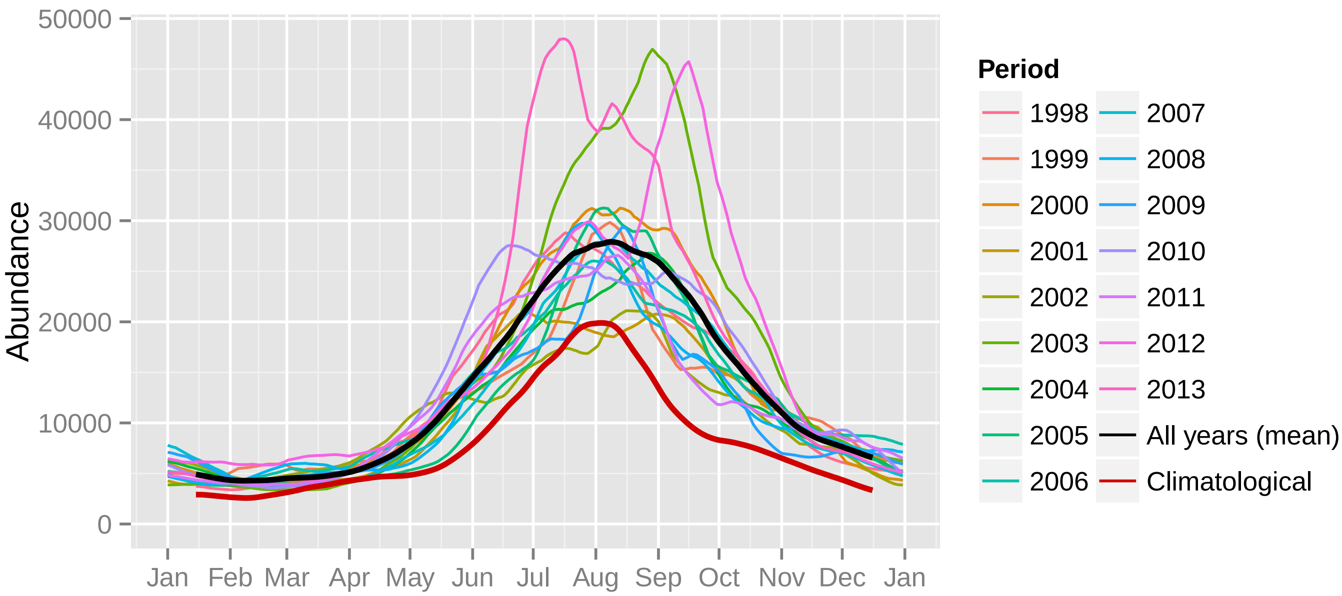

Figure 105: The same data as the preceding figure, but with a 30-day moving average applied.

Climatological Model

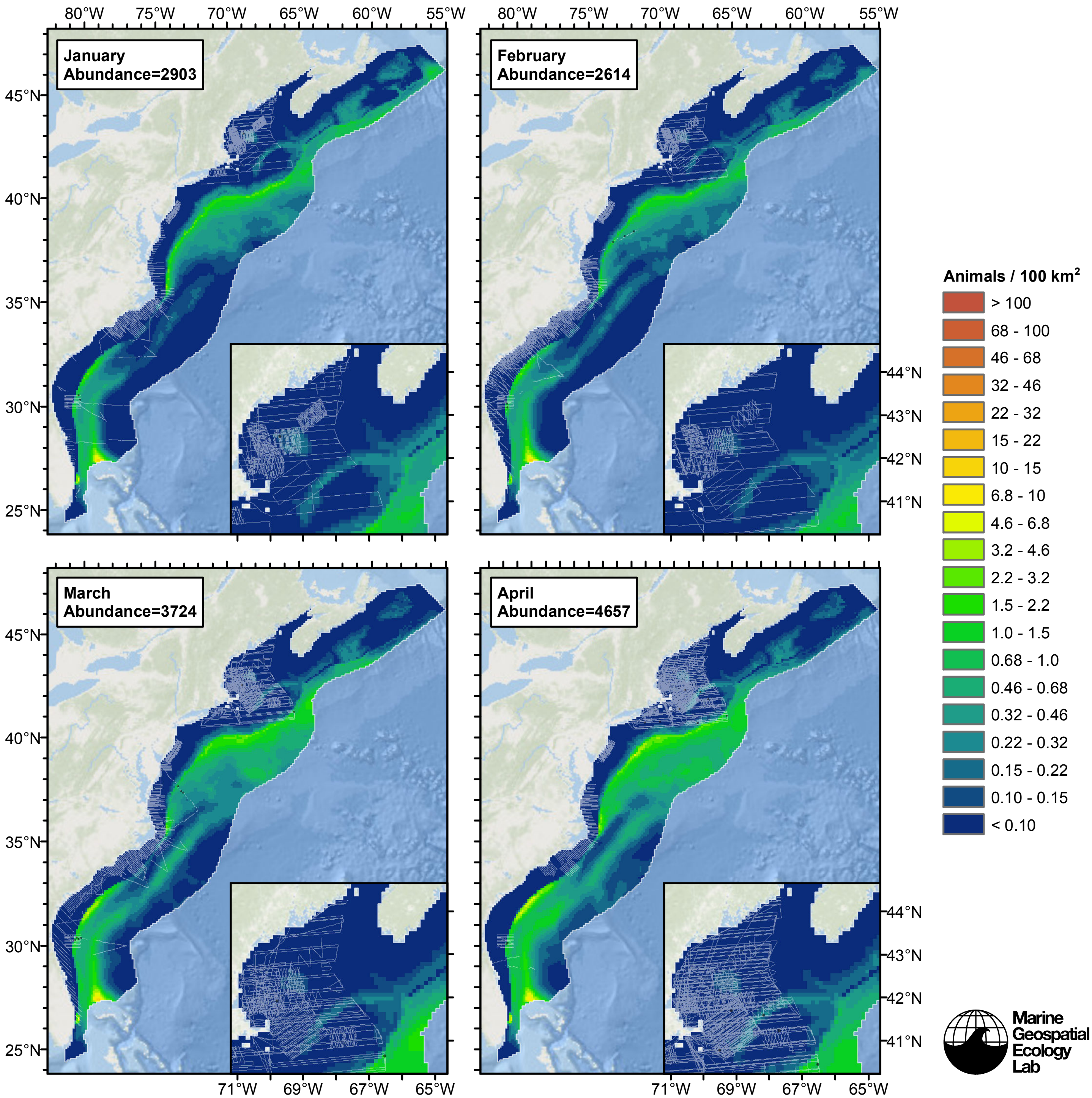

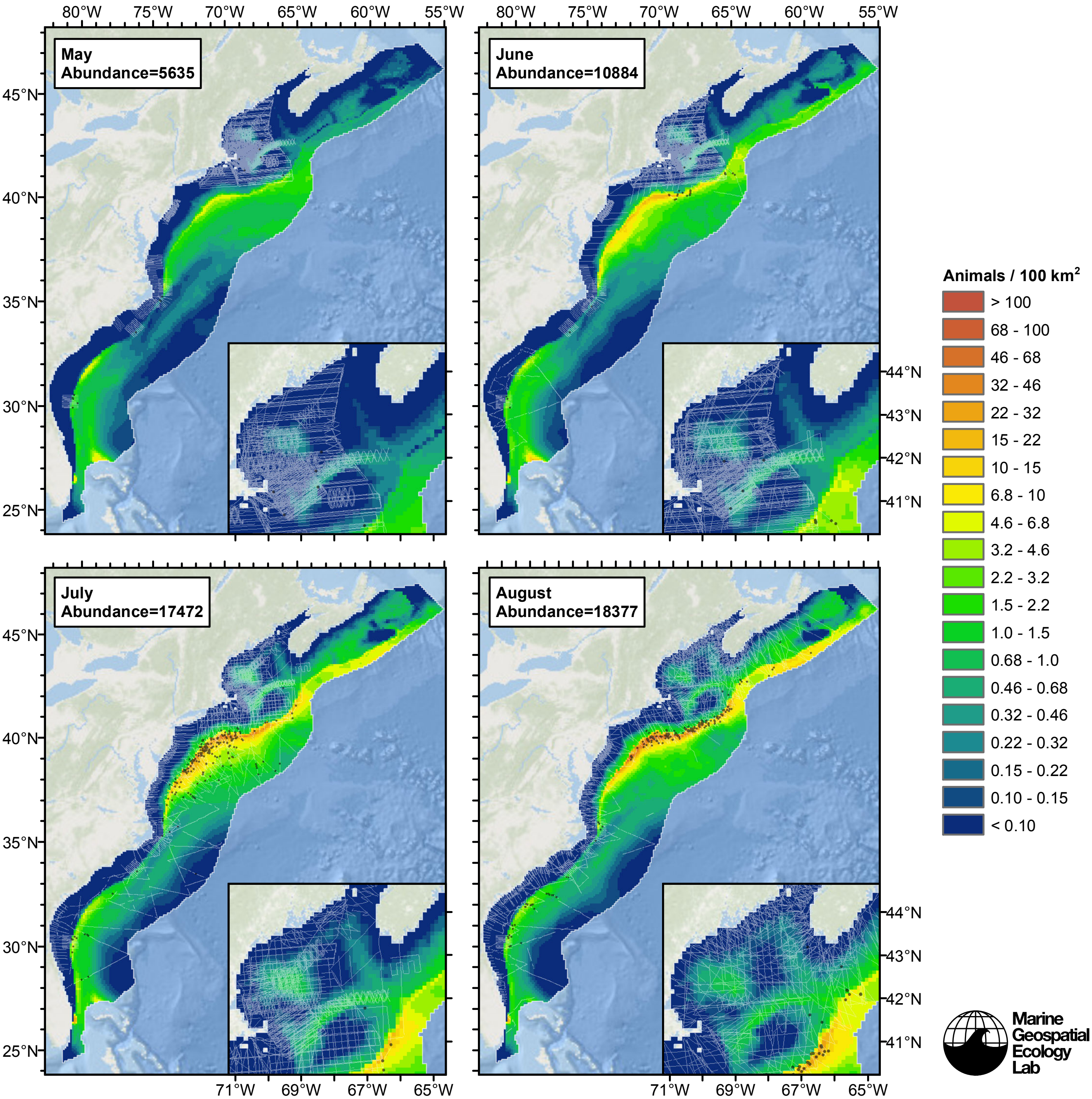
May
Abundance=5635
June
Abundance=10884
July
Abundance=17472
August
Abundance=18377
80°W
75°W
70°W
65°W
60°W
55°W
45°N
40°N
35°N
30°N
25°N
44°N
43°N
42°N
41°N
71°W
69°W
67°W
65°W
Animals / 100 km²
> 100
68 - 100
46 - 68
32 - 46
22 - 32
15 - 22
10 - 15
6.8 - 10
4.6 - 6.8
3.2 - 4.6
2.2 - 3.2
1.5 - 2.2
1.0 - 1.5
0.68 - 1.0
0.46 - 0.68
0.32 - 0.46
0.22 - 0.32
0.15 - 0.22
0.10 - 0.15
< 0.10
Marine
Geospatial
Ecology
Lab

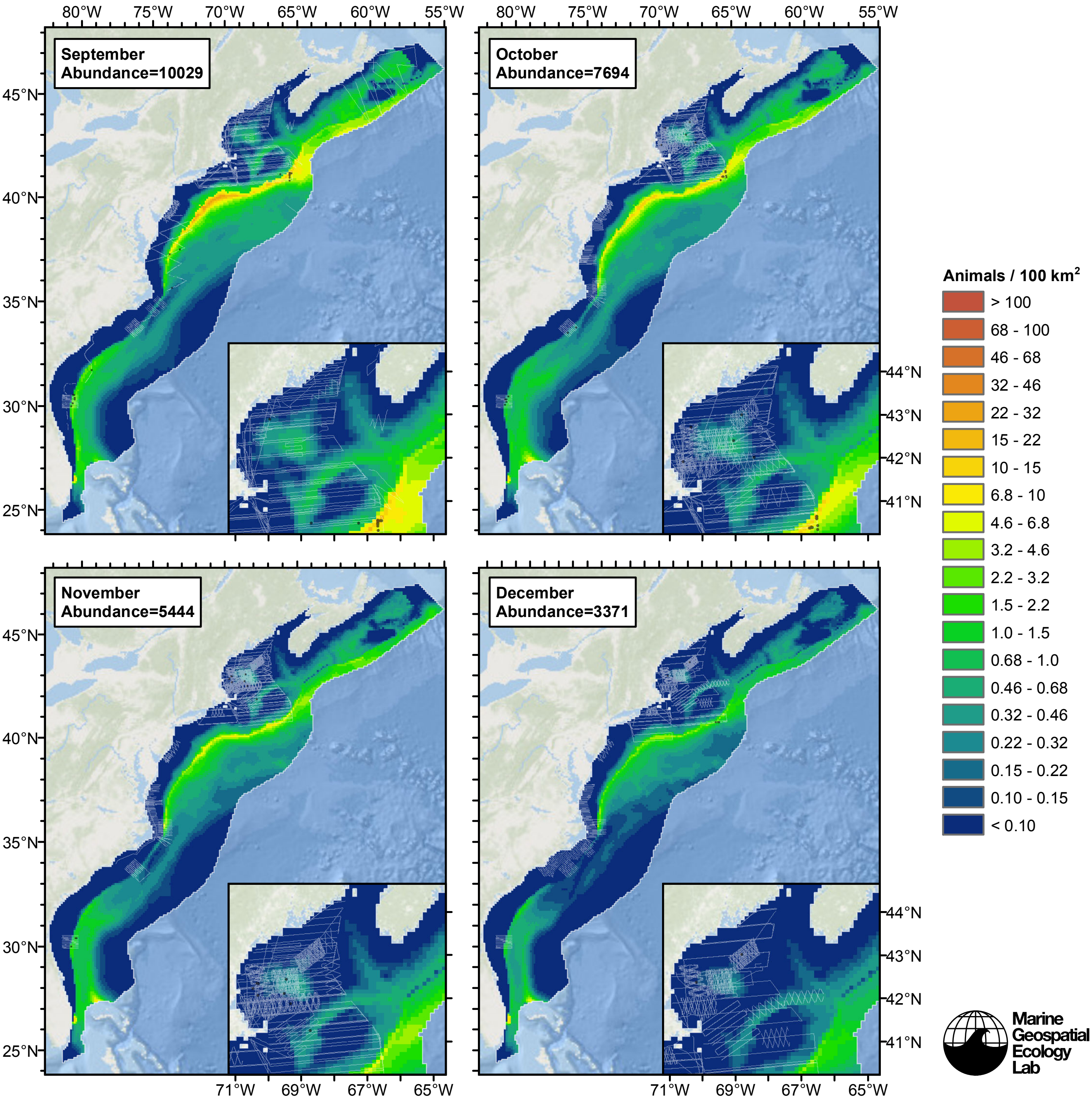

September
Abundance=10029
October
Abundance=7694
November
Abundance=5444
December
Abundance=3371
80°W
75°W
70°W
65°W
60°W
55°W
45°N
40°N
35°N
30°N
25°N
44°N
43°N
42°N
41°N
71°W
69°W
67°W
65°W
Animals / 100 km^2
> 100
68 - 100
46 - 68
32 - 46
22 - 32
15 - 22
10 - 15
6.8 - 10
4.6 - 6.8
3.2 - 4.6
2.2 - 3.2
1.5 - 2.2
1.0 - 1.5
0.68 - 1.0
0.46 - 0.68
0.32 - 0.46
0.22 - 0.32
0.15 - 0.22
0.10 - 0.15
< 0.10
Marine
Geospatial
Ecology
Lab

Contemporaneous Model

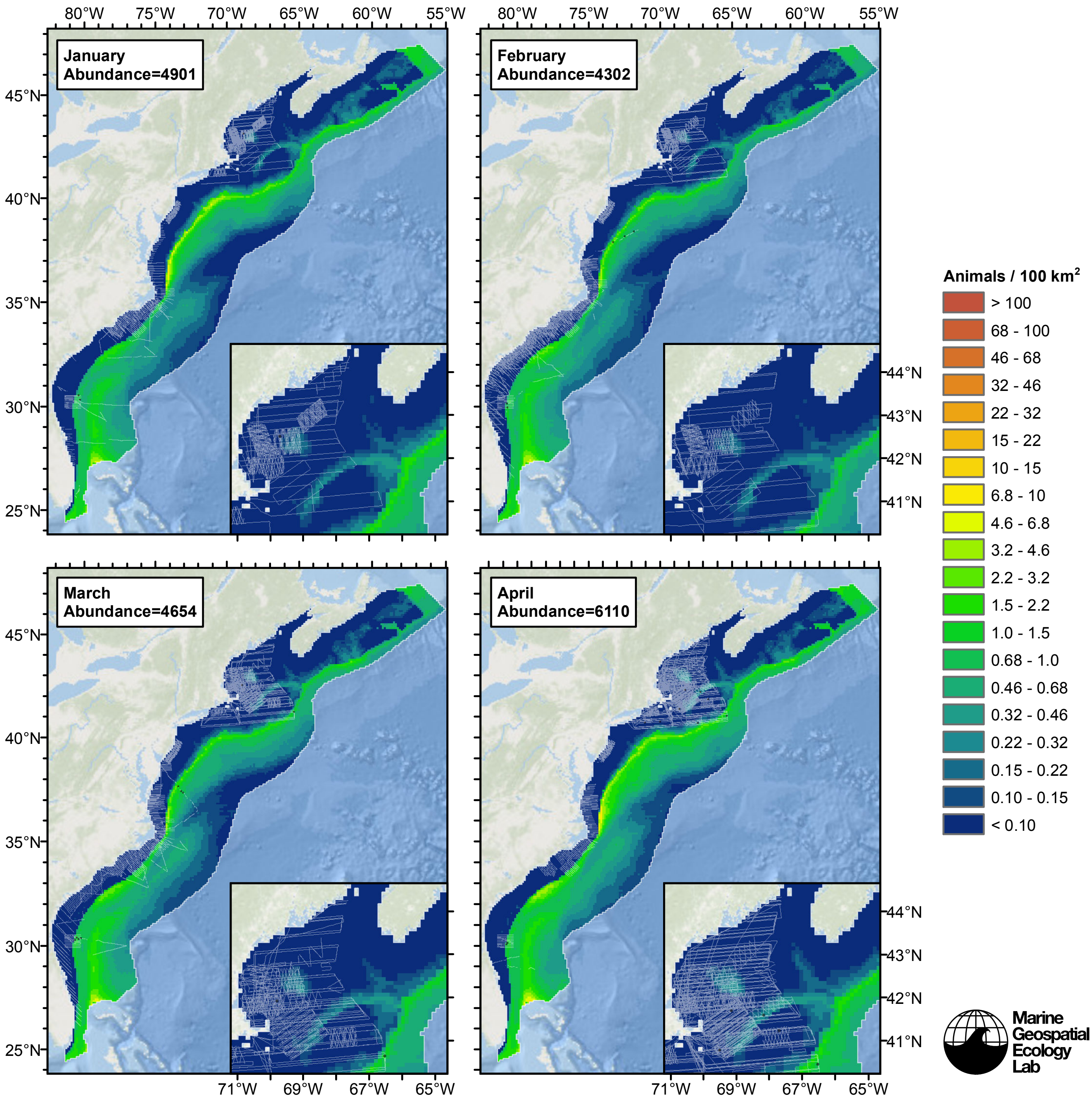

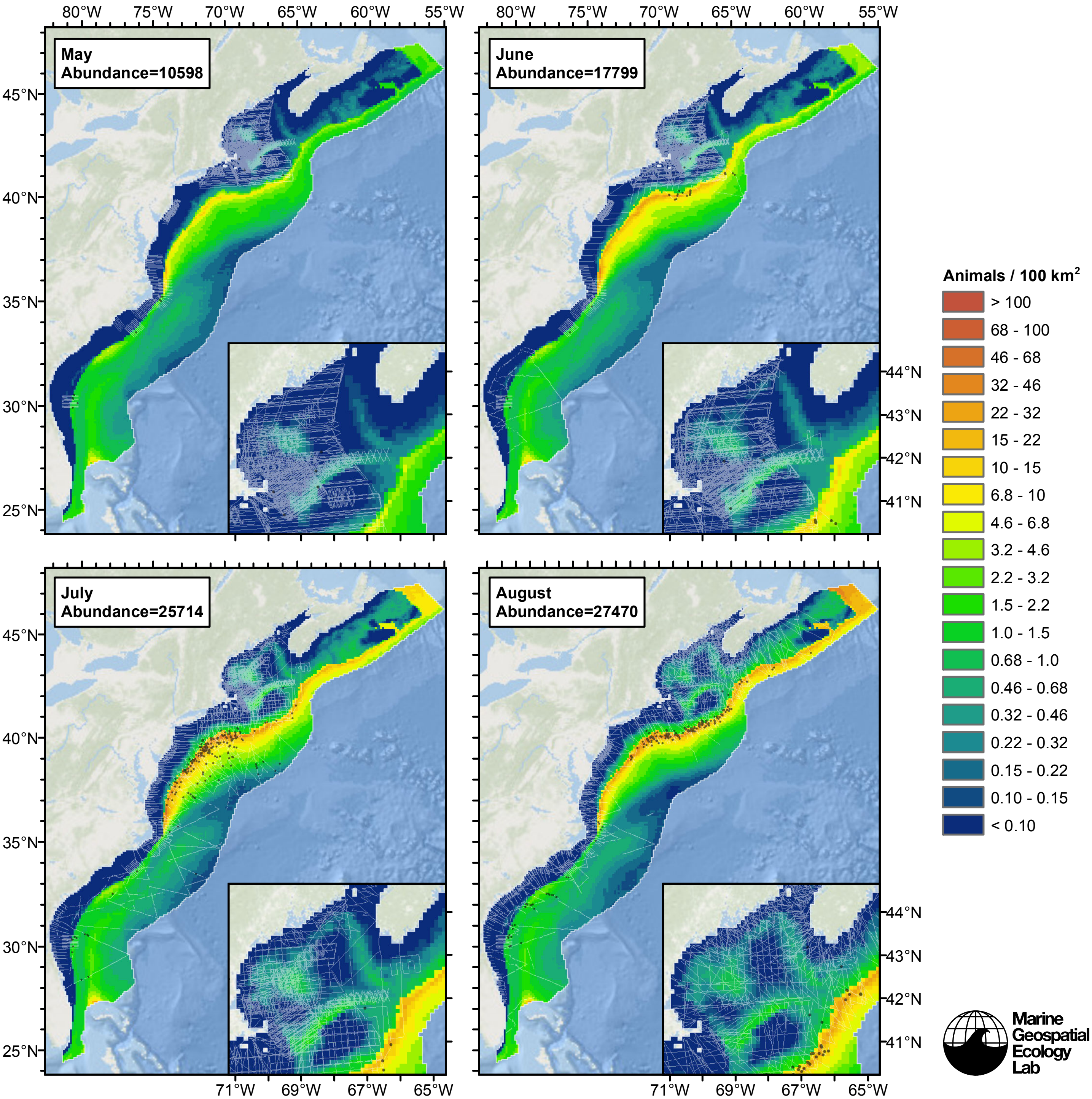

Marine Geospatial Ecology Lab

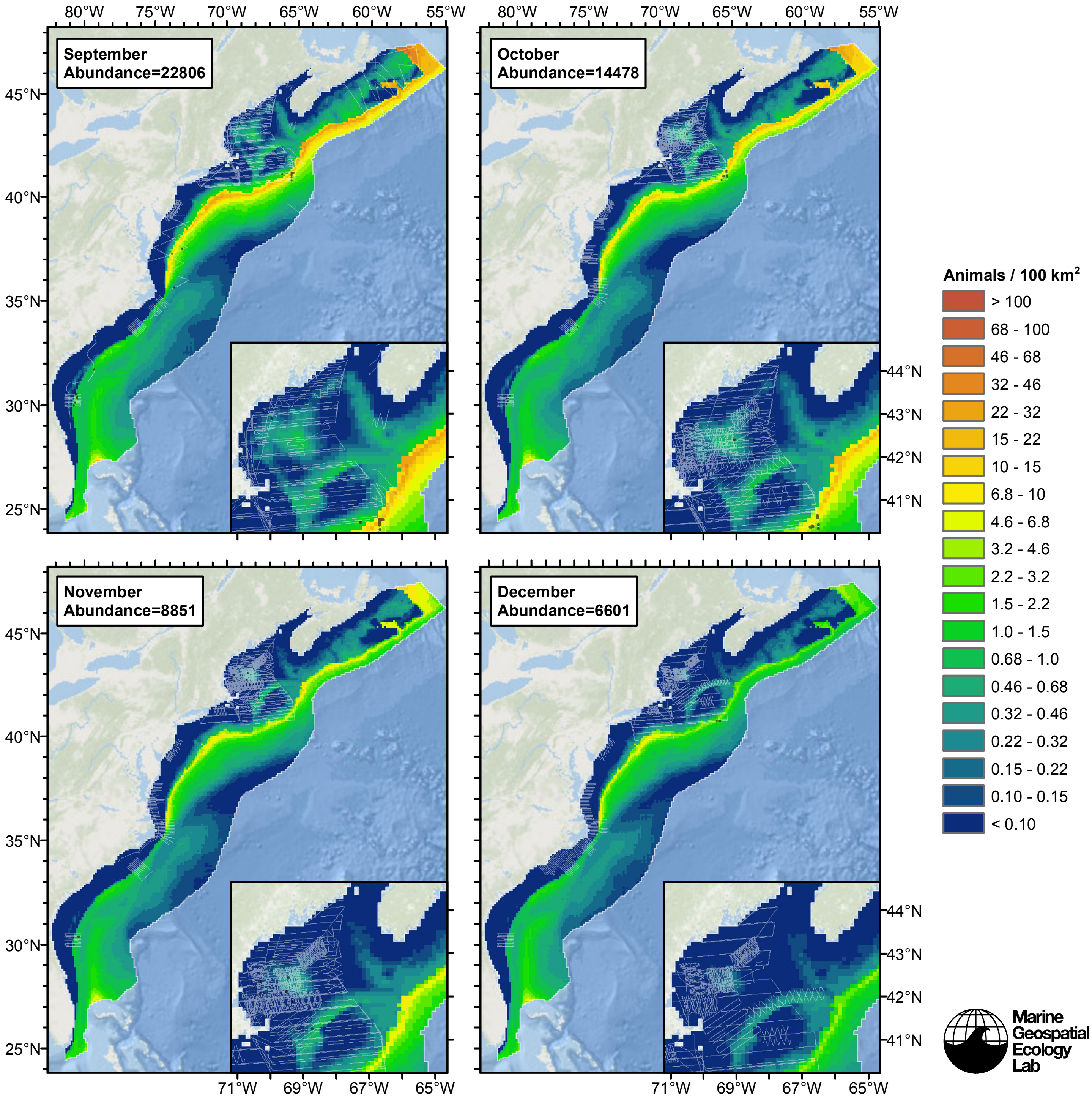
September
Abundance=22806
October
Abundance=14478
November
Abundance=8851
December
Abundance=6601
80°W
75°W
70°W
65°W
60°W
55°W
45°N
40°N
35°N
30°N
25°N
44°N
43°N
42°N
41°N
71°W
69°W
67°W
65°W
Animals / 100 km^2
> 100
68 - 100
46 - 68
32 - 46
22 - 32
15 - 22
10 - 15
6.8 - 10
4.6 - 6.8
3.2 - 4.6
2.2 - 3.2
1.5 - 2.2
1.0 - 1.5
0.68 - 1.0
0.46 - 0.68
0.32 - 0.46
0.22 - 0.32
0.15 - 0.22
0.10 - 0.15
< 0.10
Marine Geospatial Ecology Lab

Climatological Same Segments Model

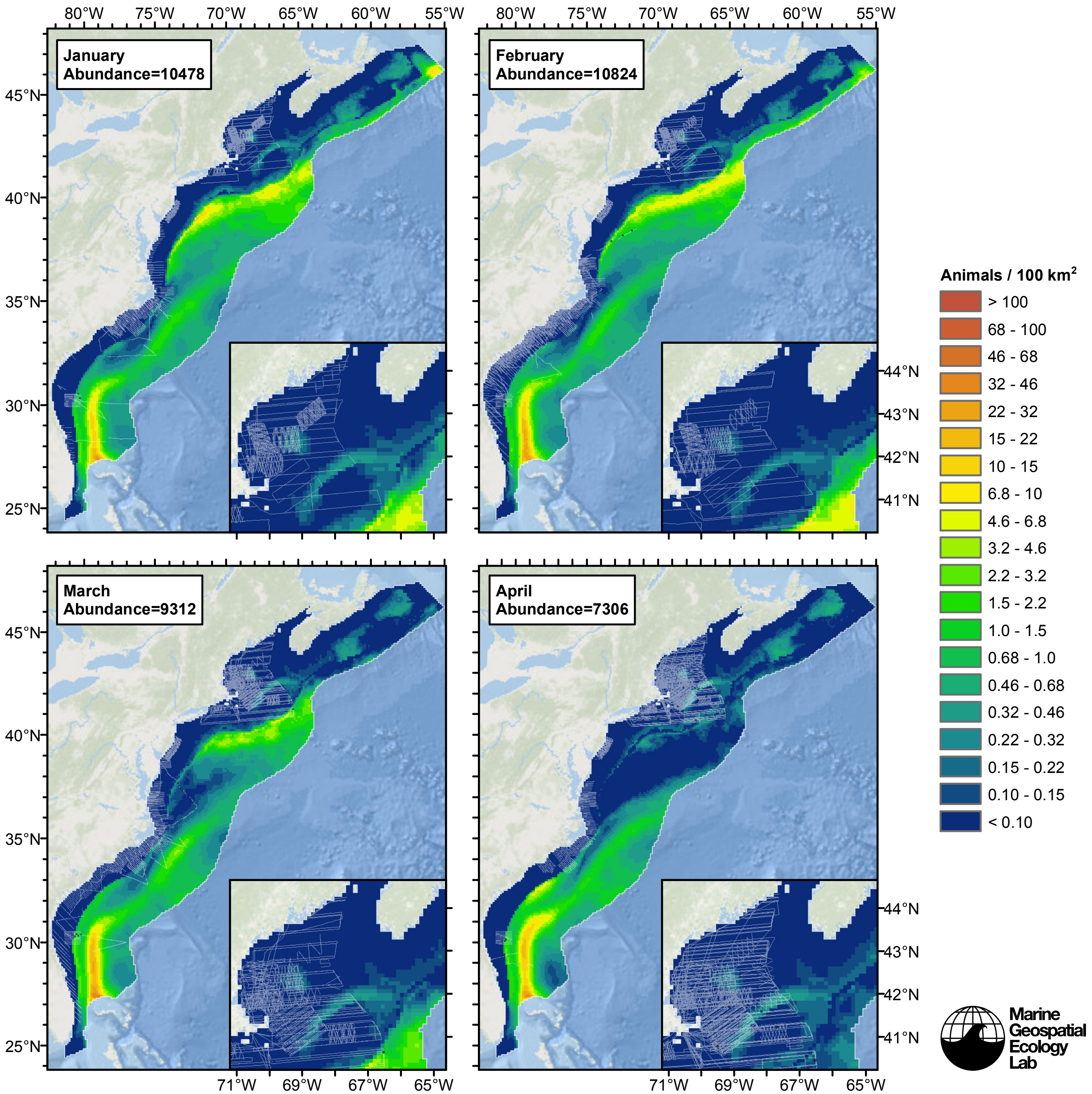

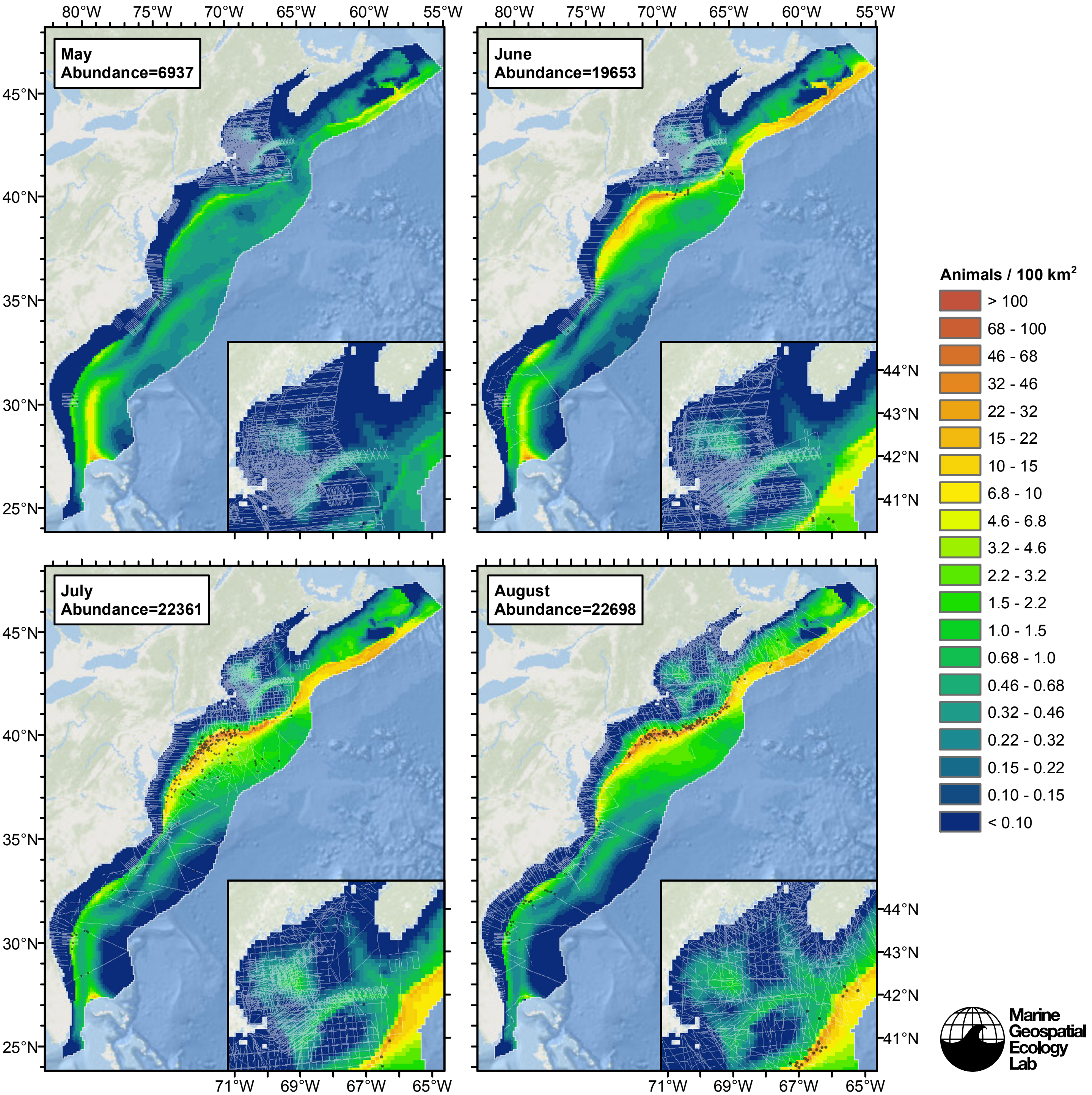
May
Abundance=6937
June
Abundance=19653
July
Abundance=22361
August
Abundance=22698
80°W
75°W
70°W
65°W
60°W
55°W
45°N
40°N
35°N
30°N
25°N
44°N
43°N
42°N
41°N
71°W
69°W
67°W
65°W
Animals / 100 km^2
> 100
68 - 100
46 - 68
32 - 46
22 - 32
15 - 22
10 - 15
6.8 - 10
4.6 - 6.8
3.2 - 4.6
2.2 - 3.2
1.5 - 2.2
1.0 - 1.5
0.68 - 1.0
0.46 - 0.68
0.32 - 0.46
0.22 - 0.32
0.15 - 0.22
0.10 - 0.15
< 0.10
Marine
Geospatial
Ecology
Lab

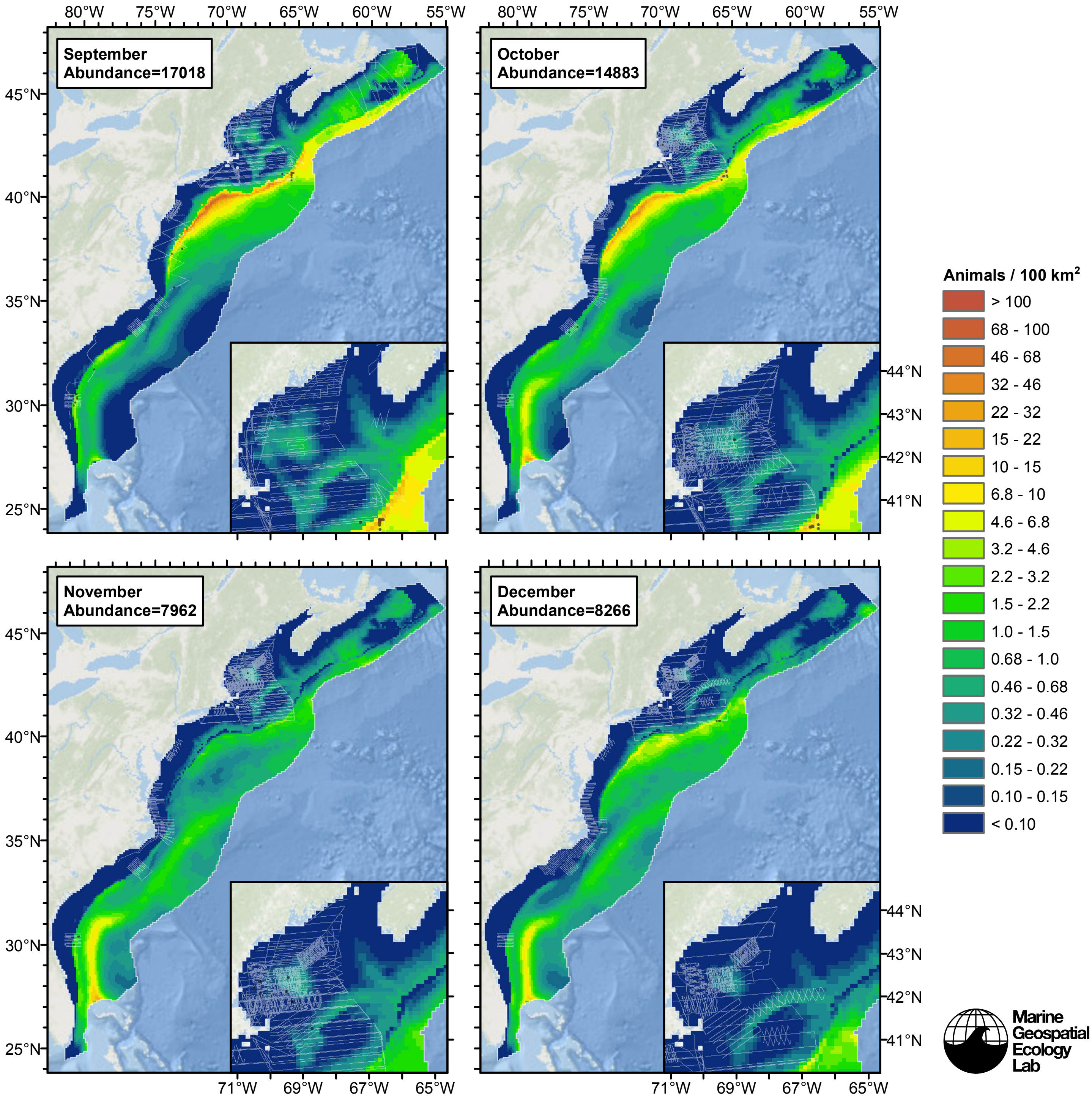

Discussion

The majority of Risso's dolphins were sighted in the Slope and Abyss region. Here, the climatological models achieved better fits than the contemporaneous models, explaining 2.3-4.8% more deviance, suggesting that climatological predictors are more suitable for modeling Risso's dolphins in this region. In the Shelf region, where fewer Risso's dolphins were sighted, the contemporaneous models achieved better fits, explaining 0.7-2.2% more deviance than the climatological models.

The predicted mean total abundance ranged widely across the models, with the climatological model that considered all segments predicting the smallest abundance and the other two predicting nearly 70% more. The models were most similar in the winter months. The greatest differences occurred the late summer months of August and September, with the contemporaneous model predicting much higher abundance along the Scotian Shelf, particularly in the deep Laurentian

Channel leading into the Gulf of St. Lawrence, and a large submarine canyon known as the “Gully” (see Temporal Variability section). We are skeptical of these predictions. Lawson and Gosselin (2009) reported only six sightings of Risso’s dolphins on the entire Scotian Shelf and near Cape Breton Island during the Canadian TNASS summer aerial survey in 2007. Hooker et al. (1999) reported no sightings during seven years of vessel-based cetacean research trips to the Gully; all were conducted in June-August months.

We made several attempts to contact J. Lawson regarding the Canadian TNASS survey, in the hope of incorporating it into our models to improve our predictions in Canadian waters, but we received no response. We remain hopeful that a collaboration can be established in the future, and the Canadian TNASS data may be incorporated into a new version of our models.

Prior abundance surveys conducted across the broader east coast of the U.S. and Canada by NOAA estimated 14400-20400 Risso’s dolphins for the months of June-August, although the spatial extents of these predictions did not exactly match that of our study area. In comparison, our climatological model that considered all segments predicted 10900-18400, while the contemporaneous model predicted 17800-27500.

Given the climatological model’s closer match to NOAA’s estimates, and that the contemporaneous model predicted what seemed to be spurious high abundance in Canada, we selected the climatological model that considered all segments as our best estimate of Risso’s dolphin distribution and abundance.

We also considered the climatological model that was fitted to the same segments as the contemporaneous model. This model predicted the highest total mean abundance, with June-August abundance ranging from 19700-22700. But this model displayed what we believe is an unlikely “bump” in wintertime abundance, in which abundance was low in November-December, then increased roughly 25% in January-March, then fell below the November-December level in April-May. For this reason, we preferred the climatological model that was fitted to all segments.

The literature suggested that Risso’s dolphins occupy the mid-Atlantic continental shelf edge year round, and may expand northward during spring, summer and fall, contracting southward in winter (Waring et al. 2014; CETAP 1982). Because our model reproduced that pattern, we suggest that our monthly predictions be used for federal regulatory purposes and marine spatial planning applications, so that the seasonality of the species be accounted for. But we urge caution in winter. Our model predicted roughly 85% lower abundance in January than in August. If this is correct, it suggests that the bulk of the population migrates out of the study area in winter, perhaps south to the Caribbean or far offshore. With so little survey effort off the shelf in winter, we have little evidence on which to base such a claim. To resolve this uncertainty, we strongly recommend that additional off-shelf surveys be performed in winter months.

References

Barlow J, Forney KA (2007) Abundance and density of cetaceans in the California Current ecosystem. Fish. Bull. 105: 509-526.

CETAP (1982) A characterization of marine mammals and turtles in the mid-and north Atlantic areas of the US outer continental shelf. Final Report. Bureau of Land Management, Washington, DC. Ref. AA551-CT8-48.

Carretta JV, Lowry MS, Stinchcomb CE, Lynn MS, Cosgrove RE (2000) Distribution and abundance of marine mammals at San Clemente Island and surrounding offshore waters: results from aerial and ground surveys in 1998 and 1999. Administrative Report LJ-00-02, available from Southwest Fisheries Science Center, P.O. Box 271, La Jolla, CA USA 92038. 44 p.

Hiby L (1999) The objective identification of duplicate sightings in aerial survey for porpoise. In: Marine Mammal Survey and Assessment Methods (Garner GW, Amstrup SC, Laake JL, Manly BFJ, McDonald LL, Robertson DG, eds.). Balkema, Rotterdam, pp. 179-189.

Hooker SK, Whitehead H, Gowans S (1999) Marine Protected Area Design and the Spatial and Temporal Distribution of Cetaceans in a Submarine Canyon. Conservation Biology 13: 592-602.

Jefferson TA, Weir CR, Anderson RC, Ballance LT, Kenney RD, et al. (2014) Global distribution of Risso’s dolphin Grampus griseus: a review and critical evaluation. Mammal Review 44: 56-68.

Lawson JW, Gosselin J-F (2009) Distribution and preliminary abundance estimates for cetaceans seen during Canada’s Marine Megafauna Survey-A component of the 2007 TNASS. DFO Can. Sci. Advis. Sec. Res. Doc. 2009/031. 28 p. Available online: http://biblio.uqar.qc.ca/archives/30125408.pdf

Palka DL (2006) Summer Abundance Estimates of Cetaceans in US North Atlantic Navy Operating Areas. US Dept Commer, Northeast Fish Sci Cent Ref Doc. 06-03: 41 p.

Waring GT, Josephson E, Maze-Foley K, Rosel PE, eds. (2013) U.S. Atlantic and Gulf of Mexico Marine Mammal Stock Assessments – 2012. NOAA Tech Memo NMFS NE 223; 419 p.

Waring GT, Josephson E, Maze-Foley K, Rosel PE, eds. (2014) U.S. Atlantic and Gulf of Mexico Marine Mammal Stock Assessments – 2013. NOAA Tech Memo NMFS NE 228; 464 p.